

Copyright

by

Federico Macias Aguayo Jr.

2016

**The Dissertation Committee for Federico Macias Aguayo Jr. Certifies that this is
the approved version of the following dissertation:**

**External Sulfate Attack of Concrete: An Accelerated Test Method,
Mechanisms, and Mitigation Techniques**

Committee:

Kevin J. Folliard, Supervisor

Michael D.A. Thomas, Co-Supervisor

David W. Fowler

Maria C.G. Juenger

Harovel Wheat

**External Sulfate Attack of Concrete: An Accelerated Test Method,
Mechanisms, and Mitigation Techniques**

by

Federico Macias Aguayo Jr., B.S.C.E; M.S.E

Dissertation

Presented to the Faculty of the Graduate School of

The University of Texas at Austin

in Partial Fulfillment

of the Requirements

for the Degree of

Doctor of Philosophy

The University of Texas at Austin

May 2016

Dedication

To my family that has always been there for me, there is no way I would have made it this far without y'all. To my best friend, Nikki, you made all this work well worth it towards the end. And to the most important person in my life, my son, Isaiah, I love you and this is all for you.

Acknowledgements

First, I would like to thank my supervisor and friend, Dr. Kevin Folliard. Thank you for giving me this opportunity to work under your supervision and spreading the contagious “concrete bug” on me. Your leadership, guidance, and most importantly your friendship have been such a great experience and I cannot thank you enough for all that you have taught me. I feel that I am a better person because of you and I hope that I can even be half the researcher and advisor that you are. To be an assistant faculty has always been my dream and now it’s a reality, and I owe it all to you. I am extremely grateful for all your support and am excited to continue working with you as your neighboring colleague at Texas State.

To my co-supervisor, Dr. Michael Thomas, it has been a privilege working under your supervision and I thank you for the opportunity. Your knowledge and guidance is unquestionably something that I don’t take for granted. You and Dr. Folliard make working in this industry so exciting and I hope to work with you more in the future.

To the rest of my PhD committee: Dr. Maria Juenger, Dr. David Fowler, and Dr. Harovel Wheat, thank you very much for the guidance throughout my undergraduate and graduate time here at UT. Dr. Juenger, you’ve been so kind and patient with me, I cannot thank you enough for all your support. I truly do appreciate your constructive criticism for my writing and I believe that I am a better writer because of you. Dr. Fowler, it has been a pleasure working under your supervision. Thank you so much for being very active and a huge support during my job-hunt. Lastly but certainly not least, thank you Dr. Wheat for being a member of my committee. Your unconditional love and support for us “concrete nerds” is amazing and I really do appreciate it.

I would also like to personally thank my former PhD mentor, Dr. Anthony Bentivegna. There is no way I would be in this position without your guidance and friendship. I look forward to many years of friendship and hard work.

To my lab mates, thank you so much for all the good times and experiences. Thano Drimalas, your incredible selflessness personality to put aside your responsibilities and help others, especially me, is something I truly admired. You have become one of my closest friends in the past few years and I've enjoyed all our trips together. I look forward to many years of working with one of my best friends. Racheal Lute, from the very first rumors I heard about you returning to the lab, I couldn't wait to meet you. Since then, it has been an incredible three years and I couldn't imagine them without you. I'm super pumped to be staying in Texas and continuing to hang. Chris Clement, Mitchell Dornak, Jose Zuniga, Phil Pesek, Ted Moffat, Huang Yi, Stephen Stacey, and Nick Tiburzi, thank you so much for all the lab help, good laughs, good beer, and strong friendships all these years. I also want to thank all of the undergraduates that have helped me over the years. Especially those towards the end who made my post-knee surgery so much easier to deal with.

I would also like to thank the staff at our amazing laboratory. Sherian Williams, thanks for putting up with all my travel mistakes over the last 7 years. You made my life so much easier and smoother at the lab I don't know what I would have done without you. Mike Rung, I appreciate your help so much over the years. No matter how busy you were, you always tried your best to help me out with any issue I had at the lab and I really appreciate it.

Lastly, I want to give the upmost thank you to my family. You have been so supportive and patient these last nine years it's incredible that you have been willing to put up with me. To my parents, regardless of you ever understanding why I pursued a

Doctoral degree in concrete, you never doubted me one bit and if anything, you only gave me more support to continue with what I love to do. To my sisters, I can't imagine life without y'all. Thank you for always supporting me. Isaiah Federico Aguayo and Nikki Weaver, I'm incredibly blessed to have a family with you two. I'm looking forward to all the great years together.

External Sulfate Attack of Concrete: An Accelerated Test Method, Mechanisms, and Mitigation Techniques

Federico Macias Aguayo Jr., Ph.D.

The University of Texas at Austin, 2016

Supervisor: Kevin J. Folliard

Co-Supervisor: Michael D. A. Thomas

Abstract

Sulfate attack of concrete is perhaps the least understood of the major durability mechanisms plaguing reinforced concrete infrastructures. Many studies have attempted to better understand the underlying mechanisms in which the various modes of deterioration by sulfate attack manifest; however, several controversies still exist. Moreover, ASTM C 1012 (2012), which is the most commonly referred standardized laboratory test method to determine sulfate resistance of blended portland cement mixtures, does not always link well to field performance and may take up to 18 months to complete.

The research program presented in this dissertation investigates various issues pertaining to the mechanisms, testing methods, and factors influencing external sulfate attack. The primary focus of this research study was to investigate and propose a reliable, and innovative accelerated test method to evaluate the sulfate performance using concrete specimens. The research program was divided into the following four key

components: (1) design a method that can obtain results within a reasonable timeframe (less than six months); (2) design a method that uses concrete specimens and thus links more closely to field performance; (3) develop a better understanding on the role and mechanisms of sulfate attack on concrete through a comprehensive research program including field and laboratory investigations; and (4) investigate the use of calcium sulfate (gypsum) used as an additive to mitigate the potential of sulfate attack in blended portland cement mixtures using high-calcium fly ash.

The findings in this dissertation led to the development of a potential accelerated test method for determining sulfate resistance by vacuum impregnating concrete (or mortar) samples with sulfate solution to accelerate the ingress and onset of chemical reactions between the hydrated cement paste and sulfate ion (SO_4^{2-}). The effects of binder type, water-to-cementitious ratio (w/cm), curing regime, sulfate type and concentration are examined. In comparison to the conventional ASTM C 1012 method, results showed a higher rate of expansion with significant distress observed in samples subjected to the accelerated test method and placed in a 5% Na_2SO_4 solution. Similar trends, but at a relatively lower expansion rate, were also observed in samples placed in a 0.89% Na_2SO_4 solution. Physical measurements, chemical analysis and microstructural studies were performed periodically on the specimens.

Table of Contents

Dedication	iv
Acknowledgements	v
Abstract.....	viii
List of Tables	xvi
List of Figures.....	xvii
Chapter 1: Introduction	1
1.1 Background	1
1.2 Scientific Network	3
1.3 Problem Definition.....	4
1.4 Research Objective	6
1.5 Research Scope and Limitations	7
1.6 Objectives.....	8
1.7 Content of Dissertation and Summary of Papers	8
Chapter 2: A Review on Sulfate Attack Mechanisms and Test Methods for Evaluating Sulfate Resistance	11
2.1 Introduction.....	11
2.2 Sulfate Attack.....	11
2.3 Internal sulfate attack	13
2.4 Thaumasite attack	14
2.5 Physical Sulfate Attack	15
2.6 External Sulfate Attack	17
2.6.1 Mechanism of various sulfate types	17
2.6.1.1 Magnesium Sulfate	17
2.6.1.2 Sodium Sulfate	19
2.6.1.3 Calcium Sulfate.....	20
2.7 Testing Methods for Evaluating Sulfate Resistance	20
2.7.1 European Standard	21

2.7.1.1 CEN/TR 15697 (2008).....	21
2.7.2 U.S. Standards.....	21
2.7.2.1 ASTM C 452 (2015)	21
2.7.2.2 ASTM C 1012 (2012)	22
2.7.2.3 USBR 4908 (1986)	23
2.7.3 Canadian Standard	24
2.7.3.1 CSA A3004-C6; CSA A3004-C8	24
2.7.4 Additional Testing Methods	27
2.8 Summary	30
Chapter 3: Deterioration of Mortar Bars Using High-Calcium Fly Ash Immersed in Sodium Sulfate Solutions	31
3.1 Abstract	31
3.2 Introduction.....	32
3.3 research Significance	34
3.4 Materials and Experimental Procedures	34
3.4.1 Materials	34
3.4.2 Length Changes	36
3.4.3 Scanning Electron Microscopy	37
3.4.4 X-Ray Diffraction	38
3.5 Experimental Results and Discussion.....	39
3.5.1 Expansion and Visual Appearance	39
3.5.1.1 C1 Mixtures	39
3.5.1.2 C2 Mixtures	43
3.5.2 Microstructural changes.....	46
3.5.3 X-Ray diffraction	52
3.6 Summary and Conclusion	58
3.7 Future Research	58
Chapter 4: An Accelerated Method to Evaluate Mixtures Subjected to Chemical Sulfate Attack Part I: Induced Internal Cracking.....	59

4.1 Abstract	59
4.2 Introduction	60
4.3 Materials and Methods	62
4.3.1 Materials	62
4.3.2 Mortar Testing	64
4.3.2.1 Accelerated Test Method – Induced Cracking (IC)	65
4.3.3 Performance limits for ASTM C 1012	66
4.4 Results	67
4.4.1 5% Na ₂ SO ₄ Solution	67
4.4.2 0.89% Na ₂ SO ₄	72
4.6 Discussion	75
4.6.1 Implication of the Accelerated Method	75
4.6.1.1 Effect of maturity from drying regime	75
4.6.1.2 Effect of cement type and C ₃ A content	76
4.6.1.3 Effect of induce cracking on the pore structure	76
4.7 Conclusion	77
Chapter 5: An Accelerated Method to Evaluate Mixtures Subjected to Chemical Sulfate Attack Part II: Vacuum Impregnation	78
5.1 Abstract	78
5.2 Introduction	79
5.2.1 Sulfate Attack Mechanisms	80
5.2.2 Sulfate Attack Test Methods	82
5.3 Materials and Experimental Methods	83
5.3.1 Materials and Mixture Proportions	83
5.3.2 Methods	85
5.3.2.1 Sample preparation	85
5.3.2.2 ASTM C 1012	86
5.3.2.3 Accelerated Test Method – Vacuum Impregnation (VI)	86
5.3.2.4 Maturity testing	90

5.4 Results and discussion	91
5.4.1 Accelerated performance testing – Vacuum impregnation.....	91
5.4.1.2 Expansion and mass change in 5% Na ₂ SO ₄	91
5.4.1.3 Expansion and mass change in 0.89% Na ₂ SO ₄	96
5.4.1.4 Influence of curing	100
5.4.1.5 Mass change of mortar pre- and post-vacuum impregnation.....	105
5.6. Conclusion	106
Chapter 6: Sulfate Resistance of Concrete: Simultaneous Evaluation of an Accelerated Method and Outdoor Exposure Site	108
6.1 Abstract	108
6.2 Introduction.....	109
6.3 Experimental Methods	110
6.3.1 Materials	110
6.3.2 Mixture Proportions	112
6.3.3 Specimens, exposure conditions and tests conducted.....	116
6.3.3.1 Casting and curing	116
6.3.3.2 Outdoor exposure site and field investigation	116
6.3.3.2 Accelerated laboratory testing of concrete specimen exposed to sulfate	120
6.3.3.3 Removal of concrete surface.....	121
6.3.3.3 Non-solution renewal.....	123
6.3.3.4 Modified ASTM C 1012.....	123
6.4 Results and Discussion	124
6.4.1 Field performance of concrete specimens.....	124
6.4.2 Expansion Results	124
6.4.2 Performance of concrete specimens in controlled laboratory conditions ..	129
6.4.2.1 Accelerated performance test.....	129
6.4.2.2 Expansion results for surface removal specimens	131
6.4.2.3 Expansion results for non-solution renewal specimens	132

6.5 Conclusions.....	134
Chapter 7: Sulfate Resistance of Mortar Bars in Calcium, Magnesium, and Sodium Sulfate Using a Vacuum Impregnation Technique.....	137
7.1 Abstract	137
7.2 Introduction.....	138
7.2.1 Mechanisms of Sulfate Attack.....	139
7.2.1.1 Magnesium Sulfate	139
7.2.1.2 Sodium Sulfate	140
7.2.1.3 Calcium Sulfate.....	141
7.3 Research Significance.....	142
7.4 Experimental Program	142
7.4.1 Materials	142
7.4.2 Mortar Testing	144
7.4.2.1 Accelerated Mortar Bar Testing – Vacuum Impregnation	145
7.4.3 Exposure Conditions	146
7.4.4 Microstructural Charaterization	147
7.5 Results.....	148
7.5.1 ASTM C 1012 Expansion	148
7.5.2 Accelerated Sulfate Testing	151
7.5.2.1 Sodium Sulfate.....	151
7.5.2.2 Magnesium Sulfate	153
7.5.2.3 Calcium Sulfate.....	157
7.5.3 Microstructural Characterization	161
7.5.3.1 X-Ray Diffraction	161
7.5.3.2 Scanning Electron Microscope	163
7.6 Discussion	169
7.7 Conclusions.....	170
Chapter 8: Evaluation of the Effect of Gypsum Addition on the Sulfate Resistance of High-Calcium Fly Ash Mortars.....	172

8.1 Abstract	172
8.2 Introduction	173
8.3 Experimental Procedures	174
8.3.1 Cementitious materials and calcium sulfate	174
8.3.2 Mixture Proportions – Equivalent tricalcium aluminate content (C_3A_{eq}) ..	176
8.3.3 Methods of investigation.....	179
8.3.3.1 Mortar bar testing.....	180
8.3.3.2 Microstructural characterization	181
8.3.3.3 Isothermal Calorimetry	183
8.4 Results and Discussion	184
8.4.1 Mortar bar expansion	184
8.4.1.1 ASTM C 452.....	184
8.4.1.2 ASTM C 1012.....	185
8.5 Microstructural Evaluation	191
8.5.1 XRD Rietveld analysis.....	191
8.5.2 SEM/EDS.....	198
8.7 Heat of Hydration	200
8.8 Conclusion	203
Chapter 9: Conclusions and Recommendations	204
9.1 Conclusions.....	204
9.1.1 Accelerated Performance Testing	204
9.1.2 Field Performance	205
9.1.3 Mechanisms of Sulfate Attack.....	206
9.2 Future Work	207
Appendix A – Rietveld Analysis for Cementitious Materials	209
Appendix B –Procedure for Performing the Accelerated Vacuum Impregnation Technique	214
Appendix C – Calcium Sulfate Addition Sample Calculation	215
References	216

List of Tables

Table 2.1: Requirements for sulfate resistant cements in Canada (CSA A3001-13).....	26
Table 2.2: Review of external sulfate attack test methods.....	29
Table 3-1: Chemical compositions of cementitious materials (% by mass).....	35
Table 3-2: Phase compositions of cements (% by mass)*	35
Table 3-3: Mixture proportions (% by mass).....	37
Table 4-1: Chemical compositions of cementitious materials (%).....	63
Table 4-2: Mortar bar mixture proportions and exposure conditions	64
Table 4-3: Performance limits as per ACI 318 for expansion in ASTM C 1012	67
Table 5-1: Chemical composition of cementitious materials (Wt. %).....	84
Table 5-2: Mixture proportions.....	85
Table 6-1: Chemical composition of cements	112
Table 6-2: Chemical composition of supplementary cementitious materials	112
Table 6-3: Proportions of cementitious materials (% by mass)	114
Table 6-4: Mixture proportions by mass.....	114
Table 6-5: Fresh and hardened properties of concrete mixtures	115
Table 7-1 Chemical Composition of Cementitious Materials	143
Table 7-2 Mixtures and associated cation selected for study	144
Table 8-1: Mineralogical analysis of cementitious materials	175
Table 8-2: Phase composition analysis for cements (Bogue Calculation).....	175
Table 8-3: Bogue and measured Rietveld results for the C_3A content in cements*	178
Table 8-4: Mixture Proportions and equivalent C_3A contents of fly ash cement blends	179
Table 8-5: Quantitative Rietveld analysis of fly ash/cement blends with varying gypsum replacements prior to sulfate exposure	193

List of Figures

Figure 2-1: Chemical reactions between sulfate ions and cement hydrates (adapted from Chabreliie, 2010).....	12
Figure 2-2: XRD patterns of ettringite and thaumasite (adapted from Erlin and Stark, 1966)	15
Figure 3-1: Accelerated mortar bar expansion results for Type I mixtures exposed to 5 and 0.89% Na ₂ SO ₄	42
Figure 3-2: Visual appearance in mortar bars showing deterioration in: (a) C1 in 5% Na ₂ SO ₄ after 1 year; (b) C1 in 0.89% after 18 months; (c) C1 + 30%HC in 5% Na ₂ SO ₄ around 4 months; (d) C1 + 30%HC in 0.89% Na ₂ SO ₄ at 4 months	43
Figure 3-3: Accelerated mortar bar expansion results for Type I/II mixtures exposed to 5 and 0.89% Na ₂ SO ₄	45
Figure 3-4: Visual appearance of mortar bars showing deterioration in: (a) C2 mixture (5S) in 5% Na ₂ SO ₄ after 15 months; (b) C2 mixture in 0.89% Na ₂ SO ₄ after 15 months; (c) C2 + 30%HC in 5% Na ₂ SO ₄ around 4 months; and (d) C1 + 30%HC in 0.89% Na ₂ SO ₄ at 4 months	46
Figure 3-5: SE images coupled with EDS spectrums showing C1 mixture after 4 months exposure in: (a) 5% Na ₂ SO ₄ ; and (b) 0.89% Na ₂ SO ₄	48
Figure 3-6: SE image coupled with EDS spectrum showing significant ettringite formation in C1-30HC mixture after 4 months exposure in 5% Na ₂ SO ₄	49
Figure 3-7: SE images coupled with EDS showing C1-30HC mixture after 4 months exposure in 0.89% Na ₂ SO ₄	50
Figure 3-8: SE image of C1-30HC mixture after 4 months exposure in 0.89% Na ₂ SO ₄ ..	52
Figure 3-9: Rietveld analysis for control mixture (C1-Cont) after 1 year exposure in 5% Na ₂ SO ₄	53
Figure 3-10: XRD traces of control (C1-Cont) and binary (C1-30HC) mixtures.....	54
Figure 3-11: Rietveld results for mortars using cement C1 submerged in 5% Na ₂ SO ₄ after 56Days	56

Figure 3-12: Rietveld results for mortars using cement C1 submerged in 5% Na ₂ SO ₄ after 1yr	57
Figure 4-1: Curing cycle to introduce microcracks in the cement paste.....	66
Figure 4-2: 18 month expansion and mass change results using C1012 (top) and accelerated method (bottom) for Type I cement, 5% Na ₂ SO ₄	69
Figure 4-3: 18 month expansion and mass change results using C1012 (top) and accelerated method (bottom) for Type I/II cement, 5% Na ₂ SO ₄	71
Figure 4-4: 18 month expansion and mass change results using C1012 (top) and accelerated method (bottom) for Type V cement, 5% Na ₂ SO ₄	71
Figure 4-5 18 month expansion and mass change results using C1012 (top) and accelerated method (bottom) for Type I cement, 0.89% Na ₂ SO ₄	73
Figure 4-6 18 month expansion and mass change results using C1012 (top) and accelerated method (bottom) for Type I/II cement, 0.89% Na ₂ SO ₄	74
Figure 4-7: 18 month expansion and mass change results using C1012 (top) and accelerated method (bottom) for Type V cement, 0.89% Na ₂ SO ₄	75
Figure 5-2: a) Internal view of sample placement; b) external view of pressure tank used for vacuum impregnation	89
Figure 5-3: a) Vacuum Impregnation setup; and b) Pressure gauge illustrating the pressures experienced in the tanks	90
Figure 5-4: 18 month expansion and mass change results using C1012 (top) and accelerated method (bottom) for Type I (C1) cement, 5% Na ₂ SO ₄	93
Figure 5-5: Visual appearance of mortar bars showing deterioration in: (a) C1 tested using ASTM C 1012 in 5% after 1 year; (b) C1 tested using ASTM C 1012 in 0.89% after 18 months; (c) C1 tested using vacuum impregnation in 5% around 4 months; (d) C1 tested using vacuum impregnation in 0.89% sodium sulfate at 6-9 months	94
Figure 5-6: 18 month expansion and mass change results using C1012 (top) and accelerated method (bottom) for Type I/II (C2) cement, 5% Na ₂ SO ₄	95
Figure 5-7: 18 month expansion and mass change results using C1012 (top) and accelerated method (bottom) for Type V (C5) cement, 5% Na ₂ SO ₄	96

Figure 5-8: 18 month expansion and mass change results using C1012 (top) and accelerated method (bottom) for Type I (C1) cement, 0.89% Na ₂ SO ₄	98
Figure 5-9: 18 month expansion and mass change results using C1012 (top) and accelerated method (bottom) for Type I/II (C2) cement, 0.89% Na ₂ SO ₄	99
Figure 5-10: 18 month expansion and mass change results using C1012 (top) and accelerated method (bottom) for Type I/II (C2) cement, 0.89% Na ₂ SO ₄	100
Figure 5-11: Comparison of expansion results for mortar bars cured in in a moist curing room until a strength of 20 MPa (2,850 psi) was reached and cured following the ASTM C 1012 procedures	102
Figure 5-12: Comparison of expansion results for mortar bars moist cured for 28 days and cured following the ASTM C 1012 procedures	103
Figure 5-13: Comparison of expansion results for vacuum and non-vacuum impregnated mortar bars moist cured for 28 days	104
Figure 5-14: Comparison of expansion results for vacuum and non-vacuum impregnated mortar bars cured following the ASTM C 1012 procedures.....	105
Figure 5-15: Mass gain/loss of mortar bars pre- and post-vacuum impregnation	106
Figure 6-1: Outdoor sulfate exposure site located in Austin, TX	117
Figure 6-2: Updated outdoor exposure site using above-grade horse troughs for concrete exposure to sulfate environments.....	119
Figure 6-3: Orientation of concrete prisms placed in outdoor sulfate exposure site	120
Figure 6-4: a) Concrete sample holder; and b) Internal view of sample placement	121
Figure 6-5: a) Modified concrete prisms; and b) View of samples after surface removal	122
Figure 6-6: Expansion results for $w/cm = 0.40$ concrete prisms outdoor in field.....	127
Figure 6-8: Expansion of concrete prisms with $w/cm=0.40$ tested using Modified ASTM C 1012, DS, and OD accelerated method	130
Figure 6-9: Expansion of concrete prisms with $w/cm=0.55$ tested using Modified ASTM C 1012, DS, and OD accelerated method	131

Figure 6-10: Expansion results for concrete prisms subjected to surface removal of the surface	132
Figure 6-11: Expansion results for concrete prisms placed in sodium sulfate without replacing the solution during measurements.....	133
Figure 6-12: Visual degradation of concrete prisms placed in 5% Na ₂ SO ₄ with no solution replacement	134
Figure 7-2: Expansion results for ASTM C 150 cements investigated using ASTM C 1012 method.....	149
Figure 7-3: Expansion results for binary mixtures using ASTM C 1012 method	151
Figure 7-4: Expansion of control mixtures using accelerated method and submerged in sodium sulfate solution	152
Figure 7-5: Expansion of binary mixtures using accelerated method and submerged in sodium sulfate solution	153
Figure 7-6: Expansion of control mixtures using accelerated method and submerged in magnesium sulfate solution.....	155
Figure 7-7: Mortar bars of control mixtures exposed to magnesium sulfate solution (12 months); A) Type I; B) Type I/II; C) Type V	155
Figure 7-8: Expansion of binary mixtures using accelerated method and submerged in magnesium sulfate solution.....	156
Figure 7-9: Mortar bars of binary mixtures exposed to magnesium sulfate solution (12 months); A) Type I/II-20C; B) Type I/II-30C	157
Figure 7-10: Type I mixture stored after one year exposure in calcium sulfate	158
Figure 7-11: Expansion of control mixtures using accelerated method and submerged in calcium sulfate solution	159
Figure 7-12: Expansion of binary mixtures using accelerated method and submerged in calcium sulfate solution	160
Figure 7-13: Expansion of binary mixtures using accelerated method and submerged in calcium sulfate solution	160

Figure 7-14: XRD patterns from mortar bar samples in magnesium sulfate comparing the composition of the outer deteriorated surface (left) and the interior sample (right).....	162
Figure 7-15: XRD patterns from mortar bar samples in calcium sulfate comparing the composition of the outer deteriorated surface (left) and the interior sample (right).....	162
Table 7-3: Quantitative Rietveld analysis of cementitious mixtures (error $\pm 3\%$)	163
Figure 7-16: Severe ettringite formation for Type I mortar mixtures submerged in calcium sulfate (left) and magnesium sulfate (right)	164
Figure 7-17: SEM image of the surface of a mortar bar submerged in calcium sulfate .	165
Figure 7-18: Visual observation of cracks forming in Type I/II mixture in calcium sulfate (left) large deposits of gypsum surrounding aggregate evident in magnesium sulfate up to 400 microns into sample (right)	167
Figure 7-19: SEM images for type I/II control mixture in magnesium sulfate showing depth of sulfate penetration and various deleterious sulfate products formed.....	168
Figure 7-20: Time to failure (Failure indicated as $\geq 0.10\%$ expansion or fracture)	169
Figure 8-2: Length change for cements tested using ASTM C 452	185
Figure 8-3: Length change for blended C1/HC with varying gypsum dosages in 5% Na ₂ SO ₄ solution (% gypsum addition)	186
Figure 8-4: A) Mixture C1.0 after 28 days exposure; and B) Mixture C1.4 after 9 months exposure in 5% Na ₂ SO ₄ solution.....	187
Figure 8-5: Length change for blended C2/HC with varying gypsum dosages in 5% Na ₂ SO ₄ solution (% gypsum addition).....	188
Figure 8-6: Length change for blended C5/HC with varying gypsum dosages in 5% Na ₂ SO ₄ solution (% gypsum addition).....	190
Figure 8-7: Length change for blended OW/HC with varying gypsum dosages in 5% Na ₂ SO ₄ solution (% gypsum addition).....	191
Figure 8-8: Phase content of reaction products prior to sulfate exposure and different levels of SO ₃	194
Figure 8-9: Phase content of reaction products after six months exposure to 5% Na ₂ SO ₄ and different levels of SO ₃	195

Figure 8-10: Ettringite formation as a function of time in 5% Na ₂ SO ₄ in blended C1/HC mixture with varying gypsum dosages	197
Figure 8-11: Ettringite formation as a function of time in 5% Na ₂ SO ₄ in blended OW/HC mixture with varying gypsum dosages	198
Figure 8-12: EDS point analysis of left) outer edge portion of sample; and right) bulk paste matrix	199
Figure 8-13: BSE images of samples prior to exposure of A) C1.4 showing large deposits of ettringite near the edge; and B) C1.0 with abundant monosulfate	200
Figure 8-14: Heat flow curve for paste samples maintained at an isothermal temperature of 35 °C (95 °F)	201
Figure 8-14: XRD patterns of paste samples pre-and post-exposure to 5.0% Na ₂ SO ₄	202
A.1: X-Ray Diffraction Pattern and Rietveld Analysis for Type I Cement	209
A.2: X-Ray Diffraction Pattern and Rietveld Analysis for Type I/II Cement	210
A.3: X-Ray Diffraction Pattern and Rietveld Analysis for Type V Cement	211
A.4: X-Ray Diffraction Pattern and Rietveld Analysis for Class H Oil Well Cement ...	212
A.5: X-Ray Diffraction Pattern and Rietveld Analysis for High-Calcium Class C Fly Ash	213

Chapter 1: Introduction

1.1 BACKGROUND

Deterioration of concrete structures from external sources of sulfate has long been recognized and studied by many researchers across the world. Among the early investigations in the United States, the earliest were those reported by Bates, Phillips, and Wig of the National Bureau of Standards in 1913 (Bellport, 1968; Bates et al., 1913). Several structures were reported having significant damage and deterioration located along the water line in contact with the structures, as well as areas that were fully submerged and exposed to an evaporation front. Although the mechanisms of the chemical (and/or physical) attack was not clearly understood, it was believed that the primary cause of deterioration was the availability of sulfate ions from the groundwater near the structures.

Today, the mechanisms of sulfate attack are better understood by practitioners and researchers. Several comprehensive research programs across the globe were initiated including the Portland Cement Association (PCA), U.S. Army Corps of Engineers, U.S. Bureau of Reclamation, the National Bureau of Standards (NBS, now NIST), and the Canadian National Research Council (NRC) among others, to investigate long-term sulfate performance in both lab and field-scale testing. Several factors were investigated in determining the ones that were most influential on sulfate performance including water-cement ratio (w/c), cement content, cement types, chemical and mineral admixtures, and various types of coatings. The findings from these studies now recognize two types of attack that result from external sources of sulfate:

- **physical sulfate attack** in which, due to phase changes (crystallization and cyclic hydration/dehydration) in the penetrating sulfate solution,

internal stresses are developed in the concrete pores and ultimately lead to cracking and erosion of the concrete surface above the water line; and

- **chemical sulfate attack** where, the sulfate source leads to an alteration of hydration products in the cement paste that result in volumetric expansion in the hardened concrete, and associated cracking

The damage associated with physical sulfate attack has brought significant interest to many concrete researchers and practitioners due to the numerous litigation cases in Canada and in the western parts of the United States (Haynes, 2002). In many cases, however, attack by soluble sulfates on concrete can occur and lead to both physical and chemical damage simultaneously (Nehdi et al., 2014). Although both have been extensively studied, the latter form of attack remains a controversial and complex topic among concrete researchers and is the primary focus of this dissertation.

Fortunately, the number of reported field cases in which sulfate attack has been cited as the primary cause of deterioration for a concrete structure is rare. The production of commercially available sulfate resisting cements (SRC) as well as appropriate use of supplementary cementitious materials (SCMs) to combat this undesirable durability issue has led to major improvements in sulfate performance. Moreover, researchers and practitioners have made significant effort in providing guidelines and specification to determine sulfate concentrations, and recommended prescriptive measures for reducing the likelihood of attack for new concrete construction. The American Concrete Institute 201.2R *Guide to Durable Concrete* (2008) is the most commonly referred guideline for providing sulfate resistance in the United States. It is reported that increased resistance to chemical sulfate attack can be achieved from the use of appropriate cement type, SCM, low w/cm and good construction practice (ACI 201.2R, 2008; Skalny, 2002).

With significant pressure on the concrete industry to reduce its environmental impact, the production of more sustainable concrete mixtures through the use of SCMs, among others, has been an increasing trend over the last few decades. Additionally, the development of newly available binders such as calcium sulfoaluminate and alkali-activated binders, have been popular choices of materials for niche application. The use of these materials has led to a significant reduction in the amount of CO₂ emissions from cement production. However, many durability issues still arise when using these materials and raise many concerns, especially when exposed to aggressive sulfate environments. The complicated nature of this attack has led to ongoing effort to better understand the mechanisms and deterioration seen in field concrete structures in order to develop solutions that are more efficient. Furthermore, a reliable and robust test method is needed in order to determine appropriate preventive measures for these new materials.

1.2 SCIENTIFIC NETWORK

The research conducted in this dissertation was initially developed and funded by Lafarge, Inc. (now LafargeHolcim). Under the branch of LafargeHolcim, the Lafarge Research Center (LCR) in Lyon, France developed a scientific network in 2011 to build up a comprehensive database of commonly referenced concrete mixtures used in the field for building, housing, and small concrete structures of civil engineering. Various parameters were evaluated including mechanical strength and their durability resistance using both concrete performance tests and durability indicators (i.e., sulfate attack, freeze-thaw, salt scaling, etc.). The purpose of this study was to build up a scientific and technical network of academic and engineers to prepare the new performance-based approach. The network included several leading research laboratories across the world:

- Lafarge Research Center, Lyon, France
- Hunan University, Changsha, China
- Indian Institute of Technology Madras, Chennai, India
- University of New Brunswick, Fredericton, New Brunswick, Canada
- University of Texas at Austin, Austin, TX, USA

As a part of a larger research initiative, the latter two research laboratories initiated a comprehensive PhD program aimed at investigating and delving deeper into a specific durability mechanism. At the University of New Brunswick (UNB), Dr. Michael D.A. Thomas along with Yi Huang (PhD student) lead efforts in investigating salt scaling and deterioration of concrete through field and laboratory studies. Here at the University of Texas at Austin, under the supervision of Dr. Kevin J. Folliard, research efforts were aimed at studying external sulfate attack and investigate ways to improve and develop new accelerated sulfate test methods that accurately reflect concrete performance in the field.

1.3 PROBLEM DEFINITION

Sulfate attack of concrete continues to be one of the least understood forms of concrete deterioration in the world. Despite the few documented cases of sulfate attack in the field, there is debate and controversy on the mechanisms and the linkage between laboratory tests and field performance. This is especially the case when producing concrete using high amounts of supplementary cementitious materials and other natural pozzolans. For instance, concrete containing high-calcium fly ash have has typically been considered to perform very poorly in sulfate-rich environments (Dhole et al., 2011; Dhole, 2008; Drimalas, 2007; Shehata et al., 2008; Radomski, 2003; Tikalsky &

Carrasquillo, 1989). Furthermore, performance is typically made worse with increasing replacement of high-calcium fly ash when evaluated using the standardized test method ASTM C 1012; however, Drimalas (2007) reported observing an opposite trend in which performance was slightly improved with higher replacement of high-calcium fly ash for concrete specimens stored in an outdoor exposure site. On the other hand, high-calcium fly ash when used in combination with silica fume or Class F fly ashes in ternary mixtures at low water-cement ratios can be considered acceptable when appropriately evaluated using performance testing, such as ASTM C 1012 (Dhole et al., 2011). Dhole et al. (2013) reported that it was ultimately the nature of the reactive glassy phases present in high-calcium fly ashes that would dictate their sulfate performance.

The problem that exists today, however, is ASTM C 1012/1012M is the only test method available for concrete producers to determine sulfate resistance of concrete mixtures. The method involves using mortar bars that are submerged in a 5% sodium sulfate solution (33,800 ppm SO_4^{2-}) and monitored for their expansion periodically. Although this method is generally accepted across the world, there are many issues and arguments that arise among several researchers when using this method. Some of them include the following:

- There is an extensive period until significant results are obtained (up to 18 months) even with an extremely aggressive sulfate concentration (33,800 ppm SO_4^{2-}) especially when SCMs are being considered for use in these aggressive sulfate environments;
- There are several studies that have shown ASTM C 1012 does not always accurately replicate field performance;
- There is a large discrepancy in performance with poor reproducibility across labs;

- There are several sulfate types that are available in the field whereas ASTM C 1012 specifies only sodium sulfate as the testing solution (more recently, the use of magnesium sulfate has been allowed); and
- There is no accelerated test method that evaluates the sulfate performance of concrete specimens (ASTM C 1012 evaluates the sulfate performance of standard mortars)

This dissertation provides a multi-scale study (lab and field) of concrete, mortar, and paste specimens, and on their performance due to external sulfate attack. Several potential accelerated test methods are investigated using both concrete and mortar specimens. The findings present a newly accelerated method to evaluate the sulfate resistance of plain and blended portland cement systems.

1.4 RESEARCH OBJECTIVE

The primary objective of this research is to develop a concrete performance test method to determine sulfate resistance reliably, quickly and that comes to as close as possible to the mechanisms encountered in field concrete. In general, the research program requires a holistic approach that includes laboratory and field concrete exposed in various sulfate environments and conditions. Furthermore, determine the major influential factors that contribute to the mode of deterioration seen in external sulfate attack and achieve a greater understanding on the mechanisms and performance in the field. In order to accomplish this, the research was divided into the following two avenues:

The first component of the research is focused on the sulfate resistance of concrete and mortar bars under controlled laboratory environments. The performance of

paste, mortar and concrete mixtures containing varying amounts of supplementary cementitious materials, immersed in numerous sulfate types and concentrations are evaluated. Alternative accelerated test methods are proposed and compared to that of the conventional standardized test method, ASTM C 1012/1012M (2012). Additionally, the use of calcium sulfate (gypsum) used as an additive to mitigate the severity of sulfate attack in mixtures using high-calcium fly ash is investigated.

The second component of the research includes concrete samples placed outdoors under ambient conditions in Austin, TX. The site included similar sodium sulfate concentration evaluated indoors in the laboratory. The performance of these concretes is compared to the laboratory samples to achieve a greater understanding of the visual damage and deleterious products formed from external sulfate attack. These concrete samples are also used as a baseline to propose a concrete test method for determining sulfate resistance.

1.5 RESEARCH SCOPE AND LIMITATIONS

The research program is limited to the evaluation of standard mortar bars, concrete prisms, and hydrated cement paste samples exposed to multiple sulfate solutions. In order to successfully achieve an accelerated method that links well with field performance, significant effort at the beginning of the project was made to cast a wide range of concrete prisms and evaluate their sulfate performance. Although significant effort was made later to elucidate the underlying mechanisms of expansion and degradation for some these specimens, the initial scope was to investigate, develop, and propose an accelerated concrete test method for evaluating external sulfate resistance.

The research program initially included a testing program to evaluate several mitigation techniques for sulfate attack, especially those that are particularly relevant to the state of Texas. Particular emphasis was placed on issues related to high-calcium fly ashes used in sulfate environments.

1.6 OBJECTIVES

Based on the research scope presented, several key objectives were defined for this research:

- Evaluate and determine the effect of sulfate concentration, sulfate type (Na^+ , Mg^{2+} , Ca^{2+}), sulfate replenishing, curing, and specimen type (mortar versus concrete) on sulfate performance;
- Investigate, develop, and propose an accelerated method that uses either concrete and/or mortar specimens and obtain results in a timely manner (<6 months);
- Evaluate sulfate performance in both laboratory and field conditions;
- Validate the results by comparing field exposed concrete with laboratory specimens (field concrete and indoor concrete; indoor concrete and indoor mortar; accelerated and conventional testing); and
- Study the use of calcium sulfate (gypsum) as a mineral admixture to improve the sulfate performance of blended high-calcium fly ash mixtures

1.7 CONTENT OF DISSERTATION AND SUMMARY OF PAPERS

The dissertation was created and written following the outline and template provided by the Graduate School at the University of Texas at Austin; however, Chapters

3 through 8 present six potential manuscripts that have or will be submitted for publication as conference proceedings or refereed journal articles. The remainder of this dissertation is presented as described below.

In Chapter 2, a brief literature review on the types of sulfate attack and mechanisms, as well as test methods used to evaluate performance, is presented.

Chapter 3 presents the first manuscript, entitled “Deterioration of Mortar Bars Using High-Calcium Fly Ash Immersed in Sodium Sulfate Solutions.” This chapter evaluates the sulfate performance of mortars cast with different SCM contents immersed in two sodium sulfate solutions. The two sodium sulfate solutions selected were evaluated throughout the research program and thus, this manuscript was meant to set the tone of the dissertation by better understanding the mechanisms of sulfate attack involving these two sulfate concentrations.

Chapter 4 presents the first of a two part paper, entitled “An Accelerated Method to Evaluate Mixtures Subjected to Chemical Sulfate Attack Part I: Induced Internal Cracking.” The article was divided into two papers in order easily distinguish two proposed accelerated methods for evaluating sulfate resistance. In this chapter, mortar bars are subjected to a modified curing regime to introduce microcracks in the paste as a means to accelerate the ingress of sulfate and thus, accelerate the associated expansion mechanism of external sulfate attack.

Chapter 5 presents the second part of a two part paper, entitled “An Accelerated Method to Evaluate Mixtures Subjected to Chemical Sulfate Attack Part II: Vacuum Impregnation Technique.” This chapter presents an accelerated method although in this case, mortar bars are subjected to a high-vacuum pressure to drive sodium sulfate solution into the pores and initiate early reactivity between the sulfate ion and cement hydrates.

Chapter 6 presents a concrete study on external sulfate attack entitled “Sulfate Resistance of Concrete: Simultaneous Evaluation of an Accelerated Method and Outdoor Exposure Site.” This chapter presents a comprehensive research program initiated at the University of Texas at Austin to investigate the performance of concrete specimens in various sulfate environments. Field and laboratory studies are performed with the aim of developing a concrete performance test for evaluating sulfate resistance. The results presented primarily focus on the field performance. The research in this study is still ongoing to better link the performance between lab and field specimens, and propose a new standardized method.

Chapter 7 presents an article, entitled “Sulfate Resistance of Mortar Bars Exposed to Calcium, Magnesium, and Sodium Sulfate Using a Vacuum Impregnation Technique.” Whereas Chapter 5 evaluated the impact of vacuum impregnation using sodium sulfate, this chapter focuses on the performance of cementitious mixtures exposed to magnesium and calcium sulfate as the testing solution.

Chapter 8 presents an article, entitled “Evaluation of the Effect of Gypsum Addition on the Sulfate Resistance of High-Calcium Fly Ash Mortars.” The use of gypsum is investigated for improving the poor sulfate resistance of blended high-calcium fly ash mixtures. Four cements varying in tricalcium aluminate (C_3A) content and blended with a high-calcium fly ash and various gypsum additions are evaluated for their sulfate performance.

Lastly, Chapter 9 summarizes the key findings of this research program and provides some recommendation for future research related to sulfate testing and accelerated test methods.

Chapter 2: A Review on Sulfate Attack Mechanisms and Test Methods for Evaluating Sulfate Resistance

2.1 INTRODUCTION

This chapter presents a brief literature review on the existing theories and mechanisms associated with sulfate attack of concrete with emphasis on the chemical reaction between the hydrated cement paste and external sources of sulfate. Although the research described in this dissertation focuses exclusively on chemical sulfate attack, a brief discussion of other sulfate-related durability issues, such as internal sulfate attack and the thaumasite form of sulfate attack is provided.

First, the various forms of sulfate attack (chemical and physical) are discussed to review the state of the art regarding sulfate attack reactions, mechanisms, and effects of relevant concrete properties on sulfate resistance. This overview is not meant to cover all the information regarding sulfate attack but namely, reactions involving ettringite, gypsum and thaumasite formation. Following this, a brief overview of different test methods proposed by other researchers for determining sulfate resistance of cement based binders is presented. A review of more specific aspects of sulfate attack is presented in the subsequent chapters.

2.2 SULFATE ATTACK

Sulfate attack of concrete is a result of internal or external sources of sulfate ions (SO_4^{2-}) that involves several overlapping reactions with the cement paste and result in observable, measurable, or detected damage to the concrete structure. Many of the constituents of the cement paste such as calcium silicates, calcium aluminates, and calcium aluminate ferrites as well their hydrated products can be involved in these series

of chemical reaction (see Figure 2-1). The series of overlapping chemical reactions typically results in mainly three types of deleterious products formed after the concrete has hardened:

- Ettringite ($\text{Ca}_6(\text{Al,Fe})_2(\text{SO}_4)_3 \cdot \text{H}_2\text{O}$);
- Gypsum ($\text{CaSO}_4 \cdot 2\text{H}_2\text{O}$); and
- Thaumasite ($\text{CaCO}_3 \cdot \text{CaSO}_4 \cdot \text{CaSiO}_3 \cdot 15\text{H}_2\text{O}$)

The formations of the first two are the most common and well-known products of sulfate attack. They are the most reoccurring and studied of the three. Nonetheless, the thaumasite form of sulfate attack has been an increasing choice of topic among concrete researchers due to the increase production of portland limestone cements (PLCs) in Canada and parts of the United States. The following sections provide a brief description of the various sulfate-related durability problems

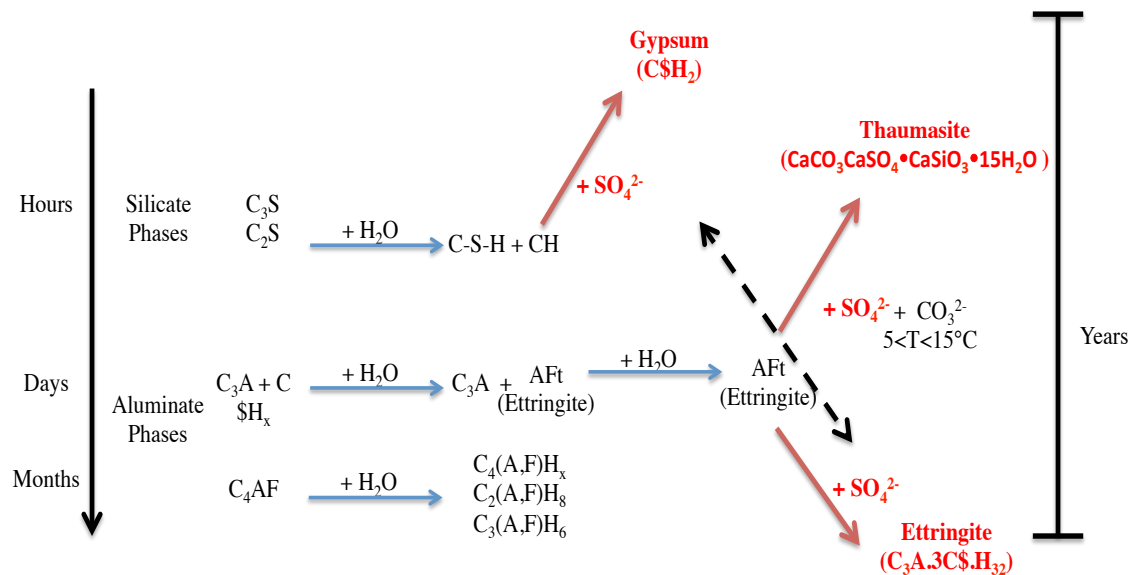


Figure 2-1: Chemical reactions between sulfate ions and cement hydrates (adapted from Chabrelie, 2010)

2.3 INTERNAL SULFATE ATTACK

One form of sulfate attack is “internal sulfate attack” which may also include “delayed ettringite formation” (DEF). DEF is a form of premature deterioration in concrete elements that are typically subjected to high curing temperatures. When the internal concrete temperature reaches a critical temperature, typically above 70°C (158°F), ettringite is typically decomposed and the sulfate ions released get trapped in the inner C-S-H of the cement paste (Folliard et al., 2005; Drimalas, 2004). These trapped sulfates are released by the C-S-H once a drop of the pH occurs in the concrete. This results in the formation of secondary ettringite in the hardened concrete from the reaction between the sulfates and monosulfate present during the initial stage of hydration. Consequently, the reaction results in significant expansion and stress development in the concrete.

The sources of sulfate present internally in the concrete (gypsum in binder, aggregate, and chemical and mineral admixtures) (Collepari, 2003; Taylor et al., 2001) contribute to this form of deterioration and pose higher risk when subjected to elevated temperatures. Many precast concrete elements that are steam-cured at temperatures in excess of 70°C (158°F), can be susceptible to damage from DEF; however, DEF can also occur in cast-in-place concrete without heat curing if the temperature rise, due to the heat of hydration of the cement, results in internal concrete temperatures in excess of 70°C (158°F), (Thomas, 1998).

The associated trigger of DEF from the reduction in the pH in concrete pore solutions can occur from a number of items such as leaching or alkali silica reaction (ASR). Delayed ettringite formation is often associated with alkali silica reaction in the field structures as ASR results in a reduction of the pH in the pore solution (Folliard et

al., 2006); however, there have been reported cases of DEF occurring in the field with no evidence of ASR in the concrete structures (Thomas et al., 2008).

2.4 THAUMASITE ATTACK

Thaumasite formation ($\text{CaCO}_3 \cdot \text{CaSO}_4 \cdot \text{CaSiO}_3 \cdot 15\text{H}_2\text{O}$) occurs in concrete due to the interaction between C-S-H, carbonate ions (CO_2 or CO_3^{2-}) and the ingress of external sulfates from soils or groundwater. Typically, this form of sulfate attack occurs at low temperatures (5-10 °C [40-50 °F]); however, it has been reported at temperatures in excess of 20°C (68 °F) although the kinetics for thaumasite formation is significantly slowed down (Irassar et al., 2003).

Thaumasite formation has often been confused with ettringite formation due to their similar chemical and crystalline composition. Figure 2-2 shows diffraction patterns for ettringite and thaumasite. However, contrary to the crystal growth formation of ettringite commonly associated with external sulfate attack, thaumasite typically leads to a complete loss of cohesion and binding properties of the concrete from the direct reaction with the C-S-H of the cement paste; this reaction can effectively turn the concrete into a mushy substance with no form at all.

Currently, there is significant concern in the concrete industry from the thaumasite form of sulfate attack due to production of portland limestone cements (PLCs) in many parts of the country. The presence of limestone is known to increase the likelihood of the thaumasite form of external sulfate attack; however, concrete made with portland limestone cement has exhibited similar overall sulfate resistance to portland cements (Hossack, 2010).

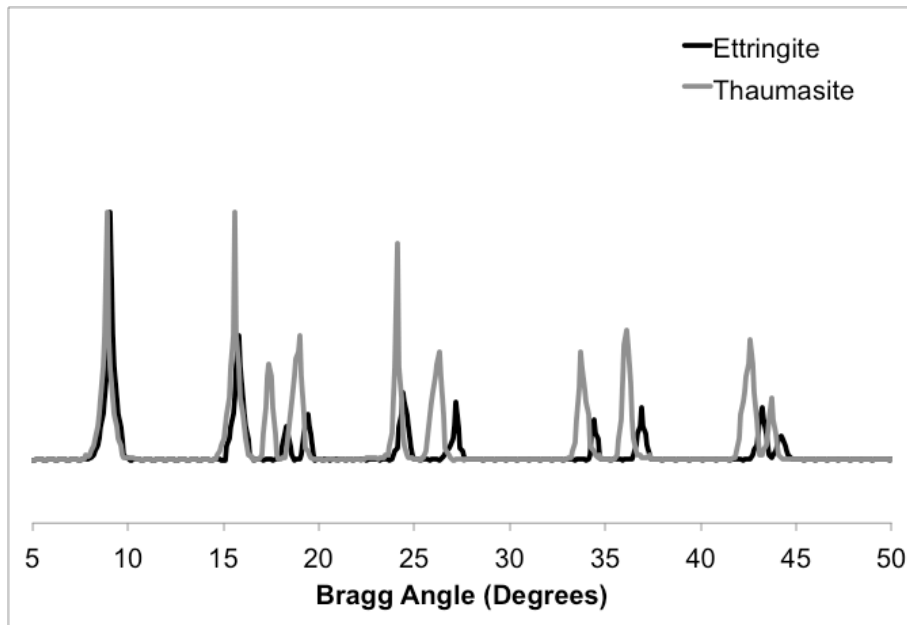


Figure 2-2: XRD patterns of ettringite and thaumasite (adapted from Erlin and Stark, 1966)

2.5 PHYSICAL SULFATE ATTACK

Physical sulfate attack (also commonly known as salt attack) is a common form of deterioration typically found in field structures that are partially buried in sulfate containing soils and exposed to an evaporation front. This form of sulfate attack results in no alteration of the cement hydrates (i.e., no formation of gypsum or ettringite) but rather only physical damage associated from salt crystallization in nanometer size concrete pores. In an initial study by the Portland Cement Association (PCA) investigating the long-term durability of concrete specimens stored in outdoor environments in Sacramento, California, it was reported that the distress observed in concrete beams partially submerged in soil containing 10% sodium sulfate was attributed to external, chemical sulfate attack (Stark, 1989). However, in 2002, a second bulletin on the PCA site determined that damage on the concrete beams was only occurring above the soil level, and that very little damage was reported below ground. Stark (2002)

proposed that the main mechanism of distress was a result of physical sulfate attack. As a result, the ACI 201.2R (2008) *Guide to Durable Concrete* recently recognized physical salt attack as a newly emerging form of concrete deterioration.

A common form of physical salt attack in concrete occurs when sodium sulfate penetrates into concrete; however, this form of deterioration can occur with any kind of salt not only sulfate salts (e.g., sodium carbonate and sodium chloride). Similarly to chemical sulfate attack, dissolved salt ions ingress through the concrete pores. Subsequently, capillary rise of the salt ions from diffusion through the concrete matrix leads to an increased concentration at the exposed surface of the concrete (Haynes et al., 1996). Evaporation from the exposed surface causes the salt ion concentration to increase as more salt ions precipitate from the evaporating water molecules (Haynes et al. 1996). Recent work by Haynes (2008) found that as the relative humidity decreases, the height of the evaporation front also decreases. As the salt ions continue to build up in the concrete pores at the surface and the temperature cycles, the salt ions change phases, thus resulting in a volume change. Crystallization from a supersaturated thenardite (Na_2SO_4) solution to mirabilite ($\text{Na}_2\text{SO}_4 \cdot 10\text{H}_2\text{O}$) conversion is triggered by a temperature drop and/or relative humidity increase, resulting in the sodium sulfate ion absorbing ten water molecules and thus increasing by 314% in volume (Hime et al., 2001). With repeated action of wetting and drying as well as temperature cycles, the concrete can suffer from significant surface distress and erosion. According to Scherer (2004), during wetting and drying cycles, it is the crystallization pressure from the formation of mirabilite during wetting that does most of the damage.

2.6 EXTERNAL SULFATE ATTACK

Typically, external sources of sulfate diffuse through the concrete pores, setting off a series of expansive reactions of sulfate ions with aluminum containing phases and/or calcium hydroxide to form ettringite or gypsum, respectively. Both of these reaction products are believed to damage concrete by an increase in the overall solid volume of the cement paste and thus encourage further penetration of sulfate ions into the concrete from significant cracking (Messad, et. al, 2012; Skalny et al., 2002). However, different types of manifestation during sulfate attack have been found which lead to concrete deterioration, including (1) expansion caused by gypsum and ettringite formation, (2) progressive loss of mass and strength, and (3) decalcification of cement paste in which softening of cement paste takes place without significant expansion (Mehta & Monteiro, 2006; Gollop & Taylor, 1992; 1995; Dhole, 2008).

2.6.1 Mechanism of various sulfate types

Many of the deteriorations listed previously are dictated by type of sulfates present in the soil, groundwater, and/or seawater. The most common types of sulfates are magnesium, sodium, and calcium sulfate, each of them with different properties and different ways of interacting with the exposed concrete. The following section highlights some of the mechanisms involving these types of sulfates.

2.6.1.1 Magnesium Sulfate

Magnesium sulfate is commonly present in soils and groundwater, as well as in many seawaters and brackish water. Depending on the concentration of Mg^{2+} in solution, magnesium sulfate is often considered by several researchers as the most aggressive of all the sulfate salts (Mehta & Monteiro, 2006; Skalny, et.al., 2002), especially in blended

portland cement-based concrete (Bonen; 1992; Dehwah, 2007). Through interaction with the already stable cement paste, magnesium sulfate will react with portlandite [CH] to form brucite [Mg(OH)₂]. Brucite has a very low solubility giving a low pH value (≈ 10.5) in saturated solution. In order to balance this pH in the pore solution, calcium is released from the C-S-H in the cement paste. Additionally, from further availability of magnesium and sulfate, these can react with the C-S-H gel to form gypsum, brucite, silica gel, and water. As a final step, during the advanced stage of attack, the brucite and silica gel can react slowly to yield magnesium silicate hydrates (M-S-H), having no binding properties.

Kunther et al. (2013) reported magnesium to be more severe at the surface of mortar, especially mixtures incorporating blends of supplementary cementitious materials such as granulated blast furnace slag (GGBFS). He observed more deterioration in mortar bars immersed in magnesium sulfate solutions than sodium sulfate solutions; however, the associated expansion was not always observed in the mortar bars and depended on the binder being tested. Moreover, the samples immersed in solutions containing different cations showed less expansion and surface deterioration than samples immersed in a purely magnesium sulfate solution.

Gollop et al. (1992; 1995) reported similar distress in sulfate attack of paste samples submerged in sodium and magnesium sulfate solutions, with the latter solution causing more distress due to the role of Mg²⁺ ions in forming M-S-H, thus decalcifying the C-S-H phases resulting in loss of binding properties. This ultimately may reduce the overall strength capacity of the structure resulting in reduced service life. This form of chemical attack is the primary reason several researchers consider the magnesium cation of sulfate attack the most aggressive.

2.6.1.2 Sodium Sulfate

It is well known that attack from solutions containing sodium sulfate as the primary associated cation can lead to several forms deleterious expansive products including ettringite and gypsum. These are generally formed from the availability of several alumina-bearing compounds present in the cement and/or supplementary cementitious materials (SCMs). In many cases, the resulting deterioration from sulfate attack is highly influenced by the initial stable phases present in the concrete. For example, the availability of leftover tricalcium aluminate [C_3A] following hydration can be made available to react with external sources of sulfate. Moreover, as the availability of gypsum decreases, ettringite [AFt] is converted to monosulfate [AFm], liberating gypsum to react with unreacted C_3A , forming additional monosulfate (Black et al., 2006); which is also available to react with external sulfates forming ettringite in the hardened state of concrete. As a result, this leads to the development of lower C_3A cement for sulfate resistance.

The formation of gypsum to cause enough volumetric expansion and induce stresses capable of severe cracking of the hardened paste has been a controversial debate, with many studies demonstrating a “mushy” appearance and loss in strength from the formation of gypsum. Despite this, several researchers (Bellmann et al., 2006; Tian & Cohen, 2000; Santhanam et al., 2003) have shown that the expansion due to the formation of gypsum can develop. Through the evaluation of physical properties and microstructural characterization, gypsum was almost always associated as a result from sulfate attack. In general, sulfate attack from sodium sulfate is typically attributed from the formation of both ettringite and gypsum with no consensus on the main mechanisms.

In very severe cases, sodium sulfate can decompose the hydrated C-S-H phases of alite (C_3S) and belite (C_2S). The continued reaction of CH with sulfate to form gypsum

results in a reduction in the pH of the pore solution and thus, Ca^{2+} ions are removed from the C-S-H phases in order to balance the system. This has shown to lead to a reduction in the CaO/SiO₂ ratio and may be accompanied with a loss of binding properties (Skalny et al., 2002).

2.6.1.3 Calcium Sulfate

Calcium sulfate (gypsum) is typically referred to as the least aggressive when compared to magnesium and sodium sulfate (Skalny et al., 2002). The primary product that results from the chemical reaction between calcium sulfate and the cement paste is ettringite through the reaction with monosulfate. Although this source of sulfate is frequently found in the field (Drimalas, 2007; Bellmann, et.al., 2012; Leemann & Loser, 2011), the amount of sulfate that is able to penetrate the concrete is limited due to the low solubility of around 1.45g/L of SO₄ at 20 °C (68 °F) (Skalny et al., 2002). In addition, no decalcification of the C-S-H phase is associated with this form of reaction as the salt itself provides the Ca^{2+} ions needed. Despite this, Drimalas (2007) and Dhole (2008) have reported significant damage in concrete placed in gypsiferous soils; however, there are very few other researchers who report on this. Further research is needed in order to confirm no other possible mechanisms exist related to calcium sulfate.

2.7 TESTING METHODS FOR EVALUATING SULFATE RESISTANCE

This section provides a review of current test standards or methods proposed by many researchers for testing the performance of plain and blended portland cements in sulfate environments. Specifically, standards from Europe, United States, and Canada are included in this section. In addition, minor references to other standards and methods developed or investigated are included at the end of the section.

2.7.1 European Standard

2.7.1.1 CEN/TR 15697 (2008)

Currently, the European Committee for Standardization (CEN) does not recommend a standard test method for evaluating the sulfate resistance of a portland or blended cement. In spite of several European countries previously having had test methods, the development of a European Standards (EN) for sulfate resisting cements has been complicated by national difference in the types of cement that are recognized to have sulfate resisting properties. However, under the terms of EU Mandate 114, committee CEN/TC 51 directed research towards the development of a performance tests for sulfate resistance. In 2008, CEN published a technical report, CEN/TR 15697:2008 “Performance Testing for Sulfate Resistance – State of the art report,” outlining the current status concerning sulfate resistance. The report draws on key material from over 129 relevant papers and reports that were entered into an Access Database. A wealth of information is provided comparing the advantages and disadvantages of different test specimen types (paste, mortar or concrete), different exposure conditions and different techniques used to assess specimen deterioration. This report is a vital step into assessing the different sulfate resistance techniques employed and their possible influence on the performance of different cements or blends of cement with pozzolans or slags.

2.7.2 U.S. Standards

2.7.2.1 ASTM C 452 (2015)

ASTM C 452 involves accelerating the expansion of mortar bars by adding gypsum to a portland cement prior to mixing. Sufficient gypsum is added to the dry portland cement so that the mixture has a sulfur trioxide (SO₃) content of 7 percent, based

on mass of mixture. The additional gypsum allows for ettringite formation to occur internally without the need for external sulfates to enter the specimen. The mortar bars have dimensions of 25 x 25 x 285 mm (1 x 1 x 11.25 in) with stainless steel gauge studs embedded into the ends for length measurements. After casting the mortar bars, they are cured in their molds for 22 to 23 hours, demolded and their lengths measured, before they are immersed in deionized water, and their 14-day expansion measured.

ASTM C 452 is rapid and does differentiate between high C_3A and low C_3A portland cement. However, it is not considered applicable for blended cements. The tests conditions of ASTM C 452 do not simulate field exposure of concrete to sulfate, which involves the ingress of sulfates in to concrete. Therefore, this method is primarily used to establish that a sulfate resisting portland cement meets the performance requirement of specification ASTM C 150 (2016)

2.7.2.2 ASTM C 1012 (2012)

Despite its controversial applicability, ASTM C 1012 (2008) has been used by many researchers to evaluate the sulfate resistance of cement based materials. This method is typically preferred over other methods not because it is deemed to be the best test or the test most linked to field performance, but rather because it is the test most commonly used, specified, and included in national and international guidelines. As per ASTM C 1012, a standard mortar mixture is cast with 1 part portland cement to 2.75 parts sand. For the control portland cement mixture, the w/cm is fixed at 0.485, and for mixtures incorporating SCMs, water is added to obtain a flow of ± 5 of that of the control portland cement mixture. The mortar bars have dimensions of 25 x 25 x 285mm (1 x 1 x 11.25 in) with stainless steel gauge studs embedded into the ends for length measurements. Nine 50 mm (2 in) mortar cubes are also cast from each mixture. After

casting the mortar bars and cubes, they are sealed and placed into a $35\text{ }^{\circ}\text{C} \pm 3\text{ }^{\circ}\text{C}$ ($95\text{ }^{\circ}\text{F} \pm 5\text{ }^{\circ}\text{F}$) water bath for $23\text{ hr} \pm 0.5\text{ hr}$. After curing, the specimens are demolded and two of the cubes are tested for strength. Once an average compressive strength of two cubes has reached 20 MPa (2,850 psi), the bars are then placed into a 5% sodium sulfate solution (33,800 ppm SO_4^{2-}). Otherwise, the bars and cubes are placed into a saturated limewater bath until strength is achieved. Upon immersion in the sulfate solution, expansion measurements are taken every 1, 2, 3, 4, 8, 13, 15 weeks and 4, 6, 9, 12, 18 months thereafter.

Although ASTM C 1012 is a much longer tests as compared to ASTM C 452, it can be applicable to blended cements, which makes it a highly effective test. ASTM C 1012 clearly simulates more closely to field exposure conditions than does ASTM C 452, in that the sources of sulfate ions are external and follow the diffusion-reaction phenomenon reported by Gollop & Taylor (1995). Therefore, this test method provides the best means of assessing the sulfate resistance of mortars made using portland cement, blends of portland cement with pozzolans or slags, and blended hydraulic cements.

2.7.2.3 USBR 4908 (1986)

The United States Bureau of Reclamation (USBR) recommends the standardized test, USBR 4908, “Procedure for length Change of Hardened Concrete Exposed to Alkali Sulfate” for researchers interested in better representing service conditions by testing actual concrete specimens. In this method, 150 x 300 mm (6 x 12 in) concrete cylinders are submerged in a sulfate solution after the specimens have reached a certain strength similar to ASTM C 1012. Additionally, this method is applicable to concrete mixes

containing portland cements, blended cements, or blends of cement and mineral admixtures.

USBR 4908 provides users three different approaches in which the specimens can be exposed to the sulfate solution:

- Method A involves continuously submerging the cylinders in a 2.1% sodium sulfate solution;
- Method B involves continuously submerging in a 10% sodium sulfate solution; and
- Method C is a wetting/drying test where the cylinders are alternately immersed for 16 hr in a 2.1% sodium sulfate solution and then dried for 8 hours under a forced air at 54 °C (130 °F).

USBR 4908 test requires at least 1 to 2 years before any significant results can be obtained. Unfortunately, there are no widely accepted expansion or mass change limits that go along with these procedures. However, USBR 4908 has the flexibility to evaluate several effects on the sulfate resistance of concrete including, permeability, mineral and chemical admixtures, and other mix design alternatives as well as various curing procedures (Stephens & Carrasquillo, 1999).

2.7.3 Canadian Standard

2.7.3.1 CSA A3004-C6; CSA A3004-C8

In Canada, concrete exposed to sulfate environments must meet the requirements of Canadian Standards Association (CSA) A23.1-09 (CSA, 2009), which imposes

maximum limits on the water-to-cementitious materials ratio (w/cm) and permits only sulfate-resistant portland cement and/or suitable blends of portland cement with supplementary cementitious materials (SCMs). Similarly to ASTM C 150 (2016), CSA A3001 (2013) imposes limits on C_3A content and expansion limits on sulfate resistant cements. Additionally, expansion limits are also included for the use of blended portland cements in sulfate environments. The requirements are summarized in Table 2-1.

CSA provides two standards for the performance of portland cements in sulfate environments that are essentially identical to the ASTM C 452 and ASTM C 1012 methods. CSA A3004-C6 “Test Method for Determination of Mortar Bar Expansion Due to External Sulphate” is primarily used to establish a sulfate resisting portland cements in which mortar bars must pass a 14-day expansion limit; whereas, CSA A3004-C8 “Test Method for Determination of Sulphate Resistance of Mortar Bars Exposed to Sulphate Solution” is used to test mortars of blended portland cements stored in a 5% sodium sulfate solution.

More recently, portland limestone cements, which may contain up to 15% limestone, have been introduced into Canada and parts of the United States. These cements are now allowed for use in concrete exposed to sulfates provided that a sufficient level of SCM to meet the prescriptive and performance requirements using a modified version of the CSA A3004-C8 in which the test procedure is ran at a lower temperature (5 °C versus 23 °C). This new procedure is proposed as a means of predicting the risk of

the thaumasite form of sulfate attack in concretes containing limestone cements (Barcelo et. al., 2014).

Table 2.1: Requirements for sulfate resistant cements in Canada (CSA A3001-13)

Cement Type	Types permitted	Requirements
Portland cement (PC)	MS or HS	<ul style="list-style-type: none"> Limits on C₃A content 14-day expansion limit for mortar bars containing gypsum (7% SO₄ by mass of cement)
Blended Portland cement containing SCM ¹	MSb or HSb	<ul style="list-style-type: none"> 6-month² expansion limit (0.10% for MSb and 0.05% for HSb) for mortar bars in 5% Na₂SO₄ at 23°C
Portland limestone cement (PLC)	PLC is not permitted in sulfate exposure classes unless it is used in combination with sufficient levels of SCM to meet the requirements shown below	
Blended Portland limestone cement containing SCM ¹	MSLb or HSLb	<ul style="list-style-type: none"> 6-month² expansion limit (0.10% for MSLb and 0.05% for HSLb) for mortar bars in 5% Na₂SO₄ at 23°C 18-month expansion limit³ (0.10% for MSLb and HSLb) for mortar bars in 5% Na₂SO₄ at 5°C Minimum SCM replacement levels of 25% Type F fly ash, 40% slag or 15% metakaolin, or of combinations of 5% silica fume with 20% Type F fly ash or 5% silica fume with 25% slag
<p>¹SCM can be combined with either PC or PLC at the concrete mixture provided it is demonstrated that such combinations meet the requirements for blended PC or blended PLC.</p> <p>²Mortar bars that exceed the 6-month expansion limit of 0.05% for Types HSb and HSLb cements are still deemed to pass provided that the 12-month expansion does not exceed 0.10%</p> <p>³If the expansion between 12 months and 18 months exceeds 0.03% the test must be continued until 24 months and the 24-month expansion is not permitted to exceed 0.10%</p>		

2.7.4 Additional Testing Methods

Many of the test methods used for determining sulfate resistance involve the immersion of mortar samples in a test solution. Others perform continuous wetting and drying cycles in order to simulate the effects of damage from salt crystallization. Additionally, many researchers use different sulfate solutions and concentrations as well as a number of various physical parameters to qualify sulfate resistance of cementitious materials. For example, Koch (1960) and Locher (1956) determined the sulfate resistance of mortar by the relative decrease in flexural strength between samples placed in sodium sulfate and companion samples stored deionized water after 28 days of exposure. The Chinese national standard GB/T 2420 (1981) followed a similar approach but using smaller mortar bars (10 x 10 x 60 mm [0.4 x 0.4 x 2.25 in]) and thus increasing the volume of sulfate solution to volume of mortar bars. However, the method exhibited high variability in flexural strength performance. On the other hand, other methods determine sulfate resistance by monitoring the expansion of samples placed in a specified sulfate solution. External sulfate attack using linear expansion measurements, such as the ASTM C 1012 (2012) test method, has been studied since 1930s by Tuthill (1936) who noticed the deterioration in concrete structures caused by sulfate bearing soils along the Colorado River and recommended appropriate pozzolanic replacement as one of the methods to reduce the damage potential (Bonakdar & Mobasher, 2010). Typically, these methods replenish the testing solution periodically whereas other test methods use the same test solution throughout the duration of the test. Mehta and Gjorv (1974) used a circulating solution in which the pH is kept constant by manual titration with H₂SO₄. Mehta (1975) then automated the aforementioned procedure by means of a continuous titration with H₂SO₄, while monitoring the pH using a pH controller. According to Mehta (1975), the procedure details were found to be adequate to yield reproducible results.

Brown (1981) used a similar experimental setup reporting that controlling the pH of the sulfate solution more accurately represents field conditions and leads to a much faster expansion of mortar bars than a typical non-controlled pH sulfate solution.

Ferraris et al. (2005) studied the specimen size effect showing that smaller size prisms (10 x 10 x 100 mm [0.4 x 0.4 x 1.5 in]) increased the expansion rate, enhancing the test results in much less time than the standard 25 x 25 x 285 mm (1 x 1 x 11.25 in) specimens. However, the test specimens were cast using paste samples, which leads to even greater disconnect from field conditions. Ferraris et al. (1997) also tested cylinders with constant length of 152 mm (6 in) and varying diameters (25, 50, 75 mm [1, 2, 3 in]) exposed to sulfate solutions from the sides concluding that the expansion from external sulfate attack is mostly governed by ionic diffusion and could hence be accelerated using smaller specimens (Bonakdar & Mobasher, 2010). A brief summary of these test methods and standards, including the test methods discussed in the previous sections, are provided in Table 2-2.

Table 2.2: Review of external sulfate attack test methods

Standard or reference	Specimens		Initial Curing	Subsequent storage condition	Property determined								
	Compositions	Size (mm)											
ASTM C 452; CSA A3004-C6	Cement/sand (c/s) = 1/2.75 w/c = 0.485 or 0.460 for air entraining cements ^{A,B}	25 x 25 x 285 (nominal gage length 250)	Moist closet for 22-23 h; followed by in water for ≥ 30 min, at $23^{\circ}\text{C} \pm 1.7^{\circ}\text{C}$	In fresh water at $23^{\circ}\text{C} \pm 1.7^{\circ}\text{C}$; replensih the water every 7 days	Length change compared to nominal gage length. Measure after 14 days								
ASTM C 1012 CSA A3004-C8	Cement/sand (c/s) = 1/2.75 w/c = 0.485 or 0.460 for air entraining cements ^C	25 x 25 x 285 (nominal gage length 250) ^D	seal in mold which is immersed in water at $35^{\circ}\text{C} \pm 3^{\circ}\text{C}$, 23.5h ± 30 min; followed with in lime water at $23^{\circ}\text{C} \pm 1.7^{\circ}\text{C}$ ^E	in 0.352 M (5.0%) sodium solfuate solution at $23^{\circ}\text{C} \pm 1.7^{\circ}\text{C}$, pH = 6.0 - 8.0. Volume of solution to mortar 4/1 ^F	Length change compared to nominal gage length. Mass change compared to nominal mass. Measuring intervals veying according to length change rate.								
USBR 4908		150 x 300 concrete cylinder		Method A: immersion in a 14 g/l Na ₂ SO ₄ solution; Method B: immersion in a 68 g/l Na ₂ SO ₄ solution; Method C: alternate immersion in a 14 g/l Na ₂ SO ₄ solution for 16 h and forced air drying for 8 h at 54 °C	Length change compared to nominal gage length. Mass change compared to nominal mass. Measuring intervals veying according to length change rate.								
Australian Standard AS 2350.14	w/c = 0.5	15 x 40 x 160 (nominal gage length 130)	2-day in sealed mold and 5-day in lime water at $23^{\circ}\text{C} \pm 1.7^{\circ}\text{C}$	In 0.352 M (5.0%) sodium solfuate solution at $23^{\circ}\text{C} \pm 1.7^{\circ}\text{C}$, pH = 6.0 - 8.0. Volume of solution to mortar 4/1	Length change compared to nominal gage length. Up to 16 week continual monitoring.								
Kock (1960)	c/s = 1/3 w/c = 0.60	15 x 40 x 160 (nominal gage length 130)	1-day in mold then, in water at 20°C till 21-day	in 0.704 M (10%) sodium sulfate solution at 20°C	flexure strength								
Locher (1956)	c/s = 1/3 w/c = 0.60	15 x 40 x 160 (nominal gage length 130)	1-day in mold then, in water at 20°C till 21-day	in 0.310 M (4.4%) sodium sulfate solution at 20°C	flexure strength								
Smolczyk (1972)	c/s = 1/3 w/c = 0.60	10 x 40 x 160	1-day in mold then, in water at 20°C till 14-day	in 0.310 M (4.4%) sodium sulfate solution at 20°C	expansion								
German (Frearson & Higgins 1995)	c/s = 1/3 w/c = 0.50	10 x 40 x 160	1-day in mold, then in water at 20°C till 14-day	in 0.1666 M (2.366%) sodium sulfate solution at 20°C	expansion								
Frearson & Higgins (1995)	<table border="1" style="display: inline-table; vertical-align: middle;"><tr><td>c/s</td><td>w/c</td></tr><tr><td>1/3</td><td>0.60</td></tr><tr><td>1/2</td><td>0.50</td></tr><tr><td>1/3</td><td>0.45</td></tr></table>	c/s	w/c	1/3	0.60	1/2	0.50	1/3	0.45	10 x 40 x 160	1-day in mold, then in water at 20°C till 14-day	in 0.310 M (4.4%) sodium sulfate solution at 20°C	expansion
c/s	w/c												
1/3	0.60												
1/2	0.50												
1/3	0.45												
Wolochow (1952a)	C/s = 1/4 standard consistency	25 x 25 x 285	2-day in mold at 23°C , then in water at 23°C till 7-day	in 0.352 M (5.0%) sodium solfuate solution at $23^{\circ}\text{C} \pm 1.7^{\circ}\text{C}$	expansion								
Kollek & Lumley (1990)	c/s = 1/4 w/c = 0.60	25 x 25 x 285	1-day in mold, then in water at 20°C till 7-day	various: 0.042, 0.084, 0.169, 0.296 (0.6, 1.2, 2.4, 4.2%), at 20°C	expansion								
French (Frearson & Higgins 1995)	c/s = 1/4 w/c = 0.50	20 x 20 x 160	1-day in mold, then in water at 20°C till 28-day	in 0.1666 M (2.366%) sodium sulfate solution at 20°C	expansion								
GB 749	c/s = 1/3.50; standard consistency	10 x 10`x 30	1 day in covered mold at 20°C , then 14 days water curing	sulfate solution (concentration not specified) $20 \pm 5^{\circ}\text{C}$	relative flexure strength after 6 months ⁶								
GB 2420	c/s = 1/2.50 w/c = 0.50	10 x 10`x 60	24 \pm 2h in mold at $20 \pm 3^{\circ}\text{C}$, then in water at 50°C for 7-days	in 3.0% sodium sulfate solution, 20°C . Volume of solution to mortar > 30:1	relative flexural strength after 28 days ⁶								

2.8 SUMMARY

There are many test methods available to determine the resistance of concrete to sulfate attack. Different studies use various parameters (expansion, strength loss, etc.) to evaluate sulfate resistance. Additionally, most of the test methods on sulfate attack include the exposure of mortar or paste samples in sodium sulfate solution to obtain results within a reasonable timeframe. However, given the complicated mechanisms involved in sulfate attack, not one parameter can be used to predict sulfate-related damage in all conditions. This is clearly evident from various methods documented in various literatures (Tittelboom et al., 2013, CEN/TR 15697, 2008; Xu et al., 1998 Bonakdar & Mobasher, 2008). Moreover, the various combinations that sulfate attack can manifest (chemical versus physical) as well as can occur in the field simultaneously make it extremely difficult to develop appropriate test methods. Thus, a holistic approach that includes laboratory and field performance of concrete exposed in various sulfate environments and conditions is needed for successful modeling of the impact of sulfate attack on the performance of a given structure.

Chapter 3: Deterioration of Mortar Bars Using High-Calcium Fly Ash Immersed in Sodium Sulfate Solutions

3.1 ABSTRACT

In this study, the performance of several binary and ternary mixtures containing a high-calcium fly ash and other pozzolans, such as Class F fly ash and silica fume, were investigated for their sulfate resistance using different sodium sulfate solutions. The mortar bars were placed in a similar sulfate solution as per ASTM C 1012/1012M (33,800 ppm SO_4^{2-}) and a less severe sulfate solution (6,000 ppm SO_4^{2-}) and monitored for their expansion. The phase composition of the mortar samples was investigated using x-ray diffraction and scanning electron microscope coupled with energy dispersive spectroscopy (SEM/EDS). The mortar bars placed in the moderate sulfate concentration resulted in less expansion and deterioration than the same bars placed in the higher sulfate concentration. Storage in sodium sulfate solutions resulted in the formation of ettringite and gypsum in both sulfate concentrations. Replacement of cement by high-calcium fly ash showed significantly higher amounts of ettringite formation especially for the mortar bars stored in the higher sulfate concentration. SEM analysis revealed ettringite to be the primary cause of disruption and deterioration observed in the mortar bars.

Keywords: Sulfate attack, Sulfate concentration, Ettringite, Gypsum, Expansion

3.2 INTRODUCTION

Although several forms of sulfate attack exist, external chemical sulfate attack of concrete has been highly considered one of the most complex forms of deterioration mechanisms. Typically, external sources of sulfates diffuse through the concrete pores, setting off a series of expansive reactions of sulfate ions with aluminum containing phases and/or calcium hydroxide to form ettringite or gypsum, respectively. The formation of these products can lead to volumetric expansion and cracking of the surface layer thus encouraging further penetration of sulfate ions into the concrete and resulting in more severe damage (Messad, et. al, 2012).

To best evaluate the sulfate resistance of concrete mixtures, test specimens can be exposed to natural sulfate conditions in the field and periodically examined over time. However, unless the concrete is very porous, field exposure cannot provide relatively rapid results and there are many uncontrolled factors (i.e., temperature, humidity, etc.). Generally, ASTM C 1012 (2012) is commonly used to determine the performance of various concrete mixtures under sulfate attack in controlled laboratory conditions. In this method, standard mortars are cast and monitored for their expansion periodically while submerged in a 5% sodium sulfate solution for up to 18 months. The sulfate concentration specified in the test solution, however, has been a subject of much scrutiny for being considered far too aggressive and not realistic of field conditions. Moreover, testing with ASTM C 1012 has been reported as having poor correlation to field performance (Dhole, 2008; Drimalas, 2007) that requires a significant time to qualify performance, making it a very unpopular test among researchers and practitioners.

The advantage of obtaining a test result in a relatively short amount of time (when compared to the service life of a structure) is typically accompanied by changes in the process of deterioration and has to be brought into question (Cohen & Mather, 1991).

Some of the early research investigating the mechanisms of sulfate of attack found that with increasing sulfate concentration, gypsum is the main phase present (Skalny et al., 2002; Tian & Cohen, 2000), whereas field studies have shown ettringite formation to be the primary phase present and main cause of deterioration in concrete structures (Leemann and Loser, 2011). In many cases, the source and type of sulfate (i.e., Na^+ , Mg^{2+} , Ca^{2+}) can also dictate the type of chemical reaction that may occur in the field (Skalny et al., 2002). Testing with magnesium sulfate is reported as being less expansive than sodium sulfate and depending on the binder composition, may result in surface deterioration rather than expansion (Gollop & Taylor, 1995; Kunther et al., 2013). However, many studies also report the opposite with magnesium being the most aggressive due to the formation of a corrosive magnesium-silicate-hydrate (M-S-H) and commonly associated with loss of binding properties rather than expansion (Bonen, 1992; Dehwah, 2007). Although calcium sulfate (gypsum) is a common source of sulfate in soils, it has not been studied as much in the laboratory and has not caused as much damage in the field, presumably due to its lower solubility in comparison to magnesium and sodium sulfate (Skalny et al., 2002).

The present study evaluates the influence of the sulfate concentration in the test solutions on the formation of sulfate products, particularly ettringite and gypsum. Mortar bars were placed in two sodium sulfate solutions (5.0% and 0.89% Na_2SO_4) and evaluated for their length change for 18 months. As a comparison, the performance was compared to that of standard mortar bars cast as per ASTM C 1012. In addition, X-ray diffraction (XRD) and scanning electron microscopy (SEM) coupled with energy dispersive spectroscopy (EDS) was used to quantify and characterize the phases present in the system at different intervals.

3.3 RESEARCH SIGNIFICANCE

Many studies have used the accelerated mortar bar method ASTM C 1012/1012M, in combination with ACI 201.2R-08 *Guide to durable concrete* (2008), to investigate the sulfate resistance of mortar mixtures, especially when testing fly ashes with calcium contents of more than 20% CaO (ACI 201.2R-08, 2008). In North America where sulfate exposure conditions are encountered, however, the sulfate levels are often less aggressive than that used in the accelerated mortar bar method. This raises significant controversy regarding the underlying mechanisms and whether the method provides a direct comparison to field performance. This study provides an evaluation of mortar bar using similar methods as per ASTM C 1012/1012M but investigate their performance using a less aggressive sulfate solution and draw any comparisons between the conventional test method.

3.4 MATERIALS AND EXPERIMENTAL PROCEDURES

Mortar bars were fully submerged in moderate and aggressive sulfate concentration and periodically monitored for their length change over time. Scanning electron microscopy (SEM), energy-dispersive spectroscopy (EDS), and X-ray diffraction (XRD) were used to identify and characterize the microstructure formed after sulfate exposure.

3.4.1 MATERIALS

Two portland cements were procured from within the state of Texas for making the mortar, a Type I cement (C1) with a high C_3A content of 10% and a moderate sulfate resistant Type I/II cement (C2) with a C_3A content of 7%. These cements were

designated as the controls and were assumed to have poor and moderate resistance to external sulfate attack based on their C_3A content as prescribed in ASTM C 150 (2015).

To evaluate the influence of sulfate concentration on binary and ternary mixtures, a wide range of supplementary cementitious materials were chosen for this study. A high-calcium (HC) fly ash and low calcium (LC) fly ash were used in combination with both portland cements at 25 and 30% and replacement by mass of cement, respectively. Additionally, 5% silica fume (SF) was used as part of a ternary blend with 35% HC fly ash. The HC fly ash had a $CaO = 28.98\%$ and is known to be susceptible to sulfate attack (Dhole, 2008; 2011; 2013; Drimalas, 2007). The chemical composition of the cementitious materials, as well as the phase composition of the cements used is presented in Tables 3-1 and 3-2, respectively.

Table 3-1: Chemical compositions of cementitious materials (% by mass)

Cement Type	SiO ₂	Al ₂ O ₃	Fe ₂ O ₃	CaO	MgO	Na ₂ O	K ₂ O	SO ₃	LOI
Type I (C1)	20.36	5.43	2.50	63.12	1.35	0.09	1.03	3.23	2.60
Type I/II (C2)	20.38	4.90	3.55	63.62	1.14	0.11	0.67	2.86	2.20
Supplementary Cementitious Materials									
Class C Fly Ash (HC)	30.76	17.75	5.98	28.98	6.55	2.15	0.3	3.64	-
Class F Fly Ash (LC)	48.48	25.01	3.56	15.92	2.5	0.3	0.71	0.72	-
Silica Fume (SF)	93.17	-	2.1	0.8	0.3	-	-	0.2	-

Table 3-2: Phase compositions of cements (% by mass)*

Cements	C ₃ S	C ₂ S	C ₃ A	C ₄ AF
Type I	62.12	11.52	10.16	7.61
Type I/II	66.06	8.60	6.98	10.80

*(Bogue calculation)

3.4.2 LENGTH CHANGES

Mixture proportions are presented in Table 3-3. A modified version of ASTM C 1012 was used to measure the expansion caused by sulfate attack. The most recent version of ASTM C 1012/1012M (2013) specifies the mortar bars and cubes to be stored in a sealed curing container on top of risers above water, and stored in a oven at $35\text{ }^{\circ}\text{C} \pm 3^{\circ}\text{C}$ ($95\text{ }^{\circ}\text{F} \pm 5\text{ }^{\circ}\text{F}$). However, mortar bars used in this study were cast and cured following the procedures outlined in the 2012 version of ASTM C 1012/1012M (2012). Other modifications include a fixed water-cementitious ratio (w/cm) of 0.485 (versus the comparable flow to the control cement mixture), reduced number of bars tested (five versus six), and the addition of a lower sodium sulfate concentration (6,000 ppm versus 33,800 ppm SO_4^{2-}).

Mortars were mixed according to ASTM C 109 (2016). Mortar bars 25 x 25 x 285 mm (1 x 1 x 11.25 in) and cubes 50 mm (2 in) were cast, sealed in double Ziploc bags and submerged in a curing tank to cure for the first 24 hours at $35\text{ }^{\circ}\text{C} \pm 3\text{ }^{\circ}\text{C}$ ($95\text{ }^{\circ}\text{F} \pm 5\text{ }^{\circ}\text{F}$). Following the first 24 hours of curing, the mortar bars and cubes were then demolded and transferred to a saturated limewater curing tank at $23\text{ }^{\circ}\text{C} \pm 3\text{ }^{\circ}\text{C}$ ($73\text{ }^{\circ}\text{F} \pm 3\text{ }^{\circ}\text{F}$). The mortar bars and cubes were allowed to cure until two cubes reached an average compression strength of 20 MPa (2,850 psi) or more. Once the strength was achieved, the mortar bars were removed from the limewater, measured according to ASTM C 490 (2011) and transferred to a container containing 5% Na_2SO_4 (33,800 ppm SO_4^{2-}) and 0.89% Na_2SO_4 (6,000 ppm SO_4^{2-}) solution at $23\text{ }^{\circ}\text{C} \pm 3\text{ }^{\circ}\text{C}$ ($73\text{ }^{\circ}\text{F} \pm 3\text{ }^{\circ}\text{F}$). Length change was determined in reference to an invar bar before sulfate exposure and after 7, 14, 21, 28, 56, 91, 105, 121, 182 days of exposure and every 3 months thereafter. Results were based on an average of four specimens. Samples to track the microstructural changes after various immersion periods were taken from the fifth specimen. During each

measurement, the solutions were replaced with new 5% and 0.89% sodium sulfate solution at $23\text{ }^{\circ}\text{C} \pm 2\text{ }^{\circ}\text{C}$ ($73\text{ }^{\circ}\text{F} \pm 3^{\circ}\text{F}$) to remove any significant amount of alkalis leaching into the solution and thus increasing the pH.

Table 3-3: Mixture proportions (% by mass)

Mixture	W/CM	C1 (%)	C2 (%)	HC (%)	LC (%)	SF (%)
C1-Cont	0.485	100	-	-	-	-
C1-30HC	0.485	70	-	30	-	-
C1-35HC-5SF	0.485	60	-	35	-	5
C1-25LC	0.485	75	-	-	25	-
C2-Cont	0.485	-	100	-	-	-
C2-30HC	0.485	-	70	30	-	-
C2-35HC-5SF	0.485	-	60	35	-	5
C2-25LC	0.485	-	75	-	25	-

3.4.3 SCANNING ELECTRON MICROSCOPY

A JEOL JSM-6490LV scanning electron microscope equipped with a secondary electron (SE) detector, back-scattered electron (BSE) detector, and energy-dispersive spectrometer (EDS) was used to observe the microstructural changes of the samples post-sulfate exposure. The samples were examined after 4 months of exposure to sulfate primarily due to the abrupt change in expansion noted between the two different concentrations. Cross-sections of the mortar bar were broken off and sawed down to an 8 mm (0.31 in) thick sample. Samples were prepared by epoxy impregnating, fixed grinding, polishing and placing under vacuum in a desiccator until examined in the SEM. For consistency, the SEM samples are labeled according to their mixture number and

exposed sulfate concentration. Mortar bar samples investigated using SEM were not carbon coated. Consequently, the microscope was operated at low vacuum with the pressure varying between 1-10Pa. In addition, a 15 and 20kV accelerating voltage (depending on the quality of the image) and 10 mm (0.39 in) working distance was used to optimize the image. EDS analysis was used to identify the elements present in the mortar sample.

3.4.4 X-RAY DIFFRACTION

Microstructural changes were also studied using powder collected from mortar bar samples exposed to sodium sulfate solutions. About a 12.5 – 25 mm (0.5 – 1.0 in) sample was broken off during periodic measurements and stored under vacuum for no less than three days. Samples were collected and finely ground below 45 micron (0.008 in) before prepping for the XRD. A XRD diffractometer was used to collect the pattern with a position-sensitive detector operating at 40 kV with a 30 mA using a copper target (Cu K α wavelength 1.54Å) and a nickel filter and a carbon monochromator. XRD scans were collected from 5-70° 2 θ with a step size of 0.2°/min and a dwell time of 6 seconds. The composition of the hydrated pastes was determined by quantitative X-ray diffraction (Rietveld) analysis on the diffraction patterns. Rietveld analysis is a technique to accurately determine the quantities of crystalline phases present in a sample. The procedure involves determination of calculated XRD patterns through simulation technique based on the structure files for the relevant phases expected within the sample. Simulations were carried out using the TOPAS software. The calculated pattern is refined step-by-step to take into account peak shape, instrumental factors, variations in structures, errors induced during sample preparation, and temperature effects (Dhole,

2008; Dinnebier & Billinge, 2008). Refinement is a systematic procedure in Rietveld analysis to obtain the simulated XRD pattern in close agreement with the observed XRD pattern. Results presented in this study are on refinements with a weighted profile R-factor (R_{wp}) $\leq 10\%$ (Toby, 2006).

3.5 EXPERIMENTAL RESULTS AND DISCUSSION

3.5.1 Expansion and Visual Appearance

3.5.1.1 C1 Mixtures

The accelerated mortar bar expansion results for mixtures using Type I cement at 0.89% and 5.0% sodium sulfate concentrations are presented in Figure 3-1. As expected, the mixtures placed in the less aggressive sulfate solution exhibited a significantly lower expansion rate compared to their companion bars. During the first four weeks of measurements, only small length changes were observed. Thereafter, mixtures exposed to the more aggressive solutions began to diverge away and experience higher expansions. The fastest expansion was observed for the binary mixture (C1-30HC), which began showing significant expansion at 8 weeks, and ultimately failed after only 15 weeks of exposure in 5% sodium sulfate. The control mixture (C1) observed the second best performance followed by the ternary (C1-35HC-5SF) and binary (C1-25LC) mixture, which was still measurable after 950 days of exposure.

The expansion rates differed significantly between the lower and higher sulfate concentrations. Interestingly, similar performance was observed for those bars placed in 0.89% sodium sulfate showing the same level of performance between the mixtures. With exception to the high-calcium binary mixture, all mortar bars demonstrated delayed expansion in the 0.89% sodium sulfate solution. Mixture C1-30HC exhibited a final

expansion value of 0.47% after only 15 weeks of exposure in 5% sodium sulfate and was no longer measurable at 4 months due to complete loss of cohesion of the mortar bars as shown in Figure 3-2. The bars submerged in the lower concentration had an expansion of 0.18% at 6 months and were still intact with moderate cracking observed, and by 9 months of exposure, the bars observed cracking and surface deterioration, especially at the ends and corners of the bars.

It has been reported by many researchers that the sulfate resistance of high-calcium fly ash mixtures can be improved through small additions of silica fume (3-6%) as a ternary blend (Shashiprakash & Thomas, 2001; Tikalsky & Carrasquillo, 1993). Through the addition of silica fume or natural pozzolan, the calcium hydroxide content will decrease and can reduce the severity from gypsum formation. Moreover, the pozzolanic reactivity can decrease permeability and ultimately impede the ingress of external sulfates into the paste matrix. Surprisingly, this was not the case for the ternary mixture (C1-35HC-5SF) evaluated in this testing program. Although it exhibited a slower rate of expansion in comparison to the HC binary mixtures, it is clear that the HC fly ash used in this study raises significant concerns with regards to its sulfate performance. Mortar bars placed in 0.89% sodium sulfate showed similar performance with an expansion of 0.21% at 18 months of sulfate exposure.

With exception to the binary LC mixture submerged in 0.89% sodium sulfate solution, all mixtures exhibited significant expansion at both concentrations. Remarkably, the binary LC mixture did not show any appreciable expansion having only a 0.08% expansion after 950 days of exposure in 0.89% sodium sulfate. Although significant expansion was observed in similar mortar bars placed in 5% sodium sulfate, only moderate cracking and deterioration at the ends and corners were observed on the binary LC mortar bars.

Figure 3-2 shows the visual appearance of the mortar bars at 12 and 18 months for the control mixture placed in 5% and 0.89% sodium sulfate, respectively and around 4 months for the binary HC mixture placed in both sulfate solutions. The images to the left show those mixtures placed in 5% sodium sulfate whereas, those on the left were placed in 0.89% solution. From the results showing the visual appearances, two major observations can be drawn:

- The mortar bars submerged in the 5% sodium sulfate solution clearly illustrates the aggressiveness from the concentrated sulfate solution showing severe damage and deterioration in the mortar bars; and
- The mortar bars exposed to 0.89% sodium sulfate solution exhibited similar expansion values at later times; however, the noted deterioration is significantly less than those in 5% solution

These findings demonstrate the severity of performance testing to evaluate durability issues for cementitious mixture. Although there is significant pressure to develop accelerated methods that can provide results in a timely manner, the results may not accurately reflect field-exposed concrete. In many cases, the accelerated method may change the mode of failure and thus, the deterioration that is seen on the sample (Cohen & Mather, 1991). The results in Figures 3-1 and 3-2 give some indication that this type of phenomenon could be occurring. Moreover, the mode of damage and reduced deterioration observed on the mortar bars submerged in a “more” realistic sulfate solution may help explain why relatively few cases of sulfate attack are described in the field.

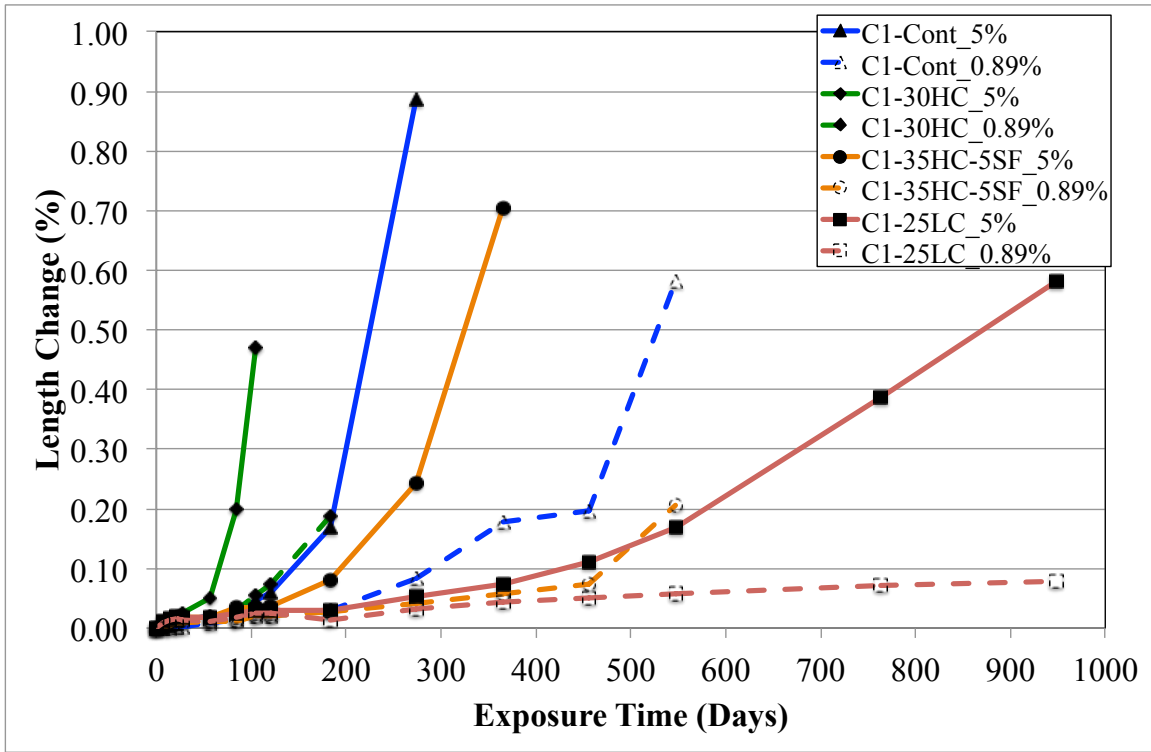


Figure 3-1: Accelerated mortar bar expansion results for Type I mixtures exposed to 5 and 0.89% Na₂SO₄

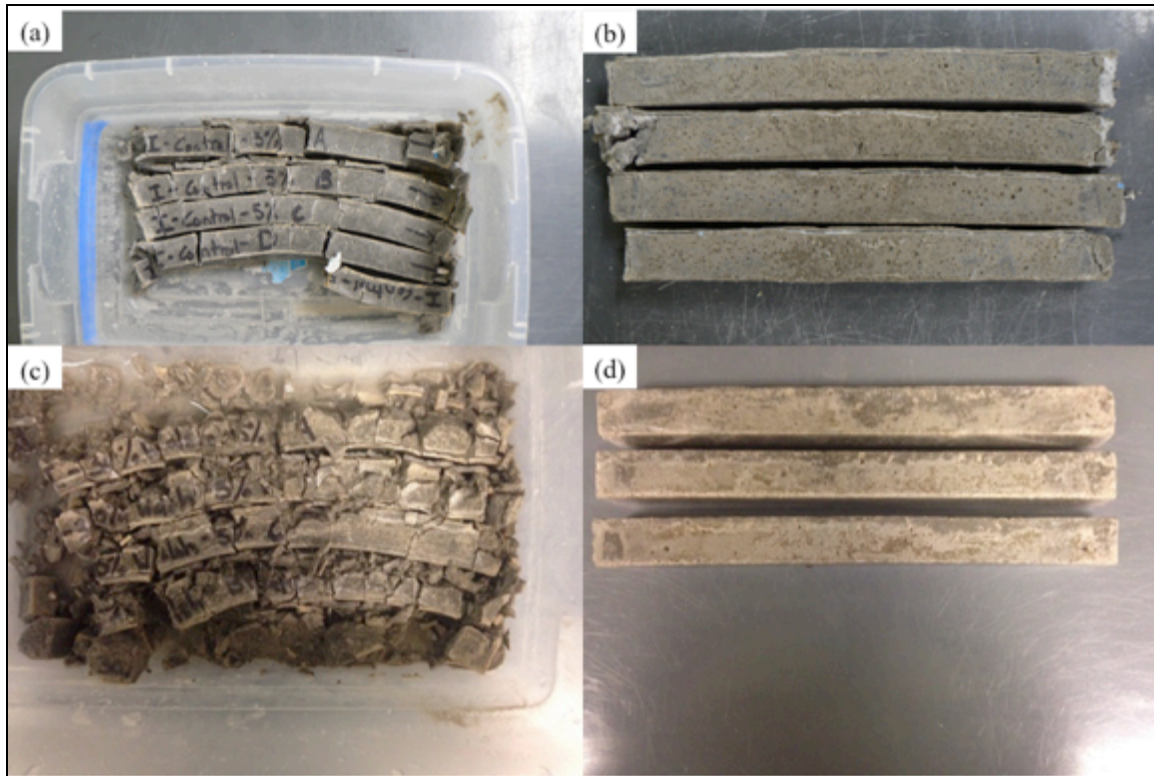


Figure 3-2: Visual appearance in mortar bars showing deterioration in: (a) C1 in 5% Na_2SO_4 after 1 year; (b) C1 in 0.89% after 18 months; (c) C1 + 30%HC in 5% Na_2SO_4 around 4 months; (d) C1 + 30%HC in 0.89% Na_2SO_4 at 4 months

3.5.1.2 C2 Mixtures

The observed length changes for mixtures using C2 (see Figure 3-3) were smaller than for the previously discussed C1 mixtures. Interestingly, the length changes are very similar for both concentrations during the first 15 weeks (before larger expansions are observed). Thereafter, it appears that cracking of the mortar bars has initiated and the mechanism is controlled by the diffusion-reaction phenomenon as described in Gollop & Taylor (1992). The mortar bars evaluated in this study typically showed cracks originating from the finished surface and progressing further towards the center of the bar leading to a warping effect.

As expected, the binary HC mixtures showed poor sulfate resistance showing significant expansion after only 12 weeks in 5% sodium sulfate solution, and after 4 months, the bars showed severe deterioration with most failing at the center of the bar (see Figure 3-4). The results suggest that the chemical composition of the mixtures prior to sulfate exposure could be affecting the performance. This is likely attributed to the reactive glassy phases and aluminates available to react in the fly ash mixture thus favoring the formation of ettringite at later ages (Dhole et al., 2013).

Santhanam et al. (2002) modeled the effects of sodium sulfate concentrations on small mortars. He describes the expansion of mortar in sodium sulfate follows a two-stage process; an initial period of very small expansion until a critical value is achieved, followed by a sudden increase in expansion. At any sodium sulfate concentration, the duration of the initial stage of expansion is unaffected; however, once the initial level of disruption is achieved, the rate of attack is proportional to the concentration (Santhanam et al., 2002). The findings in this study present similar results for the length change at both sulfate concentrations. The visual presence of moderate size cracks at the corners and finished surface of the control (C2) mortar bars seem to be in agreement with the suggested literature mentioned above (see Figure 3-4). With exception to the binary HC mixture, all mixtures observed very little change in expansion up to 15 weeks follow by a divergence in expansion rates between both sulfate concentrations.

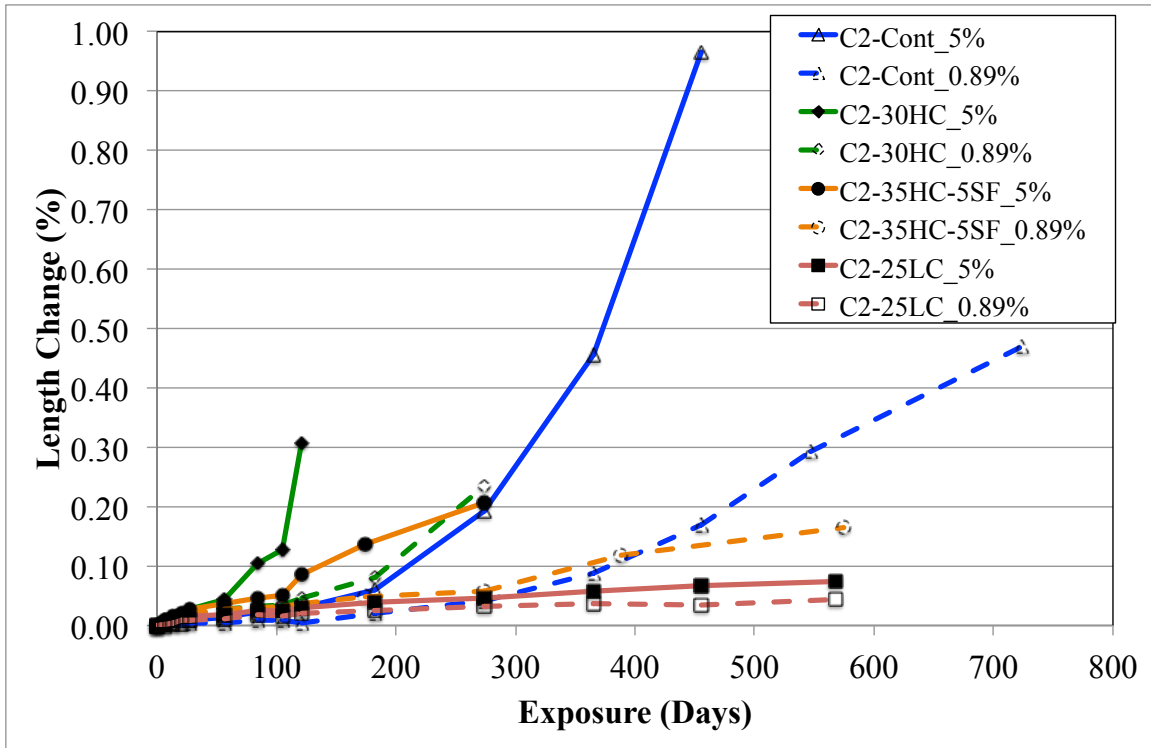


Figure 3-3: Accelerated mortar bar expansion results for Type I/II mixtures exposed to 5 and 0.89% Na₂SO₄

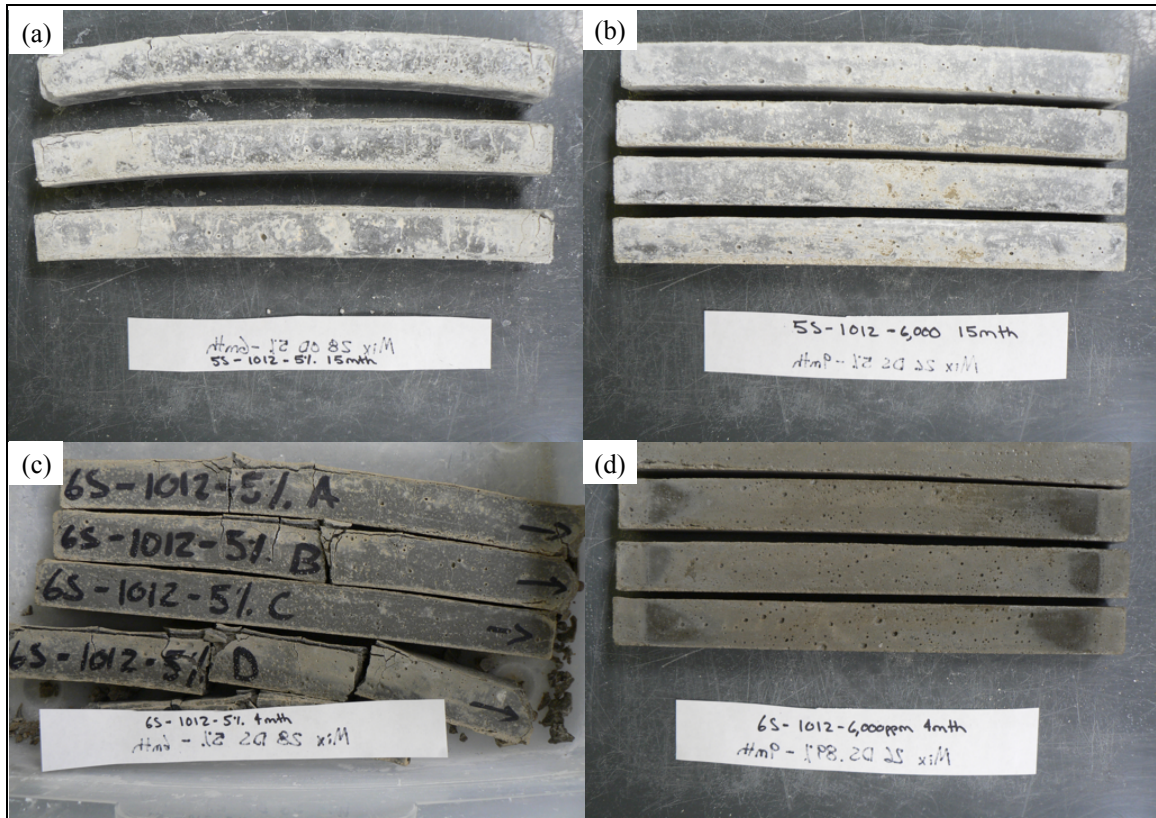


Figure 3-4: Visual appearance of mortar bars showing deterioration in: (a) C2 mixture (5S) in 5% Na_2SO_4 after 15 months; (b) C2 mixture in 0.89% Na_2SO_4 after 15 months; (c) C2 + 30%HC in 5% Na_2SO_4 around 4 months; and (d) C1 + 30%HC in 0.89% Na_2SO_4 at 4 months

3.5.2 Microstructural changes

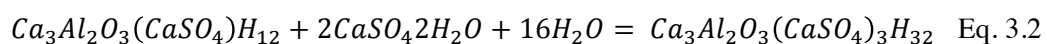
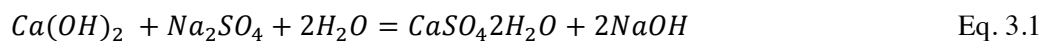
To observe and identify microstructural changes in the mortar mixture exposed to the two sodium sulfate concentrations, Secondary electron (SE) imaging combined with EDS was used to identify elements present in the sample. Additionally, X-Ray diffraction combined with the Rietveld method was performed to quantify the phases present.

For the control mixtures, ettringite deposits were found within the paste matrix in both sodium sulfate concentrations after 4 months of exposure (Figure 3-5). The higher

concentration appears more distinct and distributed throughout the matrix, which is consistent with the associated increase in length change at this period (see Figure 3-1). Interestingly, ettringite deposits were also evident in the lower sulfate concentration; however, the amount and arrangement were discontinuous and significantly less dense. In comparison to the higher concentration, the images also revealed little to no microcracking within the bulk paste matrix at the lower concentration. The results are consistent with the physical length change observed previously; the mortar bars exhibited minor cracks along the edges and higher expansion values in the higher concentration.

The HC fly ash mixture displayed a more disruptive behavior when compared to the control, as shown in Figure 3-6. Both concentrations showed significant deposits of ettringite in the pores with a remarkably high amount of microcracking in the paste matrix. Similar to the control mixture, the formation of ettringite in the 5% sodium sulfate solution appeared significantly denser and well distributed throughout the system.

It is worth mentioning an interesting observation made in several of the SEM images. In the work presented here, ettringite was commonly found to form in areas near and/or around portlandite crystals in mixtures submerged in the 0.89% sodium sulfate. Figure 3-7 shows several SE images of the binary HC mixture after 4 months of exposure in 0.89% sodium sulfate solution. The figure presents three EDS spectrums illustrating the conversion of portlandite to gypsum, followed by the formation of poorly crystalline ettringite. The above mechanism can be described by the following two chemical reactions between external sodium sulfate solution and calcium hydroxide in the hydrated cement paste (Skalny et al., 2002):



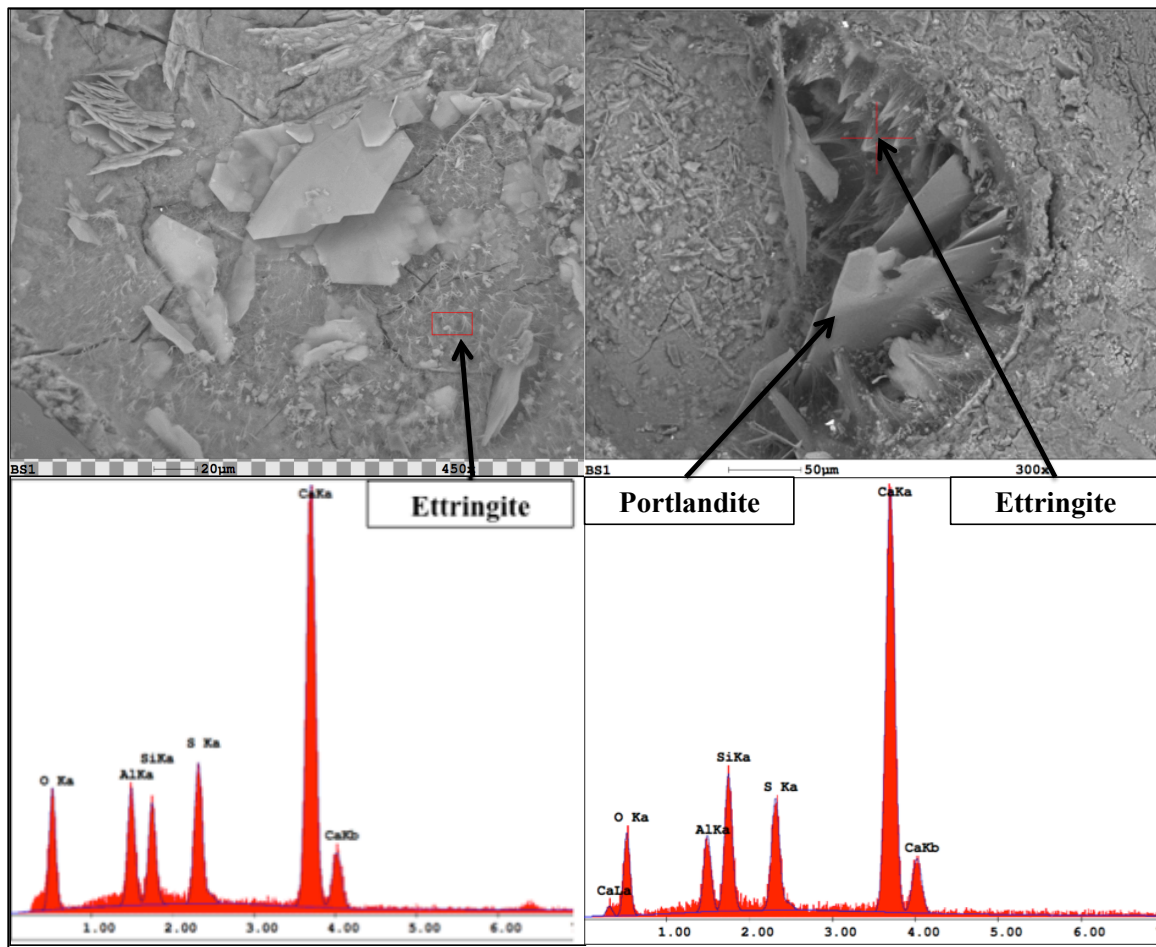


Figure 3-5: SE images coupled with EDS spectrums showing C1 mixture after 4 months exposure in: (a) 5% Na_2SO_4 ; and (b) 0.89% Na_2SO_4

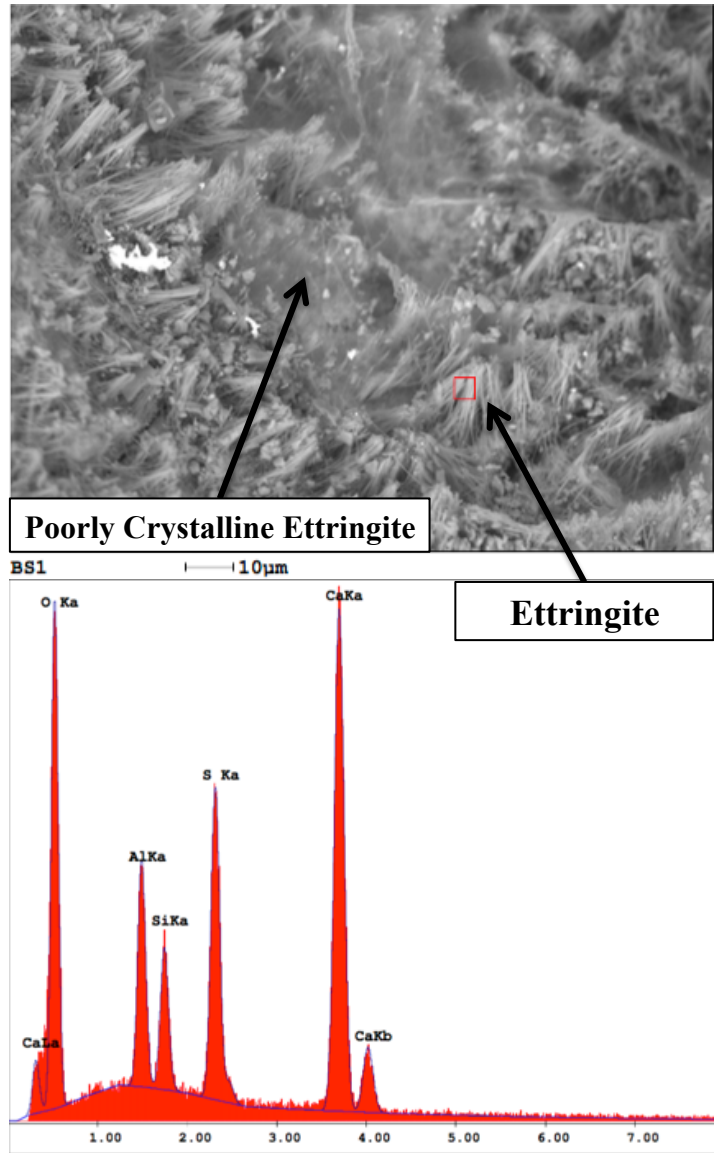


Figure 3-6: SE image coupled with EDS spectrum showing significant ettringite formation in C1-30HC mixture after 4 months exposure in 5% Na₂SO₄

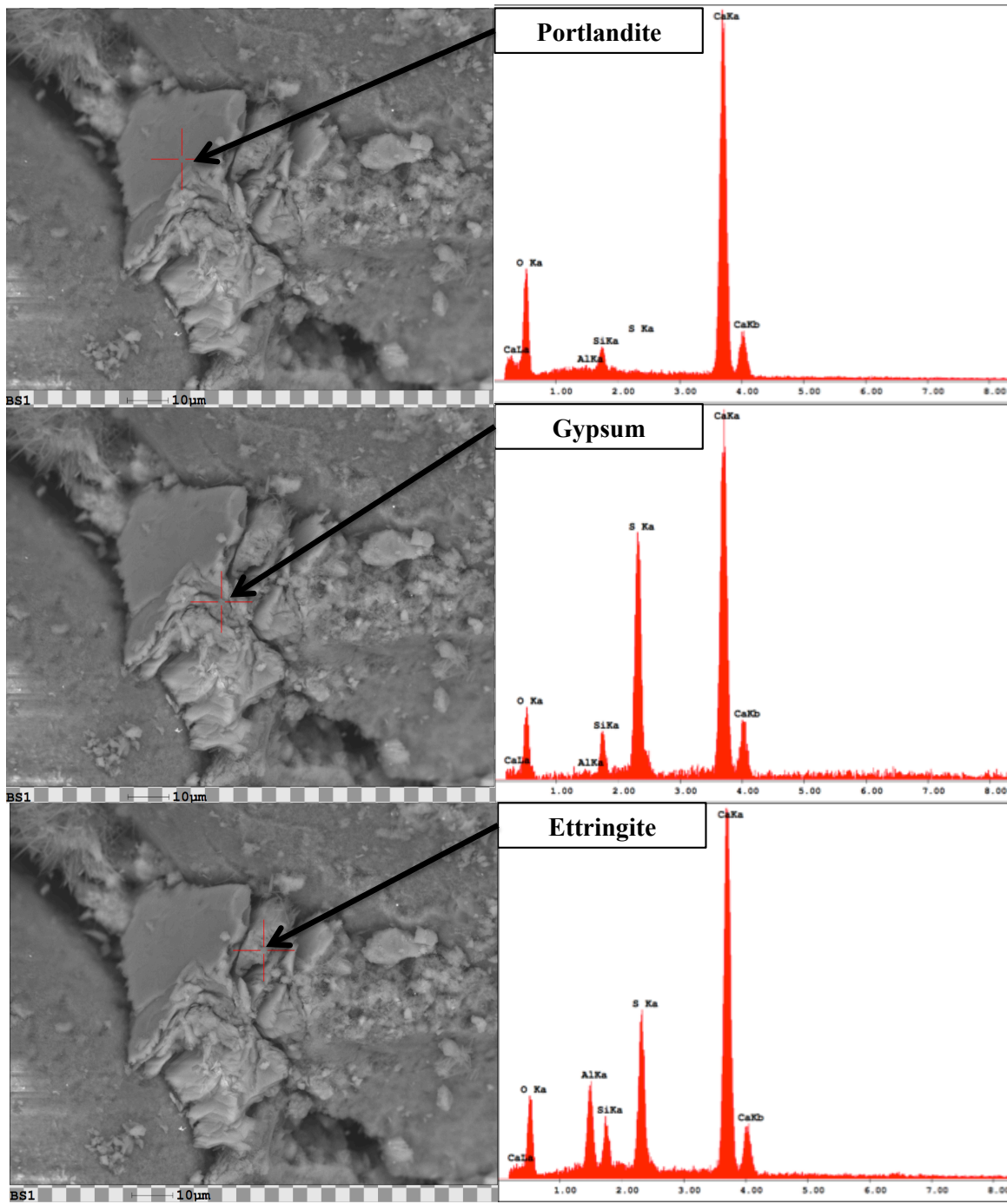


Figure 3-7: SE images coupled with EDS showing C1-30HC mixture after 4 months exposure in 0.89% Na₂SO₄

The SEM images revealed very few observation of gypsum in any of the mixtures. The main phase present, independent of the solution used was ettringite. Furthermore, in many instances the propagation of cracks was also found in areas where significant ettringite deposits were located in the paste, as shown in Figure 3-8. According to Scherer (1999; 2004), ettringite could only exert enough crystal pressure to cause expansion and cracking in small pores within a certain size range. The SEM images appear to indicate that ettringite crystal growth is the primary cause of expansion even in mixtures submerged in the lower sulfate concentration (0.89% Na_2SO_4); the aforementioned mechanism is intensified with increasing concentration and supersaturation of the pores with sulfate ions (Santhanam et al., 2002).

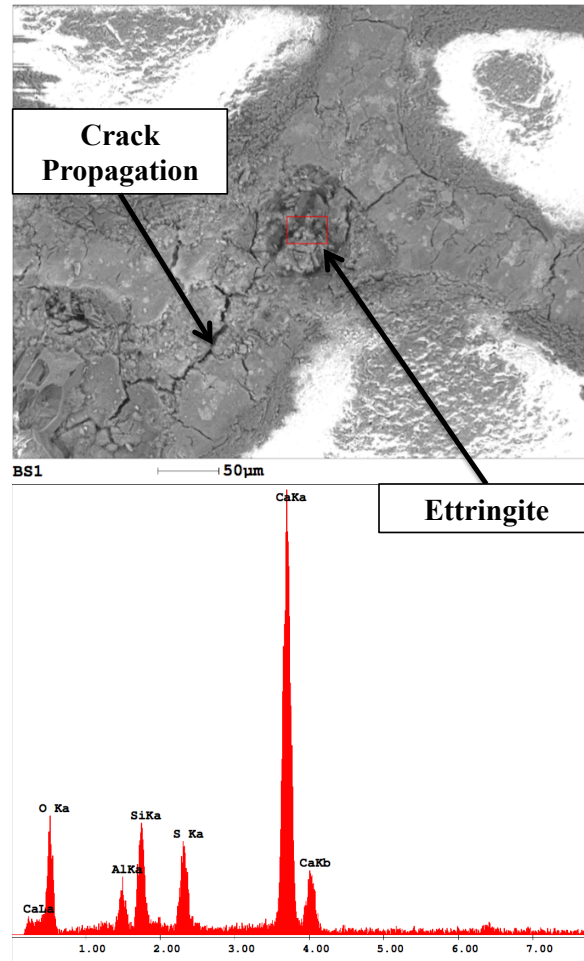


Figure 3-8: SE image of C1-30HC mixture after 4 months exposure in 0.89% Na₂SO₄

3.5.3 X-Ray diffraction

The phases present in each mixture were identified using XRD after exposure to the sulfate concentrations over time. Figure 3-9 provides the Rietveld analysis for a diffraction pattern on the control mixture (C1-Cont) after 1 year of exposure in 5% sodium sulfate. The pattern shows the chemical composition in the powder sample in terms of the normalized amounts of 11 crystalline phases present at detectable levels. For

all patterns evaluated, monosulfate (M), ettringite (E), gypsum (G), and portlandite (CH) were detected in the qualitative and quantitative Rietveld analysis.

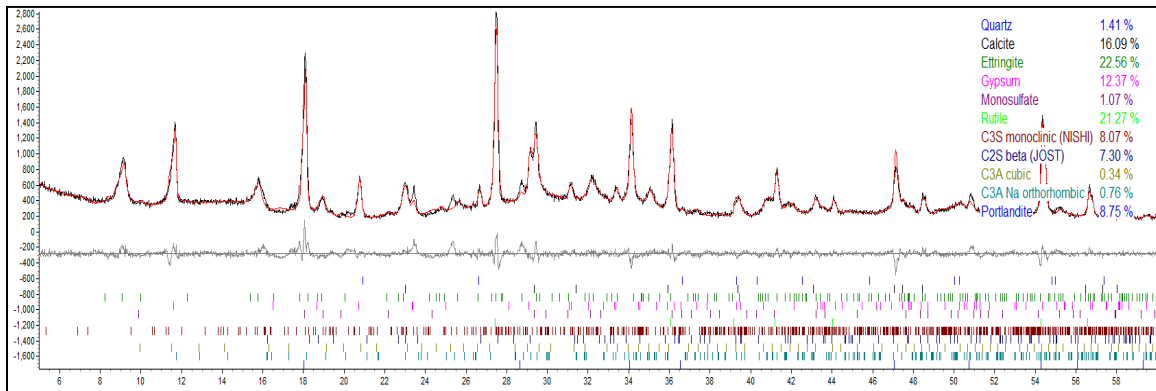
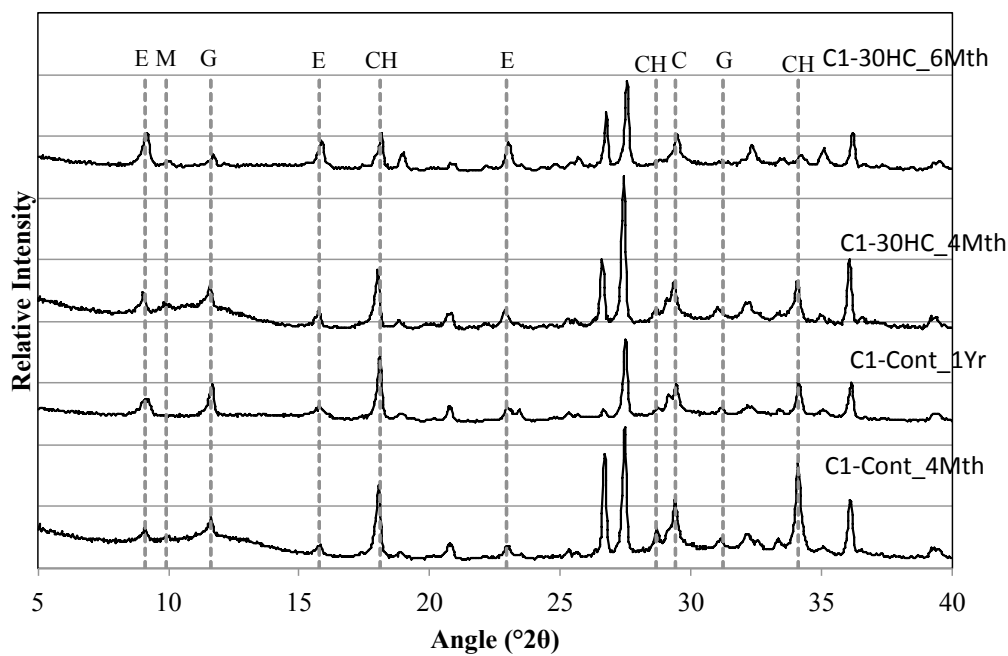


Figure 3-9: Rietveld analysis for control mixture (C1-Cont) after 1 year exposure in 5% Na_2SO_4

XRD patterns for the control (C1-Cont) and binary (C1-30HC) mixtures are presented in Figure 3-10. In both sulfate solutions, the patterns revealed traces of ettringite, gypsum, as well as portlandite. Interestingly, there is a significant drop in the portlandite intensity most likely as a result of gypsum conversion from the external sulfates. The drop is evident along the portlandite peak at about $34.1^\circ 2\theta$. A significant drop in the portlandite peak is also observed in the 0.89% sodium sulfate solution. Although ettringite is clearly evident in the 5% sodium sulfate patterns, small traces are evident in the 0.89%, which is consistent with the previous SEM results.

5.0% Na₂SO₄



0.89% Na₂SO₄

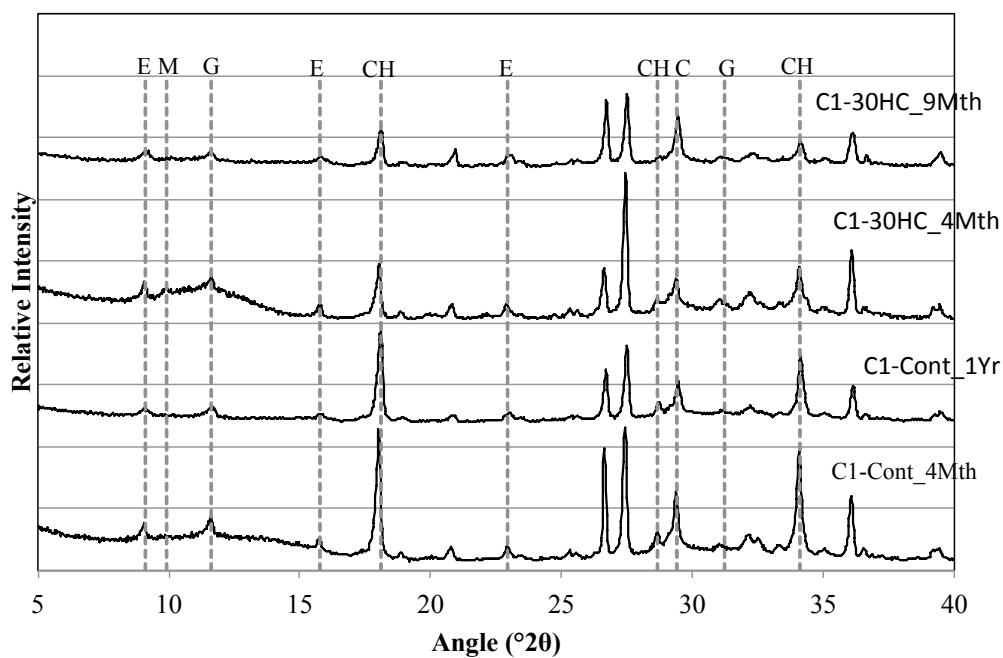


Figure 3-10: XRD traces of control (C1-Cont) and binary (C1-30HC) mixtures

The percentages of hydration products were determined using rutile (TiO_2) as an internal standard and are presented in Figures 3-11, 3-12, and 3-13. Ettringite and gypsum phases were present at similar quantities at about 56 days independent of sodium sulfate concentration; however, after one year exposure the ettringite is the dominant phase present with minor increases in the gypsum phase. Here, the further formation of ettringite leads to faster expansion. This is contradictory to what many researchers have reported. Biczok (1967) reported that the mechanisms of sulfate attack is dependent on the concentration of the sulfate solution where concentration exceeding 8,000 ppm SO_4^{2-} (1.2% Na_2SO_4), gypsum is the main phase present. According to Müllauer et al. (2014), however, ettringite was found to be the primary phase present in higher sulfate concentration (30g/L SO_4^{2-}) and responsible for expansion and damage.

Ettringite and gypsum phases were also present in mortars immersed in the lower sulfate concentration after one year of exposure; however, ettringite was found in much smaller quantities. At 0.89% sodium sulfate, the control mixture (C1) observed over 70% less ettringite whereas, the binary mixture (C1-30HC) observed over a 140% less ettringite. It is interesting to note the similar ettringite quantities present in the ternary (C1-35HC-5SF) and LC binary (C1-25LC) mixture immersed in the 0.89% sodium sulfate solution. Both mixtures also observed very similar expansion values after one-year exposure. The formation of ettringite does not necessarily result in significant expansion or damage, depending on where and under what conditions it forms (Scherer, 1999).

The Rietveld results show that ettringite and gypsum are present at both sulfate concentrations; however, the associated cracking and observed expansion appears to be from the formation of ettringite in small pores. This was also evident in the SEM images

previously discussed. Nevertheless, the presence of both may indicate deterioration attributing from both phases.

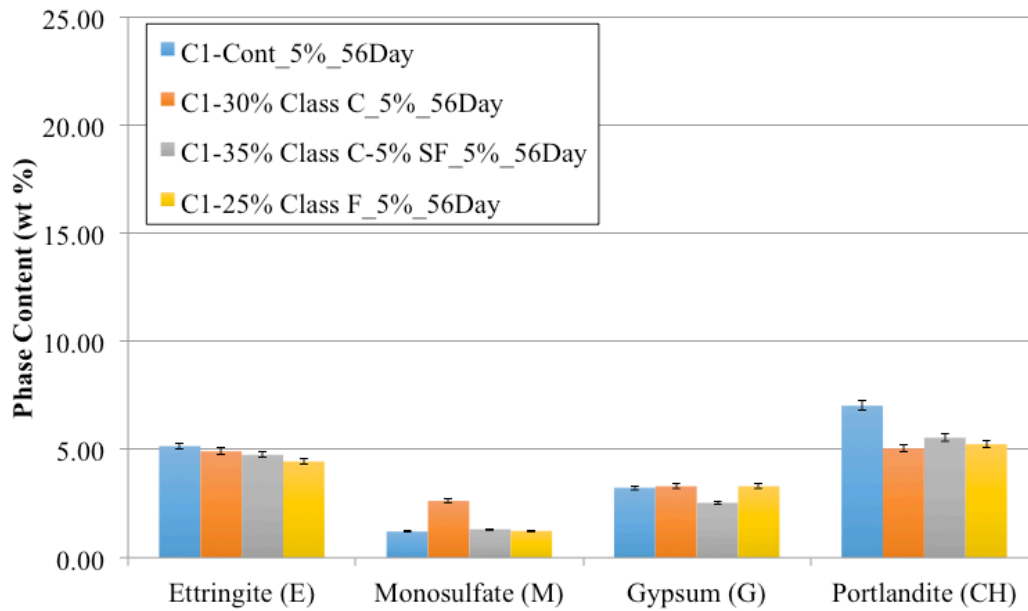


Figure 3-11: Rietveld results for mortars using cement C1 submerged in 5% Na₂SO₄ after 56Days

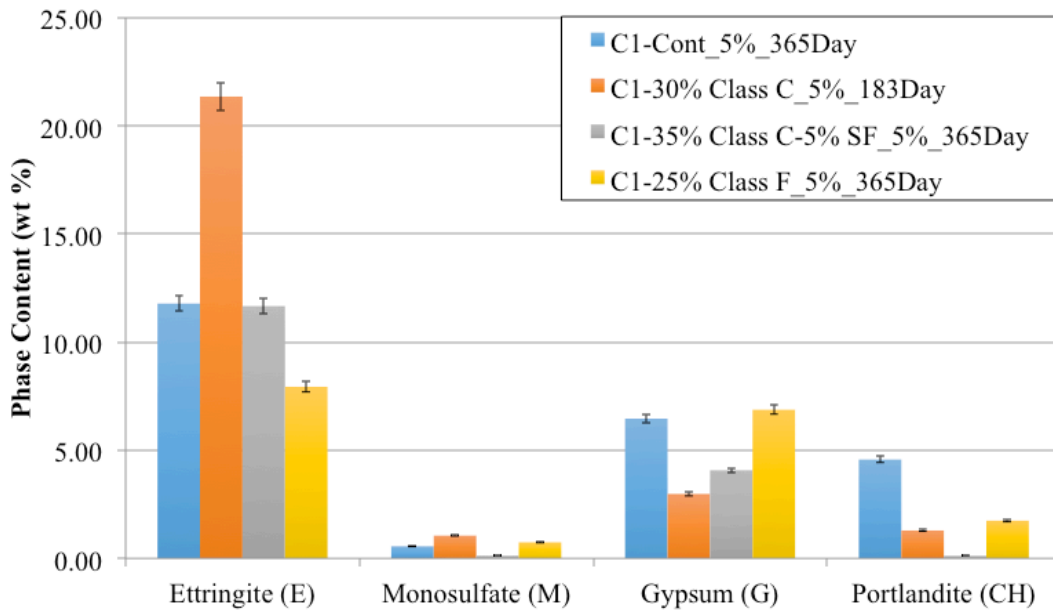


Figure 3-12: Rietveld results for mortars using cement C1 submerged in 5% Na₂SO₄ after 1yr

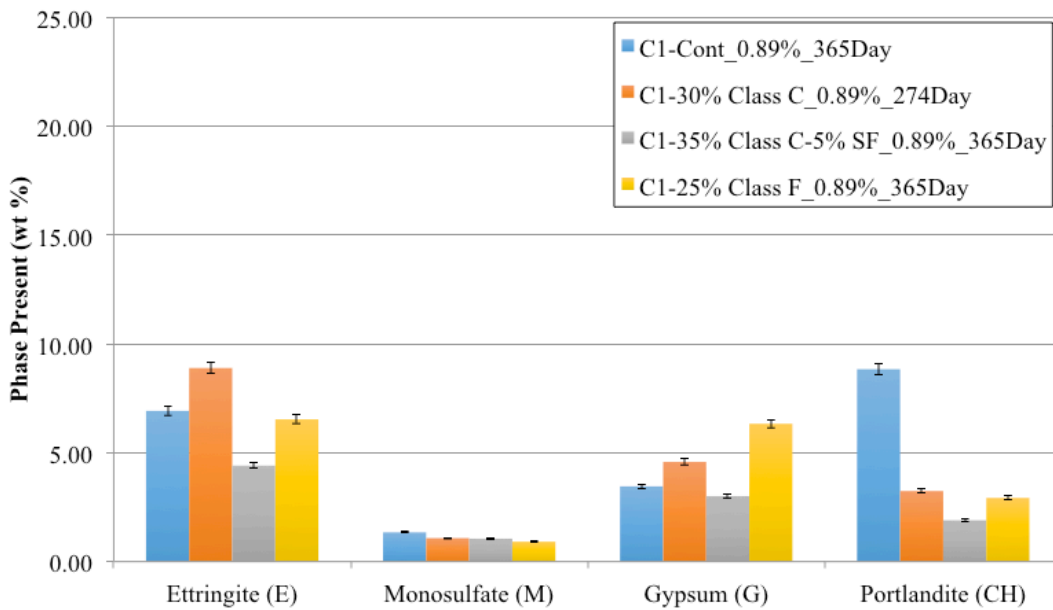


Figure 3-13: Rietveld results for mortars using cement C1 submerged in 0.89% Na₂SO₄ after 1yr

3.6 SUMMARY AND CONCLUSION

The results presented in this chapter show that test specimens are damaged primarily by the formation and ongoing crystal growth pressure of ettringite independent of sodium sulfate concentration. Microcracking was observed in the test samples, which led to an enhanced ingress of sulfate ions and consequently, accelerated the disintegration; however, the rate of attack is proportional to the concentration and supersaturation of the pores with sulfate ions (Santhanam et. al., 2002). Gypsum was observed in very few instances when evaluated using the SEM; however, traces of gypsum formation were evident in the XRD patterns and in relative amounts based on the Rietveld analysis of the diffraction patterns. Lastly, significant differences in the mode of failure were evident between the two concentrations investigated.

3.7 FUTURE RESEARCH

This study shows that regardless of sulfate concentration, ettringite is the main component to the expansion mechanism and ultimately leading the cementitious mixtures to deleterious sulfate attack. Additional research needs to be conducted on other mixtures including various cement types as well as the addition of other supplementary cementitious materials such as slag, silica fume, and other natural pozzolans. Further research should be conducted at even lower concentration of sulfate such as 0.22% Na_2SO_4 (1,500 ppm SO_4^{2-}) and 0.022% Na_2SO_4 (150 ppm SO_4^{2-}) corresponding to the class 1 and 2 potential exposure in ACI 201.2R *Guide to durable concrete* (2008). More long-term sulfate attack durability tests need to be performed on concrete specimens submerged in various sulfate concentrations in the laboratory and benchmarked to actual field performance or the performance in outdoor sulfate exposure sites.

Chapter 4: An Accelerated Method to Evaluate Mixtures Subjected to Chemical Sulfate Attack Part I: Induced Internal Cracking

4.1 ABSTRACT

The sulfate resistance of concrete is typically assessed using the standardized test method ASTM C 1012/C1012M (2008). This method involves the use of standard mortar mixtures immersed in a 5% sodium sulfate solution and monitored for their expansion at regular intervals for at least 12 months (longer when incorporating supplementary cementitious materials). The length of the test limits the ability for concrete producers to reliably guarantee the maximum service life for a concrete structure placed in these aggressive environments. As a result, reliable and reproducible accelerated test methods to evaluate sulfate resistance are needed. Two proposed accelerated test methods to evaluate the sulfate resistance of cementitious mixtures were investigated. Results are presented in two parts; this chapter present the impact of induced internal cracking as a method to accelerate sulfate attack and Chapter 5 focuses a novel technique in which mortar samples are vacuum impregnated with sodium sulfate (Na_2SO_4) solution to accelerate the ingress of sulfate ions into the pores. The first method allows for the use of mortar bars to be cast and placed similarly to that of ASTM C 1012/C1012M, however, the samples are placed in high-temperature oven for 24 hours in order to intentionally induce microcracking of the paste matrix to accelerate the ingress of sulfate solution. Thereafter, the mortar bars are immersed in a sodium sulfate solution and monitored for their expansion at regular intervals. The resulting expansion of the mortar bars and mass change were measured and compared to their companion bars not subjected to the drying regime. Mixtures cast using Type I cement showed a faster rate of expansion and lead to

a quicker onset of deterioration when compared to ASTM C 1012/C1012M; however, mortars cast using Type I/II and Type V cement did not show any appreciable change in rate of expansion.

4.2 INTRODUCTION

In order for a concrete structure to be designed for its maximum service life, careful consideration must be made when evaluating the suitability of a concrete mixture for its intended environment. This is especially true for concrete exposed to sulfate-bearing soils, groundwater and/or seawater where external sources of sulfate can penetrate the concrete and lead to severe deterioration of the structure. Commonly known as external sulfate attack (ESA), this form of concrete deterioration has been known to reduce the long-term durability of concrete structures for decades.

Several researchers (Crammon, 2003; Drimalas et al. 2011; Skalny et al., 2002) have documented the various forms of deterioration from external sulfate attack and include, but not limited to, expansive related surface cracking, loss of binding properties, increasing permeability, and ultimately further penetration and increasing severity of attack. Depending on the environmental settings as well as the properties intrinsic to the concrete (i.e., water-cement ratio, permeability, chemical composition, etc.), the chemical and physical processes in the sulfate attack mechanism can occur simultaneously making this form of deterioration very complex and challenging to understand especially in the field.

Many long-term laboratory and field studies have demonstrated that with adequate curing, low water-cement ratio, and use of a sulfate-resistant binder having a low tri-calcium aluminate content (generally <5% C_3A) sulfate attack can be mitigated

and/or prevented in the field (Drimalas et al., 2011; Monteiro & Kurtis, 2003; Ouyang et al., 1988; Stark, 1989). With the support of the aforementioned research, ACI 201.2R *Guide to Durable Concrete* (2008) prescribes the use of certain cementitious materials and maximum water-cement ratio as an alternate method to meet sulfate resistant requirements, depending on the class of severity of potential sulfate exposure. Other available cementitious materials are allowed to be used as long they are able to meet the performance requirements designated in ACI 201.2R (i.e., performance testing using ASTM C 1012/C1012M for determining sulfate resistance). However, sulfate attack is a slow process and standardized test methods such as ASTM C 1012/C1012M (2008) can take more than 12 to 18 months to perform. Consequently, the length of the test limits the ability for concrete producers to quickly and reliably evaluate the potential of a given mixture for deleterious sulfate attack, prohibiting appropriate preventive measures for attack.

Although several researchers have proposed various versions of accelerated test methods, there is still no general consensus to which method most accurately predicts field performance. Brown (1981) demonstrated that controlling the pH of the sulfate solution more accurately represents field conditions better and leads to a much faster expansion of mortar bars than a typical non-controlled pH sulfate solution. Brown's investigation showed the controlled sulfate environment accelerated the rate of sulfate attack regardless of whether a strength loss or a linear expansion criterion was used. Mehta (1975) also reporting similar results showing significant strength loss in cube paste samples after 28 days of testing using an automated system controlling the pH of the testing solution.

Different samples sizes and shapes have also been used to accelerate the sulfate attack performance test. Ferraris et al. (2005) studied the specimen size effect showing

that smaller size prisms (10 x 10 x 100 mm [0.4 x 0.4 x 1.5 in]) increased the expansion rate, enhancing the test results in much less time than the standard 25 x 25 x 285 mm (1 x 1 x 11.25 in) specimens. However, the test specimens were cast using paste samples, which further deviates from field mixtures and conditions. Ferraris et al. (1997) also tested cylinders with constant length of 152 mm (6 in) and varying diameters (25, 50, 75 mm) exposed to sulfate solutions from the sides only concluding that the expansion from external sulfate attack is mostly governed by ionic diffusion and could hence be accelerated using smaller specimens (Bonakdar & Mobasher, 2010).

The acceleration of sulfate attack on mortar bars placed in a high-temperature oven to intentionally introduce internal microcracks in the cement paste was investigated in this study. Since DEF may occur when the internal concrete temperature reaches the critical temperature (e.g., 70°C (158°F)) (Folliard, et al., 2005) during the early stages of hydration, a lower temperature of 60°C (140°F) was used in this investigation. For comparison, the specimens with the same mixture proportions were evaluated in accordance with the ASTM C 1012/1012M (2008) method unless otherwise noted. The performance was evaluated through mass and expansion measurements.

4.3 MATERIALS AND METHODS

4.3.1 Materials

Three different clinker types were used for this study: a Type I cement (LS) with a high-C₃A clinker ($\approx 10\%$ C₃A), a Type I/II cement (MS) with moderate-C₃A clinker ($\approx 7\%$), and a Type V cement (HS) with a low-C₃A clinker ($\approx 3\%$ C₃A). The C₃A content was used as a measure of sulfate resistance requirements for all cements. The ASTM C

150 Type I and I/II cements were procured locally from central Texas, and the Type V cement was procured from California.

Each of the cements studied was also blended (as a percent replacement by mass of cement) with supplementary cementitious materials (SCMs) including a Class C and Class F fly ash. Additionally, a densified silica fume was used as part of a ternary blend in mixtures with Class C fly ash. Each of the fly ashes and silica fume used in the research program conformed to the requirements designated in ASTM C 618 (2015) and ASTM C 1240 (2015), respectively. Table 4-1 and 4-2 provide a detailed overview of the chemical compositions of the cementitious materials and mixture proportions of the mortar used in this study.

Table 4-1: Chemical compositions of cementitious materials (%)

Cements	Chemical Composition								Compound Composition of Clinker (Bogue)			
	SiO ₂	Al ₂ O ₃	Fe ₂ O ₃	CaO	MgO	Na ₂ O	K ₂ O	SO ₃	C ₃ S	C ₂ S	C ₃ A	C ₄ AF
Type I (LS)	19.71	5.21	2.54	63.58	1.16	0.13	0.90	3.06	70.35	3.45	9.52	7.72
Type I/II (MS)	20.38	4.90	3.55	63.62	1.14	0.11	0.67	2.86	66.07	8.60	6.98	10.80
Type V (HS)	20.98	3.66	3.71	62.95	4.55	0.24	0.34	2.70	66.88	9.71	3.42	11.29
Supplementary Cementitious Materials												
Class C Fly Ash	30.76	17.75	5.98	28.98	6.55	2.15	0.3	3.64				
Class F Fly Ash	48.48	25.01	3.56	15.92	2.5	0.3	0.71	0.72				
Silica Fume	93.17	-	2.1	0.8	0.3	-	-	0.2				

Table 4-2: Mortar bar mixture proportions and exposure conditions

	LS	MS	HS
100% Cement	5% & 0.89% Na ₂ SO ₄ at 23 °C following 20 MPa maturity		X
30% Class C Fly Ash			X
25% Class F Fly ash			X
35% Class C Fly Ash + 5% Silica Fume			
	LS	MS	HS
100% Cement	5% & 0.89% Na ₂ SO ₄ at 23 °C following 20 MPa maturity and 24 hr in 60 °C oven		X
30% Class C Fly Ash			X
25% Class F Fly ash			X
35% Class C Fly Ash + 5% Silica Fume			

4.3.2 Mortar Testing

All mixtures were tested using a 5% (33,800 ppm SO₄²⁻) and 0.89% (6,000 ppm SO₄²⁻) sodium sulfate solution to evaluate the influence of sulfate concentration on the rate of expansion. Mixtures were proportioned and cast following the procedures prescribed in ASTM C 1012/1012M (2008). The quantity of sand was 2.75 times by weight of cementitious materials (portland cement, fly ash, and/or silica fume) and the water-to-cementitious ratio (*w/cm*) was kept constant at 0.485 for all mixtures. For each mixture, twenty 25 x 25 x 285 mm (1 x 1 x 11.25 in) mortar bars, with a gauge length of 250 mm (10 in) and a sufficient number of 50 mm (2 in) cubes for determining strength were prepared. Immediately after casting, the molds were placed in large polyethylene bags, sealed, and submerged underwater at 35 °C ± 3 °C (95 °F ± 5 °F). All prisms were stripped from the molds at 23.5 hr ± 0.5 hr and subsequently transferred to a limewater bath. While the mortar bars remained in the lime bath, the mortar cubes were tested

periodically for their compressive strength until a strength of 20 MPa (2,850 psi) was achieved.

4.3.2.1 Accelerated Test Method – Induced Cracking (IC)

For the accelerated test method to evaluate sulfate resistance, mortar bars were subjected to a high-temperature, drying-cycle to intentionally induce internal microcracks in the cement paste to accelerate the ingress of sulfate solution. When a compressive strength of 20 MPa was achieved from an average of two mortar cubes, half of the mortar bars (10) were subjected to a modified heat treatment regime similar to that used for DEF testing in Fu (1996) and Folliard, et al. (2005). The specimens were placed in an environmental cabinet at 60°C (140°F) for 24 hours to allow complete temperature equilibrium of the samples with the environment. All prisms were then allowed to cool to room temperature in limewater at 23 °C ± 2 °C (73 °F ± 4 °F) for a minimum of 1 hour and subsequently measured for their initial length and mass prior to being transferred to a container containing 5% and 0.89% sodium sulfate solutions. Figure 4-1 illustrates the time-temperature profile for accelerated performance test.

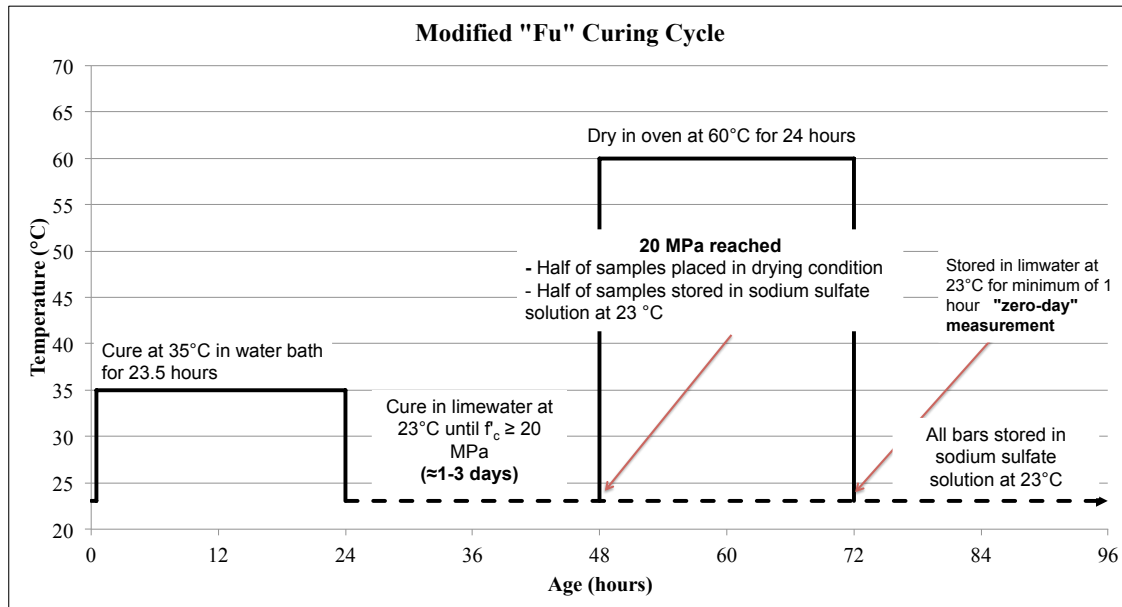


Figure 4-1: Curing cycle to introduce microcracks in the cement paste

Lengths and weights were measured at regular intervals with the sodium sulfate solution replaced every time in order to reduce the effects of leaching on the observed expansion (Wang, 1994). The expansion was determined by taking the average of the readings of four mortar bars. The duration of the test was 18 months unless sufficient damage occurred to prevent length-change measurements to be taken before the 18 months.

4.3.3 Performance limits for ASTM C 1012

The performance of different mixtures was evaluated by using the limits prescribed in ACI 318-14 (2014) building code requirements. Table 4-3 presents the maximum expansion for each sulfate exposure class. A mixture is considered to qualify for a Class 1 moderate exposure if it can keep expansion below 0.10% for 6 months when tested for sulfate attack using ASTM C 1012. Similarly, a mixture qualifies for a Class 2

severe sulfate exposure if the maximum expansion exhibited is below 0.10% for 12 months. Finally, a Class 3 very severe exposure requires the mixtures to keep expansion below 0.10% for 18 months when tested using ASTM C 1012 (ACI 201.2R, 2008)

Table 4-3: Performance limits as per ACI 318 for expansion in ASTM C 1012

Sulfate exposure class	Maximum expansion in ASTM C1012/C1012M-10 ¹⁵ test		
	Expansion (maximum) at 6 months, %	Expansion (maximum) at 12 months, %	Expansion (maximum) at 18 months, %
S1 Moderate	0.10	—	—
S2 Severe	0.05	0.10*	—
S3 Very Severe	—	—	0.10

*Twelve-month limit for S2 applies when expansion at 6 months exceeds to 0.05% limit.

4.4 RESULTS

4.4.1 5% Na₂SO₄ Solution

Figure 4-2 shows the expansion and mass change results for the Type I cement in combination with fly ash and/or silica fume in ternary blends for both the traditional ASTM C 1012 and proposed accelerated method. For clarity, the expansion and mass change results are presented alongside each other; the ASTM C 1012 results are presented at the top while the proposed accelerated method below it. The expansion and mass change up to 18 months (80 weeks) in 5% Na₂SO₄ is reported.

As expected, the control mixture (100% Type I cement) exhibited poor performance using the conventional ASTM C 1012 method and exceeded the expansion criteria at 6 months (0.17%), and was no longer measureable at 9 months. It is worth noting this is an important criterion when evaluating blended cements (cement + SCMs)

for sulfate resistance using ASTM C 1012 (ACI 201.2R, 2008). The Type I under investigation must exhibit poor performance and subsequently be improved when combined with an SCM to meet sulfate performance requirements.

The mixture containing 30% Class C fly ash exhibited faster deterioration than the control, exceeding the 0.10% expansion limit after 8 weeks, and completely disintegrating after 3 months. Note the sharp decline in the expansion value after 3 months for the blended mixture using Class C is a result of only one mortar bar available to measure. The performance of this mixture was somewhat improved when adding silica fume to the mortar. However, these mixtures still exceeded the expansion criteria of 0.10% expansion after 9 months in solution (0.24%) and were no longer measurable after 12 months. Research by Drimalas (2007), Dhole (2007), and Clements (2009) reported similar performance using a similar high-calcium ($\text{CaO} \approx 29\%$) fly ash in sulfate environments. Mixtures incorporating Class F fly ash exhibited the best performance of all the mixture using the Type I cement but still exceeded the 0.10% expansion limit after 18 months of measurements (0.17%).

The results for the mortars subjected to the drying regime to induce internal cracking and accelerate the sulfate ingress exhibited similar trends to the conventional ASTM C 1012 method but with a higher rate of expansion. For all mixtures using this method, the expansion limit of 0.10% was exceeded in 6 months or less; additionally, all mortar bars were no longer measurable after 12 months of measurements. The significant increase in rate of expansion was more notable in mixture that demonstrated “better” performance in ASTM C 1012 (I + 30% C ash + 5% SF and I + 25% F ash). These mixtures exhibited an expansion of $\geq 0.10\%$ in a third of the time that was originally reached in ASTM C 1012. The expansion rate for the control and binary mixture using Class C fly ash only observed a three and one month increase in terms of time to failure

($\geq 0.1\%$ expansion), respectively. Note on the binary mixture using Class C fly ash, only two mortar bars were measurable following the 12-week measurement as these bars completely disintegrated from sulfate exposure.

For the mass change results, there is a greater increase in the mass gain for the mortar bars subjected to drying regime. The initial mass uptake was on average an increase of 1.33% for all mixtures. In other words, the mixtures subjected to the drying regime increased in mass on average by 1.33% after one week of exposure in sodium sulfate solution. This is likely attributed to the significant amount of sulfates penetrating into the mortar bars and thus, accelerating the method.

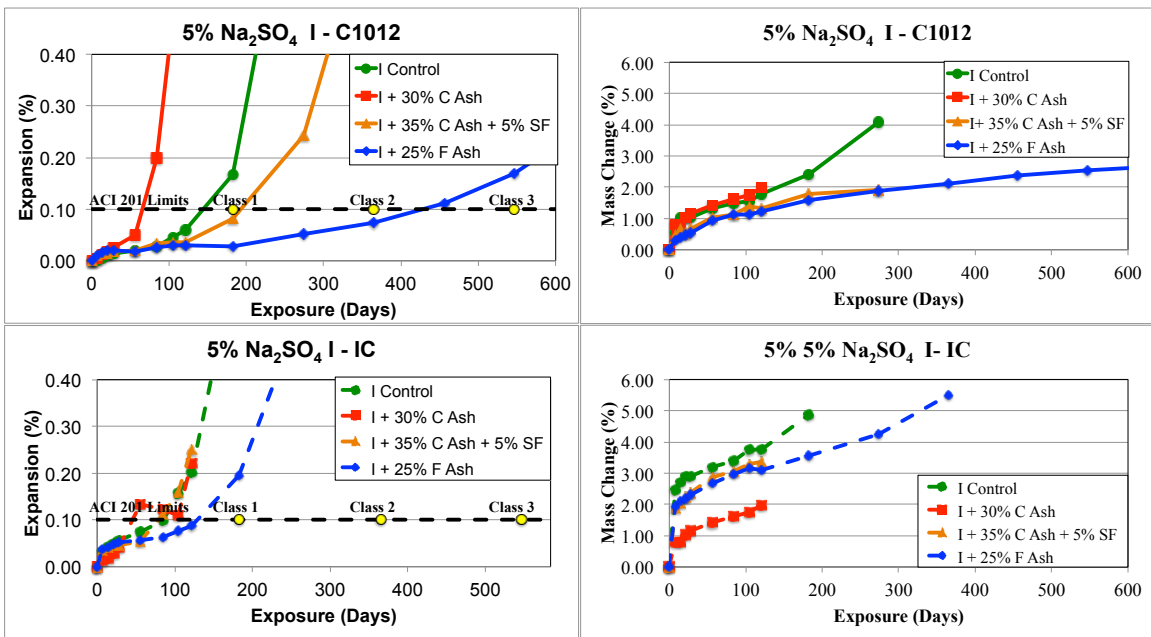


Figure 4-2: 18 month expansion and mass change results using C1012 (top) and accelerated method (bottom) for Type I cement, 5% Na_2SO_4

Figure 4-3 and 4-4 shows the expansion and mass change data up to 18 months (80 weeks) for all cement-fly ash and ternary blend mortar bars using Type I/II and Type V cement, respectively.

The control mixtures, tested using the traditional ASTM C 1012 method, exhibited better performance when compared to the Type I cement. These mixtures exceeded the maximum expansion of 0.10% at 9 month (0.19%) and 12 month (0.10%), respectively. All the bars cast with 30% Class C fly ash observed similar poor performance. Surprisingly, the ternary mixture (I/II + 35% C ash + 5% SF) had an inadequate performance under sulfate attack, exhibiting an increase in rate of expansion compared to the control, and surpassing the 0.10% expansion after 6 months of exposure.

When considering the results of the proposed accelerated method, the results are not as dramatic when compared to the Type I cement. For all the mixtures, the amount of expansion was notably higher at every measurement interval when compared to ASTM C 1012; however, all of the mixtures did not experience an increase in the rate of expansion and thus, did not exceed the 0.10% limit significantly faster than the traditional method. One thing interesting to note from the mass change results is the amount of initial mass uptake of sulfate solution was not as significant between the two methods.

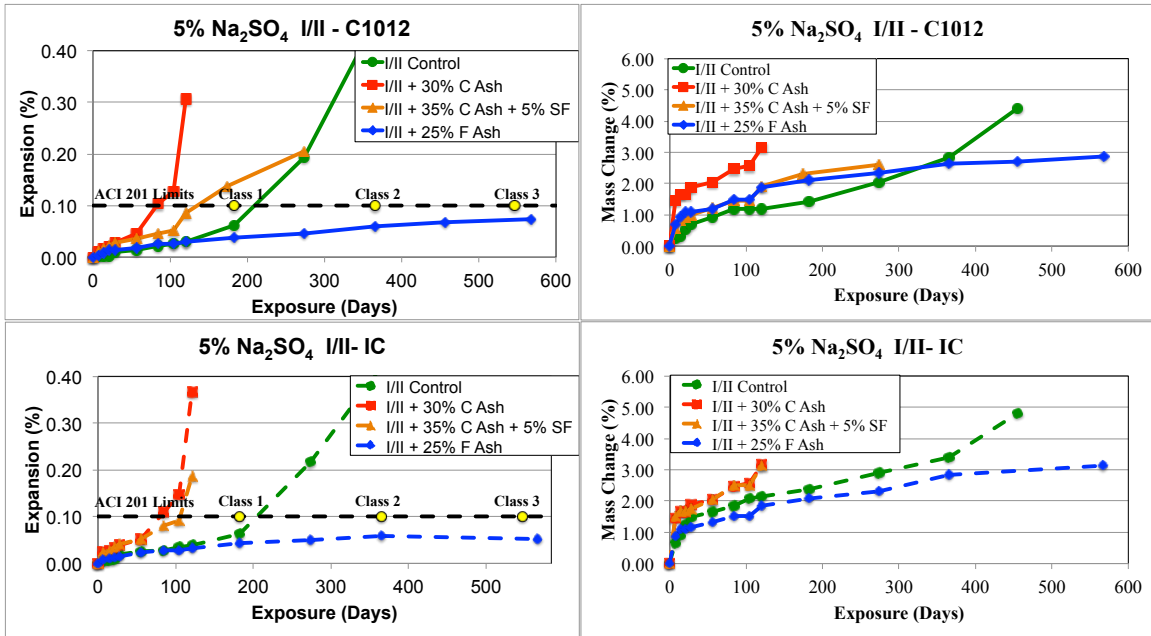


Figure 4-3: 18 month expansion and mass change results using C1012 (top) and accelerated method (bottom) for Type I/II cement, 5% Na₂SO₄

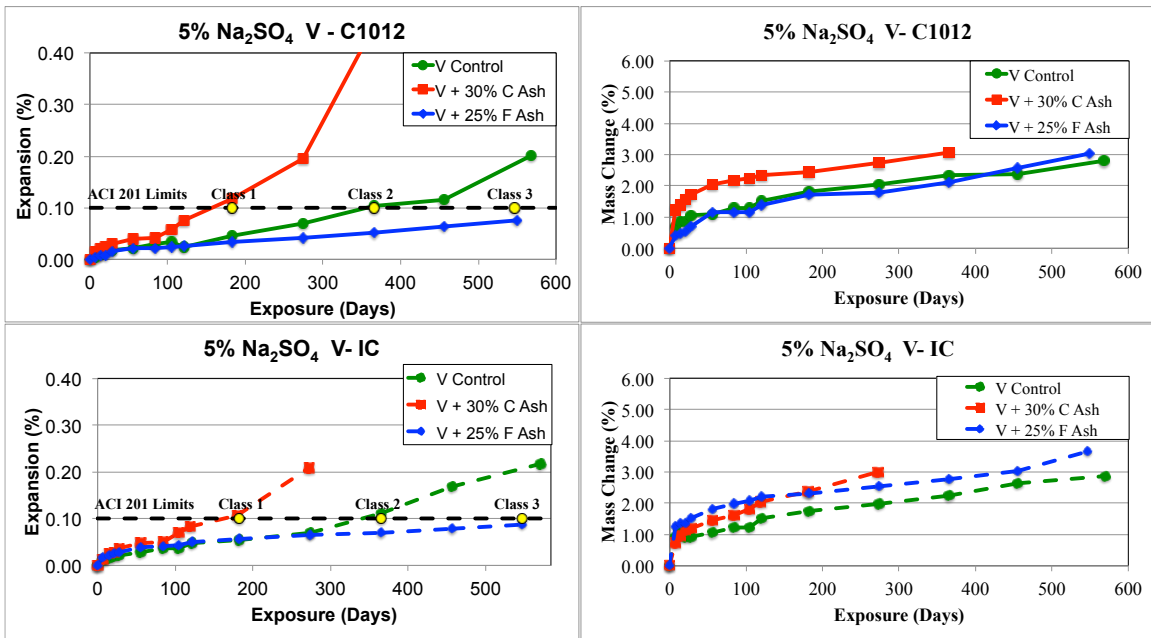


Figure 4-4: 18 month expansion and mass change results using C1012 (top) and accelerated method (bottom) for Type V cement, 5% Na₂SO₄

4.4.2 0.89% Na₂SO₄

Figure 4-5 shows the expansion and mass change results for the ASTM C 1012 and accelerated methods after 18 months (80 weeks) of exposure to 0.89% sodium sulfate. Although the rate of expansion was less, the trends are very similar to those mixtures placed in 5% sodium sulfate. Control mixtures observed a final expansion value of 0.57% at 9 months exposure in the accelerated method, whereas in the conventional method, it did not fail until 18 months at a similar expansion value (0.59%). When comparing between times of the final expansion, the accelerated method decreased the duration of the by more than half; a similar trend was observed when comparing between the time to failure as per ASTM C 1012 ($\geq 0.10\%$ expansion).

As expected, the binary mixture using 30% Class C showed poor sulfate resistance failing at 9 and 6 months for ASTM C 1012 and the accelerated method, respectively. The ternary mixture (Type I + 35% C Ash + 5% SF) and binary mixture using 25% Class F showed improved performance in comparison to those placed in 5% sodium sulfate (see Figure 4-2). The lower concentration resulted in significantly less expansion and measurements out to 18 months or longer; however, the accelerated method clearly showed faster rates of expansion when compared to ASTM C 1012. After 6 month of exposure, the ternary mixture began experiencing a significant increase in expansion rate exceeding the 0.10% criteria after 15 months. Thereafter, the mortar bars showed significant sign of cracks and deterioration with high expansion; however, the mortar bars were still intact and measurable after 18 months. Similar mortar bars tested in ASTM C 1012 just exceeded the limit at 18 months with an expansion of 0.10%. Interestingly, the Class F mixture did not exceed the expansion limit at all after 18 months of testing using ASTM C 1012 but did in the accelerated method.

The mass change in the mixtures using Type I showed a constant increase in the mass uptake up to 18 months (or failure) for all mixtures subjected to the accelerated method. The control mixture and Class F binary mixture showed significant uptake in the first few weeks. Although the mixture with 30% Class C and ternary (I + 35% C Ash + 5% SF) mixture showed less mass uptake in the first few weeks, they were still significantly higher than those bars cast and tested as per the procedures described in ASTM C 1012. The lower mass uptake may be owed to the tighter pore structure from the pozzolanic reaction of the silica fume. The mass loss associated with the Class C mixture is a result of the significant deterioration and spalling from the mortar bars resulting in a reduction in the average mass change.

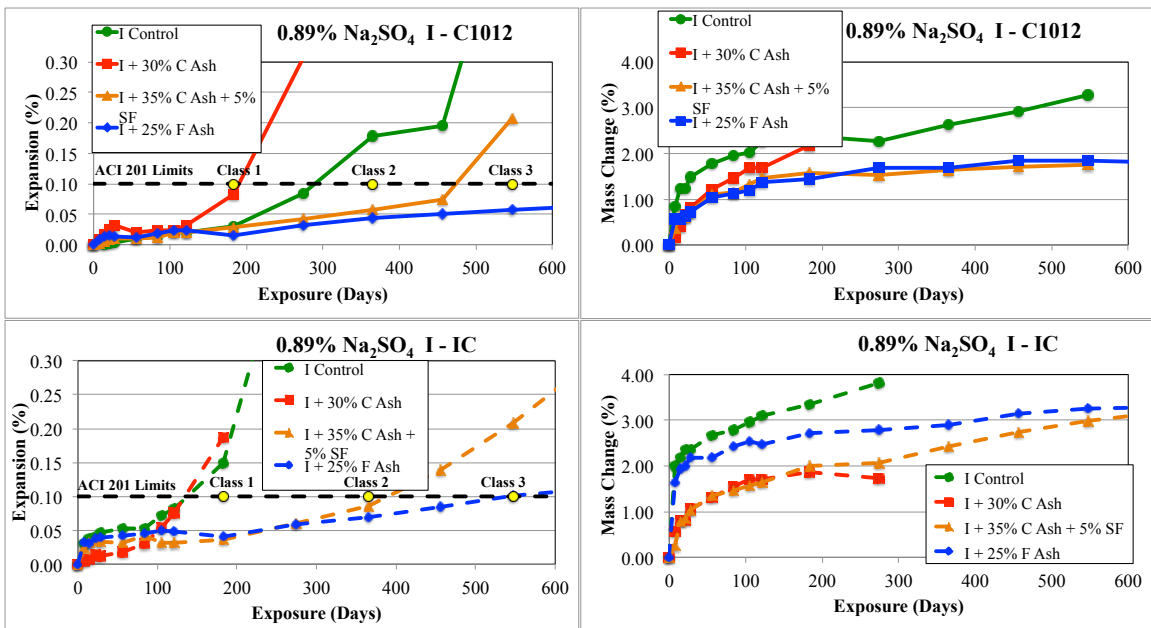


Figure 4-5 18 month expansion and mass change results using C1012 (top) and accelerated method (bottom) for Type I cement, 0.89% Na₂SO₄

Similar to the results presented for the mortar bars immersed 5% sodium sulfate, mixtures using Type I/II and Type V did not show a substantial increase in expansion

when using the accelerated method. Interestingly, the Class C mixture showed better performance when tested using the accelerated method. Higher expansions were observed after 6 months exposure using ASTM C 1012 and were no longer measurable after 9 months because they disintegrated. On the other hand, the control mixture showed worse sulfate resistance in terms of expansion having expansion value of 0.30% at 18 months; whereas, only 0.09% (and less than 0.10% expansion limit) for similar mortar bars tested using ASTM C 1012. With exception to the control mixture, no significant changes in expansions were observed for mixtures using Type V (see Figure 4-7). However, there were significant differences noted between the mass changes.

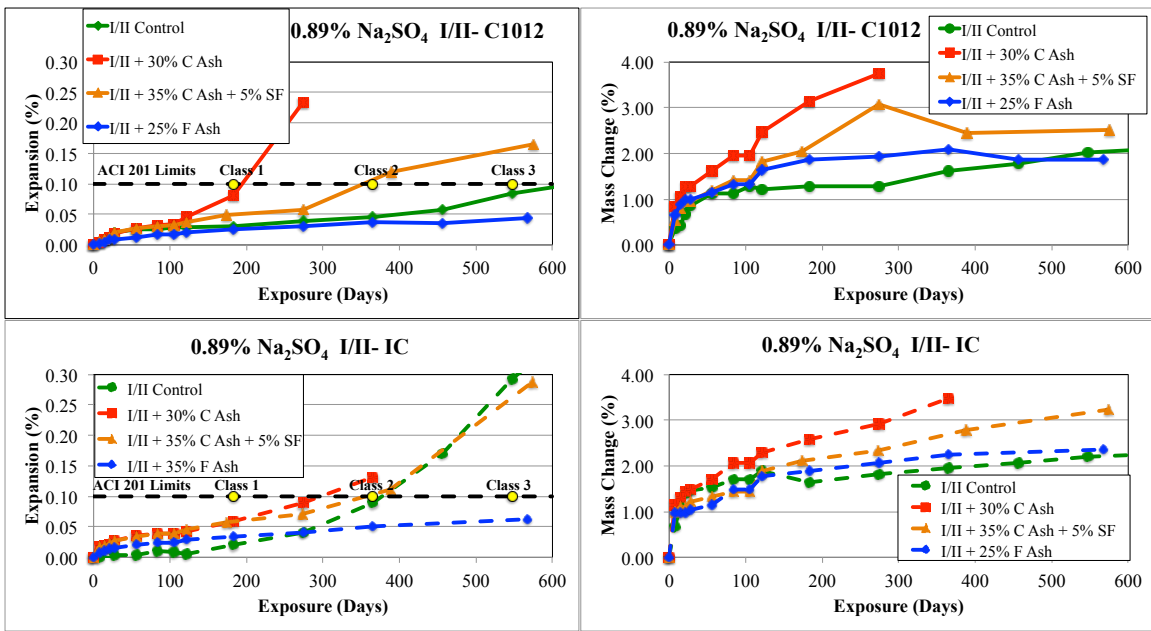


Figure 4-6 18 month expansion and mass change results using C1012 (top) and accelerated method (bottom) for Type I/II cement, 0.89% Na_2SO_4

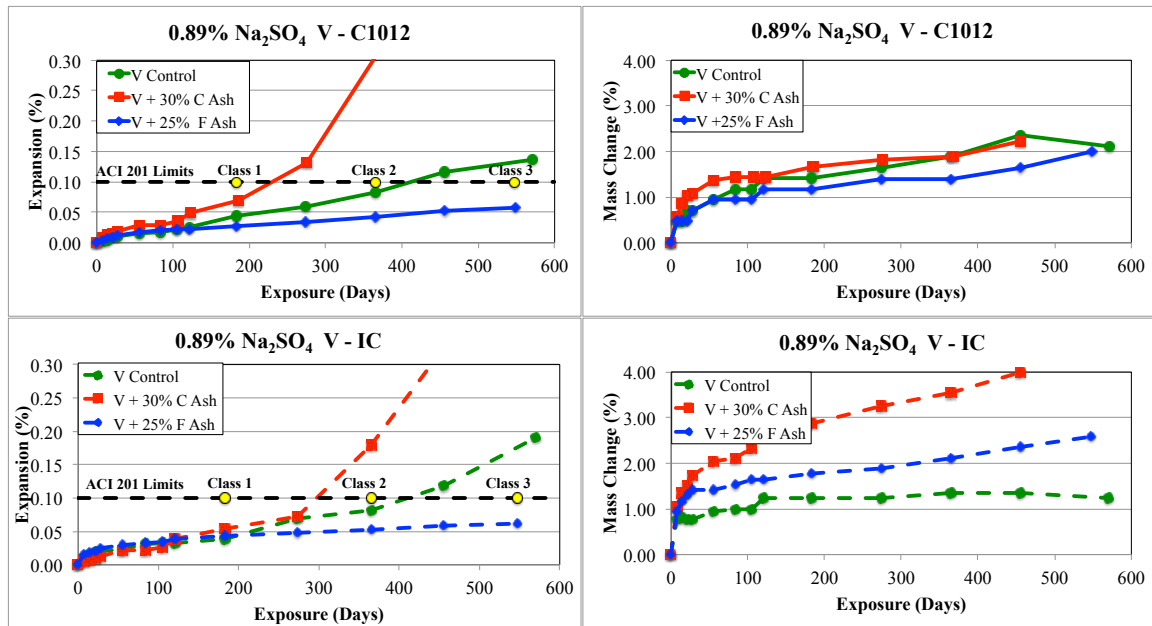


Figure 4-7: 18 month expansion and mass change results using C1012 (top) and accelerated method (bottom) for Type V cement, 0.89% Na_2SO_4

4.6 DISCUSSION

4.6.1 Implication of the Accelerated Method

The results indicate that, of the various cements and blended cements investigated, mixtures using Type I cement observed a significant increase in terms of expansion exceeding the 0.10% limit by less than half the time when compared to ASTM C 1012. However, those using Type I/II and Type V did not always follow similar trends. Several possible explanations exist for this type of performance seen.

4.6.1.1 Effect of maturity from drying regime

First, it is possible that the maturity of the mortar may be influenced when subjected to the drying regime at 60°C. For those mortar bars tested following ASTM C 1012, they were immediately immersed in sulfate solution upon achieving the specified strength (20 MPa) whereas the second-half of mortar bars are placed in an oven for an

additional 24 hours at 60°C (140°F). Although placed in a dry environment with very little (if any) humidity, the relatively high temperature may be influencing the microstructure of the mixture prior to sulfate exposure, especially for mixtures in combination with SCMs. Mehta (2008) pointed out that this was a significant contributing factor in how well a cementitious mixture would perform in a sulfate environment. The reduction of concrete permeability from the use of supplementary cementitious materials, lowering the water-to-cement ratio (w/cm), and reducing the aluminate and sulfoaluminate hydrates in the matrix can significantly decrease the risk to external sulfate attack

4.6.1.2 Effect of cement type and C_3A content

The cements evaluated in this study had varying amounts of tricalcium aluminate (C_3A) content. The C_3A content is said to play a major role in the susceptibility of mixtures to external sulfate attack (Stark, 1989). Consequently, the performance observed in mixtures using Type I/II and Type V cement using the accelerated method is likely a result of the reduction of the C_3A content. Although the mortar bars are assumed to experience microcracking in the bulk paste matrix, the lower C_3A content in the binder system does not promote the conversion of the aluminate-bearing phases to ettringite and thus, no significant expansion is observed.

4.6.1.3 Effect of induce cracking on the pore structure

Lastly, the purpose of the drying regime to intentionally induce microcracks in the paste may actually be improving the resistance due to the increase in pore space available for crystal growth. The initial low expansion could be explained by the ability of the mortars to accommodate ettringite crystal growth. When the volume of the pore space is finally exceeded, expansion occurs and this can be noted by the measured length change.

An increase in the pore size as well as the amount of pores available would thus allow ettringite room to form. The increase in mass may be attributed to the abundance of ettringite formed in these mixtures; however, significant expansion pressure to overcome tensile strength can only be exerted by ettringite which forms in small pores with a certain size range (Mullauer et al., 2013; Scherer, 1999).

4.7 CONCLUSION

The work described in this study was based on mortar bars subjected to a high-temperature (60 °C) for 24 hours prior to sulfate exposure to intentionally induce microcracks in the paste matrix to accelerate the ingress of sulfate ions into the bar. Although the results show a significant increase in the rate of expansion for mortars cast using Type I cement, similar trends were not as prevalent for those mixtures using Type I/II and Type V. Suggestions based on the physical parameters measured (i.e., mass and length change) indicate the drying regime may have a big influence on the maturity as well as creating additional pore space available for ettringite to form and thus, not having a significant impact on the observed expansion. Furthermore, regardless of the induced microcracking of the mortar bars, the lower C_3A content in the Type I/II and Type V cements do not promote the conversion of ettringite. Whereas, with the Type I cement, you expose a microstructure with much higher C_3A and hence, a higher chance for sulfate attack. Microstructural observation of the mortar bars post-drying should be considered to determine the extent of impact from the accelerated method and its influence on sulfate ingress and chemical reaction.

Chapter 5: An Accelerated Method to Evaluate Mixtures Subjected to Chemical Sulfate Attack Part II: Vacuum Impregnation

5.1 ABSTRACT

External sulfate attack continues to be a major threat to the long-term durability of concrete structures. In order for preventive measures to be taken, the combination of concrete materials must satisfy standardized values when tested using performance testing such as ASTM C 1012/C1012M. A study was carried to design and develop an innovative accelerated test that determines the susceptibility of cementitious mixtures to sulfate attack while keeping the duration of the test fairly short. This chapter presents an accelerated test method that can produce results in less than one-half the time of ASTM C 1012/C1012M. The method described herein uses similar mortar bars as per ASTM C 1012 in which the porosity of each sample is filled with a sodium sulfate solution in order to accelerate the ingress and onset of chemical reactions between the sulfate (SO_4^{2-}) and hydrated cement paste. Thereafter, the mortar bars are immersed in a solution at the same concentration and monitored for their expansion at regular intervals as per ASTM C 1012/C1012M. The mortar bars impregnated with sulfate solution failed significantly earlier than their companion bars cast and not impregnated. Visual observations of the bars demonstrated the severity of attack when fully impregnated. The resulting expansion of the mortar bars and mass change were measured and compared to their companion bars that were not impregnated with sulfate solution. In addition, the influence of curing age and sulfate concentration are also examined.

5.2 INTRODUCTION

Deterioration of concrete as a result of chemical reactions between the hydrated cement phases and external sulfate ions has been a subject of major controversy for many decades. Commonly known as external sulfate attack, this form of deterioration can cause severe damage to concrete structures that resulting in premature failure. Consequently, appropriate test methods are needed to determine the resistance of concrete under sulfate exposure.

Test methods for determining sulfate resistance are continuously being studied by many researchers. The majority of these test methods are based on a simple expansion approach originated in the early 19th century with expansion limits as the main acceptance criterion for the selection of cementitious materials. Additionally, existing laboratory tests typically evaluate the sulfate resistance of the binder through experiments on paste or mortars specimens that are often tested in severely aggressive conditions to obtain results within a reasonable timeframe. Moreover, the use of mortar or paste specimens leads to an even greater disconnect from the complicated mechanisms encountered in field conditions (Cohen & Mather, 1991). However, accelerated test methods are most suitable since sulfate attack is typically a long-term process.

In this study, the general aspects of sulfate attack in blended cement materials are discussed, followed by a brief overview of different test methods proposed by other researchers for determining sulfate resistance of cement based binders. Additionally, an alternative test method is presented in which mortar bars are vacuum impregnated prior to static immersion in sulfate solution as a means of accelerating the ingress of sulfates. This study evaluates the performance of mortar bars cast using a combination of cementitious materials. For comparison, the specimens with the same mixture proportions were evaluated in accordance with the ASTM C 1012/1012M (2008) method.

5.2.1 Sulfate Attack Mechanisms

Sulfate attack comprises a series of chemical reactions between sulfate ions and the constituents of the cement paste. It is generally agreed that the two main reaction products responsible for the observed deterioration are gypsum and/or ettringite (ACI 201.2R, 2008; Skalny et al. 2002); however, the formation of these phases and damage associated from them remains somewhat unclear. The migration of sulfate ions into the concrete can be accompanied by a gradual dissolution of portlandite and decomposition of the calcium silicate hydrate (C-S-H) phase. Depending on the type and concentration of the sulfate ion the concrete structure is subjected to, the severity of damage can lead to either volumetric changes and/or gradual strength loss in the concrete structure (Skalny et al., 2002). For example, attack from solutions containing sodium sulfate as the primary associated cation typically involved the formation of ettringite and gypsum and in very severe cases, decomposition of the C-S-H phase as increasing amounts of Ca^{2+} are released (Gollop et al. 1992; 1995). On the other hand, soils and seawater containing sulfates of magnesium can lead to the formation of other deleterious products such as brucite ($\text{Mg}(\text{OH})_2$) and gradual decomposition of C-S-H. Magnesium sulfate has a far more reaching reaction as compared to that of other sulfates because of its reaction with calcium silicates, in addition to the formation of gypsum and/or ettringite (Dhole 2008; Drimalas, 2007). The formation of brucite has a very low solubility giving a low pH value of 10.5 only in saturated solution (Skalny et al., 2002) destabilizing calcium silicates and releases more calcium to balance the pH of the pore solution. Other commonly found sulfates in soils and groundwater include potassium and calcium. Many times these sulfates are found in combinations thereby the process of sulfate attack becomes more complex (Neville, 1995).

It is generally agreed that the use of appropriate combination of cement and supplementary cementitious materials (SCMs), as well as minimizing permeability, is the key to ensuring good long-term performance for concrete exposed to sulfate-rich environments (ACI 201.2R, 2008). The use of a sulfate resistant portland cement such as Type II and Type V can reduce the severity of attack by limiting the C_3A level of the cement. When sulfate ions, coming from an internal or external source, react with C_3A in the presence of moisture, ettringite is formed, causing considerable expansion and cracking of the concrete structure. As such, in order to control the resistance against sulfate attack ASTM C 150 limits the C_3A content to 5% and 8% for Type V and Type II, respectively.

The use of SCMs and a low water-to-cementitious materials ratio (w/cm) can improve the resistance of concrete to sulfate attack by significantly reducing the permeability of concrete and slow down the ingress of external sulfate ions into the concrete (ACI 201.2R, 2008). Previous research has linked the reduction in sulfate expansions when SCMs are used to the decrease in portlandite content caused from pozzolanic reactions of the SCMs (Seraj, 2015; Janotka, et. al, 2011, Shehata et al., 2008; Khatib & Wild, 1998; Khatri & Sirivivatnanon, 1997). The conversion of portlandite to C-S-H creates a highly dense microstructures and reducing ionic diffusivity. Furthermore, the depletion of portlandite in the system limits the amount of gypsum formed from external sulfates in the hardened concrete. The use of low-calcium Class F fly ash typically improves sulfate resistance (compared to Class C) [Dhole et al., 2011], whereas Class C fly ashes can impart inferior sulfate resistance as a result of the presence of reactive calcium-aluminate glass and crystalline phases (Dhole et al., 2013).

5.2.2 Sulfate Attack Test Methods

Many of the test methods used for determining sulfate resistance involve the immersion of mortar samples in a test solution. Others perform continuous wetting and drying cycles in order to simulate the effects of damage from salt crystallization. Additionally, many researchers use different sulfate solutions and concentrations as well as use various physical parameters to qualify sulfate resistance of cementitious materials. For example, Koch (1960) and Locher (1956) determined the sulfate resistance of mortars by the decrease in flexural strength between samples placed in sodium sulfate and companion samples stored deionized water. Other tests, such as the ASTM C 1012 (2008) test method, monitor the expansion of mortar bars placed in a 5% sodium sulfate solution and can satisfy the standard if the mortar bars observe an expansion $\leq 0.10\%$. ASTM C 1012 replenishes the testing solution periodically whereas other test methods use the same test solution throughout the duration of the test. Mehta and Gjorv (1974) used a circulating solution in which the pH is kept constant by manual titration with H_2SO_4 . Mehta (1975) automated the aforementioned procedure by means of a continuous titration with H_2SO_4 , while monitoring the pH using a pH controller. According to Mehta, the procedure details were found to be adequate to yield reproducible results. Brown (1981) used a similar experimental setup reporting that controlling the pH of the sulfate solution more accurately represents field conditions and leads to a much rapid expansion of mortar bars than a typical non-controlled pH sulfate solution.

Ferraris et al. (2005) studied the specimen size effect showing that smaller size prisms (10 x 10 x 100 mm [0.4 x 0.4 x 1.5 in]) increased the expansion rate, enhancing the test results in much less time than the standard 25 x 25 x 285 mm (1 x 1 x 11.25 in) specimens. However, the test specimens were cast using paste samples, which further differs from field conditions. Ferraris et al. (1997) also tested cylinders with constant

length of 152 mm (6 in) and varying diameters (25, 50, 75 mm [1. 2. 3. in]) exposed to sulfate solutions from the sides concluding that the expansion from external sulfate attack is mostly governed by ionic diffusion and could hence be accelerated using smaller specimens (Bonakdar & Mobasher, 2010).

Other researchers have proposed other innovative techniques to determine sulfate resistance. More recently, Huang et al. (2015) used an electrical pulse cycle as an external electrical field to accelerate the migration of sulfate into mortar bars and thus accelerate the attack. They found that the electrical pulse resulted in significant mechanical strength loss due to the formation of massive sulfate products.

5.3 MATERIALS AND EXPERIMENTAL METHODS

5.3.1 Materials and Mixture Proportions

Three ASTM C 150 cements with varying tricalcium aluminate (C_3A) content were chosen for the study. Table 5-1 presents the chemical composition of the ASTM C 150 Type I (C1), Type I/II (C2), and Type V (C5) portland cements. Several mixtures were cast in this study that included plain and blended cements of Class C fly ash (CA), Class F fly ash (FA), and ternary mixes of Class C fly ash mixed with silica fume (SF). All supplementary cementitious materials were used as a percent replacement of mass of cement. For comparison between the various methods investigated in this dissertation, including the method presented in this chapter, mixtures proportions were matched to those previously discussed in Chapter 4.

Table 5-1: Chemical composition of cementitious materials (Wt. %)

Cements	Chemical Composition								Compound Composition of Clinker (Bogue)			
	SiO ₂	Al ₂ O ₃	Fe ₂ O ₃	CaO	MgO	Na ₂ O	K ₂ O	SO ₃	C ₃ S	C ₂ S	C ₃ A	C ₄ AF
Type I (C1)	19.71	5.21	2.54	63.58	1.16	0.13	0.90	3.06	70.35	3.45	9.52	7.72
Type I/II (C1)	20.38	4.90	3.55	63.62	1.14	0.11	0.67	2.86	66.07	8.60	6.98	10.80
Type V (C1)	20.98	3.66	3.71	62.95	4.55	0.24	0.34	2.70	66.88	9.71	3.42	11.29
Supplementary Cementitious Materials												
Class C Fly Ash (CA)	30.76	17.75	5.98	28.98	6.55	2.15	0.3	3.64				
Class F Fly Ash (FA)	48.48	25.01	3.56	15.92	2.5	0.3	0.71	0.72				
Silica Fume (SF)	93.17	-	2.1	0.8	0.3	-	-	0.2				

Table 5-2: Mixture proportions

Portland Cements		Supplementary Cementitious Materials		
Cement Type	w/cm	CA (Wt. %)	FA (Wt. %)	SF (Wt. %)
C1	0.485	-	-	-
	0.485	30	-	-
	0.485	-	25	-
	0.485	35	-	5
C2	0.485	-	-	-
	0.485	30	-	-
	0.485	-	25	-
	0.485	35	-	5
C5	0.485	-	-	-
	0.485	30	-	-
	0.485	-	25	-

5.3.2 Methods

5.3.2.1 Sample preparation

Standard mortars were used for all of the mixtures prepared in this study. All mortar mixtures were proportioned and prepared following the procedures prescribed in ASTM C 1012/1012M (2008) with sand to cementitious (cement + SCMs) ratio of 2.75:1, and constant water-to-cementitious ratio (w/cm) of 0.485.

ASTM C 1012 specifies a 5% (33,800 ppm SO_4^{2-}) sodium sulfate solution for evaluating sulfate resistance of mortars. However, this concentration has often been regarded as too aggressive and not indicative of field exposure. As part of this study, a 0.89% (6,000 ppm SO_4^{2-}) sodium sulfate solution was used to evaluate the influence of sulfate concentration on the rate of expansion. The latter sulfate concentration corresponds to moderate Class 2 sulfate exposure according to ACI 201.2R *Guide to*

durable concrete (2008). This concentration was used in each of the methods investigated presented in the following sections.

5.3.2.2 ASTM C 1012

For the samples tested as per ASTM C 1012, twelve 25 x 25 x 285 mm (1 x 1 x 11.25 in) mortar bars, with a gauge length of 250 mm (10 in) and a sufficient number of 50 mm (2 in) cubes for determining strength were prepared. Immediately after casting, the molds were placed in large polyethylene bags, sealed, and submerged underwater at $35\text{ }^{\circ}\text{C} \pm 3\text{ }^{\circ}\text{C}$ ($95\text{ }^{\circ}\text{F} \pm 5\text{ }^{\circ}\text{F}$). All prisms were stripped from the molds at $23.5\text{ hr} \pm 0.5\text{ hr}$ and subsequently transferred to a limewater bath. While the mortar bars remained in the lime bath, the mortar cubes were tested periodically for their compressive strength until strength of 20 MPa (2,850 psi) was achieved.

When the mortar cubes reached 20 MPa, the mortar bars were measured for their initial length in reference to a standard invar. After the initial measurement, half of the mortar bars (6 for 5% Na_2SO_4 , 6 for 0.89% Na_2SO_4) were submerged in sodium sulfate solution at $23\text{ }^{\circ}\text{C} \pm 3\text{ }^{\circ}\text{C}$ ($73\text{ }^{\circ}\text{F} \pm 4\text{ }^{\circ}\text{F}$). Thereafter, the mortar bars were measured regularly after 1, 2, 3, 4, 8, 12, 15 weeks and 4, 6, 12, 15, and 18 months in solution unless failure occurred first; both sodium sulfate solutions (5% & 0.89% Na_2SO_4) were replaced with a new solution after each measurement.

5.3.2.3 Accelerated Test Method – Vacuum Impregnation (VI)

Sample prepared for the accelerated test method were cast similarly to the bars previously mentioned in ASTM C 1012; however, immediately after casting the mortar

bars were placed in a moist curing room at 100% relative humidity (RH) and $23\text{ }^{\circ}\text{C} \pm 2\text{ }^{\circ}\text{C}$ ($73\text{ }^{\circ}\text{F} \pm 4\text{ }^{\circ}\text{F}$) for 28 days prior to testing.

For the accelerated method presented in this chapter, a novel vacuum impregnation technique was used in which the specimens are immersed in a sulfate solution and subjected to a high-vacuum to accelerate the ingress of sulfate ions. The vacuum impregnation step can be considered as a means of accelerating the test by reducing the amount of time needed to obtain a sufficient amount of sulfate ions to cause damage in the samples (Messad et al., 2010). The porosity of each sample is filled with a sodium sulfate solution by sealing the specimens in a large vessel and introducing a negative pressure to drive the solution into the sample. Saturation of the pores in the sample eliminates the latent-diffusion phenomenon that is commonly associated with external sulfate attack. Figure 5-1 depicts an illustration of the proposed method intent to ingress sulfate ions into the mortar bars. The testing solution used for impregnation was the same concentration as that used in the ASTM C 1012 method (in this case 5% and 0.89% Na_2SO_4). Subsequently, specimens are measured for their length change at intervals similarly to the ASTM C 1012 method with the sulfate solution replaced after each measurement.

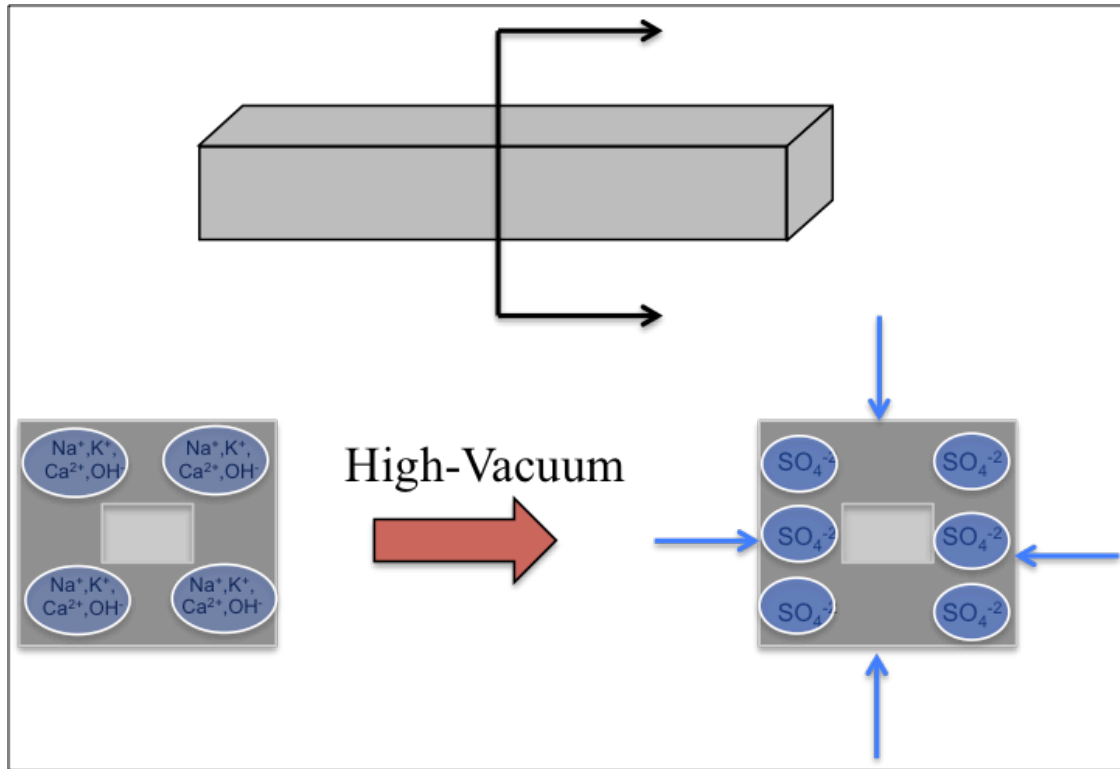


Figure 5-1: Illustration of vacuum impregnation method on a cross-section of a mortar bar

The technique used was similar to the AFPC-AFREM (1997) method for measuring the water porosity of concrete. Specimens were dried in an oven at $35\text{ }^{\circ}\text{C} \pm 3\text{ }^{\circ}\text{C}$ ($95\text{ }^{\circ}\text{F} \pm 5\text{ }^{\circ}\text{F}$) for a minimum of 14 days; the AFPC-AFREM (1997) method dries the sample at $105\text{ }^{\circ}\text{C} \pm 5\text{ }^{\circ}\text{C}$ until constant mass. The purpose of the drying period was to evaporate the pore water and permit the now-empty pores to be occupied by sodium sulfate. Investigation at the beginning of research project confirmed that without subjecting the bars to a drying period, the testing solution was unable to penetrate through the specimen. The results were confirmed through evaluation of the mass change in which there were no significant differences noted pre- and post-vacuum of the samples.

Following the drying period, the specimens are placed vertically in a sample holder and situated in a pressure tank designed for resisting high pressures. The samples were sealed and a vacuum pressure of 6.7 kPa (27.95 inches mercury) was maintained for 4 hours. Then, enough sodium sulfate solution was introduced to entirely cover the specimens. The specimens covered with the sulfate solution were left under vacuum for an additional 20 hours completing a 24 hour cycle. Figure 5-2 illustrates the external and internal views of the pressure tanks with samples placed in it. Figure 5-3 presents the overall test setup used in the laboratory. A step-by-step description of the procedures for performing the vacuum impregnation is provided at the end of this dissertation in Appendix B.

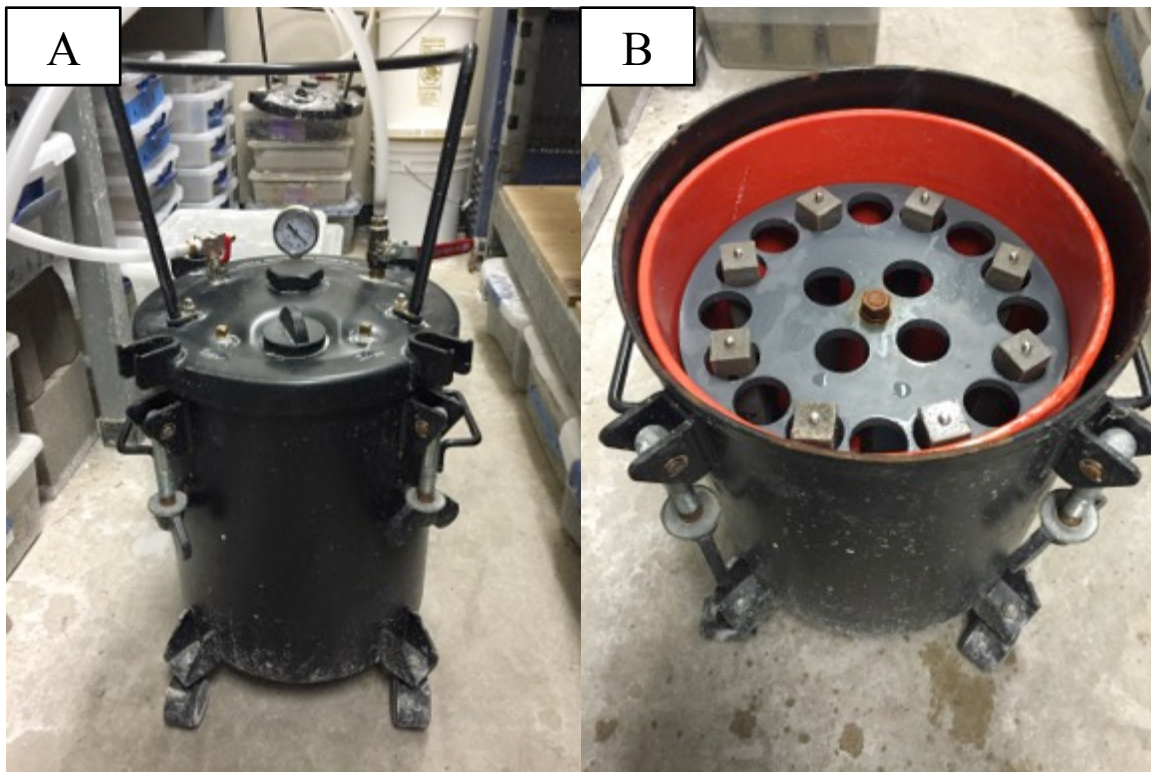


Figure 5-2: a) Internal view of sample placement; b) external view of pressure tank used for vacuum impregnation

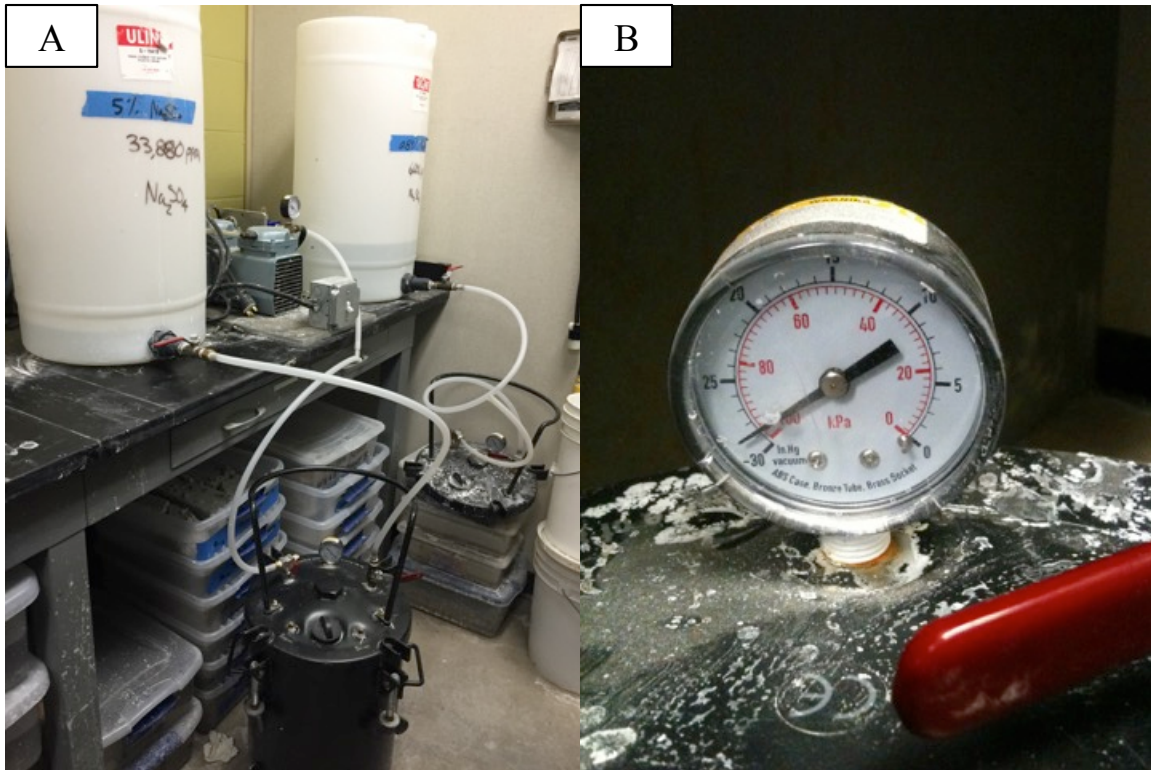


Figure 5-3: a) Vacuum Impregnation setup; and b) Pressure gauge illustrating the pressures experienced in the tanks

5.3.2.4 Maturity testing

Mortar bars were also prepared to evaluate the influence of curing and maturity on sulfate performance. All samples were proportioned and mixed according to ASTM C 1012 and subjected to following curing regimes:

- 28 day moist cure at 100% relative humidity (RH) and $23\text{ }^{\circ}\text{C} \pm 2^{\circ}\text{C}$ ($73\text{ }^{\circ}\text{F} \pm 4\text{ }^{\circ}\text{F}$) and placed in sulfate solution (not subjected to vacuum impregnation);

- Standard moist curing at 100% relative humidity (RH) and $23\text{ }^{\circ}\text{C} \pm 2^{\circ}\text{C}$ ($73^{\circ}\text{F} \pm 4\text{ }^{\circ}\text{F}$) until a strength of 20 MPa (2,850 psi) was achieved in two 50 mm (2 in) cubes and subsequently placed in sulfate solution; and
- Submerged underwater at $35\text{ }^{\circ}\text{C} \pm 3\text{ }^{\circ}\text{C}$ ($95\text{ }^{\circ}\text{F} \pm 5\text{ }^{\circ}\text{F}$) for 24 hours similar to ASTM C 1012 and subsequently testing following the aforementioned vacuum impregnation procedure

5.4 RESULTS AND DISCUSSION

The following section details the average measured expansion (% length change) of mortar bars cast in this study. Each of the average expansions was calculated from 4 mortar bars. Failure of the mortar bars is defined as length change exceeding 0.10% or fracture. The age of the mortar bars corresponds to the amount of time they were immersed in sodium sulfate solution.

5.4.1 Accelerated performance testing – Vacuum impregnation

5.4.1.2 Expansion and mass change in 5% Na_2SO_4

In 5% sodium sulfate solution, all of the mortar bars showed a significant increase in the rate of expansion when subjected to the vacuum impregnation technique. Figure 5-4 displays the results for plain and blended mixtures using C1 cement. With exception of the blended mixture using Class F fly ash, all mixtures exhibited rapid expansion and exceeded the failure criteria ($\geq 0.10\%$ expansion or fracture) after only 12 weeks of exposure. The blended FA mortar bar (C1 + 25%FA) remained $< 0.10\%$ expansion up to 4 months of exposure followed by a rapid increase in expansion thereafter and failing after 6 months of exposure. Relative to the performance in ASTM C 1012, all plain and blended mixtures reduced the duration of the test by over half. Remarkably, the time to

failure for the blended FA mixture was reduced by over 9 months relative to the ASTM C 1012 performance. This is a significant reduction in the duration of the test compared to companion mortar bars tested using ASTM C 1012.

Interestingly, although the mortar bars showed significant deterioration and crumbling along the sample (see Figure 5.5), there was still a large increase in the mass from the ingress of sodium sulfate into the bars. It is likely that the abrupt expansion observed in mortar bars is attributed to the development of cracks near and around the surface and subsequently leading to a significant amount of sulfate ingress as shown by the large mass change in Figure 5-4. In addition, the driving of the sodium sulfate solution into the mortar bars through the vacuum impregnation technique may be attributed to expansive reaction products forming near the center of the mortar, especially for a relatively small 25 mm (1 in) cross-sectional sample. Therefore, it is likely that the perceived expansion noted below is a better representation of observed linear expansion in the sample. Conversely, mortar bars tested using ASTM C 1012 typically observed scaling and minor deterioration at the surface before any significant expansion was recorded (see Figure 5-5).

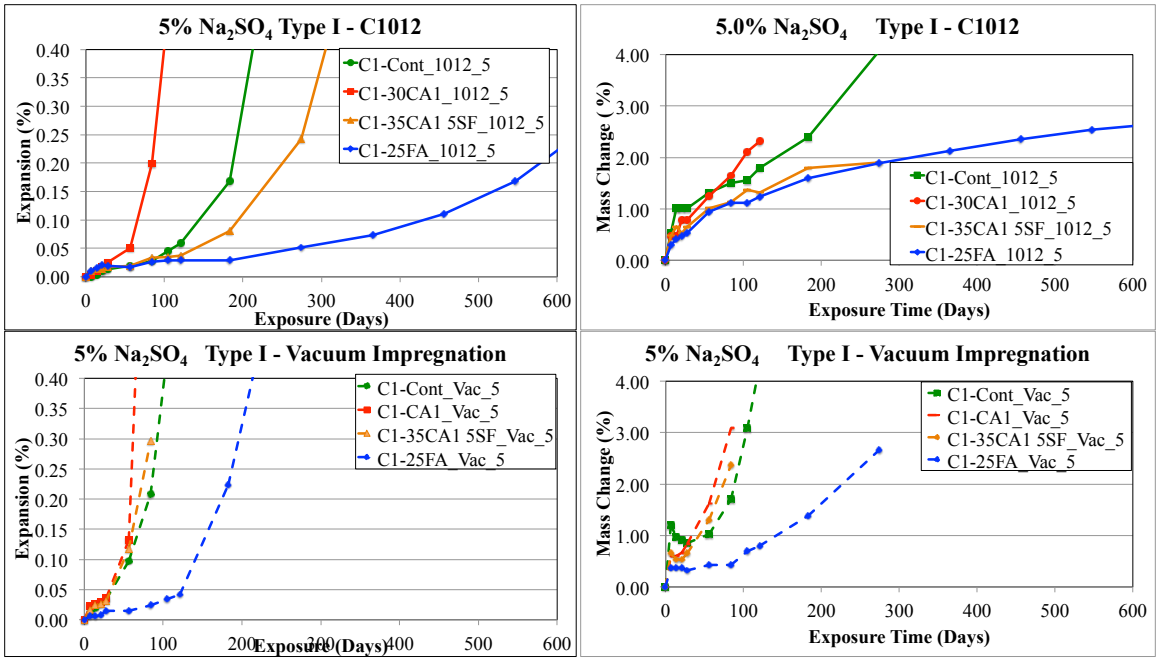


Figure 5-4: 18 month expansion and mass change results using C1012 (top) and accelerated method (bottom) for Type I (C1) cement, 5% Na₂SO₄

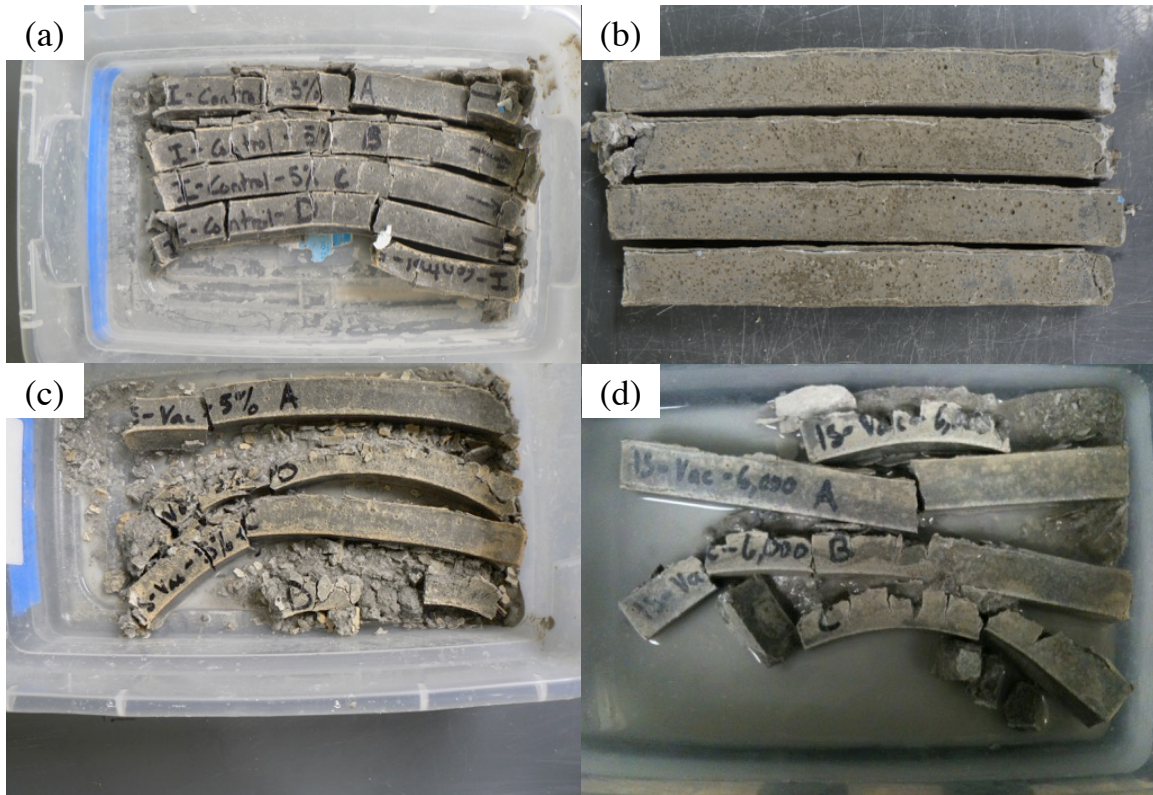


Figure 5-5: Visual appearance of mortar bars showing deterioration in: (a) C1 tested using ASTM C 1012 in 5% after 1 year; (b) C1 tested using ASTM C 1012 in 0.89% after 18 months; (c) C1 tested using vacuum impregnation in 5% around 4 months; (d) C1 tested using vacuum impregnation in 0.89% sodium sulfate at 6-9 months

Similar trends are seen in samples mixed using plain and blended C2 and C5 cements as shown in Figures 5-6 and 5-7. All C2 mixtures exceeded the 0.10% expansion by 6 months, whereas C5 mixtures all failed by one year of exposure. The expansion and the time to failure showed good correlation with the associated tricalcium aluminate (C_3A) content and ASTM C 150 designation for low, moderate, and high-sulfate resistant cements for the C1, C2, and C5 cement, respectively. For the plain cements tested in 5% sodium sulfate solution, the time to failure was reached at 12 weeks, 15 weeks, and 4 months for the C1, C2, and C5 cements, respectively.

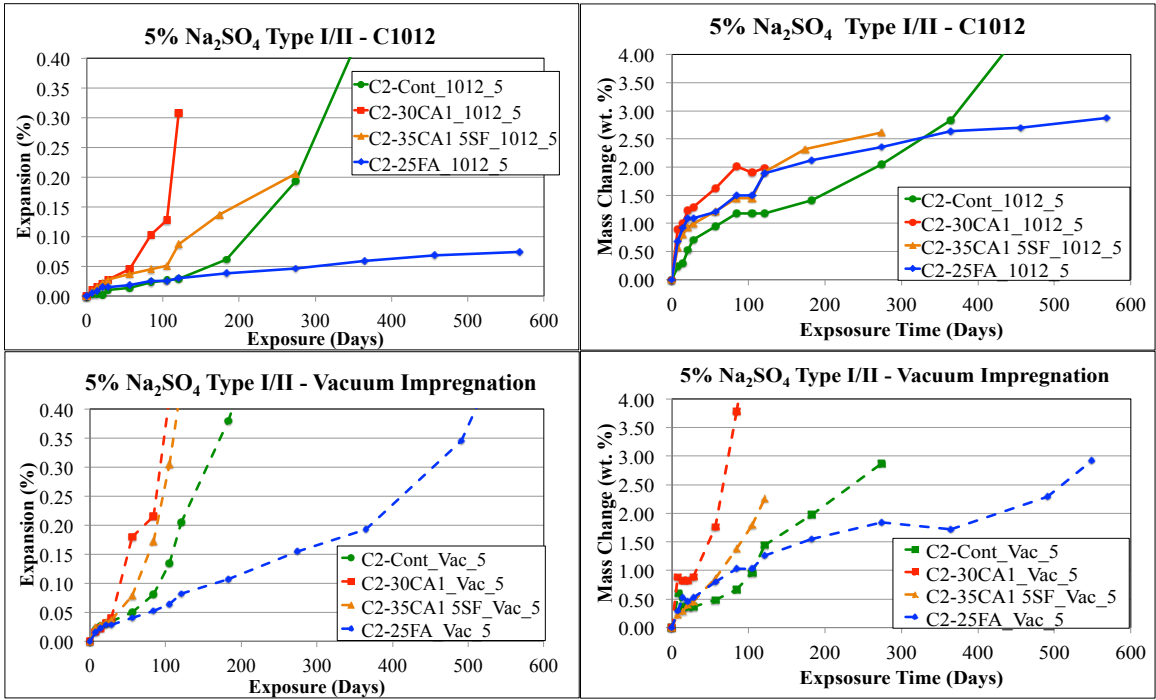


Figure 5-6: 18 month expansion and mass change results using C1012 (top) and accelerated method (bottom) for Type I/II (C2) cement, 5% Na₂SO₄

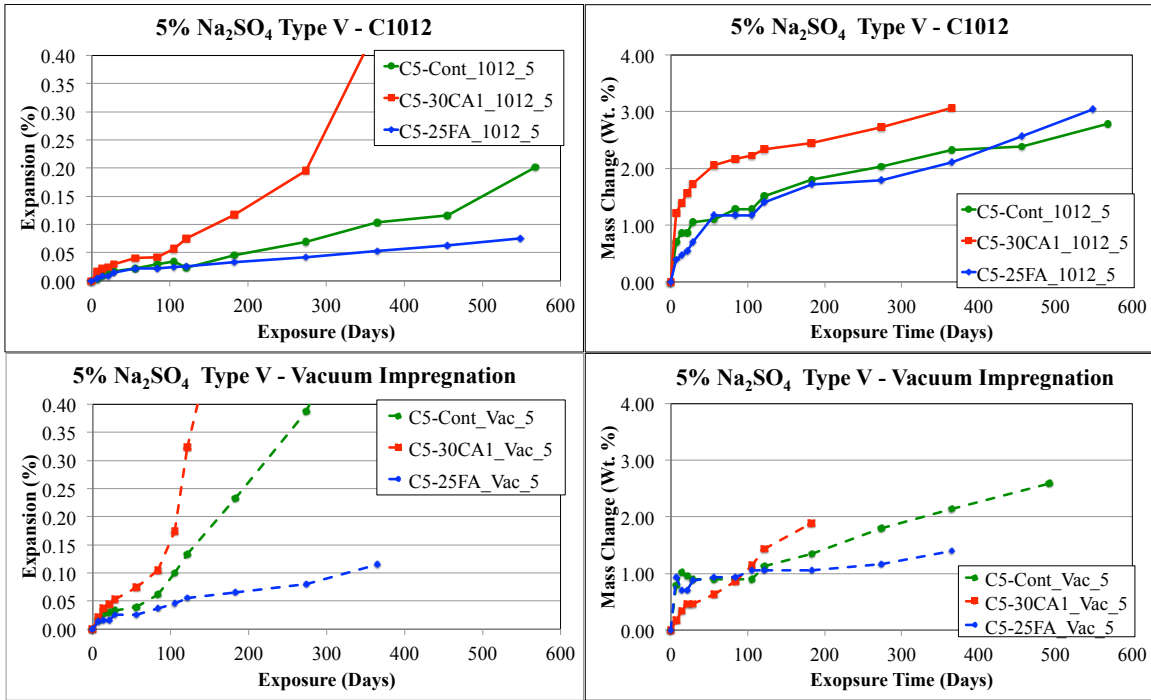


Figure 5-7: 18 month expansion and mass change results using C1012 (top) and accelerated method (bottom) for Type V (C5) cement, 5% Na₂SO₄

5.4.1.3 Expansion and mass change in 0.89% Na₂SO₄

Companion mortar bars were also tested using the methods discussed previously in 0.89% sodium sulfate solution. Figure 5-8 shows the expansion values for plain and blended C1 mixtures. After 6 months, the C1 and C1 + 30CA mortar bars were completely deteriorated and no longer measurable. At nine months, the ternary (C1 + 35CA + 5SF) mixture exceeded the 0.10% expansion (0.19%) and showed significant signs of cracks and slight warping of the bars. Interestingly, the ternary blend showed better performance when tested in 0.89% sodium sulfate, whereas in 5% observed a quicker onset of expansion (see Figure 5-4).

With the exception of the plain C5 and blended C5 + 25FA mixture, all mortar bars observed an expansion $\geq 0.10\%$ after 18 months of exposure in 0.89% sodium sulfate when tested using the accelerated method. Contrary to the expansion results of mortar

bars in 5% sodium sulfate, the sulfate performance of plain and blended C5 mixtures was not significantly affected by the accelerated method in 0.89% sodium sulfate solution. In fact, at fifteen months the expansion is higher for the C5 mortar bars tested using ASTM C 1012.

It is widely known that the sulfate concentration and type have a significant impact on the sulfate attack mechanisms. Typically, expansion is associated from the formation of ettringite crystal in very small pores within a certain size range (Scherer, 1999; 2004). Additionally, the mechanism is intensified with increasing concentrations and supersaturation of the pores with sulfate ions (Santhanam et al. 2002). The relatively low sulfate concentration, 0.89% Na_2SO_4 , used in this study may not be generating enough expansive pressure, especially for plain C5 and blended C5 + 25FA mixtures where the availability of aluminates for conversion to ettringite is substantially less. Nonetheless, the vacuum impregnation exhibited shorter durations in the time to failure for plain and blended C1 and C2 mixtures. This is a substantial benefit in terms of cost due to the significantly less sulfate powder required to make the 0.89% sodium sulfate solution.

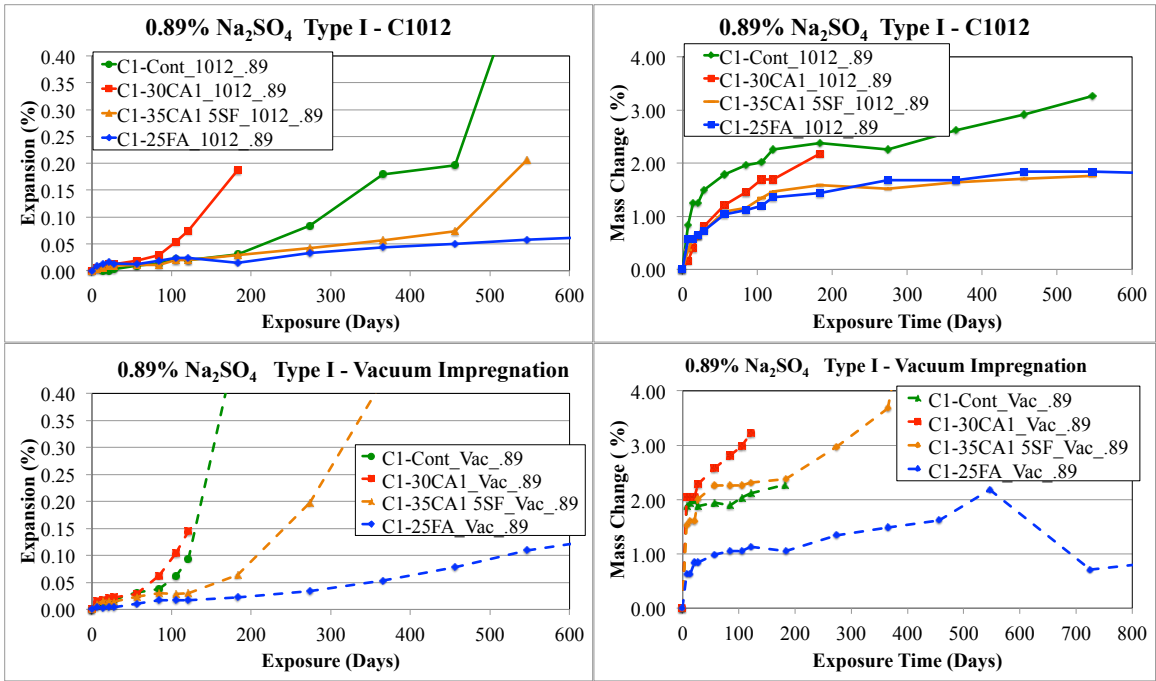


Figure 5-8: 18 month expansion and mass change results using C1012 (top) and accelerated method (bottom) for Type I (C1) cement, 0.89% Na₂SO₄

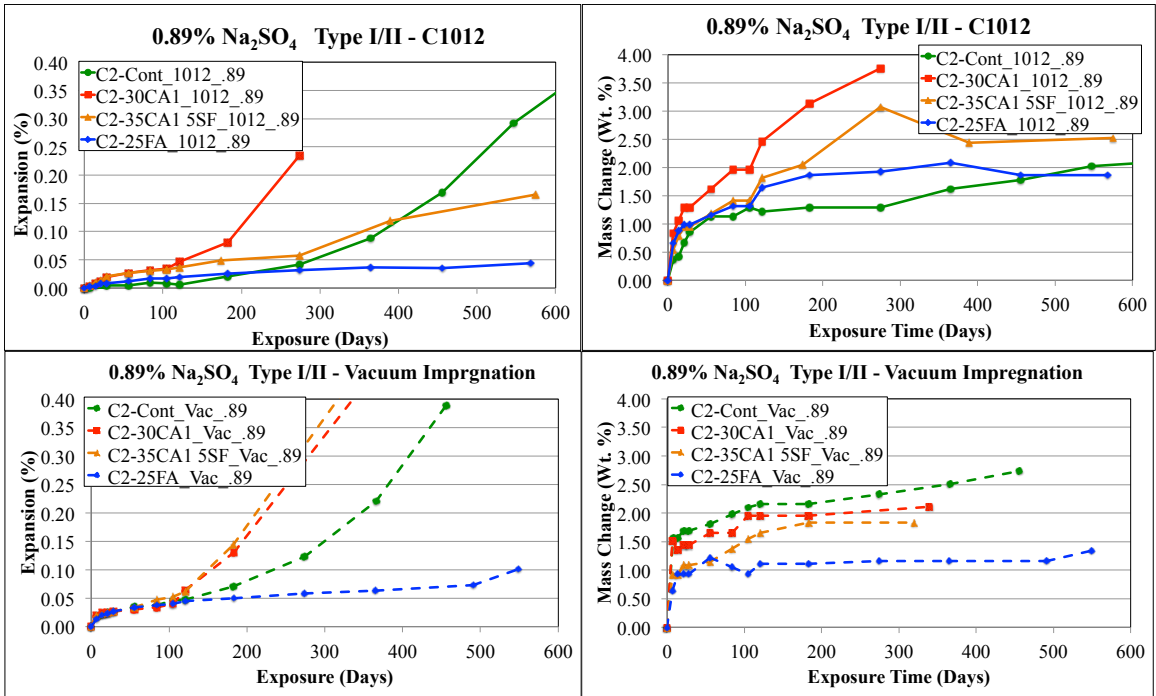


Figure 5-9: 18 month expansion and mass change results using C1012 (top) and accelerated method (bottom) for Type I/II (C2) cement, 0.89% Na₂SO₄

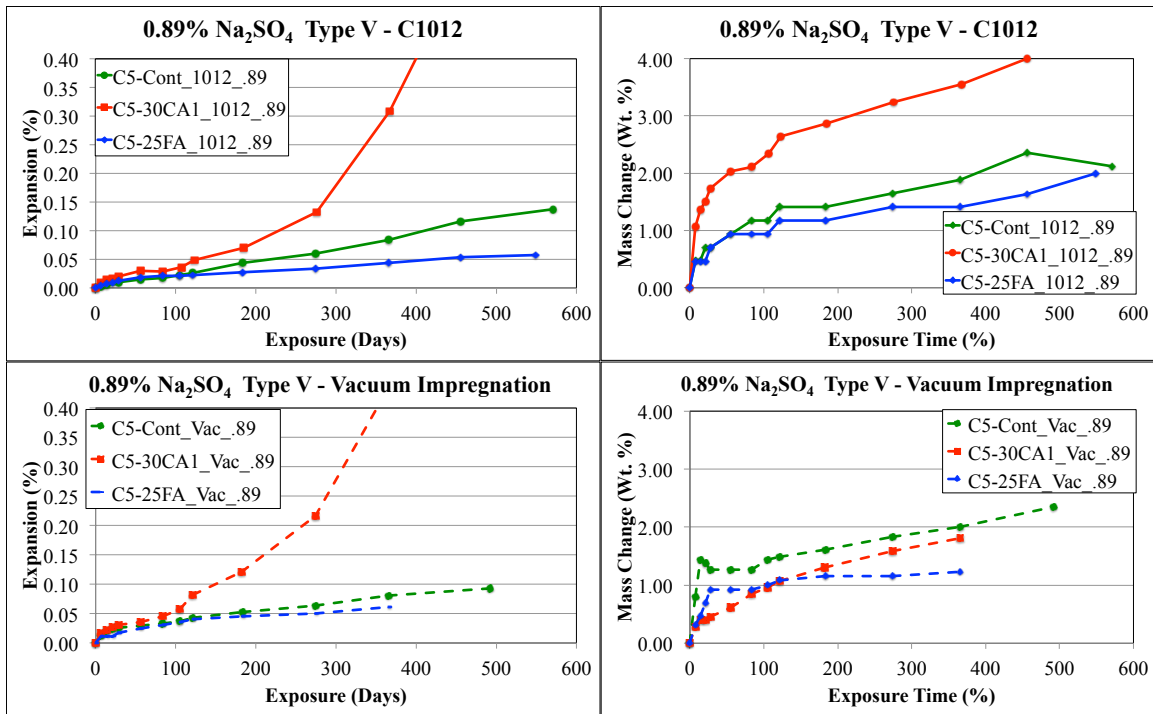


Figure 5-10: 18 month expansion and mass change results using C1012 (top) and accelerated method (bottom) for Type I/II (C2) cement, 0.89% Na₂SO₄

5.4.1.4 Influence of curing

The rate of expansion from the vacuum impregnation method was generally more rapid than the conventional ASTM C 1012 test, especially for mixtures placed in 5% sodium sulfate. However, the curing of the mortar bars raised some concern on the observed sulfate performance.

While the mortar bars tested following ASTM C 1012 were cured underwater for 24 hours at 35 °C ± 3°C (95 °F ± 5 °F) and subsequently monitored until a strength of 20 MPa (2,850 psi) is achieved (typically 1-3 days), the mortar bars subjected to the vacuum impregnation were cured in a moist room at 100% relative humidity (RH) and 23 °C ± 2 °C (73 °F ± 4 °F) for 28 days prior to testing. Thus, it was of interest to investigate the influence of the aforementioned curing regimes on sulfate performance. Figure 5-11

shows the expansion results for mortar bars cured in a moist curing room until a strength of 20 MPa (2,850 psi) was achieved from an average of two 50 mm (2 in) mortar cubes. These mixtures are designated as “2850” in the figure. The results are for mortar bars cast using plain and blended C1 cement and stored in 5% sodium sulfate solution. For comparison purposes, the results are plotted against companion mortar bars tested following ASTM C 1012.

Interestingly, very little differences were noted between the two curing regimes in terms of expansion values. Generally, slightly higher expansion rates were observed for the mortar bars placed in the moist curing room. The ternary mixture (C1 + 35CA + 5SF) showed the highest increase in expansion rate, failing after only 6 months of exposure. It is likely that the high volume of SCM content contributed to a slower degree of hydration in the mixture. The required compressive strength (20 MPa [2,850 psi]) used in this study might have not been enough to activate the pozzolanic reaction in the SCM and thus, it is likely the mortar bars exhibited a higher permeability prior to sulfate exposure leading the faster ingress of sulfate ions and early degradation. Mortar bars cured underwater at 35 °C (95 °F) showed better sulfate resistance most likely attributed to the increase of activation energy from the higher curing temperature and thus resulting in a less permeable microstructure.

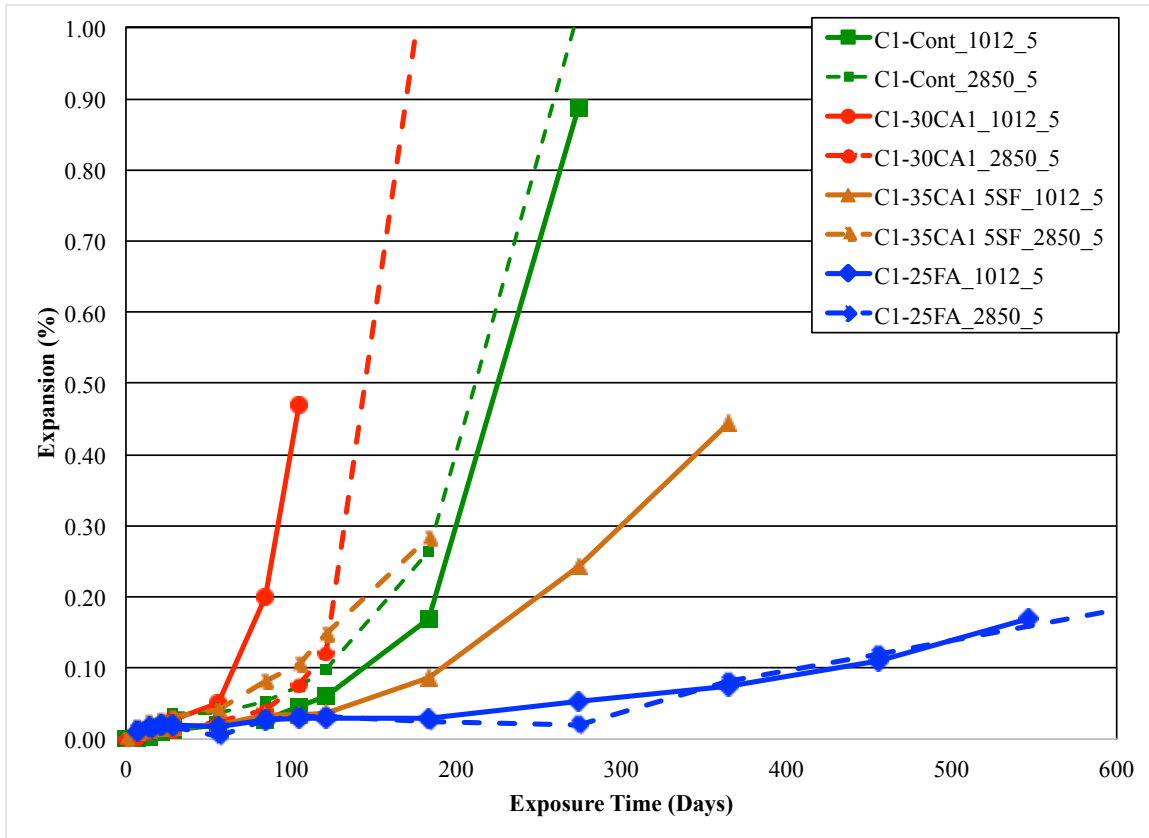


Figure 5-11: Comparison of expansion results for mortar bars cured in in a moist curing room until a strength of 20 MPa (2,850 psi) was reached and cured following the ASTM C 1012 procedures

Figure 5-12 shows the expansion results for the sets of mortar bars that were cured in a moist curing chamber at $23\text{ }^{\circ}\text{C} \pm 2\text{ }^{\circ}\text{C}$ ($73\text{ }^{\circ}\text{F} \pm 5\text{ }^{\circ}\text{F}$) for 28 days prior to placement in sulfate solution. Again, the ternary blend showed a higher onset of expansion in comparison to the to ASTM C 1012 curing regime. Interestingly, the added moist curing time did very little in improving the performance of the ternary mixture showing only a slightly lower expansion rate and with no change in the time to failure. The results emphasize the significance of appropriate curing procedures needed for

mixtures using high volume SCMs in order for the added benefits to play a contributing factor in improving the durability.

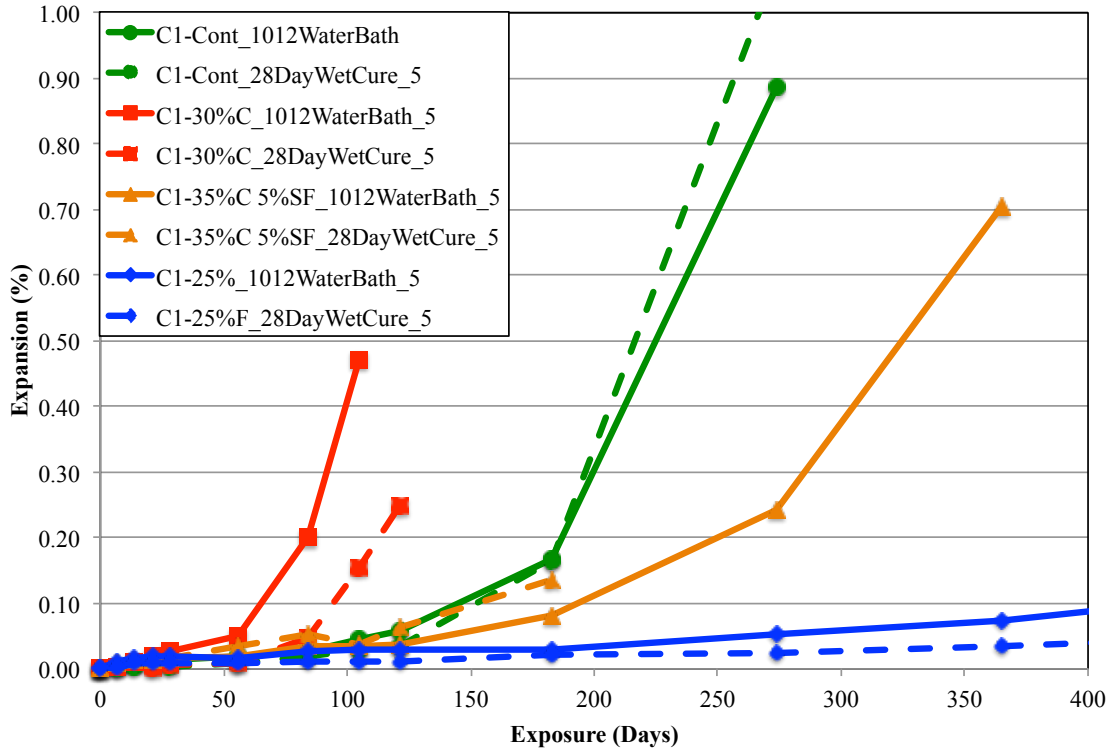


Figure 5-12: Comparison of expansion results for mortar bars moist cured for 28 days and cured following the ASTM C 1012 procedures

The comparison of expansion results between vacuum and non-vacuum impregnated mortar bars both moist cured for 28 days is presented in Figure 5-13. The results show the acceleration of the expansion from the use of the vacuum impregnation technique was not influenced by the selected curing regime. However, sulfate resistance was slightly better when the mortar bars are heat cured at 35 °C (95 °F) underwater prior to vacuum impregnation as evidence in Figure 5-14.

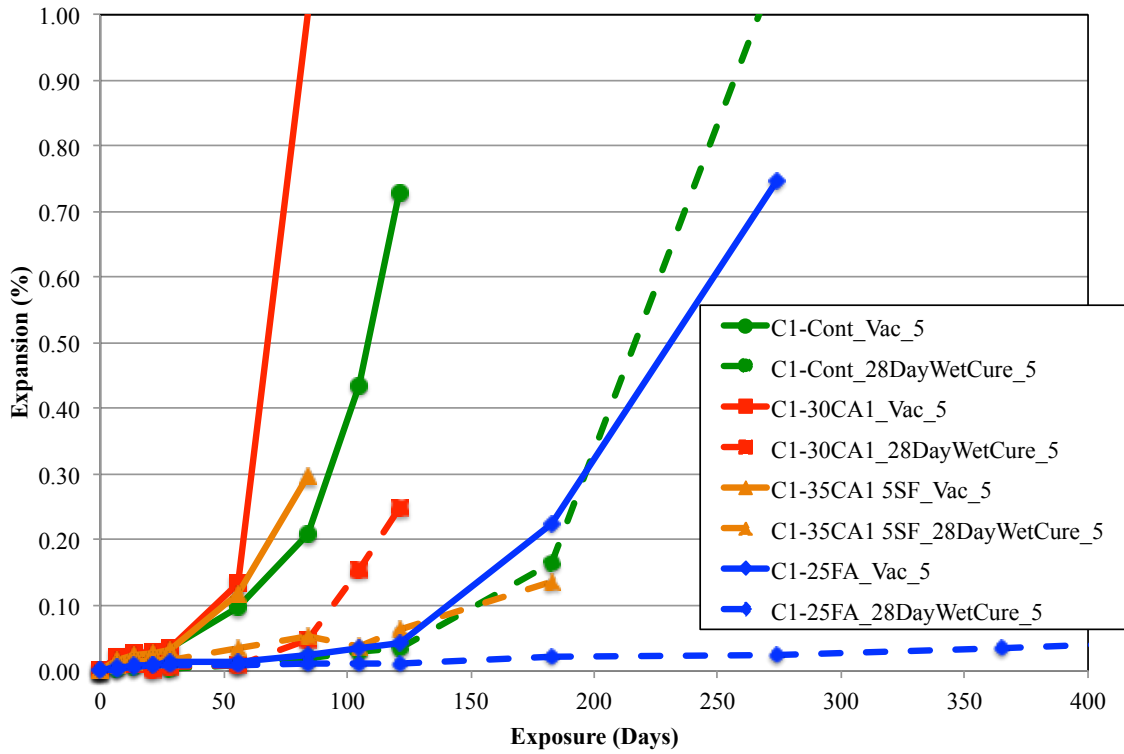


Figure 5-13: Comparison of expansion results for vacuum and non-vacuum impregnated mortar bars moist cured for 28 days

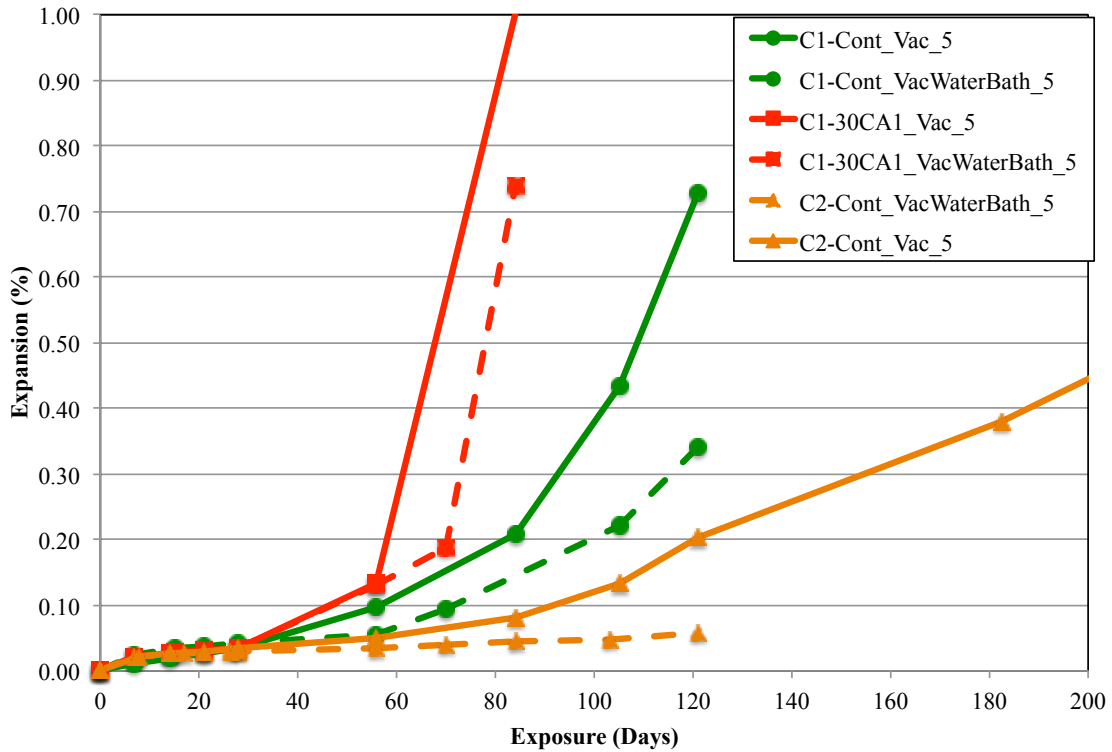


Figure 5-14: Comparison of expansion results for vacuum and non-vacuum impregnated mortar bars cured following the ASTM C 1012 procedures

5.4.1.5 Mass change of mortar pre- and post-vacuum impregnation

Figure 5-15 presents the mass change of the plain and blended C1 mixtures both pre- and post-vacuum impregnation. The exhibited mass loss in the mortar bars is associated to the drying regime where specimens are placed in an oven at $35\text{ }^{\circ}\text{C} \pm 3\text{ }^{\circ}\text{C}$ ($95\text{ }^{\circ}\text{F} \pm 5\text{ }^{\circ}\text{F}$) for a minimum of 14 days prior to vacuum impregnation to provide space for the ingress of sodium sulfate in the empty pores. The mass gain from the mortar bars fully immersed in sodium sulfate is nearly identical to the mass loss during drying. The increased mass gain on most of the specimens is assumed to be from the excess of surface water during measuring; the mortar samples are essentially “bone dry” after drying and thus do not significantly affect the results in comparison to post-vacuum measurements.

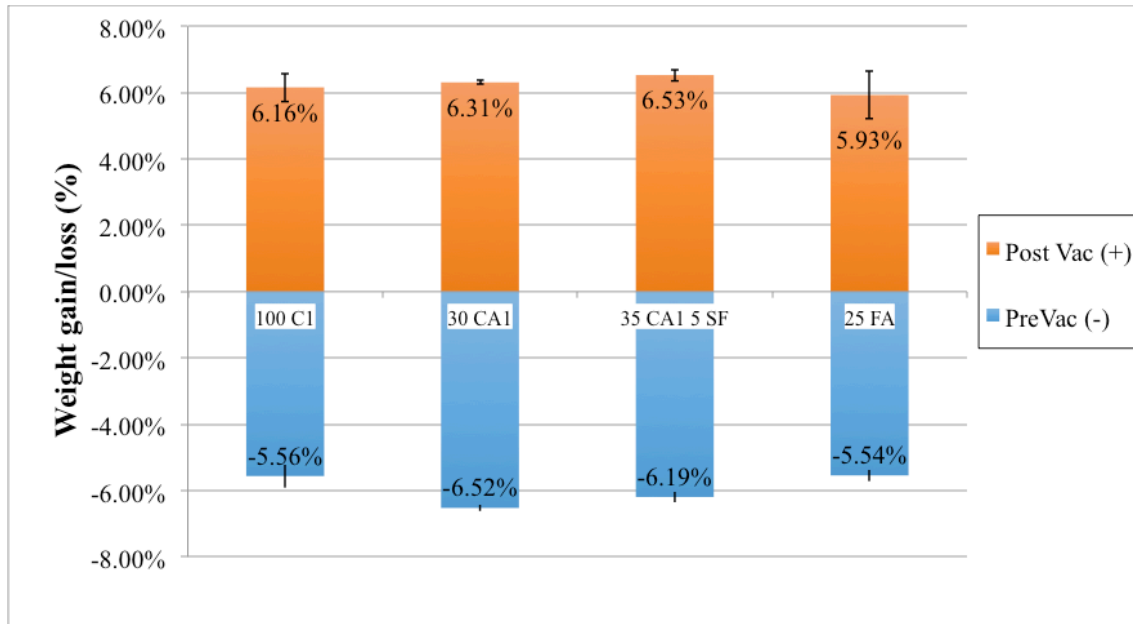


Figure 5-15: Mass gain/loss of mortar bars pre- and post-vacuum impregnation

5.6. CONCLUSION

The use of mortar bars vacuum impregnated with sodium sulfate solution prior to immersion in the test solution greatly reduced the duration of the performance test ASTM C 1012, particularly at higher sulfate concentrations (i.e., 5% Na_2SO_4). The change in mass gain and loss during vacuum impregnation confirmed the empty-pores of the mortar bars were being filled with sodium sulfate solution.

The ingress of sulfates into the mortar bars accelerated the chemical reaction between the hydrated cement phases and thus, the associated expansion from the formation of ettringite. It is likely that the depth of sulfate penetration from vacuum impregnation contributed to a series of expansive reaction near or at the center of the mortar bar and led to a better representation of the linear expansion observed from the physical measurements. Consequently, the latter resulted in macro-cracks at the surface

encouraging further penetration of sulfates into the mortar and thus, intensifying the expansion mechanism.

Although the vacuum impregnation accelerated the onset of expansion in the mortar bars, it was evident that the resistance of external sulfate attack is greatly influenced by the C_3A content of the portland cements. Furthermore, the expansion observed in mortar bars immersed in 0.89% Na_2SO_4 was relatively lower and showed less differences in performance between the ASTM C 1012 method for plain and blended C5 mixtures.

Further investigation of the accelerated method on additional cementitious mixtures is still needed. Repeatability between the observed expansion as well as development of appropriate expansion limits for the test method are still ongoing and require further consideration.

Chapter 6: Sulfate Resistance of Concrete: Simultaneous Evaluation of an Accelerated Method and Outdoor Exposure Site

6.1 ABSTRACT

It well known that concrete subjected to sulfate-bearing soils, groundwater and/or seawater can be subjected to deleterious sulfate attack. As such, preventive measures must be taken to ensure the concrete mixture is suitable for the intended sulfate environment through performance testing. The most common standardized test method for determining the sulfate resistance of a cementitious system is ASTM C 1012, which evaluates the performance of standard mortars exposed to a sodium sulfate solution. The method, however, requires a significant amount of time to obtain results making it a very unpopular test for practitioners. Interestingly, no standardized tests currently exist that evaluates concrete specimens for sulfate resistance. Moreover, from the available performance tests to assess concrete durability (i.e., ASR, freeze/thaw, salt scale, corrosion, etc.), external sulfate attack is the only durability mechanism that does not have a standardized test using concrete specimens. This chapter presents a comprehensive research program focusing on concrete specimens to develop and design a concrete test method to evaluate chemical sulfate attack. The concrete mixes were cast in combination with varying water-to-cementitious materials ratios (w/cm), cement types, and supplementary cementitious materials in field exposure and controlled accelerated laboratory testing. Concrete specimens were cast and placed in an outdoor exposure site in two different sodium sulfate solutions. Likewise, concrete specimens were also placed indoors and evaluated for their sulfate performance in controlled environment and subjected to the following four exposure conditions: 1) Modified ASTM C 1012 using

concrete specimens submerged in sodium sulfate solution, 2) Accelerated performance testing using a vacuum impregnation technique to saturate the concrete pores with sodium sulfate solution, 3) removal of the concrete surface exposing the bulk past matrix and subsequently placed in sodium sulfate solution, and 4) static immersion in sodium sulfate solution with no renewal of the testing solution at each measurement. The performance of the mixes was studied by monitoring the change in mass and length of the specimens over time. The laboratory study indicated that the accelerated method proved to be satisfactory in determining sulfate resistance within a reasonable time. Furthermore, the outdoor testing program provided a suitable baseline for determining the efficacy of the test method. In both exposure conditions, it was shown that the failure mechanism of sulfate attack was significantly influenced by the sulfate concentration. Additionally, high w/cm ratio and concrete made using high-calcium fly ash showed the worse performance in the majority of the testing.

6.2 INTRODUCTION

External sulfate attack on concrete is still a major durability topic that promotes a lot of discussion among researchers and practitioners. Performance testing and results related to this very complex form of deterioration are not always easy to perform. Moreover, natural exposure to sulfate in the soil and groundwater can involve numerous variables and contributing factors (i.e., temperature, sulfate concentration, sulfate type, etc.) that make it even more difficult to understand. Currently, ASTM C 1012 is the most commonly referred test method for determining the sulfate resistance of a cementitious system; this method evaluates the performance of mortar bars exposed to a 5% sodium

sulfate solution. However, most often in the field, concrete is exposed to a soil containing a sulfate solution of lower concentration and thus, there is often a large disconnect between lab and field performance. There is a need to develop a comparison of the accelerated ASTM C 1012 testing to concrete exposed to in-situ sulfate bearing soils

This study presents the results on over 30 concrete mixture investigated in various sulfate environments including: 1) field specimens placed in soil containing sulfates, and 2) concrete prisms placed indoors under laboratory controlled conditions. The expansion results are presented for up to 3 years of measurements on specimens placed in two sodium sulfate concentrations (5% & 0.89% Na₂SO₄).

6.3 EXPERIMENTAL METHODS

Concrete prisms and mortar bars were both cast with the same combination of cements and supplementary cementitious materials. The performance of mortar bars tested using ASTM C 1012 (*test method for expansion of blended cement, external sulfate attack*) (2008) as well as accelerated test methods were previously presented in Chapters 4 & 5 of this dissertation.

6.3.1 Materials

Three ASTM C 150 portland cements were used in this research program including a Type I (C1), Type I/II (C2) [meets the strength requirements of a Type I while having a C₃A content < 8%], and a Type V (C5) cement. The Type I and Type I/II were procured from sources within Texas; Type V was procured from a source in California. Table 6-1 provides the chemical composition of the cements.

Four supplementary cementitious materials (SCMs) were included as a part of the study and used as partial replacement of cement by mass. Two fly ashes, HC (Class C) and LC (Class F), a granulated blast furnace slag (GBFS) [designated throughout as S], and a densified microsilica used at 5% and 7% replacement levels in combination with the HC fly ash as a ternary blend at 35% and 30% replacement, respectively, were included in this study. Previous research at the University of Texas at Austin has evaluated various Class C fly ashes having a range of calcium contents and showed ambiguous performance between field and controlled laboratory exposures (Drimalas, 2007; Clements 2009). The overall program in this study used a number of Class C fly ashes but the HC fly ash chosen for this study was used as it has been shown in previous work to exhibit poor sulfate resistance when tested under laboratory conditions and thus, it was of interest to investigate its performance in the outdoor exposure site. Table 6-2 provides a detailed overview of the chemical compositions of the SCMs used throughout the program.

All mixes were prepared with a 25 mm (1 in) crushed limestone coarse aggregate and manufactured limestone sand. Both materials were procured from a local source in Central Texas and conformed to the the ASTM C 33 requirements.

Table 6-1: Chemical composition of cements

Chemical Tests	Type I (C1)	Type I/II (C2)	Type V (C5)
SiO ₂ (%)	20.84	20.38	20.62
Al ₂ O ₃ (%)	5.95	4.9	3.77
Fe ₂ O ₃ (%)	2.51	3.55	3.66
CaO (%)	62.77	63.2	62.22
SO ₃ (%)	3.43	2.86	2.95
MgO (%)	1.43	1.14	4.56
Na ₂ O (%)	0.15	0.11	0.25
K ₂ O ₃ (%)	1.00	0.67	0.34
C ₃ A (%) (Bogue)	11.52	6.98	3.42

Table 6-2: Chemical composition of supplementary cementitious materials

Chemical Tests	Silica Fume (SF)	Class C (HC)	Class F (LC)	Slag (S)
Silicon Dioxide (SiO ₂), %	93.17	30.76	48.48	35.91
Aluminum Oxide (Al ₂ O ₃), %	--	17.75	25.01	11.98
Iron Oxide (Fe ₂ O ₃), %	2.1	5.98	3.56	0.94
Calcium Oxide (CaO), %	0.8	28.98	15.92	44.1
Magnesium Oxide (MgO), %	0.3	6.55	2.5	8.9
Sulfur Trioxide (SO ₃), %	0.2	3.64	0.72	1.63

6.3.2 Mixture Proportions

A total of 33 concrete mixtures was cast and subjected to different sulfate exposure conditions during the test program. To investigate the performance of the SCMs chosen for this study, various replacement levels were used and measured in

comparison with each cement mixture used as controls. Table 6-3 describes the various cement/SCM replacements used for the concrete mixes. Two water-to-cementitious materials ratios (w/cm) were used for all the concrete mixtures, with half of the mixtures using a 0.40 and the second half a 0.55 w/cm (see Table 6-4 for concrete mixture porportioning). The use of a polycarboxylate high-range water reducer (HRWR) used to achieve a workability between 100-200 mm (4-8 in) if necessary.

It is worth noting that ACI 201.2.R, *Guide to durable concrete* (2008), does not allow the use of a 0.55 w/cm for concrete that will be subjected to sulfates exceeding ≥ 150 ppm in water or 0.10% in soil. However, the use of a 0.55 w/cm in this research program was aimed at addressing the two following objectives:

- Research from Drimalas (2007) and Clements (2009) extensively studied the performance of several concrete mixtures using 0.40, 0.45 0.50 and 0.70 w/cm in various sulfate environments. This research program was aimed at filling in those research gaps by using a w/cm of 0.55 and validate the influence of w/cm on sulfate performance; and
- Similar to ASTM C 1012, in that standard mortars are cast using a relatively high w/cm (0.485) ratio to accelerate the ingress of sulfate ions, it was deemed necessary to use a relatively high w/cm ratio for the concrete bars subjected to the accelerated test method in order for obtain results within a reasonable timescale. As such, a w/cm was chosen that was considered practical and representative of the results obtained from the field conditions.

Table 6-3: Proportions of cementitious materials (% by mass)

Mix ID	Type I	Type I/II	Type V	Class C	Class F	Silica Fume	Slag
I-Cont	100	-	-	-	-	-	-
I-30C	70	-	-	30	-	-	-
I-40C	70	-	-	40	-	-	-
I-307CSF	63	-	-	30	-	7	-
I-355CSF	60	-	-	35	-	5	-
I-15FF	85	-	-	-	15	-	-
I/II-Cont	-	100	-	-	-	-	-
I/II-30C	-	70	-	30	-	-	-
I/II-40C	-	60	-	40	-	-	-
I/II-307CSF	-	64	-	30	-	7	-
I/II-355CSF	-	60	-	35	-	5	-
I/II-25FF	-	75	-	30	-	-	-
V-Cont	-	-	100	-	-	-	-
V-30C	-	-	70	30	-	-	-
V-355CSF	-	-	60	35	-	5	-
V-50S	-	-	-	-	-	-	50
I-25F	75	-	-	-	25	-	-

***Note all mixtures cast at 0.40 and 0.55 wcm except V-50S**

Table 6-4: Mixture proportions by mass

	<i>W/CM = 0.40</i>		<i>W/CM = 0.55</i>	
	Proportions by mass		Proportions by mass	
	(kg/m ³)	(lb/yd ³)	(kg/m ³)	(lb/yd ³)
Cement +SCM	400	674	310	520
Water	160	270	171	288
Crushed Limestone	1072	1805	1100	1854
Manufactured Limestone	Adjusted	Adjusted	Adjusted	Adjusted
Air (%)	2		2	

Table 6-5: Fresh and hardened properties of concrete mixtures

<i>W/CM = 0.40</i>				
Mix ID	Slump mm (in.)	Obtained Air (%)	Unit Weight kg/m ³ (lb/yd ³)	f _c (28d) Mpa (psi)
I-Cont	102 (4)	2	86 (146)	47 (6,890)
I-30C	140 (5.5)	2.2	86 (146)	48 (7,000)
I-40C	102 (4)	1.8	85 (144)	49 (7,165)
I-307CSF	89 (3.5)	1.7	85 (144)	53 (7,735)
I-355CSF	50 (2)	1.8	85 (144)	51 (7,440)
I-15FF	50 (2)	2.2	86 (146)	49 (7,146)
I/II-Cont	50 (2)	1.8	85 (144)	58 (8,479)
I/II-30C	50 (2)	1.5	85 (144)	43 (6,578)
I/II-40C	101 (4)	1.7	87(147)	49 (7,144)
I/II-307CSF	152 (6)	2.3	85 (144)	49 (7,187)
I/II-355CSF	89 (3.5)	2	86 (145)	55 (8018)
I/II-25FF	2.5	1.9	84 (142)	41 (6,019)
V-Cont	63 (2.5)	2.7	87 (147)	59 (8,524)
V-30C	89 (3.5)	2	87 (147)	56 (8,149)
V-355CSF	89 (3.5)	2.4	86 (145)	51 (7,428)
V-50S	76 (3)	2.3	87 (147)	55 (7982)
I-25F	114 (4.5)	2.5	85 (144)	45 (6,517)
<i>W/CM = 0.55</i>				
Mix ID	Slump mm (in.)	Obtained Air (%)	Unit Weight kg/m ³ (lb/yd ³)	f _c (28d) Mpa (psi)
I-Cont	89 (3.5)	2.4	87 (147)	37 (5,357)
I-30C	102 (4)	1.6	87 (147)	36 (5,279)
I-40C	178 (7)	2.3	85 (144)	35 (5031)
I-307CSF	140 (5.5)	1.8	86 (146)	41 (5,919)
I-355CSF	165 (6.5)	1.6	84 (142)	40 (5,810)
I-15FF	200 (8)	3.1	84 (142)	34 (4,942)
I/II-Cont	165 (6.5)	1.3	84 (142)	44 (6,336)
I/II-30C	152 (6)	1.7	84 (142)	33 (4,812)
I/II-40C	178 (7)	2.1	86 (145)	35 (5,086)
I/II-307CSF	178 (7)	2.3	85 (144)	38 (5,569)
I/II-355CSF	89 (3.5)	1.7	86 (145)	37 (5,314)
I/II-25FF	165 (6.5)	1.2	84 (142)	26 (3,786)
V-Cont	140 (5.5)	2.3	86 (145)	42 (6,198)
V-30C	114 (4.5)	1.5	87 (147)	42 (6,060)
V-355CSF	89 (3.5)	1.6	86 (145)	41 (5,890)
V-50S	-	-	-	-
I-25F	127 (5)	1.8	86 (146)	27 (3,900)

6.3.3 Specimens, exposure conditions and tests conducted

Various exposure conditions were used throughout this research program. The testing conditions included an updated outdoor exposure site evaluating concrete prisms imbedded in soils containing sodium sulfate, and indoor controlled laboratory conditions. Within each exposure condition, a variety of parameters was evaluated. This section discusses in detail those parameters evaluated and the tests used to measure performance.

6.3.3.1 Casting and curing

Unless otherwise noted, concrete prisms with dimensions of 75 x 74 x 285 mm (3 x 3 x 11.25 in) were cast for all mixtures. All concrete prisms were cast, cured under wet burlap at ambient conditions for 24 hours, and then demolded and moist cured at 23 °C ± 2 °C (73 °F ± 5 °F) for an additional 27 days. When the concrete mixes reached 28 days of age, an average of three 100 x 200 mm (4 x 8 in) cylinders were broken in compression (see Table 6-5 for results) and the prisms were placed in their designated testing condition. The concretes cast with a 0.40 *w/cm* contained 31 prisms whereas those cast with 0.55 *w/cm* comprised of 26 prisms. Each prism cast was exposed to variety of testing conditions and are discussed in the following section in more detail.

6.3.3.2 Outdoor exposure site and field investigation

The development of an outdoor sulfate exposure site began in 2005 where Drimalas (2007) and Clements (2009) evaluated the sulfate resistance of several concrete mixtures in various concentrations of sodium sulfate, magnesium sulfate, and calcium sulfate. Concrete prisms were placed in large sulfate ponds containing each of the sulfate types mentioned previously and monitored for their expansion and mass change over the life of these studies and continue to date. Figure 6-1 shows the outdoor exposure site created at UT in 2005.



Figure 6-1: Outdoor sulfate exposure site located in Austin, TX

In 2011, a modification of the outdoor exposure originally designed in 2005 was made to expand the site to include additional sulfate environments tested in this research program. The update exposure site eliminated the underground sulfate ponds and included the use of above-grade horse troughs to place the concrete prisms. Figure 6-2 presents the update exposure site created in 2011. The newly built exposure site consist of eight 0.91 x 0.61 x 3.05 m (3 x 2 x 10 ft.) horse troughs, each filled half-way with sandy loam typically used for residential foundation in Austin, TX. Testing of this loam confirmed that no sulfates were present prior to placing concrete prisms. Due to the limited volume capacity of the horse trough, it was impractical to fill the trough to contain a solution of 5% sodium sulfate in the water. Consequently, it was decided to

obtain an equivalent concentration of water-soluble sulfates (SO_4^{2-}) in soil by percent mass. Thus, sulfate solutions were prepared based on theoretical assumptions of the unit weight of the sandy loam provided by the manufacture to calculate the amount of sodium sulfate needed for each trough. For this study, a 3.4% (5% Na_2SO_4) and 0.6% (0.89% Na_2SO_4) sulfate (SO_4^{2-}) by mass percent of soil were used, which matched similar concentration of those concretes placed indoors in pure sodium sulfate solution. For the outdoor troughs, anhydrous sodium sulfate was simply dissolved in water and added to the soil while thoroughly mixing to evenly distribute an equivalent sulfate ion concentration across the trough. The sulfate solutions were kept at a height of about 75 mm (3 in) above the soil. The troughs were subsequently monitored and allowed to evaporate until the solutions just reached the soil level and were then filled with water. As such, the concentration of sulfates in the trough is at a minimum when the levels are at their highest (and initial) level and at a maximum when the water has evaporated to the point where the solution reaches the soil level (Drimalas, 2007)



Figure 6-2: Updated outdoor exposure site using above-grade horse troughs for concrete exposure to sulfate environments

For the concrete prisms placed outdoors, six prisms were placed below the soil level (three in 5% Na_2SO_4 , three 0.89% Na_2SO_4), roughly 75mm (3 in) into the soil, and two prisms were placed vertically. The vertical prisms were submerged roughly 75 mm (3 in) into the soil, with the remaining portions were exposed to a wetting and drying zone and subject to wicking action (i.e., physical salt attack). Figure 6-3 illustrate the orientation of the prisms placed in the field exposure site. The results presented in this chapter only include those prisms fully submerged and subjected to chemical sulfate attack to provide a direct comparison to those prisms placed indoor and kept submerged in sulfate solution.

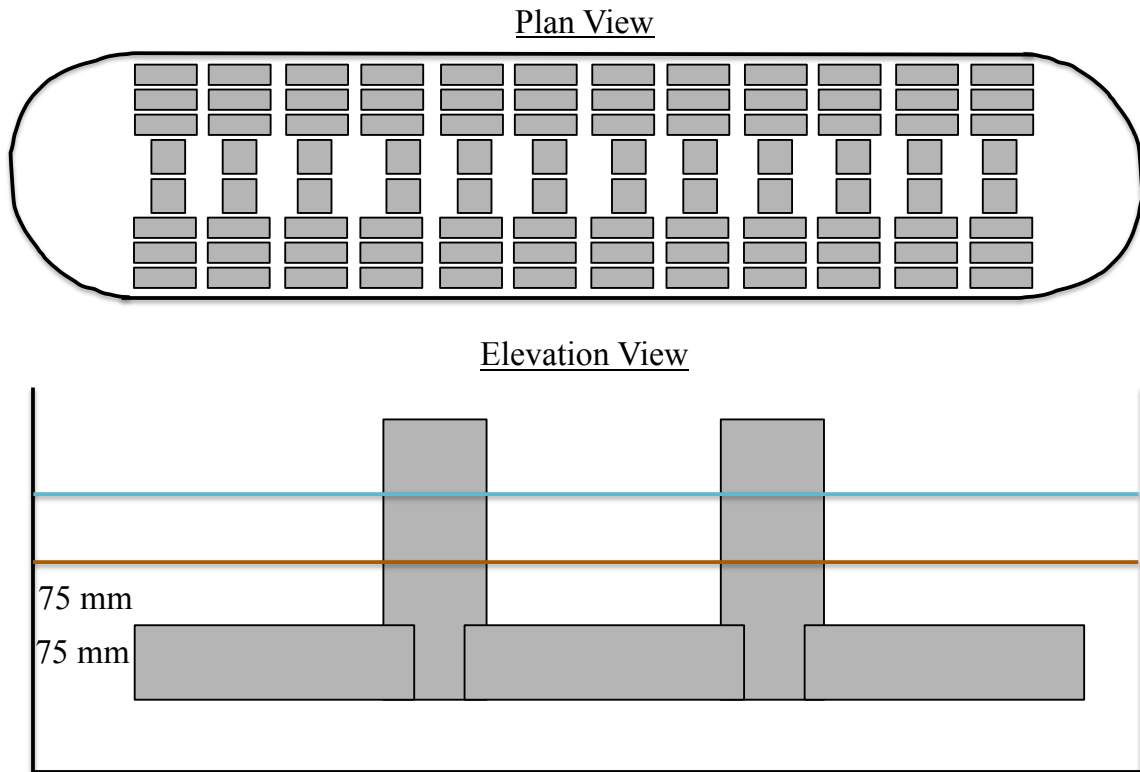


Figure 6-3: Orientation of concrete prisms placed in outdoor sulfate exposure site

6.3.3.2 Accelerated laboratory testing of concrete specimen exposed to sulfate

Concrete specimens from each mixture were subjected to a novel vacuum impregnation technique in which the specimens are immersed in a sulfate solution and subjected to high pressures to accelerate the ingress of sulfate ions. The porosity of the each concrete sample is filled with a sodium sulfate solution by sealing the specimens in a large vessel and introducing a negative pressure to drive the solution into the sample (see Figure 6-4). Subsequently, specimens are monitored for their length and mass change at 1, 2, 3, 4, 8, 12, 15, 17, and 26 weeks, and every 3 months thereafter.

Similarly to the field specimens, a 5% and 0.89% Na_2SO_4 solution were used for impregnation of the specimens. Mass changes were monitored in the concrete samples pre- and post-vacuum impregnation to confirm only sodium sulfate is introduced to the

concrete specimens. In this testing program, the concrete specimens were moist-cured for 28 days and subjected to the following two drying regimes to allow room for sodium sulfate in the water-filled pores:

- Dried in an oven at $35\text{ }^{\circ}\text{C} \pm 3\text{ }^{\circ}\text{C}$ ($95\text{ }^{\circ}\text{F} \pm 5\text{ }^{\circ}\text{F}$); (designated as “OD” throughout); and
- Dried in a shrinkage room at $23\text{ }^{\circ}\text{C} \pm 2\text{ }^{\circ}\text{C}$ ($73\text{ }^{\circ}\text{F} \pm 4\text{ }^{\circ}\text{F}$) and at 50% RH (designated as “DS” throughout)

The purpose of the two drying conditions was to investigate the influence of drying temperature on mass uptake of sulfate solution during vacuum impregnation.

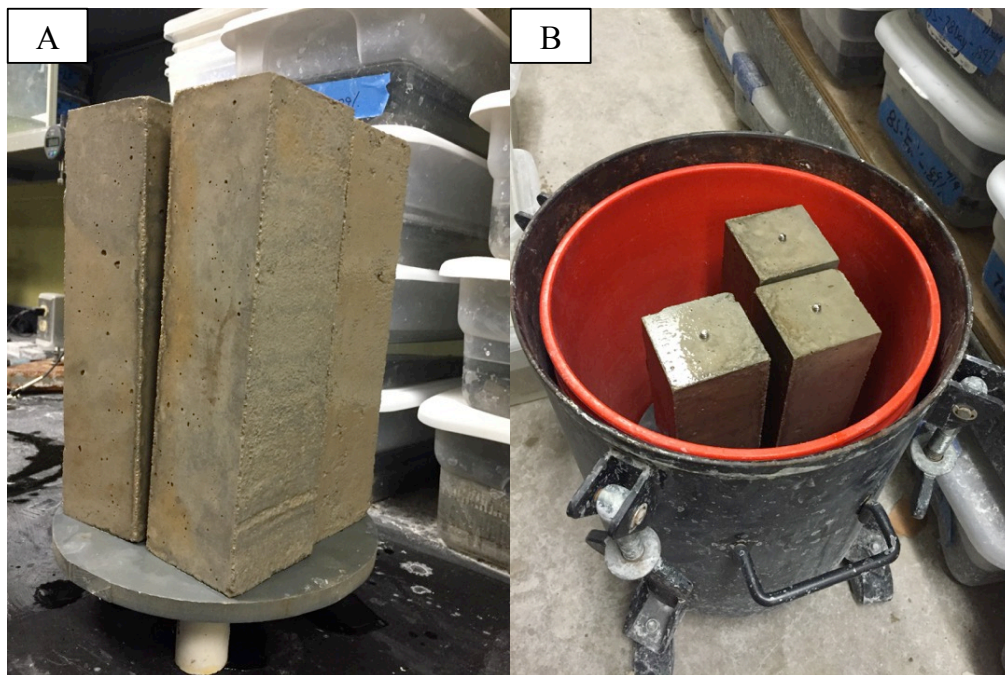


Figure 6-4: a) Concrete sample holder; and b) Internal view of sample placement

6.3.3.3 Removal of concrete surface

Kunther (2012) studied the deterioration of mortar bars that were cut from mortar slabs to remove the surface layer of dense paste and any carbonated surface layer. It was

explained that the influence of the carbonated surface could significantly impact the rate in which the sulfate attack mechanisms and associated expansion will occur. Furthermore, the removal of the surface layer of dense paste exposes more of the bulk hydration products within the sample and thus, can lead to fast deterioration. In this study, the removal of the surface was performed on concrete specimens measuring 115 x 115 x 285 mm (4.5 x 4.5 x 11.25 in) using a diamond bit concrete saw with water used as the lubricant. Prior to cutting, the specimens were moist cured for 28 days similar to the other concretes cast in the program. The modified concrete prisms were cut at each face to remove approximately 20 mm (0.75 in) of the surface; consequently, the cut prism resulted in a sample with similar dimensions as those concrete specimens cast in the rest of the program. An average of three prisms for each testing solutions (5% and 0.89% Na_2SO_4) were cut from selected mixtures at only a $w/cm=0.40$. Figure 6-5 illustrates the concrete prisms before and after removal of the surface layer.

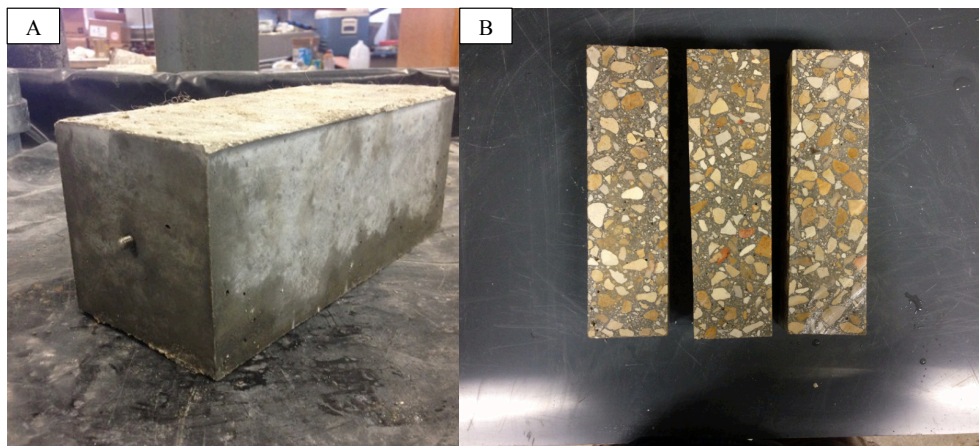


Figure 6-5: a) Modified concrete prisms; and b) View of samples after surface removal

6.3.3.3 Non-solution renewal

The performance of concrete in sulfate environments has shown to be highly influenced by the pH of the sulfate solution (Mehta, 1975; Brown, 1981; Clifton et al., 1998; Roziere et al., 2008; Planel et al., 2006). Calcium leaching of cement paste under deionized water is characterized in particular by the dissolution of portlandite ($\text{Ca}(\text{OH})_2$) and the decalcification of calcium silicate hydrates (C-S-H), leading to the diffusion of calcium ions towards the outside medium (Buil et al., 1992; Adenot & Buil, 1992; Adenot et al., 1997; Planel et al., 2006). Inevitably, the concrete pore solution reaches equilibrium with the testing solution. As a result, the leaching of alkalis leads to an increase in the pH of the testing solution typically ranging between 12-14. Field concrete elements subjected to sulfates in the groundwater are less influenced by this phenomenon due to surface runoff and constant groundwater flow maintaining a neutral pH in the water. In this study, selected concrete mixtures were evaluated for their expansion and mass change in 5% Na_2SO_4 solution in which the solution was kept the same throughout the entire test. For these specimens, enough solution was placed into the containers to ensure that the solution would not need to be renewed due to evaporation or leakage during measurements. These specimens were monitored for their expansion and mass monthly for the first 3 months and every 3 months thereafter. Although the pH was not continuously recorded, it was assumed that the solution reached equilibrium within the first few weeks of the concrete specimens being submerged.

6.3.3.4 Modified ASTM C 1012

A modified ASTM C 1012 version (designated as “MOD” throughout) in which concrete specimens (versus mortar) submerged in 5% sodium sulfate and monitored for their expansion was also investigated in this study. For comparison to field specimens,

concrete prisms were also stored in 0.89% sodium sulfate solutions. Each testing solution included three prisms stored at ambient conditions (23 °C [73 °F]). The testing solution was replaced during each measurement.

6.4 RESULTS AND DISCUSSION

This section summarizes the expansion results of the field and laboratory performance of the concrete mixtures evaluated. The field performance is first discussed, followed by the laboratory performance. The laboratory performance focuses on mixture proportions and cementitious materials also tested using mortar bars.

6.4.1 Field performance of concrete specimens

6.4.2 Expansion Results

Two sodium sulfate solutions were investigated in this study. Figure 6-6 and 6-7 presents the expansion results for the concrete prisms placed outdoors for $w/cm=0.40$ & 0.55 , respectively. The results are presented for up to 3 years of exposure or until they were no longer measurable due to deterioration. For the control mixtures using each cement type (no SCM), Type I observed the highest expansion and deterioration at both w/cm . However, mixture using Type I/II cement and a $w/cm=0.40$ observed considerably less expansion at all measurements; the performance for the Type I/II and Type V mixtures were almost indistinguishable at $w/cm=0.55$. With the exception of Type V, binary mixture blended with Class C fly ash showed significant expansion after only 6 months with most no longer measurable after 12 months of exposure in 5% sodium sulfate solution. The performance worsened at $w/cm=0.55$. Interestingly, the performance was not improved until the Class C fly ash was blended with the Type V cement. For example, mixtures I-40C and II-40C at $w/cm=0.40$ failed at 1 year while

mixture V-40C is still measurable after 2 years of exposure in 5% sodium sulfate. On the other hand, similar concrete mixtures showed better performance in 0.89% sodium sulfate and are still measurable after 3 year of exposure. The results clearly demonstrate the impact of sulfate concentration on concrete performance. For all mixtures at 0.40 and 0.55 w/cm , the expansion was considerably less for concrete prisms placed in 0.89% sodium sulfate solution.

The addition of Class C fly ash typically showed more deterioration (but not expansion) compared to the control mixtures. Generally, the performance was made worse with increasing replacement amount of Class C fly ash; the results are consistent with mortar bars testing using similar cementitious materials. Conversely, Drimalas (2007) typically showed improved performance with increasing replacement of Class C fly ash. Interestingly, the use of 15% Class F fly ash did not exhibit good performance, failing after only 1 year. However, with increasing the replacement to 25%, the performance was significantly improved, showing the least expansion of all mixtures in both sulfate concentrations.

The use of silica fume as a ternary blend to improve the performance of Class C fly ash was clearly evident from the expansion results. Although the concrete prisms exhibited some deterioration and minor cracking, the bars showed significantly less expansion and were still intact after 3 years exposure. Interestingly, the concrete prisms for the ternary mixtures using a $w/cm=0.55$ were still intact and measurable after 3 years although showing significant signs of deterioration and spalling at the corners.

The performance of concrete mixtures placed in 0.89% sodium sulfate was slightly ambiguous compared to their counterparts in 5% sodium sulfate. For example, binary mixtures blended with Class C fly ash showed increasing sulfate resistance with increasing replacement amounts. Generally, the performance was made worse for

concrete prisms placed in 5% sodium sulfate. Furthermore, similar performance was observed for mortar bars testing using ASTM C 1012. It was also noted previously that Drimalas (2007) observed a similar trend with improved performance with increasing Class C fly ash content for concrete placed in the outdoor exposure site; however, the study was carried on concrete placed in 5% sodium sulfate.

The use of 5% sodium sulfate for accelerated sulfate performance testing has commonly been considered the culprit for countless arguments and debates related to external sulfate attack. The concentration is considerably higher than what is typically documented from the field. The results from this study clearly show the disconnect between lab and field performance.

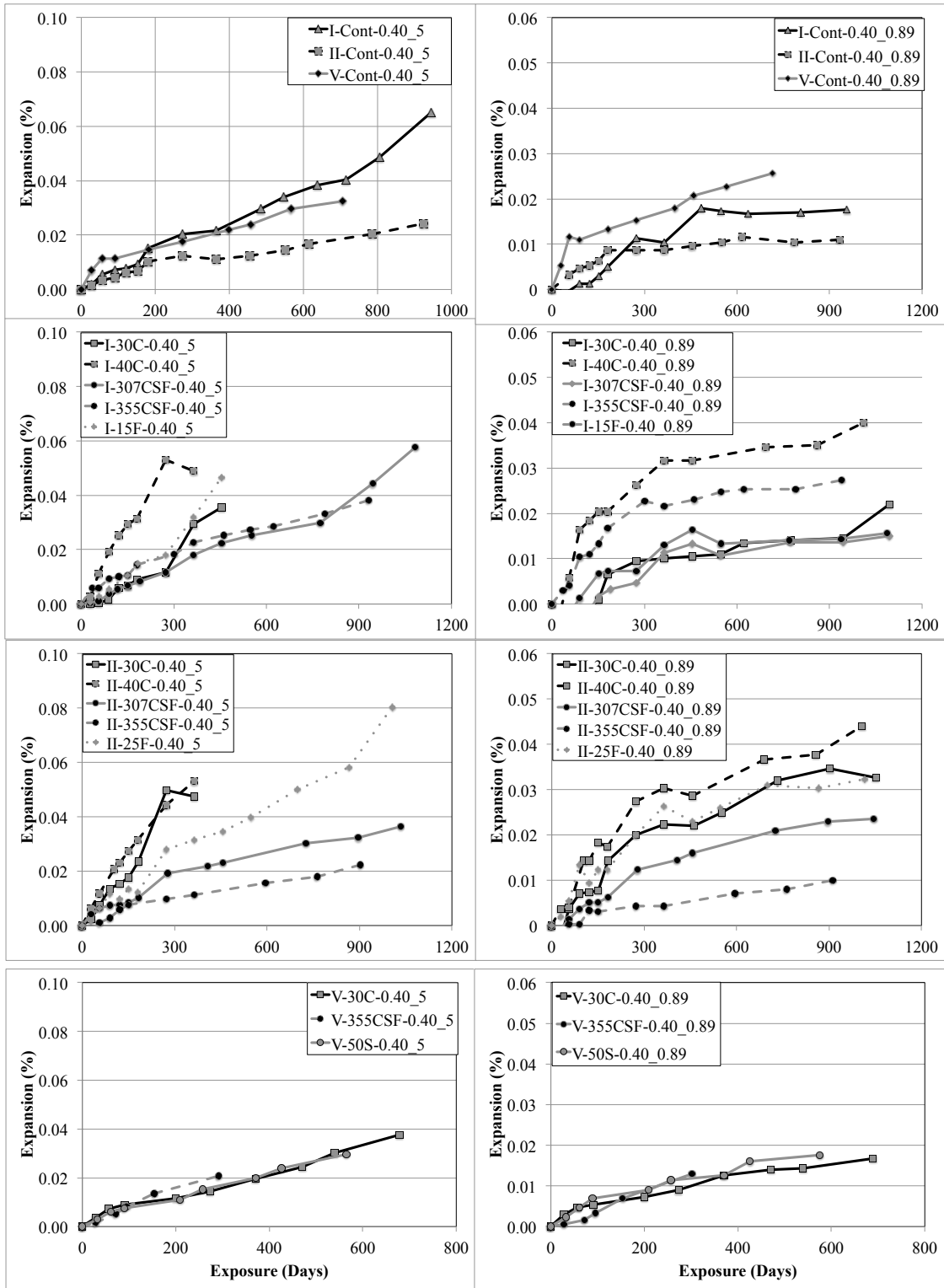


Figure 6-6: Expansion results for $w/cm = 0.40$ concrete prisms outdoor in field

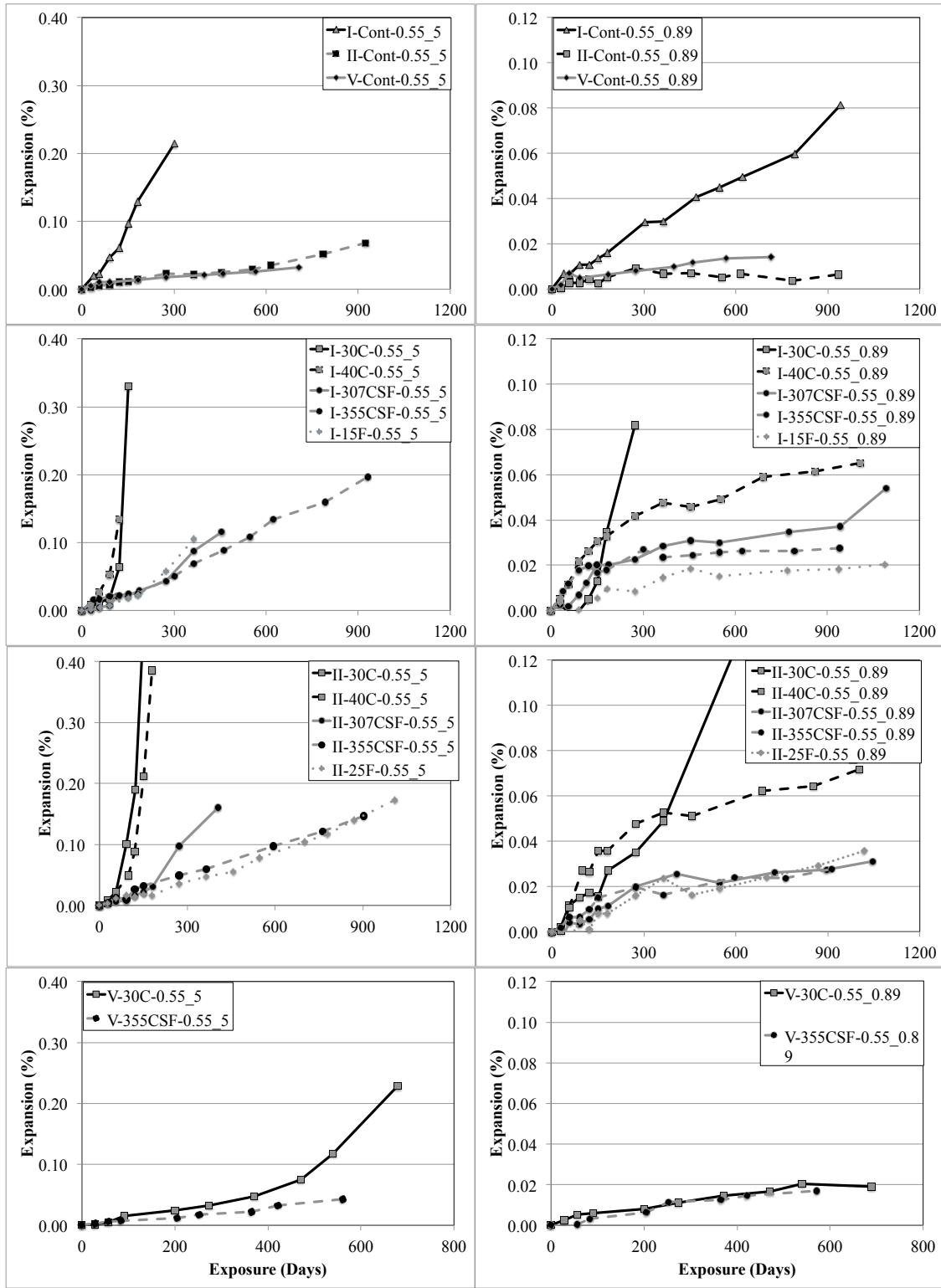


Figure 6-7: Expansion results for $w/cm = 0.55$ field concrete prisms

6.4.2 Performance of concrete specimens in controlled laboratory conditions

6.4.2.1 Accelerated performance test

The expansion results for concrete prisms subjected to the vacuum impregnation technique are present below in Figure 6-8. The results show those concrete mixtures with $w/cm=0.40$ and each cement type. For comparison, concrete also tested using the modified ASTM C 1012 method are presented below. For all mixtures, the performance was accelerated due to the vacuum impregnation. Additionally, the prisms dried in oven at 35 °C (95 °F) showed a faster onset of expansion than those prisms placed at ambient conditions and 50% RH prior to vacuum impregnation. For example, mixture I-Cont. observed an expansion of 0.11%, 0.18% and 0.98% at 924 days for the modified ASTM C 1012, DS, and OD accelerated methods, respectively. Furthermore, considering a similar 0.10% expansion limit as in the ASTM C 1012 method, mixture I-Cont. surpassed the limit at 30 month for the modified ASTM C 1012 method and 24 months for both DS and OD accelerated method. It is important to note that the expansion limit typically associated with concrete durability test methods is only 0.04% expansion as this is typically the level of expansion where concrete begins to crack in the field. Therefore, the use of 0.1% expansion as a limit for a concrete test method to evaluate sulfate performance is likely too conservative.

Interestingly, mixture I/II-Cont. appeared to be an anomaly showing the highest expansion for the OD vacuum impregnation concrete bars. It is evident that the proposed method requires further testing and repeatability to ensure its accuracy and its acceptance in the field.

The expansion levels are exacerbated for those mixtures using $w/cm=0.55$ as shown in Figure 6-9 below. The Type I control mixture subjected to the OD accelerated regime showed significant expansion early on and exceed the 0.1% expansion limit in as

little as 3 months of exposure. One possible explanation for this is the higher w/cm created a higher permeability allowing for additional sulfates to ingress. However, the trend was not as similar for mixtures subjected to DS accelerated method. The expansion rate was similar to the modified ASTM C 1012 environment and slowly tapered off after 1 year.

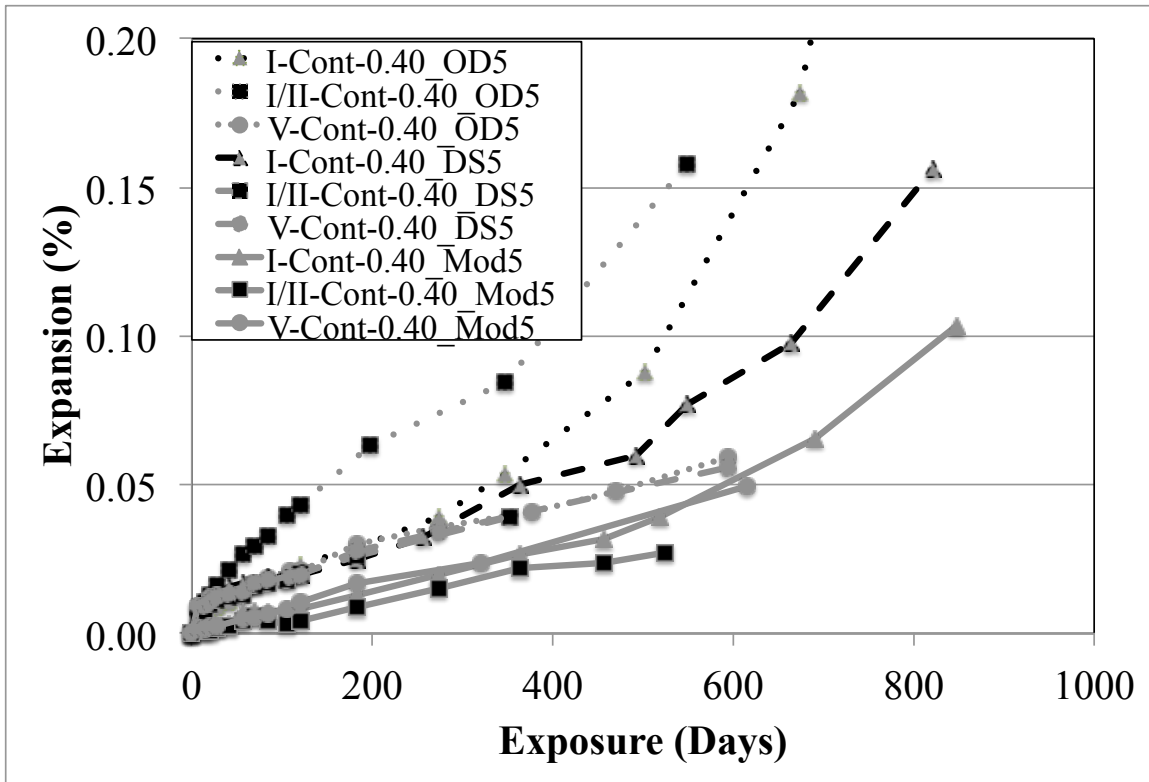


Figure 6-8: Expansion of concrete prisms with $w/cm=0.40$ tested using Modified ASTM C 1012, DS, and OD accelerated method

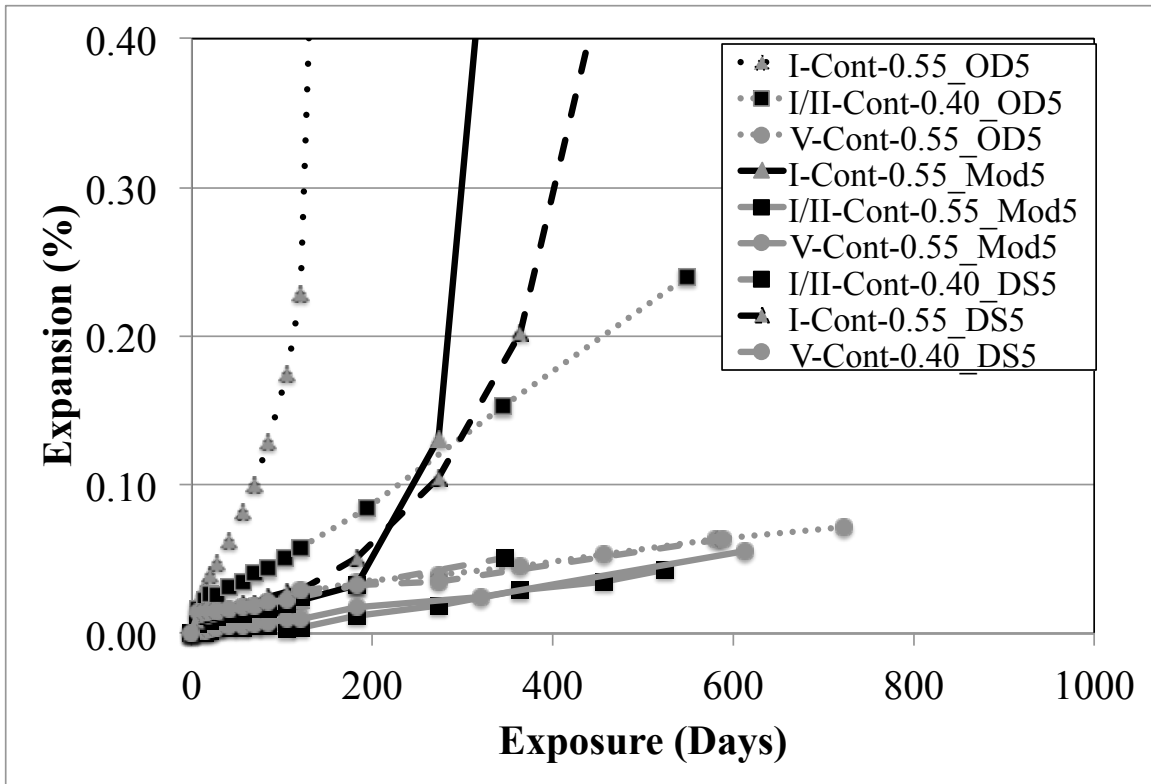


Figure 6-9: Expansion of concrete prisms with $w/cm=0.55$ tested using Modified ASTM C 1012, DS, and OD accelerated method

6.4.2.2 Expansion results for surface removal specimens

The results for the concrete specimens subjected to removal of the surface prior to immersion in sodium sulfate are presented in Figure 6-10 below. The results are presented up to 2.5 years for most mixtures. Concrete prisms using Type I exhibited significant expansion at 2 years (0.42) and were fully deteriorated after 27 months; the mixture had two concrete prisms that were fully deteriorated and the results display only the expansion measurement of one bar at 24 months. Interestingly, this was the highest expansion observed for the Type I mixture (at a $w/cm=0.40$) from the various methods used to investigate sulfate performance in this study. However, similar trends were not observed for the other mixtures evaluated using this method. Nonetheless, the expansion

considerably higher than those concrete prisms placed in sodium sulfate and not subjected to any accelerated method.

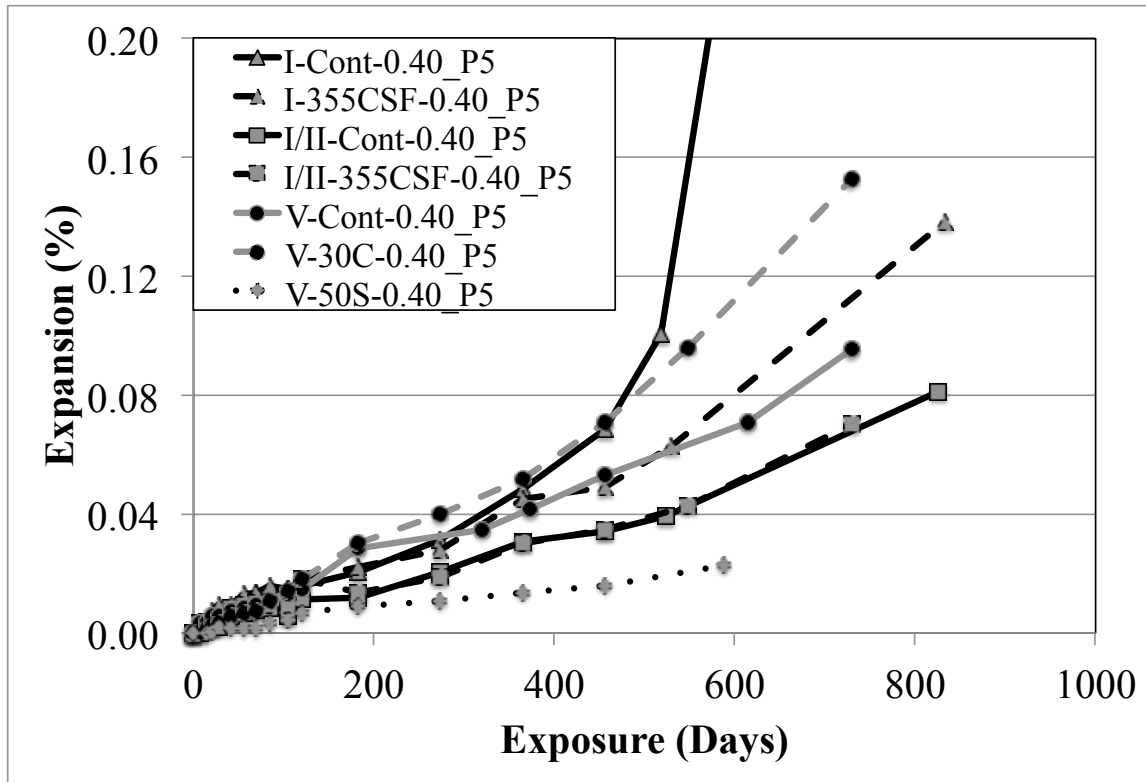


Figure 6-10: Expansion results for concrete prisms subjected to surface removal of the surface

6.4.2.3 Expansion results for non-solution renewal specimens

The expansion results for the concrete prisms placed in 5% sodium sulfate solution and without renewing the solution are presented in Figure 6-11 below. An interesting observation was made from the results in this study. The expansion for the Type I control was remarkably high after 3 years of exposure. The expansion at 3 years was approximately 0.12% and significant deterioration and cracking of the bars was notable at the ends as shown in Figure 6-12. Interestingly, similar behavior was observed

for the ternary blend mixture I-355CSF showing an expansion just slightly under 0.10% at 3 years. It is evident that the expansion rate was delayed from not replacing the testing solution; however, the final measured expansion indicates that sulfate attack can still progress in the concrete regardless of the pH in the testing solution. The expansions for the mixtures using Type I/II and Type V cement were significantly less than for Type I. Similar trends were observed in that the prisms are still experiencing expansion regardless of the solution not being swapped out.

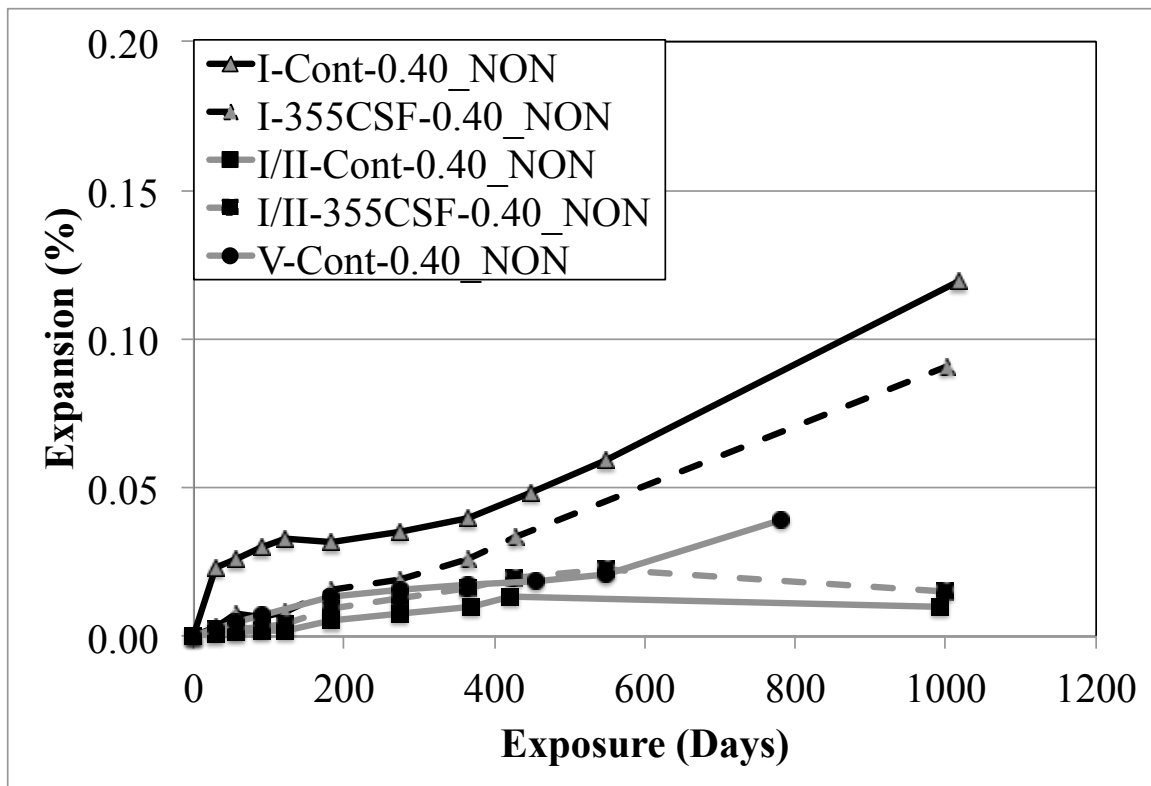


Figure 6-11: Expansion results for concrete prisms placed in sodium sulfate without replacing the solution during measurements

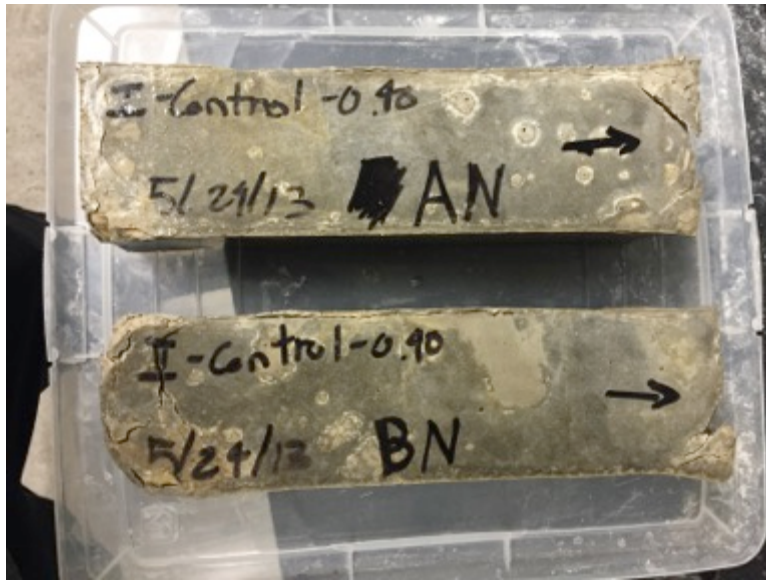


Figure 6-12: Visual degradation of concrete prisms placed in 5% Na₂SO₄ with no solution replacement

6.5 CONCLUSIONS

This study presented results from comprehensive program involving the performance of concrete specimens placed in various sulfate environments in field and controlled laboratory settings. The following are the key conclusions to date from this testing:

- Field performance of concrete specimens showed faster deterioration and higher levels of expansion than their companion prisms placed indoor and tested using the modified ASTM C 1012 method. However, concrete prisms subjected to the accelerated vacuum impregnation technique showed a faster rate of expansion (especially for concrete cast at $w/cm=0.55$) than the outdoor specimens.

- Concrete prisms placed in 5% sodium sulfate showed significantly higher expansion levels and deterioration than those placed in 0.89% for both laboratory and field conditions.
- Mixtures containing high-calcium fly ash exhibited poor sulfate resistance for both concrete prisms placed in field and laboratory conditions. Generally, the performance worsened with increasing replacement dosages at 5% sodium sulfate. Conversely, companion prisms placed 0.89% sodium sulfate showed improved performance with increasing fly ash amount. The results highlight the differences in performance related to sulfate concentration.
- Similar trends, but with reduced expansion rates, were observed in concrete prisms placed indoors at both sodium sulfate concentrations. It was clearly evident that the environmental condition outdoors (temperature, humidity, etc.) played a major role in accelerating the deterioration in field specimens. Nonetheless, indoor concrete prisms showed similar trends: (1) poor sulfate resistance for blended high-calcium fly ash mixtures; (2) significantly higher expansion at the higher sulfate concentration (5% Na_2SO_4); (3) improved performance for concrete prisms using a lower w/cm (0.40); and (4) Improved performance for high-calcium fly ash mixtures through the incorporation of silica fume as a ternary blend in small percentages.
- Interestingly, concrete prisms tested indoors in 5% sodium sulfate with no replacement of the testing solution during measurement showed significant expansion levels after 3 years of exposure. Severe deterioration and significant cracking was observed at the ends and

corners of the specimens. The performance was observed the worst for concrete mixtures using Type I cement.

- The removal of the surface layer of the concrete showed an acceleration in the rate of expansion. The control mixture using Type I cement showed the highest level of expansion from all the methods investigated in this study.
- Accelerated performance using the vacuum impregnation technique proved to be an adequate testing for determining sulfate resistance of concrete prisms. The results showed an acceleration in the rate of expansion compared to prisms testing using the modified ASTM C 1012 method. The results were improved for prisms dried using the OD method and having a higher w/cm (0.55).
- The use of 0.1% expansion as a limit for a concrete test method to evaluate sulfate performance might be too conservative, and consideration should be given to a 0.4% expansion limit, which would likely make such a test method more practical (and popular) for practitioners. Further investigation to evaluate repeatability between mixtures is necessary to confirm the results seen in this study as well as link the performance of concrete specimens placed in the field.

Chapter 7: Sulfate Resistance of Mortar Bars in Calcium, Magnesium, and Sodium Sulfate Using a Vacuum Impregnation Technique

7.1 ABSTRACT

Many research studies on chemical sulfate attack have been conducted, and considerable disagreement over the mechanisms and associated expansion and cracking process still exist. These studies have shown that several factors can influence the severity of attack, including the concentration of sulfate ions, pH level, temperature, leaching of alkalis into the solution, and the nature of the associated cation. In this chapter, the sulfate resistance of mortar bars exposed in various sulfate solutions and cation types is investigated. The availability of an accelerated method in which mortar bars are vacuum impregnated with sulfate solution prior to static immersion to accelerate the rate of expansion was selected to investigate the sulfate performance of the mortar bars. For comparison, mortar bars were also evaluated for their performance using the traditional ASTM C 1012/C1012M (2012) method in sodium sulfate. The relationship between the formation of reaction products and the expansion of portland cement mortars were investigated by x-ray diffraction (XRD)/Rietveld analysis to quantify the reaction products present and amount of linear expansion. Additionally, microstructural studies using SEM couple with EDS were used to characterize the nature of the reaction products and fronts. The results show that the sulfate resistance of cementitious materials is significantly influenced by the chemical composition and the nature of the associated cation.

Keywords: sulfate attack, sulfate resistance, sodium, magnesium, calcium, accelerated method, XRD, SEM/EDS

7.2 INTRODUCTION

Sulfate attack is one of the most complex forms of deterioration due to the fact that it involves numerous overlapping reactions, mechanisms, and internal or external sources of sulfates (Bonakdar & Mobasher, 2010; Mehta & Monteiro, 2006; Neville, 1995). For example, sulfate attack can contribute damage to concrete due to sources of sulfate present internally in the cement (gypsum in binder, aggregate, and chemical and mineral admixtures) (Collepari, 2003; Taylor et al., 2001) and subjected to high temperatures (often referred to as delayed ettringite formation). On the other hand, sources of sulfate external to the concrete member can penetrate through the pores leading to a series of chemical reactions and/or physical damage from the alteration of the hydration products in the concrete paste or repetitive crystallization of sulfate salts just under the concrete surface, respectively (Nehdi et al., 2014; Aye & Oguchi, 2011). Although the two forms can be categorized as either physical or chemical sulfate attack, they can generally be referred to as external sulfate attack (ESA), with the latter being the primary focus of this study.

Chemicals sulfate attack can generally be described by three different processes that occur (Skalny et al., 2002; Mehta & Monteiro, 2006; Messad et al., 2010), namely (1) migration of sulfate ions through the concrete pores, (2) expansive reaction of sulfate ions with aluminate-containing phases or calcium hydroxide to form ettringite and/or gypsum, respectively, and (3) expansion and associated cracking of the concrete from the surface layers to the core of the concrete.

The above-mentioned mechanism typically involves the use of sodium sulfate as the solution and many test methods focus on the physical properties (i.e., length change, mass loss, compressive strength, etc.) in order to determine sulfate resistance (ASTM C 1012, 2008; Tittelboom et al., 2013). However, it is not uncommon to find other available natural sources of sulfate in the form of magnesium and calcium sulfate present in soils and groundwater in the field (Drimalas, 2007; Dhole, 2008; Dolen et al., 2003). In fact, sulfates are more likely to co-exist with other anions and cations in the field. The rate and mechanism of sulfate attack differ depending on the nature of the associated cation. In order to better link laboratory testing with field performance, it is important to evaluate the performance in various sulfate environments that the concrete structure can encounter in the field. Laboratory studies of sulfate attack in various sulfate solutions has been the subject of considerable investigation (Whittaker & Black, 2015), but calcium sulfate has received the least attention.

7.2.1 Mechanisms of Sulfate Attack

7.2.1.1 Magnesium Sulfate

Magnesium sulfate is commonly present in soils and groundwater, as well as in seawater and brackish water. Depending on the concentration of Mg^{+} in solution, magnesium sulfate is often considered by researchers as the most aggressive of all the sulfate salts (Mehta & Monteiro, 2006; Skalny, et al., 2002). Magnesium sulfate will react with the calcium hydroxide (CH) to form brucite ($Mg(OH)_2$). Brucite has a very low solubility giving a low pH value (≈ 10.5) in saturated solution. In order to balance this pH in the pore solution, calcium is released from the C-S-H gel. Additionally, from the further availability of magnesium and sulfate, these can react with the C-S-H gel to form

gypsum, brucite, silica gel, and water. As a final step, during the advanced stage of attack, the brucite and silica gel can react slowly to yield magnesium silicate hydrates (M-S-H), which has little to no binding properties.

Kunther et al. (2013) reported magnesium to be more severe at the surface of mortar, especially for mixtures incorporating blends of supplementary cementitious materials such as granulated blast furnace slag (GGBFS). More deterioration was reported in mortar bars immersed in magnesium sulfate solutions than sodium sulfate solutions; however, the associated expansion was not always observed in the mortar bars and depended on the binder being tested. Moreover, the samples immersed in solutions containing different cations showed less expansion and surface deterioration than samples immersed in a single sulfate solution.

Gollop et al. (1992; 1995) reported similar distress in sulfate attack of paste samples submerged in sodium and magnesium sulfate solutions, with the latter forming M-S-H, thus decalcifying the C-S-H and resulting in loss of binding properties. This ultimately can reduce the overall integrity and strength of the structure, resulting in reduced service life. This form of chemical attack is the primary reason several researchers consider the magnesium cation of sulfate attack the most aggressive.

7.2.1.2 Sodium Sulfate

It is well known that attack from solutions containing sodium sulfate as the primary associated cation can lead to deleterious products, specifically ettringite and gypsum. These are generally formed from the availability of several alumina-bearing compounds present in the cement and/or supplementary cementitious materials (SCMs). In many cases, deterioration from sulfate attack is affected by the presence of unreacted cement grains. For example, the availability of leftover tricalcium aluminate [C_3A]

following hydration can be made available to react from external sources of sulfate. Moreover, as the availability of gypsum decreases, ettringite [AFt] is converted to monosulfate [AFm], liberating gypsum to react with unreacted C₃A, forming additional monosulfate (Black et al., 2006), which is also available to react with external sulfates forming ettringite in the hardened concrete.

Gypsum is generally reported to cause a “mushy” appearance and loss in strength in cement paste, without leading to expansion. However, several researchers (Bellmann et al., 2006; Tian & Cohen, 2000; Santhanam, Cohen, & Olek, 2003) have shown that the gypsum formation can also trigger expansion.

In severe cases, sodium sulfate can decalcify or decompose C-S-H. The continued reaction of CH with sulfate to form gypsum results in a reduction in the pH of the pore solution and thus, Ca⁺ ions are removed from the C-S-H phases in order to balance the system. This has shown to lead to a reduction in the CaO/SiO₂ ratio and may be associated with the loss of binding properties (Skalny et al., 2002).

7.2.1.3 Calcium Sulfate

Calcium sulfate (gypsum) is typically referred to as the least aggressive when compared to magnesium and sodium sulfate (Skalny et al., 2002). The primary product that results from calcium sulfate solution is ettringite. Although this source of sulfate is frequently found in the field (Drimalas, 2007; Bellmann, et.al., 2012; (Leemann & Loser, 2011), the amount of sulfate that is able to penetrate the concrete is limited due to the low solubility of around 1.45g/L of SO₄²⁻ at 20°C (Skalny et al., 2002). Despite this, Drimalas (2007) and Dhole (2008) have reported significant damage in concrete placed in gypsiferous soils; however, there is very few research that report on this and further

research is needed in order to confirm no other possible mechanisms related to calcium sulfate.

7.3 RESEARCH SIGNIFICANCE

In order to better link laboratory testing with field performance, it is important to evaluate sulfate performance in various sulfate environments that the concrete structure can encounter in the field. In many parts of North America where sulfate exposure conditions are encountered, various sulfate sources can co-exist in the soils and/or groundwater making the process of attack more complex. As a result, there is a need to investigate the deterioration mechanisms triggered by the most common sulfate types. The primary goal of this chapter is to shed light on the mechanisms of sulfate attack of commonly referenced sulfates in the field: sodium, magnesium, and calcium sulfate

7.4 EXPERIMENTAL PROGRAM

7.4.1 Materials

Three ordinary portland cements were used throughout the program: a Type I cement with a high- C_3A clinker (11% C_3A), a Type I/II cement with moderate- C_3A clinker (7%), and a Type V cement with a low- C_3A clinker (4% C_3A). The C_3A content was used as a measure of sulfate resistance and conformed to the ASTM C 150/C150M (2015) requirements for all cements. The Type I and I/II cements were procured locally from central Texas; the Type V cement was procured outside of the state in California.

A high-calcium Class C fly ash used as a supplementary cementitious material were also incorporated at various as a percent mass of cement. Although the study mainly focuses on the influence of sulfate solutions on binder type, further evaluation

was done to highlight the performance of high-calcium fly ash in magnesium and calcium sulfate solutions. The chemical compositions and analysis for the cements and fly ash used are provided in Table 7-1; the mixture proportion investigated is provided in Table 7-2.

Table 7-1 Chemical Composition of Cementitious Materials

	Type I	Type I/II	Type V	Class C
Blaine fineness, cm ² /g	4260	4010	3740	3840
Loss of ignition	2.6	2.2	0.9	0.37
SiO ₂ , %	20.84	20.38	20.62	30.76
Al ₂ O ₃ , %	5.95	4.90	3.77	17.75
CaO, %	62.77	63.62	62.22	28.98
MgO, %	1.43	1.14	4.56	6.55
SO ₃ , %	3.43	2.86	2.95	3.64
Na ₂ O, %	0.15	0.11	0.25	2.15
K ₂ O, %	1.00	0.67	0.34	0.3
TiO ₂ , %	0.20	0.02	0.06	-
MnO, %	0.05	0.05	0.05	-
Fe ₂ O ₃ , %	2.51	3.55	3.66	5.98
Compound Composition, (Bogue)				
Alite	53.59	66.12	66.02	-
Belite	19.32	8.55	9.31	-
Aluminate	11.52	6.98	3.80	-
Ferrites	7.64	10.80	11.14	-
Calcite	2.42	3.70	0.40	-

Table 7-2 Mixtures and associated cation selected for study

Mix No.	Cement	Class C Fly Ash	C1012	Accelerated Method (Vacuum Impregnation)		
			Associated Cation			
			Na ⁺	Na ⁺	Mg ²⁺	Ca ²⁺
1	Type I	-	✓	✓	✓	✓
2	Type I/II	-	✓	✓	✓	✓
3	Type V	-	✓	✓	✓	✓
4	Type I	20%	✓	✓	✓	✓
5	Type I	30%	✓	✓	✓	✓
6	Type I	40%	✓	✓	✓	✓
7	Type I/II	20%	✓	✓	✓	✓
8	Type I/II	30%	✓	✓	✓	✓
9	Type I/II	40%	✓	✓	✓	✓
10	Type V	30%	✓	✓	✓	✓
11	Type V	40%	✓	✓	✓	✓

7.4.2 Mortar Testing

All mixtures were proportioned and mixed according to ASTM C 1012/C1012M (2008) with a cement to sand ratio of 2.75 and water-to-cementitious ratio (*w/cm*) of 0.485. Each mixture included twenty-four 25 x 25 x 285 mm (1 x 1 x 11.25 in) mortar bars with a gauge length of 250 mm (10 in) and a sufficient number of 50 mm (2 in) mortar cubes for determining the compressive strength. Immediately after casting, the molds (bars and cubes) were placed in large polyethylene bags, sealed, and submerged underwater at 35 °C ± 3 °C (95 °F ± 5 °F). [Note: Contrary to most recent version of ASTM C 1012/10120M (2013) where molds are cast and stored over water, and in air at 35 °C (95 °C), these prisms were placed under water.]

All bars were stripped from the molds at 23.5 hr ± 0.5 hr and subsequently transferred to a limewater bath. If a compressive of 20 MPa (2,850 psi) was achieved with the mortar cube, another cube was tested to confirm the results; if the cube did not

reach the prescribed strength, the rest of the cubes were placed in the limewater bath and tested at a later time. All mortar bars were stored in limewater until a compressive strength of 20 MPa (2,850 psi) was reached. When the prescribed compressive strength was achieved, the 6 mortar bars were measured for their initial expansion and placed in a 5% sodium sulfate solution and periodically measured; the sulfate solution was also exchanged out during each measurement.

7.4.2.1 Accelerated Mortar Bar Testing – Vacuum Impregnation

In this study, the remaining mortar bars (18 bars) were tested using a modified version of ASTM C 1012. The performance of mortar bars in various sulfate solutions was evaluated using a novel vacuum impregnation technique in which the specimens are immersed in a sulfate solution and subjected to high-vacuum in accelerate the ingress of sulfate. This method reduces the reliance on the latent diffusion-reaction phenomenon by purposely driving sulfates into the mortar bars.

In order to facilitate sulfate penetration into the mortar bars, the water-filled pores must be dried prior to vacuum impregnation. This allows the now-empty pores to be filled with the sulfate solution at the same concentration to be used for the test. Following this, the mortar bars are stored immediately in a closed vessel under high vacuum, while sulfate solution is introduced into the system. The vacuum impregnation technique is accomplished by performing the following:

- Once strength is achieved, mortar bars are placed at 35°C (95°C) for drying for a minimum of 14 days (or constant mass is achieved). At the end of the drying period, bars are weighed and measured for their length;

- Following the drying period, bars are then placed in a large tank and subjected to a high-vacuum for 4 hours;
- Still under vacuum, the tank containing the mortar bars is introduced with sulfate solution (at the same concentration that is being considered for testing, in this case 5.00% Na₂SO₄, 4.24% MgSO₄, and 4.79% CaSO₄) to entirely cover the specimens. Vacuum is adjusted if needed;
- After 20 hours of immersion (24 hour cycle), vacuum is released and bars are weighed and measured for their initial length (“zero-measurement”)
- The bars are stored at 23 °C (73 °F) in solution at the same concentration as that used in the vacuum impregnation technique;
- Expansion and mass change are measured regularly and visual degradation noted for at least 12 months

7.4.3 Exposure Conditions

All of the mortar bars were vacuum impregnation and immersed in 5% sodium sulfate solution for direct comparison to the traditional ASTM C 1012 method. In this study, the addition of a magnesium sulfate and calcium sulfate solution were investigated at the same sulfate ion concentration as that of the sodium sulfate (33,800 ppm SO₄²⁻); the equivalent magnesium and calcium sulfate concentration were 4.24% and 4.79%, respectively. For the bars immersed in calcium sulfate, the limited solubility (1440 ppm at 20°C) [Skalny et al., 2002] of gypsum did not allow for complete dissolution of the calcium sulfate into water. Consequently, gypsum was precipitated out of solution and accumulated at the bottom (Figure 7-1). Despite this, enough gypsum powder was added

to achieve an “equivalent” target concentration (same sulfate ion concentration as sodium and magnesium sulfate) and mixed thoroughly.

After the initial measurements were recorded (length and mass) following vacuum impregnation, mortar bars were immersed in solution at the same concentration as that used in the accelerated testing. Expansion and mass change were then monitored and recorded by taking the average of the readings of 6 mortar bars.

7.4.4 Microstructural Characterization

In order to characterize the formation of deleterious products from sulfate exposure, mortar bar samples were removed after 1 year of exposure. Small pieces of mortar bar samples were broken off and examined using a scanning electron microscope combined with energy-dispersive spectroscopy (SEM/EDS), and X-ray diffraction (XRD). Sample observed under SEM were sliced into thin 6 mm (0.31 in) sections, grinded, and polished to obtain a quality images and perform semi-quantitative analysis using the EDS detector.

Samples evaluated using XRD were performed using finely-ground powder samples sieved through a 45 micron (0.008 in). Cross-sectional slices were taken to obtain the outer 6 mm (0.25 in) edge (deteriorated zone) and interior sample from each mortar bar sample. It was assumed that 6 mm (0.25 in) would be sufficient in obtaining representative data on the cement hydrate products that were affected by the ingress of external sulfates. Both the outer edge and core were finely ground and X-rayed. Figure 7-1 illustrates the method in obtaining the samples. The samples were scanned from 5 - 60° 2 θ at a scan rate of 0.2° per min with a 6 second dwell time. Quantitative analysis was performed on a diffraction pattern using rutile (TiO₂) as the internal standard.

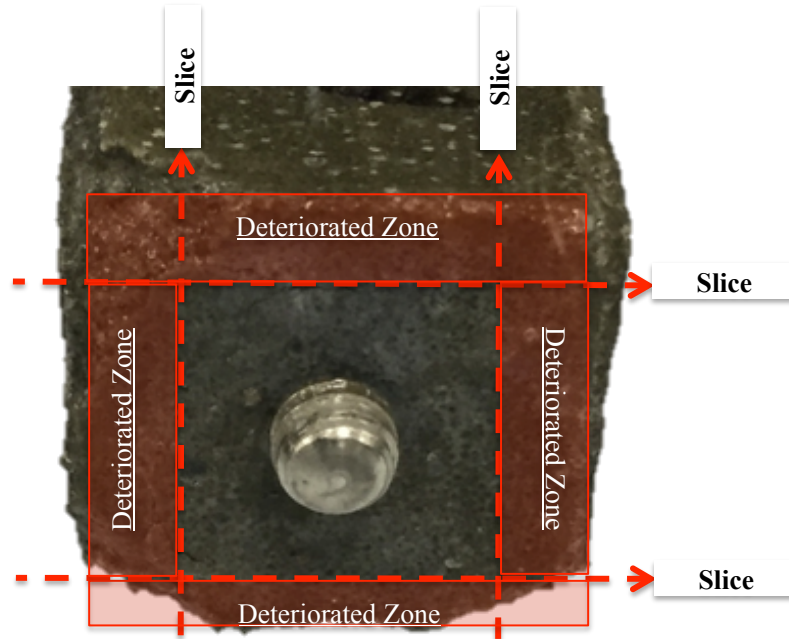


Figure 7-1: Illustration of sample obtained for XRD

7.5 RESULTS

The following section presents the average expansion of the mortar bars cast for each mix design. The first section below provides details on the expansion using the traditional ASTM C 1012 method; following that, the performance in various sulfate solutions using the accelerated method is presented. For all mixtures (and methods), failure of the mortar bars is defined as 0.10% expansion or fracture (whichever is first).

7.5.1 ASTM C 1012 Expansion

Figure 7-2 shows the expansion results for each binder type use in the study. ASTM C 1012 monitors sulfate performance by submerging standard mortars in a 5%

sodium sulfate solution. Thereafter, the length is measured and visual degradation is recorded periodically. From the results presented below, it is obvious that the tricalcium-aluminate content (C_3A) play a significant role in the sulfate performance of cementitious mixtures. The Type I cement had the least resistance to external sulfate, which was expected. It is also important to note that the Type I exceeded the ACI 201 (2008) expansion limit of 0.10% at 6 months. This would mean that that additional preventive measured would be needed in order satisfy sulfate resistance requirements in the lowest exposure class. With decreasing the C_3A contents, the expansion was significantly extended with the Type V ($C_3A \approx 3.5$) showing the most resistance, with expansions less than the 0.10% limit after one year of exposure.

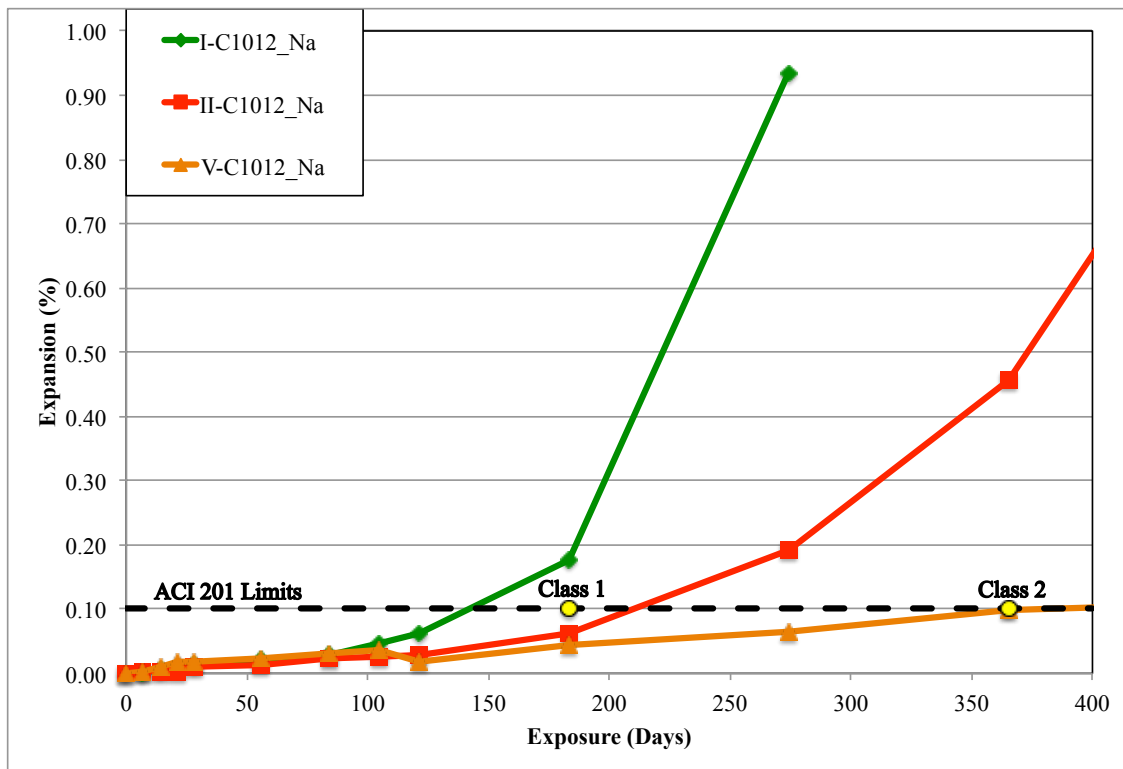


Figure 7-2: Expansion results for ASTM C 150 cements investigated using ASTM C 1012 method

The expansion results for the binary mixtures including a high-calcium Class C fly ash are presented in Figure 7-3. With the addition of the Class C fly ash, the performance is substantially influenced and in all cases, made worse. All mixtures were no longer measurable after only 9 months of exposure with the majority deteriorating completely after only 6 months of exposure. Increasing fly ash replacement generally led to a faster time to failure in all the cements studied. Type I/II cement with 20% fly ash was the only mixture to observe an expansion of less than 0.10% after 6 months of exposure (Class 1 exposure class). The sulfate resistance worsened by increasing the fly ash content to 30 percent, surpassing the expansion criteria after only 15 weeks (0.13%).

It is not surprising to see such poor sulfate resistance with the addition of Class C fly ash. The performance of binary mixtures with Class C fly ashes, specifically in sodium sulfate, has been a major issue with regards to its sulfate resistance (Drimalas, 2007; Dhole, 2008). The availability of reactive calcium-aluminates in glass phases commonly found in these fly ashes can lead to the formation of reactive aluminate hydrates in the hardened concrete. These hydrates are then able to react with the diffusion of external sources of sulfate to form ettringite and/or gypsum and lead to volume change. With increasing dosages, the aforementioned mechanism can further reduce sulfate resistance.

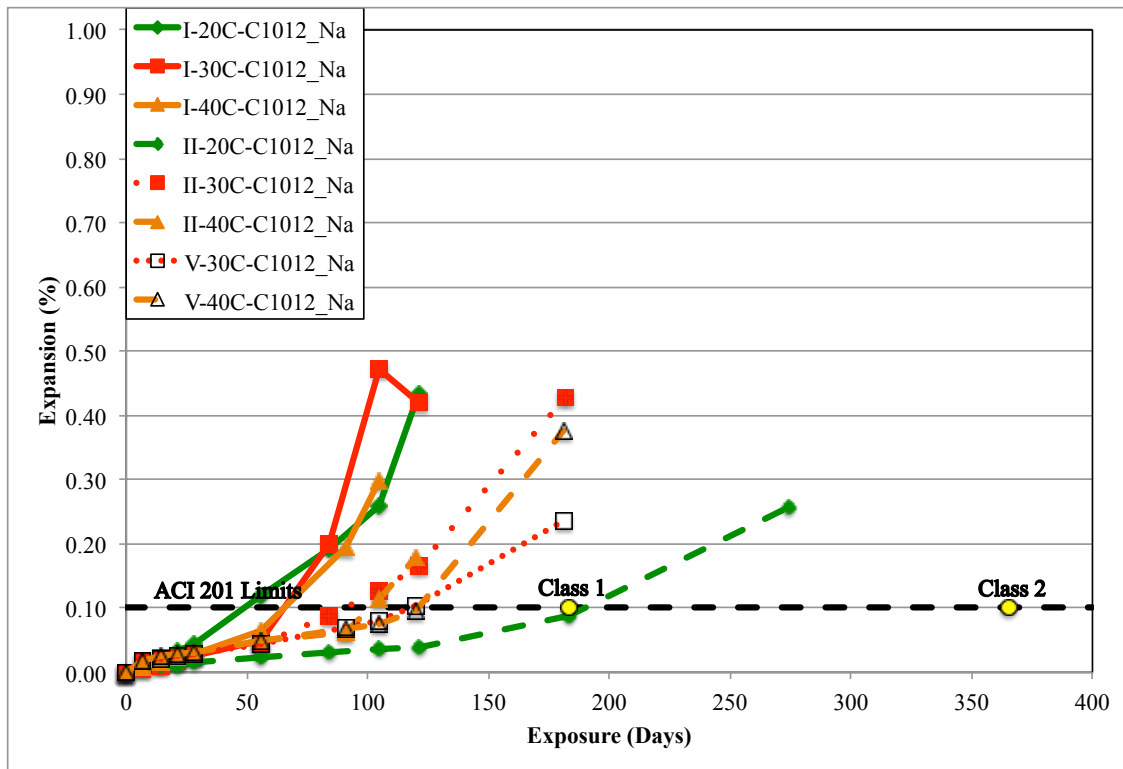


Figure 7-3: Expansion results for binary mixtures using ASTM C 1012 method

7.5.2 Accelerated Sulfate Testing

7.5.2.1 Sodium Sulfate

With the availability of an accelerated test method to evaluate sulfate performance, the results and visual degradation observed were obtained significantly faster in sodium sulfate. The results presented in Figure 7-4 show the rate of expansion for the Type I cement. Results obtained for the Type I cement were significantly quicker with the expansion exceeding the 0.10% after only 2 months of exposure. The results displayed for the Type I/II and Type V cement also exhibited similar trends when compared to their companion samples when tested using the ASTM C 1012 method (see Figure 7-2). In all cases, the mortars exceeded the 0.10% expansion criteria set by ACI 201 in less than 6 months. More specifically, the time to reach 0.10% expansion for

Type I, I/II and V mortar mixtures in sodium sulfate solution was 8, 15, and 17 weeks, respectively.

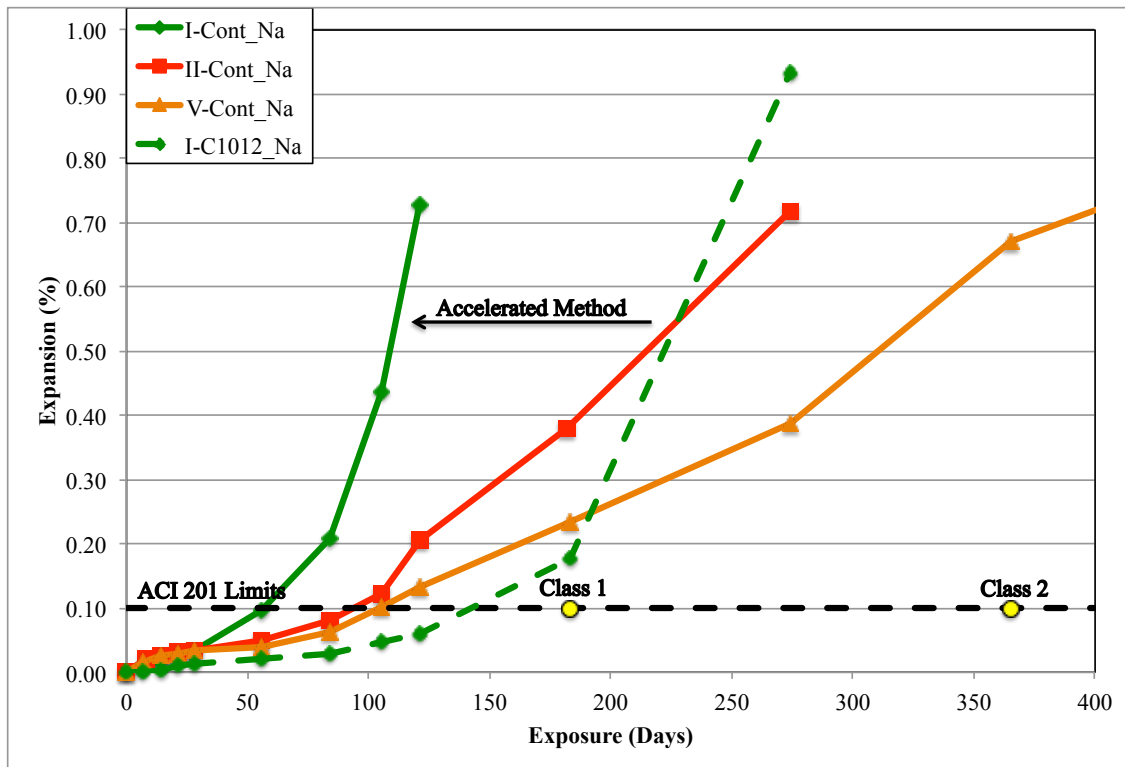


Figure 7-4: Expansion of control mixtures using accelerated method and submerged in sodium sulfate solution

The expansion results for the binary mixture including Class C fly ash were not significantly affected when tested using the accelerated method (see Figure 7-5). Generally, all mixtures observed a higher expansions values when compared to ASTM C 1012; however, the time to reach an expansion >0.10% did not significantly change from the ASTM C 1012 method. The results demonstrate just how severe some high-calcium fly ashes can behave in sulfate environments. One of the interesting things to note, regardless of the how the binary mixtures performed, the rate of expansion was not

significantly influenced by the vacuum impregnation technique. The expansion results demonstrate that although the vacuum method is able to accelerate the ingress of sulfate ions into the mortar bars, the time for the associated expansion mechanism still requires some time to begin reacting.

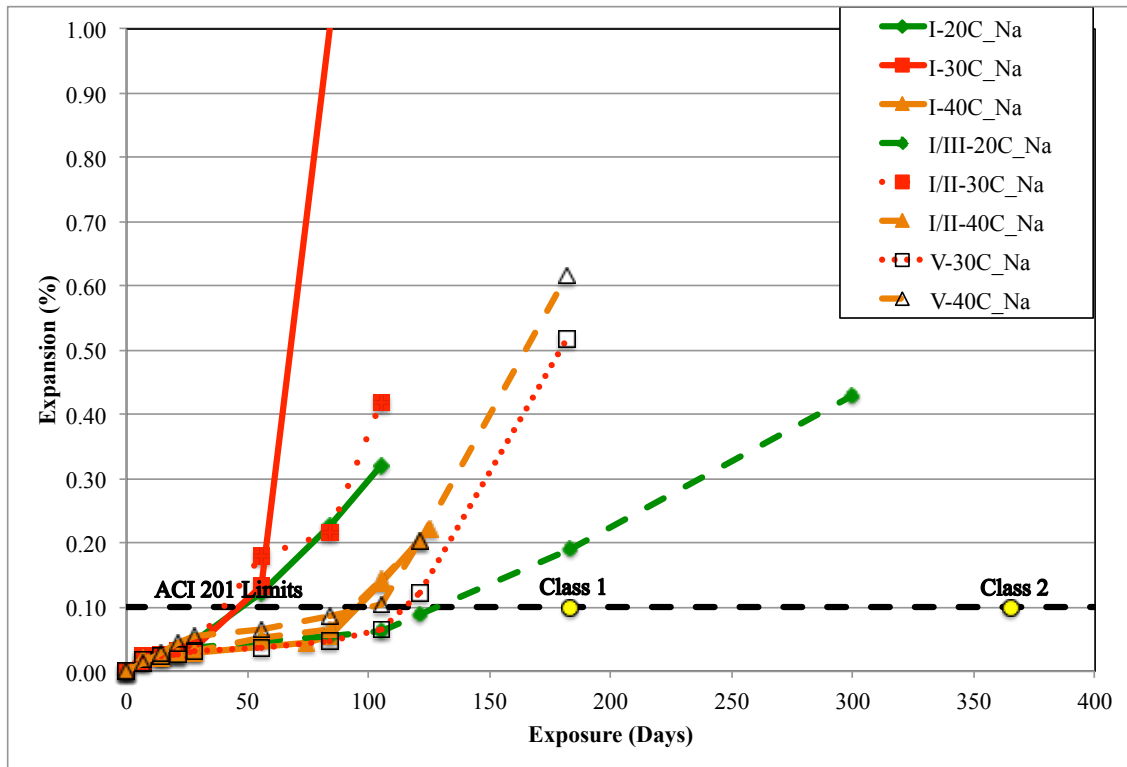


Figure 7-5: Expansion of binary mixtures using accelerated method and submerged in sodium sulfate solution

7.5.2.2 Magnesium Sulfate

The expansion results for each of the binders in magnesium sulfate solution are presented in Figure 7-6. The graph also includes, for comparison, the expansion of mortar bar sample prepared and submerged according to ASTM C 1012 from a report by Drimalas et. al. (2010). Expansion data from this reference were used because the

experimental program presented in this chapter did not include samples tested according to ASTM C 1012 and submerged in magnesium sulfate solution. There are considerable differences noted in the final expansion value as well as the expansion rate. Mortar bars immersed in magnesium sulfate experienced a steady rate of expansion compared to similar mortar immersed sodium sulfate. Although all the mortar mixtures exceeded the 0.10% expansion, the rate at which they did was much slower than in sodium sulfate. Additionally, the overall expansion values after one year of exposure is only about a half of the expansion for the Type I and I/II cements and about a sixth for the Type V cement. An interesting observation, though, is the rate of expansion for the accelerated method when compared to the referenced Type I/II mortar bars. For the Type I/II sample tested using the traditional method, the expansion slowly increased, and did not exceed the 0.10% expansion at the age of 1 year. Although the final expansion value at 1 year did not significantly vary between the two methods, the time to reach 0.10% was reduced by more than half demonstrating the advantage of using the accelerated testing for performance testing.

For all cement-only mixtures, the mortar bars are still measurable with minor deterioration at the corners (see Figure 7-7). Interestingly, the ultimate expansion observed in the Type I and I/II cements were nearly identical (about 0.38%) at 1 year of exposure. Type V exhibited the best performance with no major visual degradation noted after one year of exposure (see Figure 7-8).

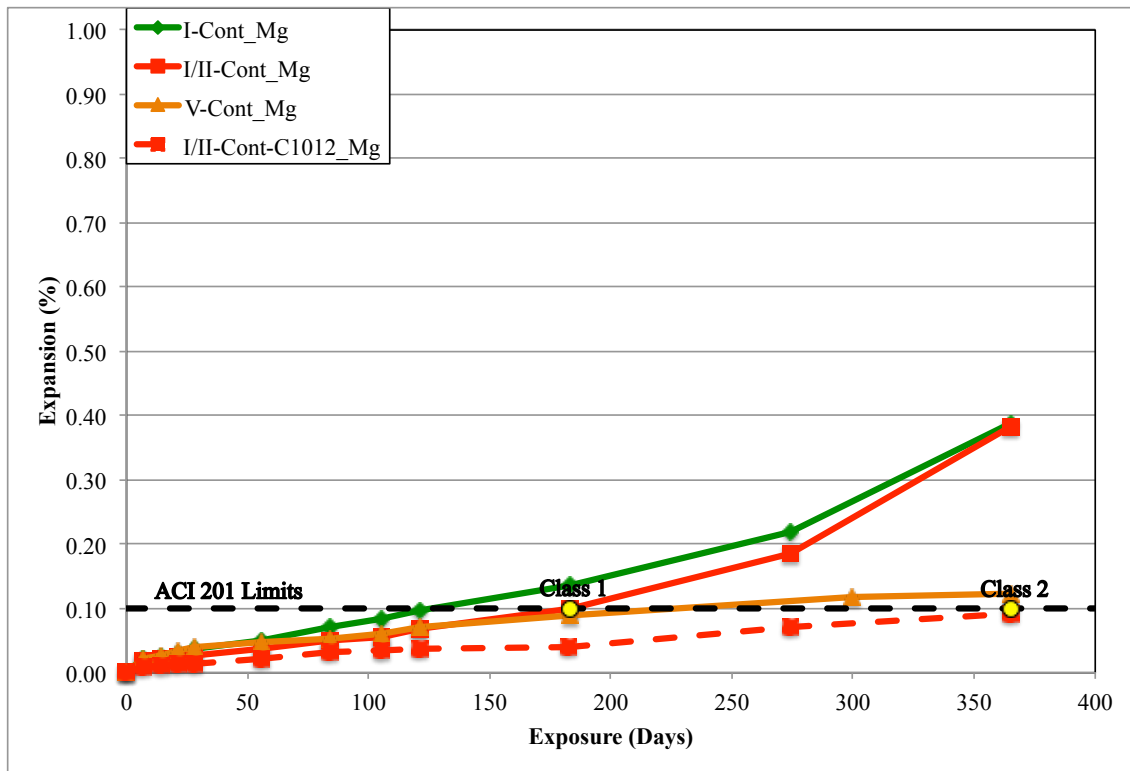


Figure 7-6: Expansion of control mixtures using accelerated method and submerged in magnesium sulfate solution

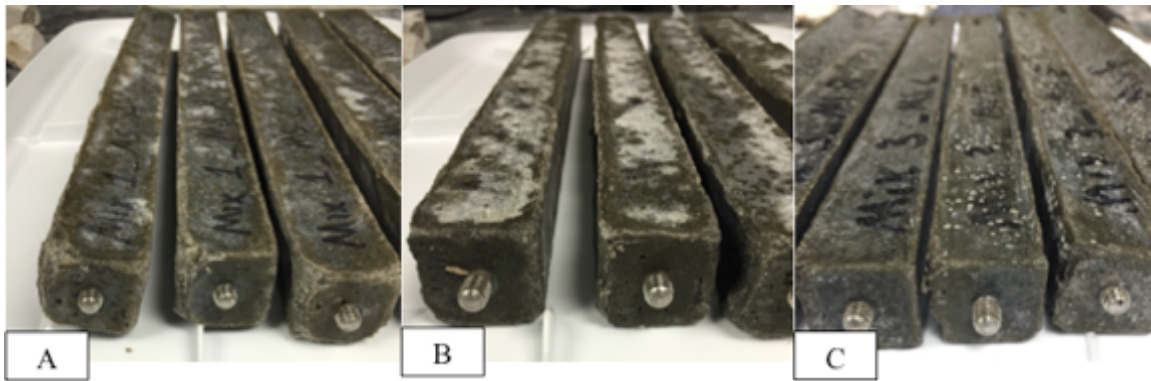


Figure 7-7: Mortar bars of control mixtures exposed to magnesium sulfate solution (12 months); A) Type I; B) Type I/II; C) Type V

A similar trend, but with higher expansion values, was found for the binary mixtures immersed in magnesium sulfate solution (see Figure 7-8). The expansion of all

mixtures generally increased at a steady rate; however, the expansion increased with increasing amounts of SCMs. For all mixtures, with the exception of the Type I + 30% Class C fly, the mortar bars were measurable out to 1 year, with a relatively lower rate of expansion; however, severe deterioration and in some cases warping of the mortar bars were noted after one year (see Figure 7-9). Regardless of the rate, all mixtures exhibited an expansion $>0.10\%$ in less than 6 months and thus failed the expansion criteria for Class 1 exposure in ACI 201.

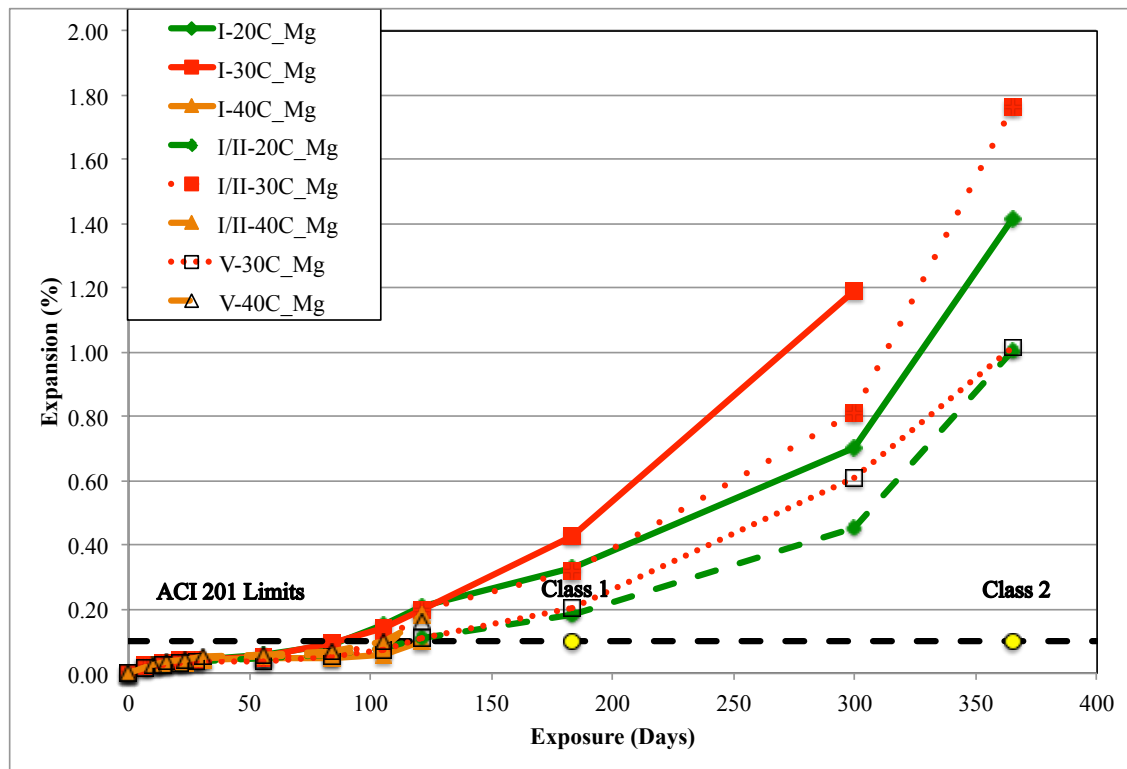


Figure 7-8: Expansion of binary mixtures using accelerated method and submerged in magnesium sulfate solution

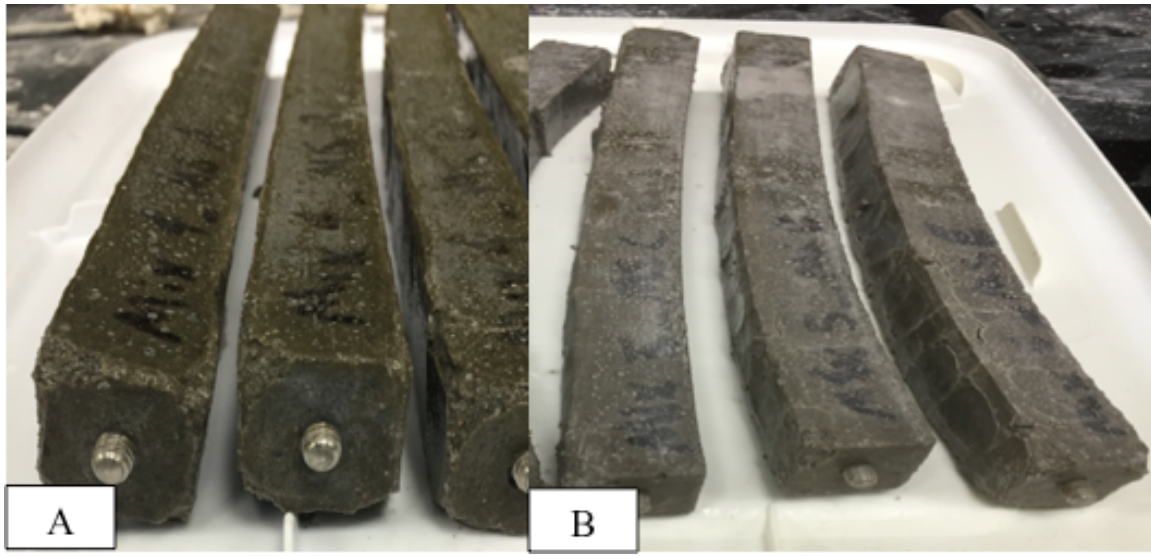


Figure 7-9: Mortar bars of binary mixtures exposed to magnesium sulfate solution (12 months); A) Type I/II-20C; B) Type I/II-30C

7.5.2.3 Calcium Sulfate

It is generally believed that calcium sulfate does contribute to significant damage to concrete structures due to its limited availability of soluble sulfate ion that are able to penetrate and react (Skalny et al., 2002). Consequently, very few studies have reported on the performance in calcium sulfate solutions in a laboratory setting. Mortar bars were cast and evaluated using an “equivalent” sulfate ion concentration as those used in the previous sections. Figure 7-10 illustrates the gypsum that precipitates on the mortar bars and at the bottom of the container as a result of the low solubility from calcium sulfate. Figure 7-11 presents the expansion results for all three binders using the accelerated test method. For comparison purposes, the expansion of mortar bar samples prepared according to Drimalas et. al., (2010) and submerged in calcium sulfate solution is included as a means of relative performance comparison

As expected, a slow rate of expansion was seen in each of binders evaluated when exposed to calcium sulfate; however, the Type I mixture began exhibiting a significant

increase expansion after 6 months and ultimately failed (no longer measurable) after 1 year of exposure, with an expansion of about 0.50%. The results are surprising considering the general assumption that calcium sulfate is less aggressive than sodium and magnesium sulfate. Moreover, the mortar bars were deteriorated and no longer measurable after 1 year of exposure; similar mortar placed in magnesium sulfate exhibited a lower expansion value as well as less deterioration. The results for the expansion study as well the visual appearance (see Figure 7-10), proved that calcium sulfate can be deleterious to cementitious mixtures, especially for high- C_3A cements.

The results using the accelerated method did not seem to significantly effect the relative rate of expansion when compared to ASTM C 1012; however, the results are only presented up to one year. For both the Type I/II and V cements, the level of expansion was less than 0.10% at 1 year of exposure.



Figure 7-10: Type I mixture stored after one year exposure in calcium sulfate

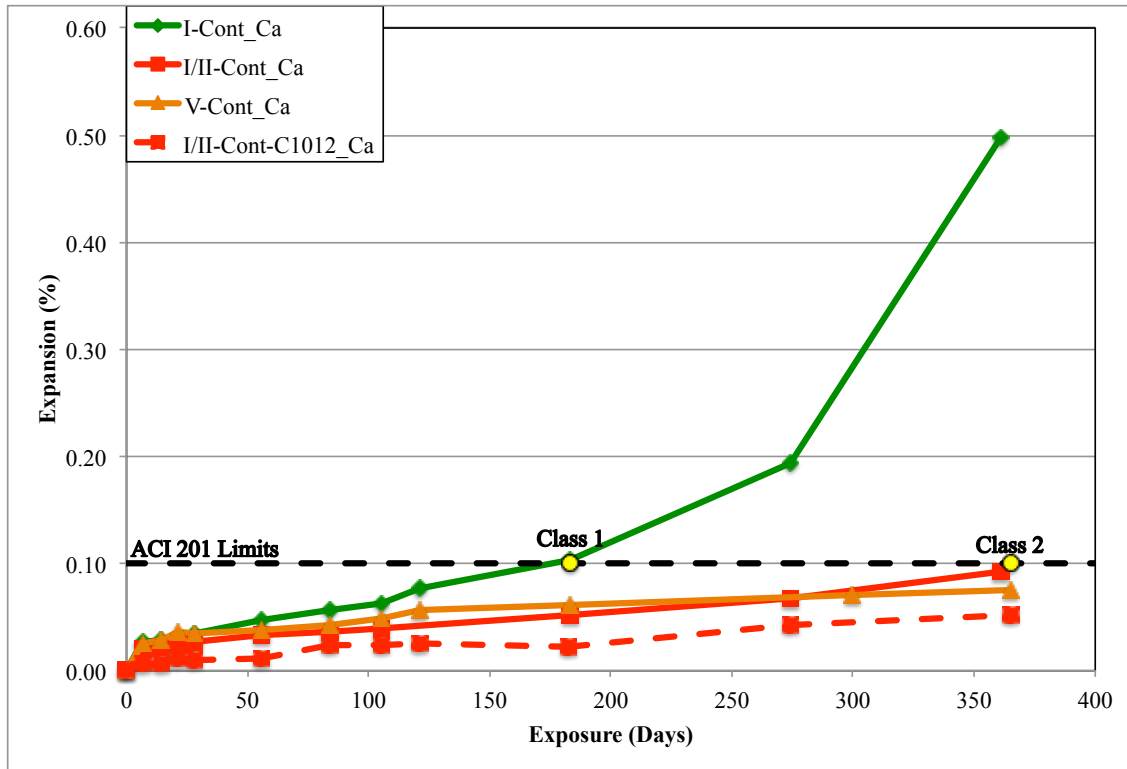


Figure 7-11: Expansion of control mixtures using accelerated method and submerged in calcium sulfate solution

With the exception of the binary mixtures using Type I cement, relatively lower levels of expansion were observed (see Figure 7-12). The results from the binary mixture using Type I correlate well with previous control performance; the higher rate of expansion confirm the significant influence of the C_3A content on sulfate performance. Additionally, the addition of high-calcium fly ash decreased sulfate resistance. Although relatively lower levels of expansion were observed in some these mixtures, deterioration and cracking is evident on the mortar bars (see Figure 7-13).

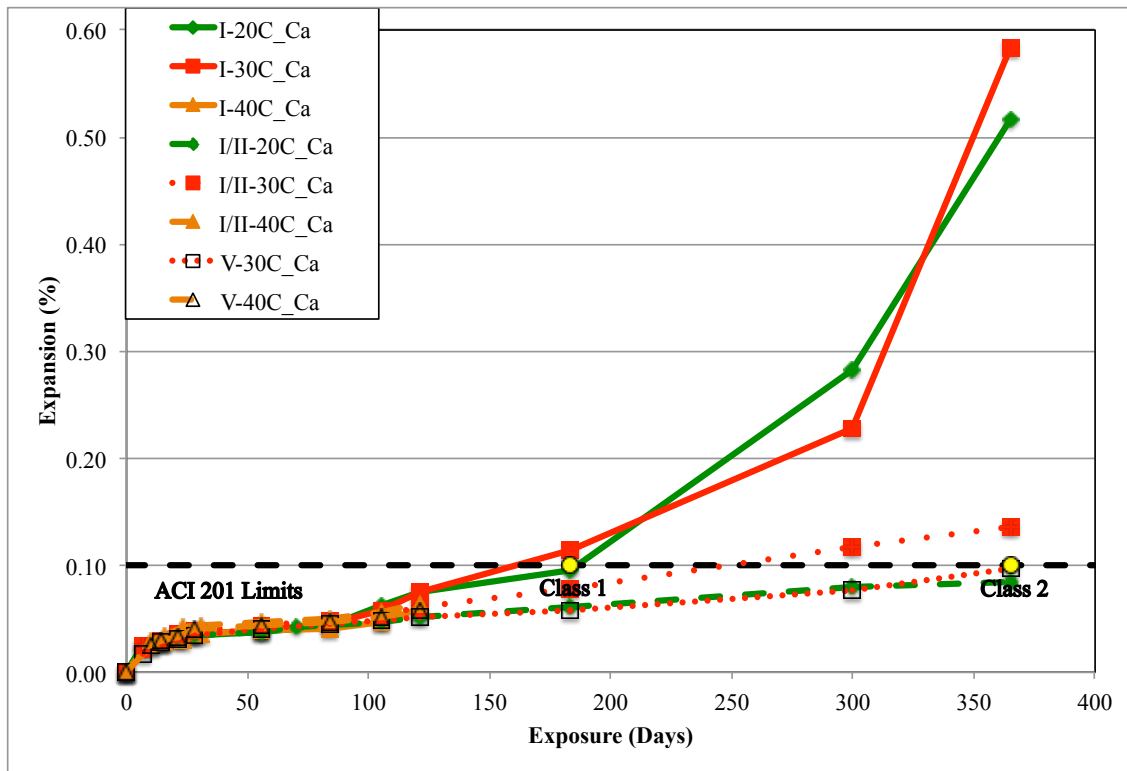


Figure 7-12: Expansion of binary mixtures using accelerated method and submerged in calcium sulfate solution

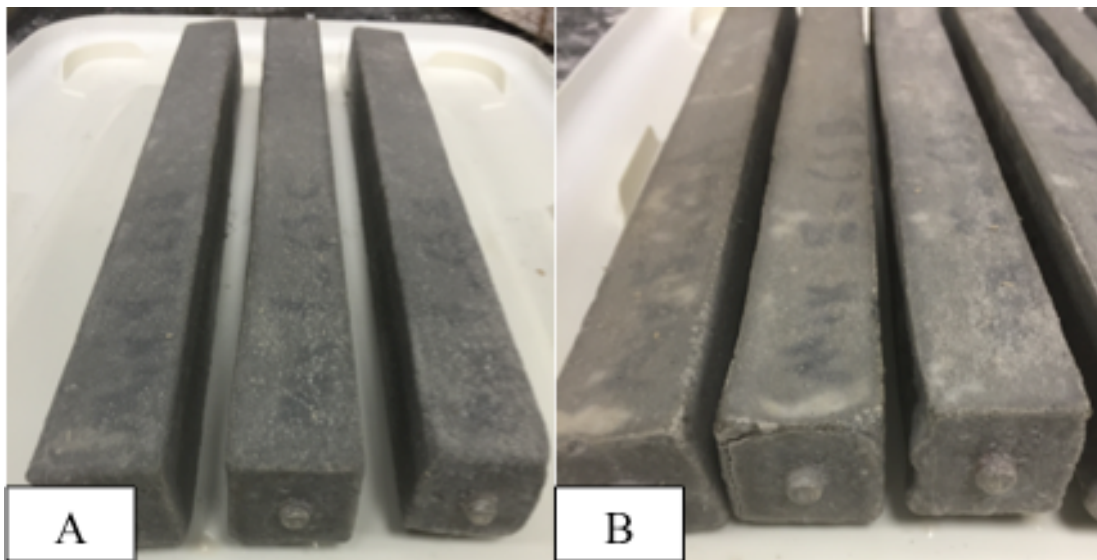


Figure 7-13: Expansion of binary mixtures using accelerated method and submerged in calcium sulfate solution

7.5.3 Microstructural Characterization

7.5.3.1 X-Ray Diffraction

Qualitative X-Ray diffraction analysis was performed on mortar bar samples after one-year exposure in magnesium and calcium sulfate solution in order to identify deleterious sulfate phases. XRD patterns were obtained for the outer 6 mm (0.25 in) deteriorated portions as well as the central piece of the mortar prisms (see Figure 7-1). To a lesser degree, this method was used as an indirect means to evaluate the level of penetration and damage on hydration products. Figure 7-14 and 7-15 shows the XRD patterns over the range from 5° to 50° 2θ for the mortar bars stored in magnesium and calcium sulfate solutions, respectively.

Although there are many similarities between the X-ray diffraction patterns, they also showed differences when comparing the two sulfate solutions. For example, mortar bars immersed in magnesium sulfate clearly showed the presence of ettringite, gypsum and calcium hydroxide (Ca(OH)₂). Mortar bars immersed in calcium sulfate showed significant signs of gypsum, although this may be attributed to some extent to calcium sulfate precipitating onto the mortar bar during testing (see Figure 7-10). Regardless of the solution type, however, ettringite and gypsum is evident in the XRD patterns in all the mixtures.

Figures 7-14 and 7-15 also present the XRD patterns for the core sample that were assumed unaffected by the ingress of external sulfate after one year of exposure. In mortar bars exposed to magnesium sulfate, significant differences in the intensity of the calcium hydroxide peak were noted between the deteriorated and core sample. This may be attributed through the formation of brucite from the reaction with magnesium and calcium hydroxide (Bonen & Cohen, 1992); however, the results from the XRD pattern alone is not sufficient to confirm this.

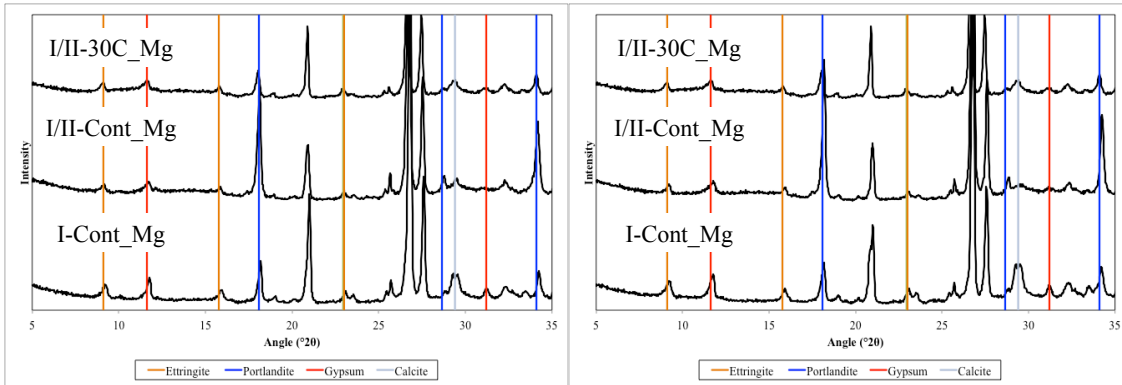


Figure 7-14: XRD patterns from mortar bar samples in magnesium sulfate comparing the composition of the outer deteriorated surface (left) and the interior sample (right)

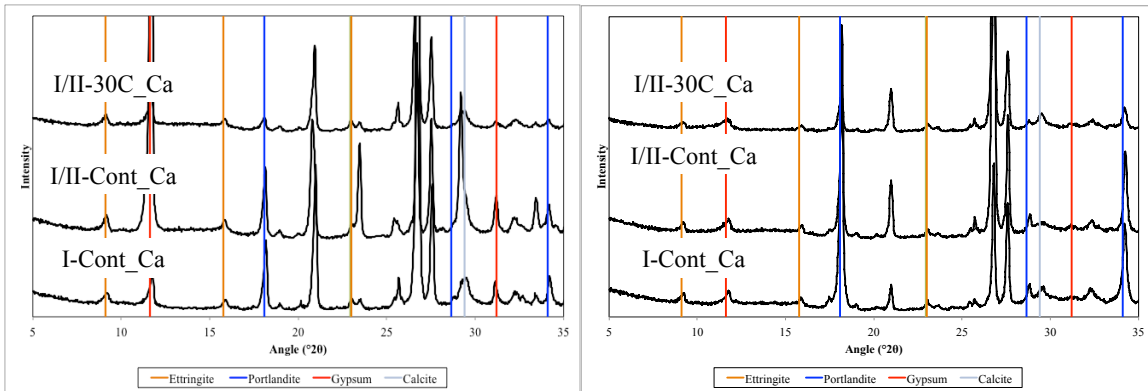


Figure 7-15: XRD patterns from mortar bar samples in calcium sulfate comparing the composition of the outer deteriorated surface (left) and the interior sample (right)

Although the XRD patterns showed the presence of several deleterious by-products from sulfate attack, the trends were not clear and the phase amount was not easily distinguishable. As a result, Rietveld analysis was performed on the cementitious mixtures (see Table 7-3). Based on these findings, the indication of either brucite or M-S-H forming is further supported based on the significant reduction in portlandite content. Additionally, the similar amounts of ettringite present in the Type I and I/II cement correlate fairly well with expansion results showing similar expansion after one year of

exposure; however, there is significant debate whether expansion fully associated with ettringite formation.

Table 7-3: Quantitative Rietveld analysis of cementitious mixtures (error $\pm 3\%$)

Deteriorated Sample	Ettringite (%)		Gypsum (%)		Portlandite	
Mixture/Solution	Calcium	Magneisum	Calcium	Magneisum	Calcium	Magneisum
Type I- Control	7.02	6.78	10.02	4.53	2.33	2.32
Type I/II - Control	6.06	6.71	36.23	6.28	1.76	2.80
Type I/II - 30C	7.45	9.69	6.52	3.11	0.96	0.92
Core Sample	Ettringite (%)		Gypsum (%)		Portlandite	
Mixture/Solution	Calcium	Magneisum	Calcium	Magneisum	Calcium	Magneisum
Type I- Control	5.60	4.07	4.20	2.75	8.25	8.35
Type I/II - Control	8.88	4.13	16.83	1.46	7.32	6.28
Type I/II - 30C	4.59	5.46	3.53	2.70	3.05	2.54

7.5.3.2 Scanning Electron Microscope

Scanning electron microscope was used to better elucidate the mechanisms seen in the mortar bars submerged in magnesium and calcium sulfate solutions. It was evident from the XRD patterns that various deleterious sulfate products were present but it was unclear to what extent it may have had on the visual damage observed on the mortar bars. Figure 7-16 shows a backscattered electron image for the Type I mixture submerged in magnesium and calcium sulfate solution taken after one year of exposure. In both solutions, the surface of the sample shows large deposits of ettringite formation in the hardened cement paste confirming the results seen in the XRD pattern. This was evident up to 200 and 100 microns into the sample for calcium and magnesium sulfate solutions, respectively. Interestingly, mortar bars stored in magnesium sulfate observed well-formed ettringite crystals near the deteriorated surface, whereas calcium sulfate displayed less stable and crystalline form of ettringite as shown in Figure 7-17. The Type I mortar bars stored in calcium sulfate showed much more cracking and deterioration at the

surface than similar bars stored in magnesium after one year of exposure. The SEM images confirm those results observed visually from the mortar bars.

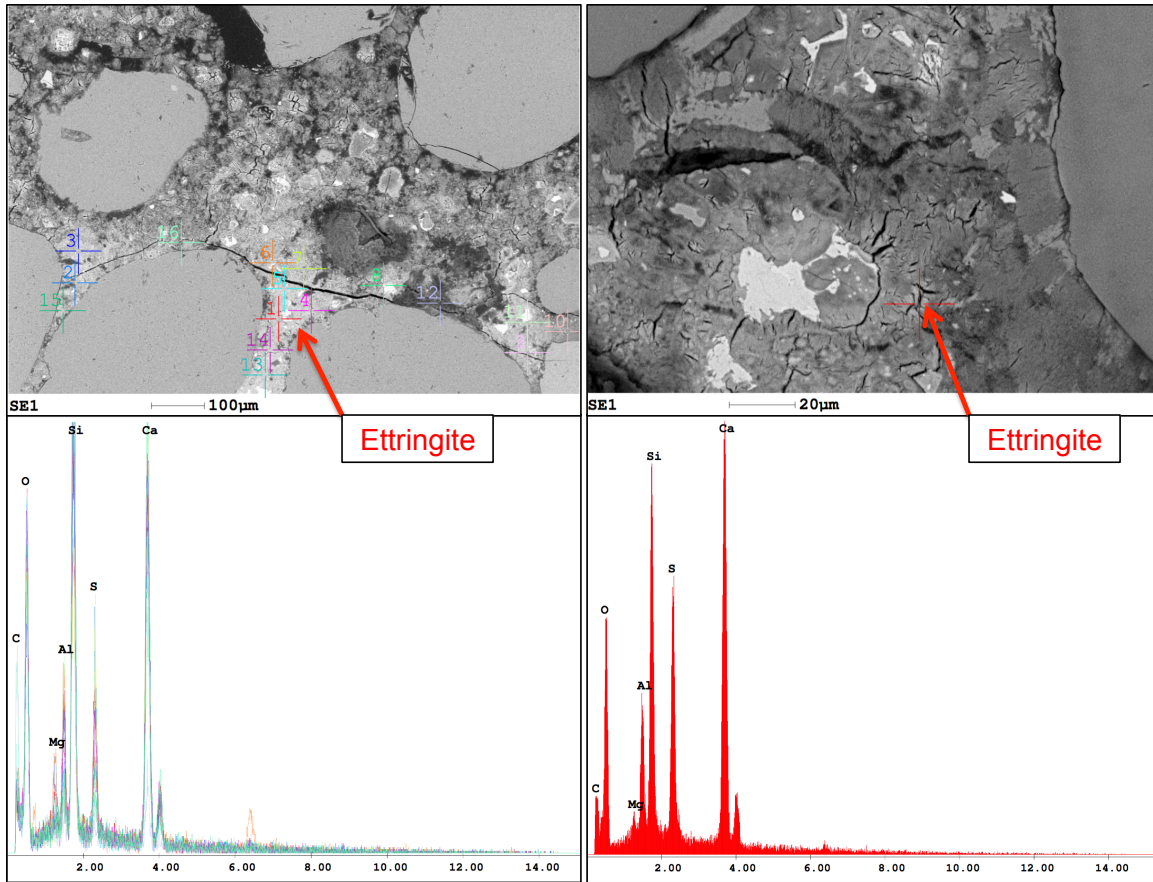


Figure 7-16: Severe ettringite formation for Type I mortar mixtures submerged in calcium sulfate (left) and magnesium sulfate (right)

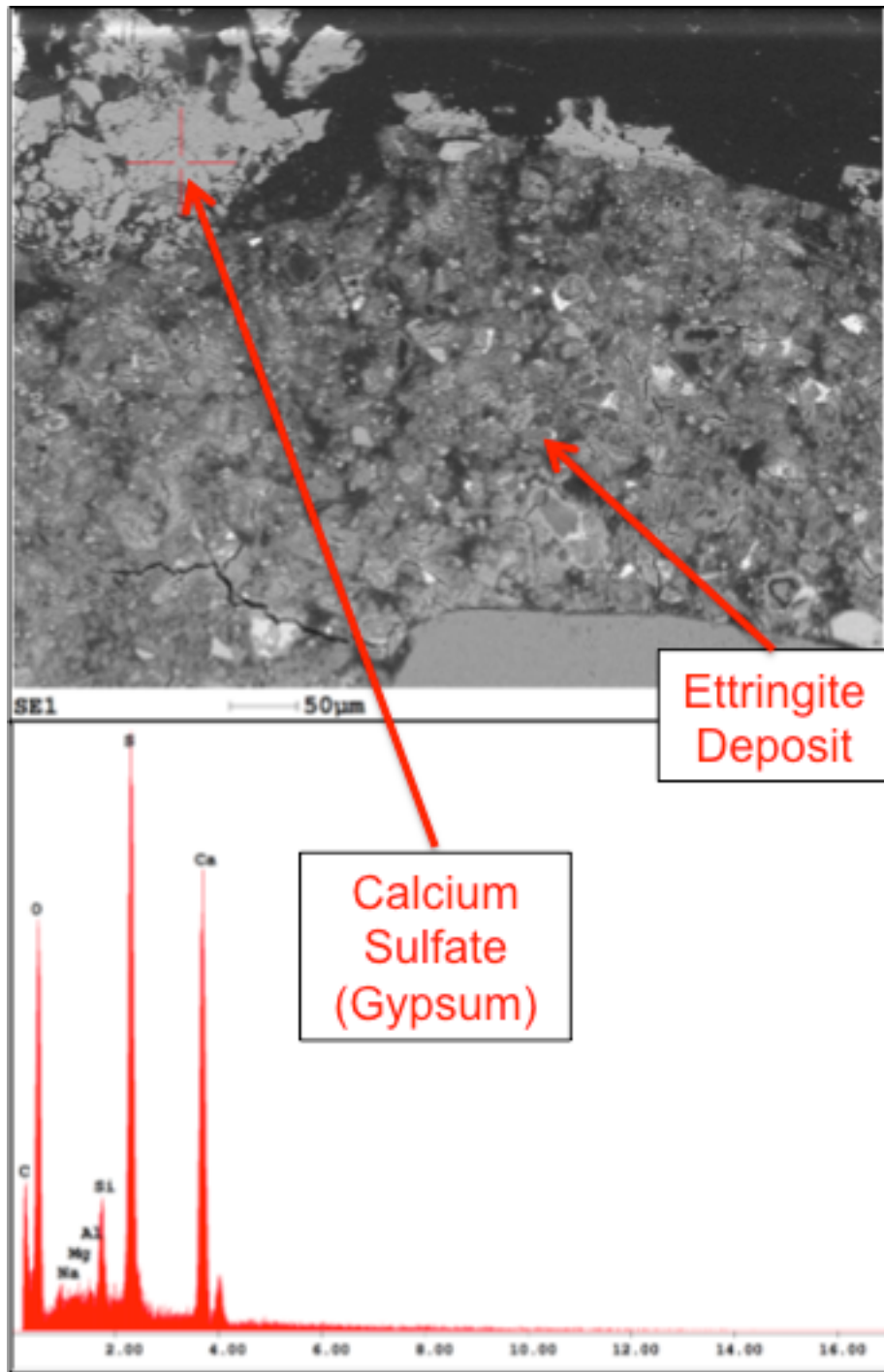


Figure 7-17: SEM image of the surface of a mortar bar submerged in calcium sulfate

Less damage was seen in the Type I/II mixtures with minor cracks surrounding the paste matrix as shown in Figure 7-18. However, mortar bars that were exposed to magnesium sulfate showed significant signs of gypsum surrounding several of the aggregates in the paste. Although ettringite was evident along the deteriorated surface of the mortar bars, the abundant amount of gypsum available in the system may contribute to expansion observed in the mortar bars exposed to magnesium sulfate (see Figure 7.5) [Tian & Cohen, 2000]. Several researchers have observed the formation of gypsum in samples exposed to magnesium sulfate (Bonen & Cohen, 1992; Kunther, Lothenbach, & Scrivener, 2013). However, it is still unclear if the formation of gypsum leads to any expansion.

Figure 7-19 shows the level of sulfate penetration and resulting products formed from exposure to magnesium sulfate. Veins of gypsum can be clearly identified as well as gypsum surrounding the aggregate. Towards the direction of the surface of the sample, the dark layered surface shows significant areas of the M-S-H phase. Interestingly, the surface observed some layers of calcite present that may have been attributed from carbonation of the sample; however, the presence of ettringite further in the paste matrix indicates that a high pH is still maintained in the system. In general, the zone inside of the calcite layer continues to change with the formation of ettringite, gypsum, and M-S-H phase.

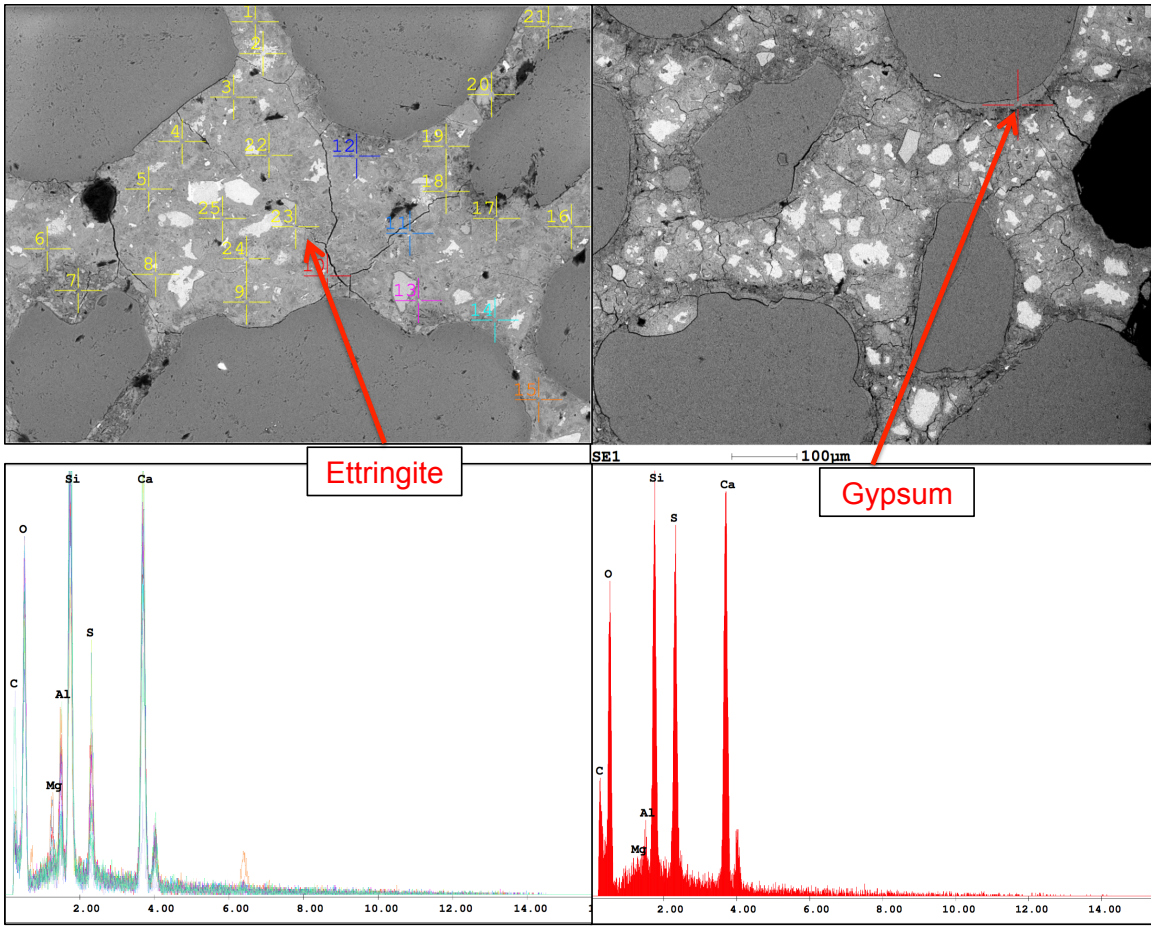


Figure 7-18: Visual observation of cracks forming in Type I/II mixture in calcium sulfate (left) large deposits of gypsum surrounding aggregate evident in magnesium sulfate up to 400 microns into sample (right)

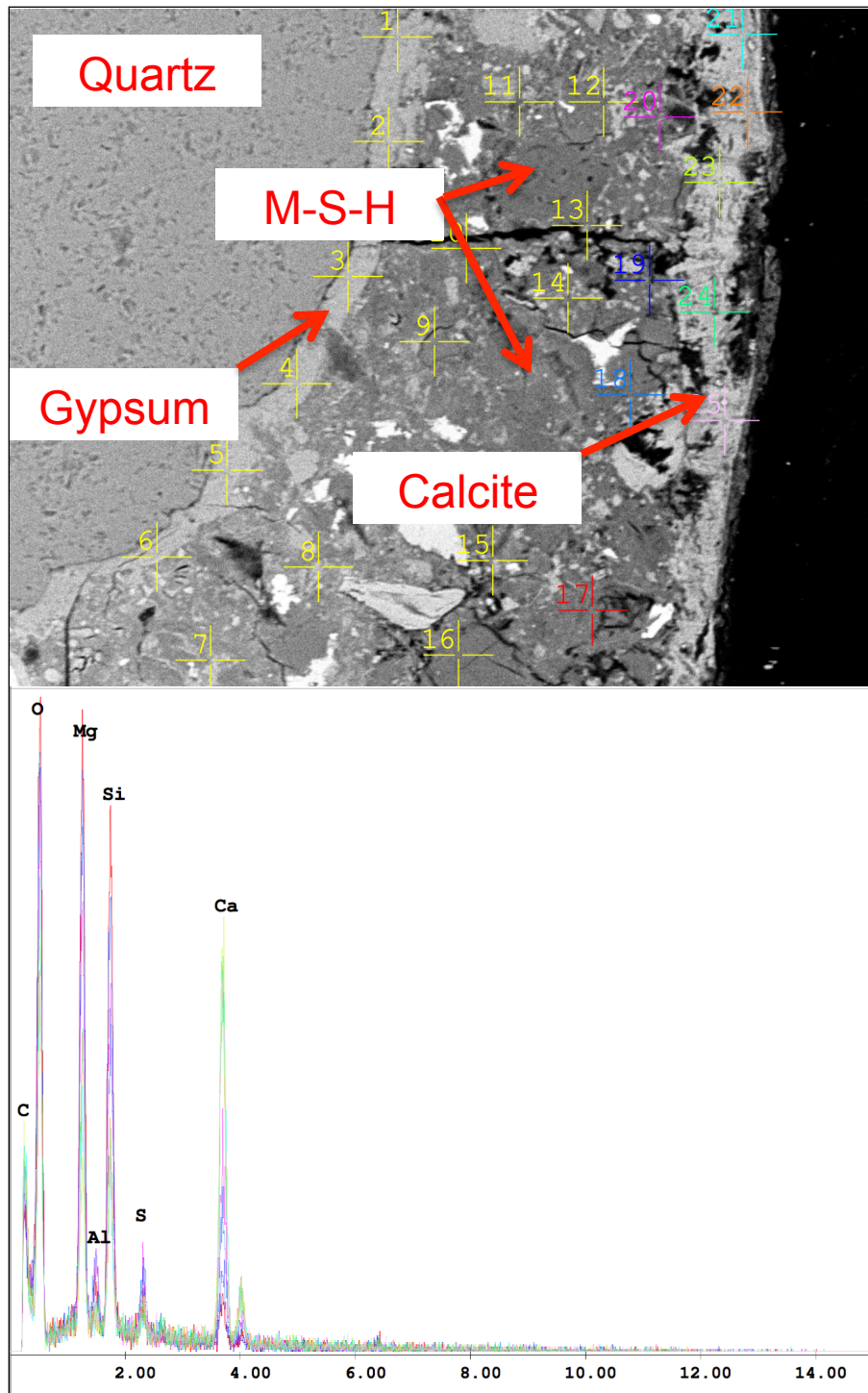
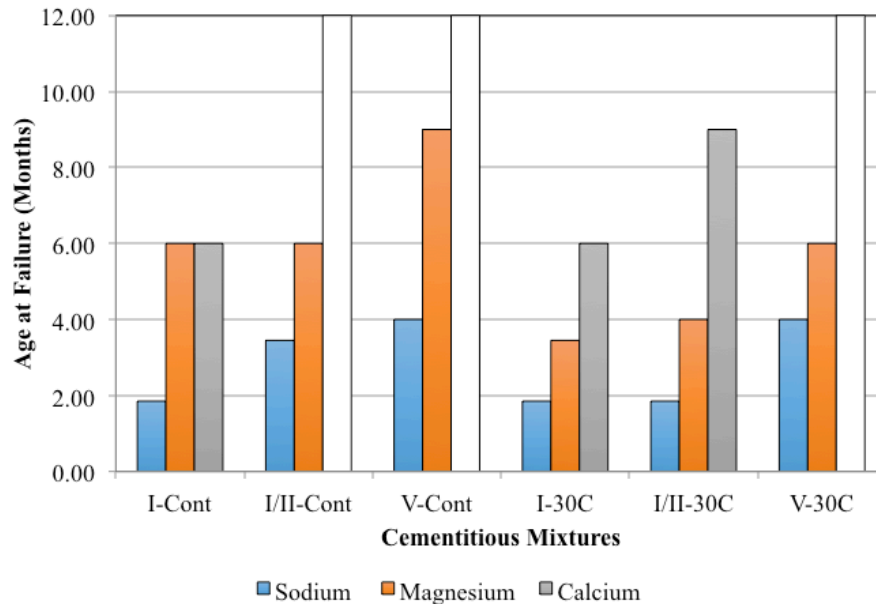


Figure 7-19: SEM images for type I/II control mixture in magnesium sulfate showing depth of sulfate penetration and various deleterious sulfate products formed

7.6 DISCUSSION

When comparing the different sulfate solutions, sodium sulfate solution showed the highest rate of expansion, along with a significantly earlier onset of expansion when tested using the accelerated method. Figure 7-20 shows the variability in time to failure for each sulfate solution type. Additionally, although the time to failure for the binary mixtures was significantly earlier in sodium sulfate and demonstrated poor sulfate resistance, the mode of failure dramatically changed when exposed to either magnesium and calcium sulfate.



* White bars indicates $\leq 0.10\%$ expansion and still measurable

Figure 7-20: Time to failure (Failure indicated as $\geq 0.10\%$ expansion or fracture)

Regardless of solution type, however, similar trends were observed with regard to the tricalcium aluminate (C_3A) content. Decreasing the C_3A content reduced the rate and magnitude of expansion. This was also evident in mixtures stored in calcium sulfate

where significant damage was only observed in those mixtures using Type I cement as the binder. Additionally, less deterioration was observed around the surface of the Type I/II and V mortar bars submerged in magnesium sulfate solution.

From the visual observations of the Type I cement stored in calcium sulfate solution for one year, it is clear that the mechanism with regards to this solution type can lead to severe deterioration. It is worth emphasizing that although calcium sulfate is commonly regarded as the least aggressive sulfate type, sulfates are available to penetrate and can lead to damage. Similar results have been reported in a long-term outdoor durability study by Drimalas (2007).

7.7 CONCLUSIONS

The performance of plain and binary mixtures in sodium, magnesium, and calcium sulfate solutions was evaluated using ASTM C 1012 and a modified accelerated method. The mechanisms of these sulfate solutions on the mortar samples were elucidated using advanced microstructural techniques including SEM/EDS and XRD. Based on the investigation, the following conclusion can be drawn:

- When investigating the performance using the accelerated method, only those mortar bars immersed in sodium sulfate demonstrated a significantly earlier onset of expansion and time to failure ($>0.10\%$); mortar bars exposed to magnesium sulfate observed the next fastest followed by calcium sulfate.
- The expansion of mortar bars was significantly influenced by the type of sulfate solution used. Sodium sulfate was found to be most aggressive solution, exhibiting the highest rate of expansion. The

Type V cement was the only binder still measurable after 12 months of exposure to the sodium sulfate. In all solutions, the effect of the tricalcium aluminate (C_3A) was evident in extending the performance. Binary mixture incorporating the high-calcium fly ash showed poor sulfate resistance when tested in sodium sulfate. Similar observations regarding the performance of high-calcium fly ash mixtures subjected to external sulfate attack have been reported (Drimalas, 2007; Dhole, 2008); However, the effects were less severe in magnesium and calcium sulfate solutions.

- The expansion in sodium sulfate experienced a two-stage process where very little expansion was observed in the first few weeks followed by a sudden increase in expansion; this was less evident in the mortar bars exposed to magnesium and calcium sulfate.
- Although the limited solubility of calcium sulfate did reduce the severity of sulfate attack as compared to sodium and magnesium sulfate, some mixtures did exhibit higher expansion.

Chapter 8: Evaluation of the Effect of Gypsum Addition on the Sulfate Resistance of High-Calcium Fly Ash Mortars

8.1 ABSTRACT

In this chapter, the addition of calcium sulfate (gypsum) to improve the sulfate resistance of blended high-calcium fly ash mixtures is investigated. The objective of this study was to investigate the effects of various gypsum contents on four different types of portland cement varying in tricalcium aluminate (C_3A) content. The addition of gypsum in these blended systems was expected to influence the sulfate resistance of mortar mixtures by increasing the availability of sulfate ions during the early stages of hydration to promote the conversion and stabilization of ettringite from aluminate-bearing phases. Several mortar mixtures varying in “equivalent” tricalcium aluminate content (cement + fly ash) were investigated for deleterious sulfate attack using the standardized method ASTM C 1012/C1012M (2008). Additionally, microstructural investigation on the formation of ettringite was studied using X-Ray Diffraction (XRD) and the Rietveld method. In general, results revealed that increasing amount of calcium sulfate tended to promote the early formation of ettringite and improve the sulfate performance when compared to simple binary system (cement + Class C fly ash).

Keywords: sulfate attack, high-calcium fly ash, calcium sulfate, gypsum, XRD, Rietveld, tricalcium aluminate

8.2 INTRODUCTION

Sulfate attack is a chemical degradation process that may occur in portland cement concrete (PCC) when it is exposed to external sources of sulfates. When concrete structures are exposed to sulfate-rich solutions, groundwater, and/or seawater, they can be susceptible to chemical sulfate attack leading to deterioration and distress that can reduce their overall strength and load capacity. While Type II and V cements are commonly specified to provide moderate and high sulfate resistance, they are less commonly available compared to a Type I cement.

It is widely known that the use of high-calcium Class C fly ashes in combination with ordinary portland cement (OPC) provides less resistance to the chemical manifestation of sulfate attack (Dhole et al., 2011; Dhole, 2007; Drimalas, 2007; Shehata et al., 2008; Radmoski, 2003; Tikalsky & Carrasquillo, 1989). Moreover, the performance is made worse with increasing replacement levels and generally, with increasing calcium (CaO) content (Drimalas, 2007). The use of low-calcium Class F fly ash, however, has shown to improve sulfate resistance (Dhole et al., 2011.). However, with increasing stringent regulation from the Environmental Protection Agency (EPA) on the coal-burning industry to reduce its environmental impact (US EPA, 2014-b; US EPA, 2014-c; Seraj, 2014), the majority of power plants have now switched coal sources to the Powder River Basin (PRB). This has consequently led to a lower quality of Class C fly ash as the predominant type available for use as a supplementary cementitious material in portland cement concrete (PCC).

This research focuses on enhancing the sulfate resistance of Class C fly ash mixtures through the addition of calcium sulfate (gypsum) used as mineral admixture with varying amounts of tricalcium aluminate (C_3A) content. The research aims at finding optimum gypsum levels for providing adequate sulfate resistance to high-calcium

fly ash mixtures through performance testing and providing insights into the mechanisms by which the optimum SO_3 content has the most significant impact in sulfate resistance.

8.3 EXPERIMENTAL PROCEDURES

8.3.1 Cementitious materials and calcium sulfate

Three commercially available ASTM C 150 cements with varying tricalcium aluminate (C_3A) content were used in this study. These cements were a Type I (C1), Type I/II (C2) and Type V (C5) cements with C_3A contents of 11.52%, 6.80%, and 3.80%, respectively. For comparison purposes, a Class H oil well cement (OW), procured from Lafarge (now LafargeHolcim) was chosen for this study to evaluate the influence of a cement with approximately no C_3A content; the compositional analysis using Bogue calculations revealed a $\text{C}_3\text{A} = 0.42\%$ for the OW cement used in this research. Table 8-1 and 8-2 presents a summary of the compositional analysis along with the phase composition for the cements investigated, respectively.

One sources of high-calcium (HC) Class C fly ash was used in all blended fly ash cement mixtures. The HC fly ash selected has been extensively studied by others researchers (Drimalas, 2007; Dhole 2008) and consistently exhibites poor sulfate resistance when used alone as a binary mixture with Type I cement. Moreover, the sulfate resistance decreases, generally, with increasing replacement of the Class C fly ash. See Table 8-2 for the bulk chemical compositional of HC fly ash.

One source of calcium sulfate dehydrate ($\text{CaSO}_4 \cdot \text{H}_2\text{O}$) was procured and used in varying combinations with the four cements. The gypsum procured meets the ASTM C 452 (2008) requirement and is from the U.S. Gypsum Company and of grade Terra Alba, Food & Pharmaceuticals (100% gypsum by weight).

Table 8-1: Mineralogical analysis of cementitious materials

	Type I (C1)	Type I/II (C2)	Type V (C5)	Class H Blend (OW)	Fly ash (HC)
SiO ₂ , (%)	20.84	20.38	20.62	21.00	30.76
Al ₂ O ₃ , (%)	5.95	4.90	3.77	3.03	17.75
Fe ₂ O ₃ , (%)	2.51	3.55	3.66	4.50	5.98
CaO, (%)	62.77	63.62	62.22	63.84	28.98
MgO, (%)	1.43	1.14	4.56	2.46	6.55
SO ₃ , (%)	3.43	2.86	2.95	3.00	3.64
Na ₂ O, (%)	0.15	0.11	0.25	0.10	2.15
K ₂ O, (%)	1.00	0.67	0.34	0.14	0.30
ZnO, (%)	0.02	0.01	0.03	0.02	-
SrO, (%)	0.09	0.08	0.07	0.09	-
Mn ₂ O ₃ , (%)	0.05	0.05	0.05	0.06	-
P ₂ O ₅ , (%)	0.20	0.02	0.06	0.13	-
TiO ₂ , (%)	0.29	0.02	0.21	0.18	-

Table 8-2: Phase composition analysis for cements (Bogue Calculation)

	C ₃ S (Wt. %)	C ₂ S (Wt. %)	C ₃ A (Wt. %)	C ₄ AF (Wt. %)
C1	53.59	19.32	11.52	7.64
C2	66.12	8.55	6.98	10.80
C5	66.02	9.31	3.80	11.14
OW	73.50	4.76	0.42	13.69

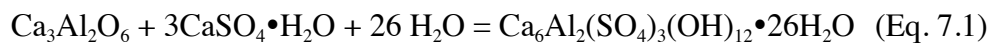
8.3.2 Mixture Proportions – Equivalent tricalcium aluminate content (C_3A_{eq})

This study focused on the effects of tricalcium aluminate content ($C_3A = 11.52\%$, 6.80% , 3.80% , and 0.42%) and gypsum used as an additive at varying replacement levels for possible improvement in the sulfate resistance of blended high-calcium fly ash mixtures. Therefore, a method for quantifying the sulfates and calcium aluminates in fly ash/cement blends was required. The gypsum required was calculated as per the procedure explained by Tikalsky (1989) and Van Aardt (1985) and loosely based on research performed by Dhole (2008); however, as a modification to the procedures performed in literature, the calcium aluminates in cement (quantified as tricalcium aluminate) used for the calculation was determined using the Rietveld method as shown in Figure 8-1. Table 8-4 presents the calculated and measured C_3A content between Bogue and Rietveld analysis along with the percent difference. The Rietveld results presented are on refinements with a weighted profile R-factor (R_{wp}) $\leq 10\%$ (Toby, 2006)

Relative to the Bogue calculation, C_3A measured using the Rietveld method resulted in significant differences in percent amounts. The C_3A content for C1 measured by Rietveld was about 30 percent lower than that calculated using Bogue equations, with the Rietveld-measured value being 7.93% , placing this cement type as a Type I/II according to ASTM C 150. Similarly, the C_3A content by Rietveld was found to be less than 5% (4.75%) for C2, placing it as a Type V cement as per ASTM C 150. Interestingly, the OW cement showed the largest difference between the two methods; however, Bogue calculations are typically not recommended for these types of cements. Results for the measured C_3A using Rietveld were based both on the cubic and orthorhombic crystal structures. As such, it was assumed that both crystal structures participated in the reaction with the sulfates available from the fly ash/cement blend as well as from the gypsum addition.

Quantifying calcium aluminates in fly ash is more difficult due to the complex nature of fly ash crystalline and glassy phases (Dhole, et.al., 2013). The reactive alumina available in fly ash is partly from crystalline and partly from the glassy phases. Based on review of available mineralogical data for high-calcium fly ash, Freeman (1992) concluded that approximately one-third of the bulk chemical alumina was estimated to be present as part of reactive calcium aluminate phases (Freeman & Carrasquillo, 1995; Dhole, 2008). Therefore, a similar estimation was used on the HC fly ash used in this study. Subsequently, the reactive alumina content can be converted to equivalent tricalcium aluminate using the molar mass ratio of $C_3A/Al_2O_3=2.65$. To allow for direct comparison of the various mixtures evaluated, the HC Class fly ash was kept at a constant 40% replacement of cement by mass for all cement/fly ash blends; thus, resulting in an equivalent tricalcium aluminate content (C_3A_{eq}) of 11.03%, 9.13%, 8.2%, and 7.65% for C1, C2, C5, and OW cements, respectively.

Lastly, sulfates in both cements and fly ash were quantified as sulfur trioxide (SO_3) and total available SO_3 contents were calculated for each blended fly ash cement mixture. The bulk SO_3 content in the fly ash was used in this part of the calculation. The gypsum requirement for each mixture is calculated using the stoichiometric equation (Van Aardt, Vissar, 1995; Dhole; 2008):



$$(SO_3)_{required} = 0.90 * C_3A_{eq} \quad (\text{Eq. 7.2})$$

$$(SO_3)_{max} = 0.70 * C_3A_{eq} \quad (\text{Eq. 7.3})$$

From the above equations, however, the SO_3 content is limited to 0.70 to avoid delayed ettringite formation. Thus, the following equation was used to calculate the gypsum requirement:

$$(SO_3)_{max} - (SO_3)_{available} = (SO_3)_{add} \quad (\text{Eq. 7.4})$$

The SO₃ addition was converted to gypsum with the molar mass ratio of CaSO₄•H₂O/SO₃=2.15. For this study four gypsum dosages at equal increments were chosen to investigate for all fly ash/cement blends, as shown in Table 8-4. Appendix C presents an example calculation of gypsum requirement for HC fly ash and Type I cement mixture.

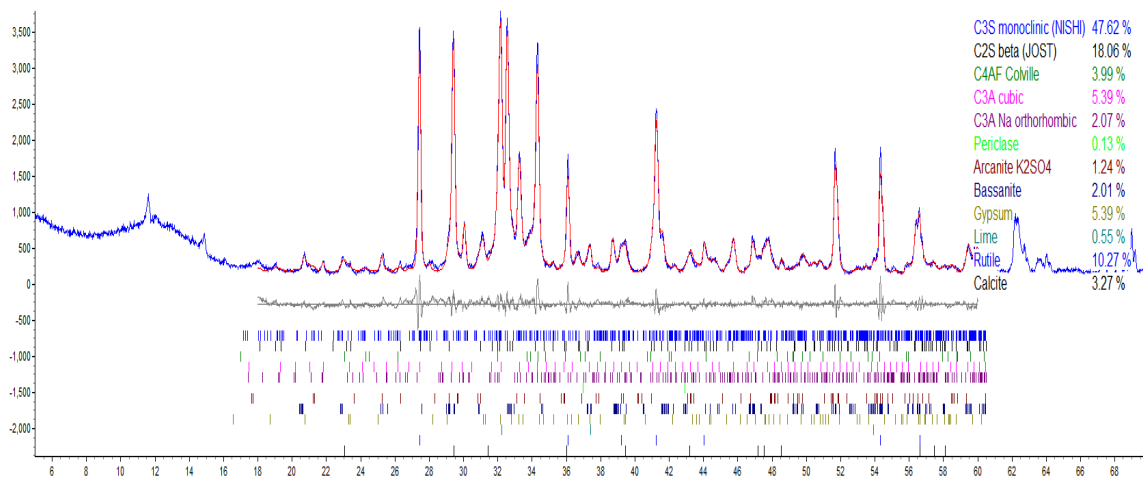


Figure 8-1: Rietveld analysis for cement C1

Table 8-3: Bogue and measured Rietveld results for the C₃A content in cements*

	C1 (Wt. %)	C2 (Wt. %)	C5 (Wt. %)	OW (Wt. %)
C ₃ A (Bogue) (Wt. %)	11.52	6.80	3.80	0.42
C ₃ A (Rietveld) (Wt. %)	7.93	4.76	3.21	2.29
% Difference	31.16%	30.01%	15.51%	449.54%

*Note: (error ± 3%)

Table 8-4: Mixture Proportions and equivalent C₃A contents of fly ash cement blends

Cement/Fly Ash Blend	Mixture ID	Gypsum (% Addition)	SO₃ (OPC + Fly Ash + Gypsum), %
C1/HC (C ₃ A _{eq} =11.41%)	C1.0	0%	3.51
	C1.1	1.01%	3.98
	C1.2	3.01%	4.91
	C1.3	6.03%	6.31
	C1.4	9.04%	7.72
C2/HC (C ₃ A _{eq} =9.51%)	C2.0	0%	3.08
	C2.1	0.85%	3.45
	C2.2	2.56%	4.18
	C2.3	5.13%	5.28
	C2.4	7.69%	6.39
C5/HC (C ₃ A _{eq} =8.58%)	C5.0	0%	3.23
	C5.1	0.70%	3.51
	C5.2	2.10%	4.07
	C5.3	4.21%	4.90
	C5.4	6.31%	5.74
OW/HC (C ₃ A _{eq} =8.03%)	OW.0	0%	3.26
	OW.1	0.61%	3.49
	OW.2	1.83%	3.96
	OW.3	3.65%	4.66
	OW.4	5.48%	5.36

8.3.3 Methods of investigation

In this research, the comparison and analysis of various blended fly ash cement mixtures was done using mortar bar testing for expansion, microstructural

characterization including X-ray diffraction (XRD), scanning electron microscopy (SEM) coupled with energy-dispersive x-ray analysis (EDS), and isothermal calorimetry.

8.3.3.1 Mortar bar testing

Standard mortar bars measuring 25 x 25 x 285 mm (1 x 1 x 11.25 in) were used for all the mortar mixtures in combination with cement/fly ash and different levels of gypsum dosages. A standard graded Ottawa sand (ASTM C 778, 2011) with sand to cementitious (portland cement & fly ash) ratio of 2.75:1 was used and the water-to-cementitious ratio (w/cm) was kept constant at a 0.485. Mixtures were prepared following the procedures outlined in ASTM C 305 (2011) except when required, the gypsum was added to the water and mixed for 15 seconds prior to the addition of cementitious materials. Mortar bars were cast and evaluated for their length change following the procedures described in ASTM C 452 and ASTM C 1012 detailed in the following sections.

8.3.3.1.1 ASTM C 452

ASTM C 452, which is applicable only to portland cements (not suitable for establishing the sulfate resistance of cement in combination with pozzolans or slag cement), covers the determination of the expansion of mortar mixtures made with cement containing high amounts of sulfates. The cement under testing is added with gypsum to obtain a total SO_3 content = 7% by mass. The gypsum used in the study must have fineness of 90% particles passing through the 45-micron sieve. This method is suitable for evaluating the expansion of mortar bar in correlation of the C_3A content of the cement used and thus provides an indication of sulfate resistance.

Two batches were prepared and cast for each cement evaluated. The initial length was recorded after 23.5 hr \pm 0.5 hr of curing in a moist room at 23 °C (73 °F). The mortar bars were submerged in deionized water and recorded for their length change after 1, 4, 7, 14, and 28 days; the deionized water was replaced after every measurement to reduce leaching of the alkalis.

8.3.3.1.2 ASTM C 1012

ASTM C 1012 was used to determine the sulfate resistance of cement in combination with HC fly ash and gypsum. After preparing three 50 mm (2 in) mortar cubes and 6 mortar bars, molds were placed in large polyethylene bags, sealed, and submerged underwater at 35 °C \pm 3 °C (95 °F \pm 5 °F). After 24 hours at 35 °C (95 °F) the bars and cubes were stripped from the molds and subsequently transferred to a limewater bath at ambient conditions. When the cubes reached a strength of 20 MPa (2,850 psi) [generally 1-3 days after casting] the bars were immersed in 5% (33,800 ppm SO₄²⁻) sodium sulfate solution at 23 °C (73 °F). Length measurements were taken at 1, 2, 3, 4, 8, 12, and 15 weeks as well as every 3 months thereafter to compare the amount of expansion for each cement with varying amounts of gypsum. Expansion results are presented up to 9 months with testing ongoing.

8.3.3.2 *Microstructural characterization*

In order to determine the type and amount of hydration/reaction phases present in the mixtures (mainly ettringite, gypsum, monosulfate, and portlandite), quantitative XRD using the Rietveld method and SEM/EDS analysis was performed on mortar bar samples prior to sulfate exposure (i.e., “zero” measurement). Samples observed under SEM were sliced into 6 mm (0.31 in) sections, grinded, and polished to obtain quality images and

identify elemental phases present using the EDS detector. EDS analysis was performed at an accelerating voltage of 20 kV and a beam current of 65 μA , with a working distance of 12 mm.

Thereafter, quantitative XRD was performed on mortar bar samples after 2, 4, and 26 weeks of exposure to 5% sodium sulfate solution. At each interval, cross-sectional slices from the mortar bars were obtained and dried using the solvent exchange method by soaking in isopropanol for 5-10 days. Afterwards, samples were stored under vacuum in a desiccator at 23 °C (73 °F). Each sample was then removed from the desiccator, ground into a fine powder passing a No. 325 (45 micron) sieve, and prepped for quantitative XRD. The composition of the hydrated pastes was determined by performing the Rietveld method on the diffraction patterns. Rietveld analysis is the technique to determine with accuracy the quantities of crystalline phases present in a sample. The procedure involves determination of calculated XRD patterns through simulation technique based on the information provided for the probably phases present. Simulations to determine the calculate diffraction pattern were carried out using the TOPAS software. The calculated pattern is refined step-by-step to take into account peak shape, instrumental factors, variations in structures, errors induced during sample preparation, and temperature effects (Dhole, 2008; Dinnebier & Billinge, 2008). Refinement is a systematic procedure in Rietveld analysis to obtain the simulated XRD pattern in close agreement with the observed XRD pattern. Results presented in this study are on refinements with a weighted profile R-factor (R_{wp}) $\leq 10\%$ (Toby, 2006). The samples were scanned from 5-60° 2 θ at a scan rate of 0.2° per min with a 6 second dwell time. Quantitative analysis was performed on a diffraction pattern using rutile (TiO_2) as the internal standard.

It is worth mentioning that analyses for quantifying the type and amount of hydration or reaction products present was based on full cross-sections of mortar bars, and as such, the results are averaged across a section that can be comprised of both damaged mortar (at surface exposed to sulfate solution) and undamaged mortar (bulk center) of a given sample. Nevertheless, this technique was used consistently throughout the study and allowed for the identification of general trends in reaction products formed.

8.3.3.3 Isothermal Calorimetry

Several studies have shown that pre-blending the gypsum with fly ash can promote early reaction of the two phases to form ettringite (Shehata et al., 2008). This is due to the fact that premixing produces a homogenous blend in which the sulfate and aluminate phases are intimately close and readily available to react. As such, cement paste mixtures were also cast to monitor the heat of hydration process and reaction products formed in samples containing C1, HC, and gypsum; selected mixtures included fly ash that was finely ground passing a No. 325 (45 micron) sieve and pre-blended with the gypsum prior to mixing. Qualitative XRD was performed to determine the probable impact of the hydration products on the sulfate resistance of paste pre- and post-sulfate exposure.

Eight different paste samples were prepared and tested using a Grace Adiabatic isothermal calorimeter. Two 20 g paste samples were prepared in 125 mL polymer cups for each mix and the *w/cm* was maintained at a 0.485. Paste samples were proportioned in each sample cup, capped, and mixed using an ultrasonic vibrator for approximately 2 minutes for consistency. The samples were placed in the isothermal calorimeter chamber and cured in a manner similar to that of the mortar bars tested as per ASTM C 1012 (35

°C ± 3 °F [95 °F ± 5 °F]) for 24 hours and monitored for their hydration curve. The samples were cured further for 3 days in saturated lime solution at 23 °C ± 2 °C (73 °F ± 4 °F), constituting a total curing period of 4 days. After 4 days, each sample was taken out and edges removed to reduce the potential of preferred orientation from the calcium hydroxide peaks thus resulting in a small cross-sectional sample from the center. The two center paste samples were broken into small pieces and either placed in reagent isopropanol, or exposed to a 5% sodium sulfate solution for 45 days prior to drying using the aforementioned solvent exchange method. Each sample was removed from the desiccator, ground into fine powder passing a No. 325 (45 micron) sieve, and tested for qualitative XRD. The sample were scanned from 5-60° 2θ at a scan rate of 0.2° per min with a 4 second dwell time.

8.4 RESULTS AND DISCUSSION

8.4.1 Mortar bar expansion

8.4.1.1 ASTM C 452

Figure 8-2 presents the length change results for the mortar bars tested using each cement type. As expected, the observed expansion had a strong correlation between the C₃A content for cements used in this study. Surprisingly, C2 cement resulted in the highest expansion of approximately 0.025% after 14 days in deionized water. The results indicated that the C2 cement had poor resistance with the addition of sulfates in the system. The higher expansion observed in the C2 cement is assumed to be from the availability of additional anhydrous cement particles available to react as compared to the other cements tested. ASTM C 150 (2016) recommends a maximum expansion value of 0.04% for a Type V cement tested at 14 days. The cements investigated recorded an

expansion of 0.024%, 0.025%, 0.016%, and 0.008% at 14 day for C1, C2, C5, and OW cements, respectively.

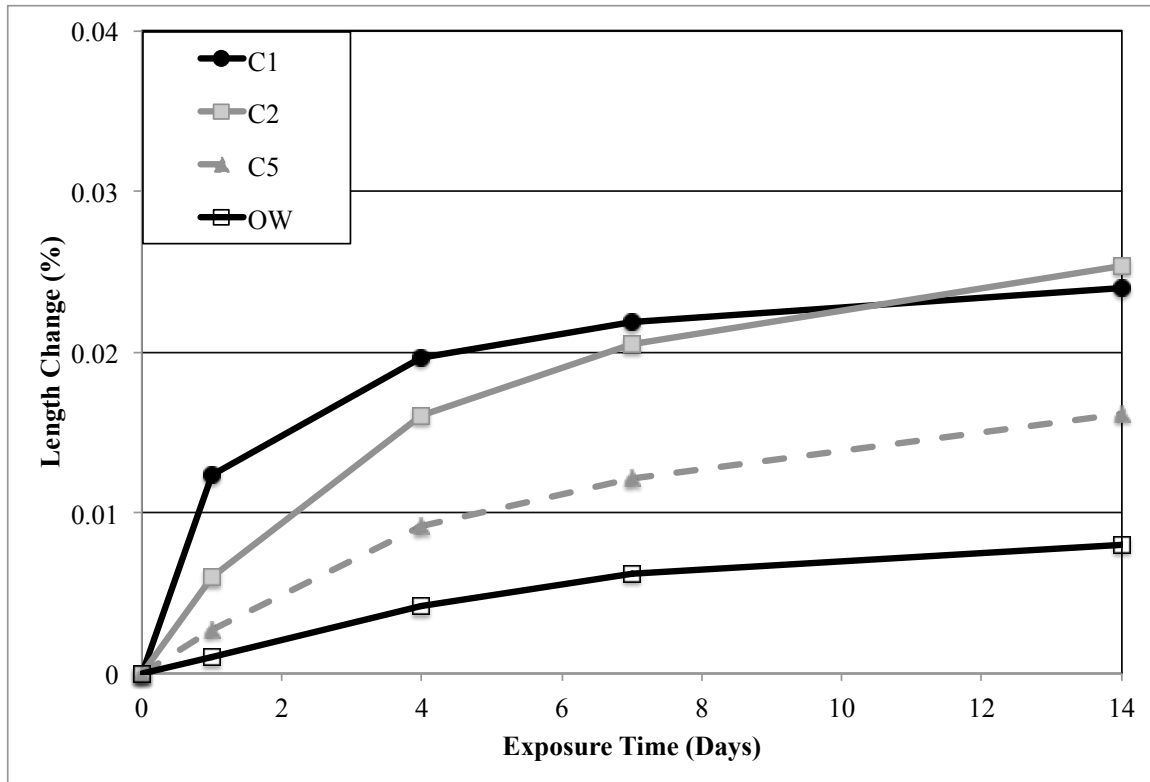


Figure 8-2: Length change for cements tested using ASTM C 452

8.4.1.2 ASTM C 1012

Figure 8-2 presents the expansion for up to 9 months for blended mixtures using C1 cement in combination with 40% HC fly ash and varying amounts of gypsum placed in 5% sodium sulfate solution. All mixtures, with the exception of C1.4, were fully deteriorated and no longer measurable after 9 months.

From the results, it is clear that the sulfate performance is significantly improved with increasing amounts of gypsum addition. Mortar bars samples containing no gypsum broke and were fully deteriorated after just 28 days of exposure and showed the worse

performance. Whereas, mixtures using 1.01% and 3.01% gypsum showed extended improvement in expansion having measurements out to 56 and 121 days, respectively. Mixture C1.3 exhibited the lowest expansion up to 183 days followed by a sudden change in the rate of expansion. Despite similar expansion values 9 months, mixture C1.4 remained intact with minor cracks around the ends and corners of the bars. The results demonstrate that the perceived expansion may not be related to ettringite formation. Figure 8-3 illustrates the disparity of damage of mortar bars samples containing 0% (C1.0) and 9.04% gypsum (C1.4) after 28 and 274 days, respectively,

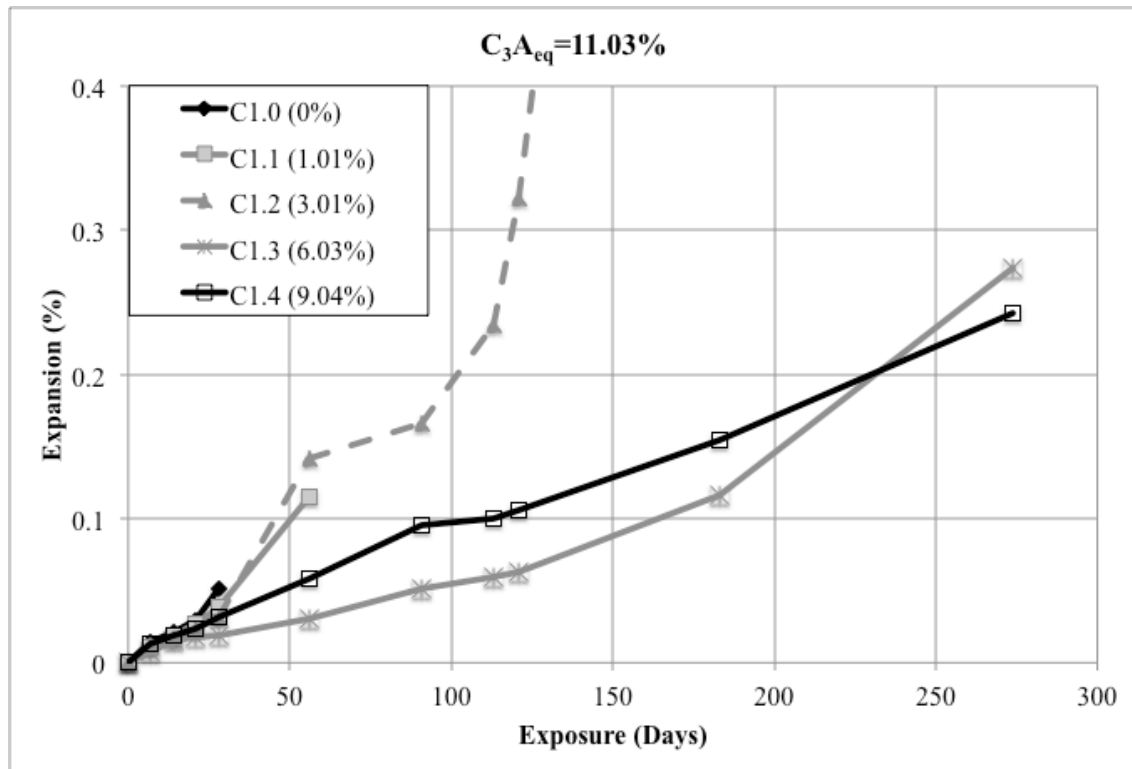


Figure 8-3: Length change for blended C1/HC with varying gypsum dosages in 5% Na_2SO_4 solution (% gypsum addition)

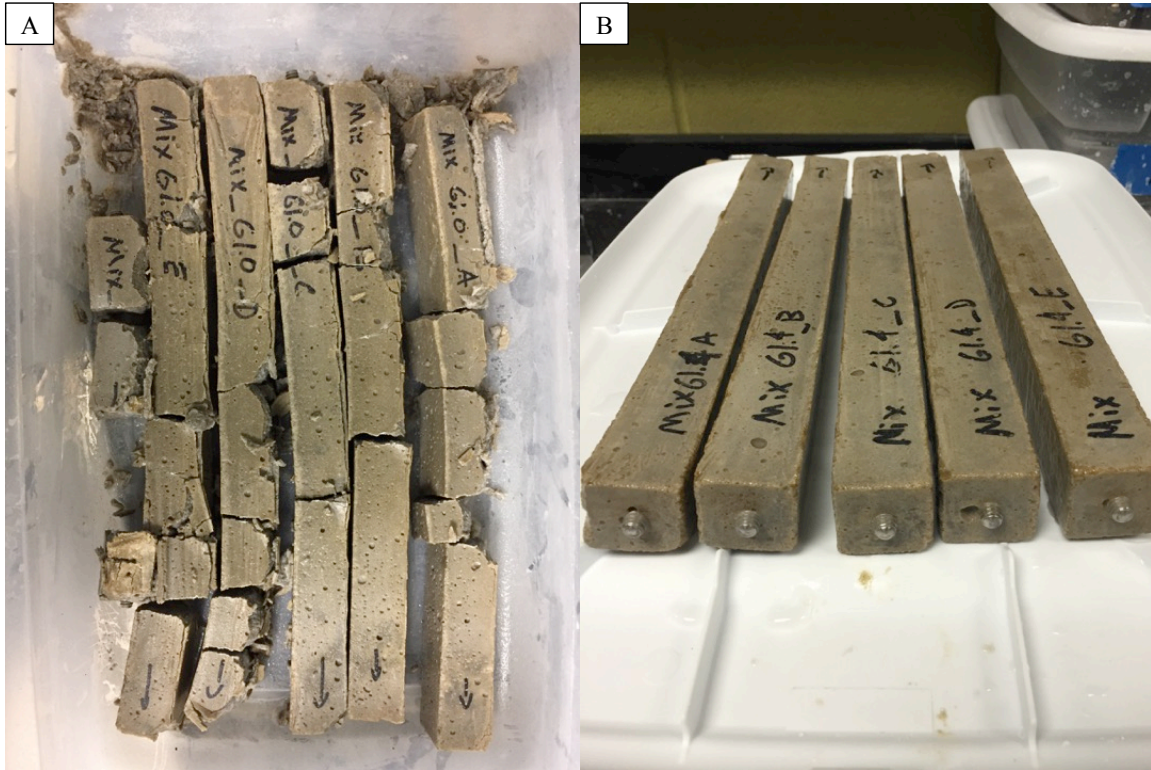


Figure 8-4: A) Mixture C1.0 after 28 days exposure; and B) Mixture C1.4 after 9 months exposure in 5% Na₂SO₄ solution

A similar trend, but with higher expansion values, was found for C2 cement (see Figure 7-5). The ternary blends of C2, HC and gypsum showed much less improvement as compared to C1 mixtures in terms of expansion. This is contradictory to previous research by Freeman & Carrasquillo (1995) where a blended Type II fly ash mixture exhibited superior performance when compared to the control. The results, however, were presented for concrete specimens and varying water-to-cementitious ratios (*w/cm*).

Interestingly, the mixture in combination with the highest gypsum content observed the highest expansion of approximately 1.16% after 274 days in sodium sulfate solution. Additionally, from the addition of gypsum, the deterioration and mode of

failure was typically less severe even with significant expansion. Additionally, the first three gypsum dosages showed various expansion values with increasing gypsum amounts; however, their time to failure was unaffected.

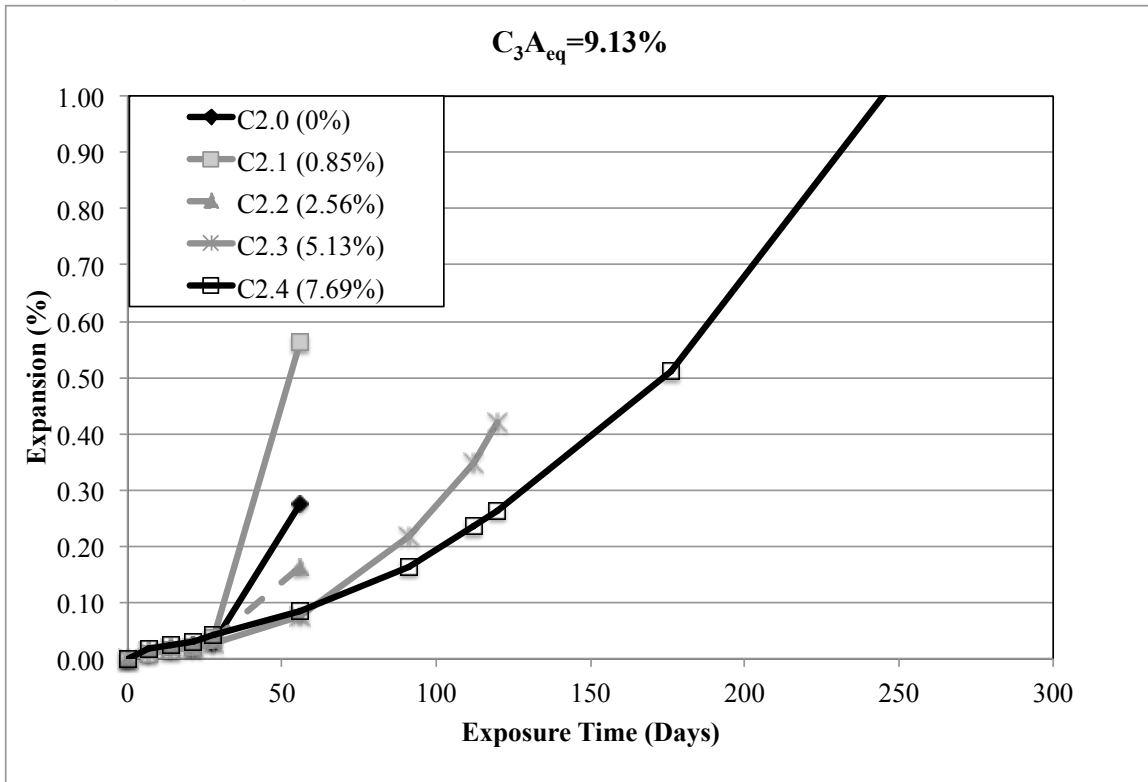


Figure 8-5: Length change for blended C2/HC with varying gypsum dosages in 5% Na₂SO₄ solution (% gypsum addition)

Figure 8-6 and 8-7 show the expansion versus time for samples using C5 and OW cement, respectively. The blended C5/HC mixtures showed interesting trends with increasing gypsum content. Mixture C5.2 showed the least expansion of approximately 0.33% after 6 months exposure; however, all mortar bars were completely broken and no longer measurable after 9 months. On the other hand, mixture C5.4 having the highest gypsum dosage (6.31%), was still measurable at 9 months despite observing minor warping and size cracks in a few of the mortar bars. Moreover, mixture C5.4 observed

the highest rate of expansion at every measurement compared to companion C5/HC mixtures.

Remarkably, blended mixtures using OW cement showed no significant effect from the addition of gypsum in the system exhibiting the highest expansion values from all of blended fly ash cements tested in this program. Although the increasing gypsum dosages extended the time to failure, significant expansion was still observed.

Although, the performance is a result of synergy of the ternary system (cement + fly ash + gypsum), OW cement are commonly known to have a $C_3A = 0\%$ in terms of Bogue calculations. Thus, it can be inferred that the observed mechanisms and deterioration is conceivably a result of the chemical and mineralogical characteristic from the fly ash having no influence from the addition of gypsum on the hydration products formed. It may also be possible that C_4AF is contributing to sulfate reactions in the OW cement, but this needs to be confirmed.

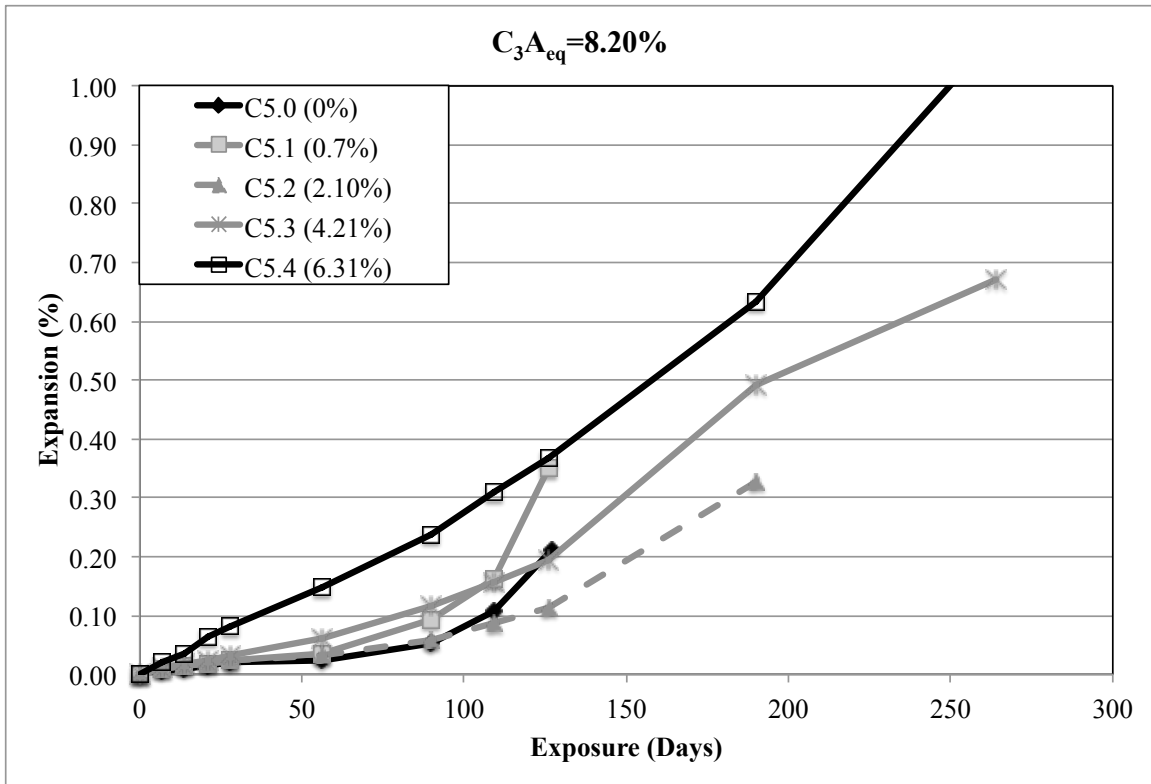


Figure 8-6: Length change for blended C5/HC with varying gypsum dosages in 5% Na_2SO_4 solution (% gypsum addition)

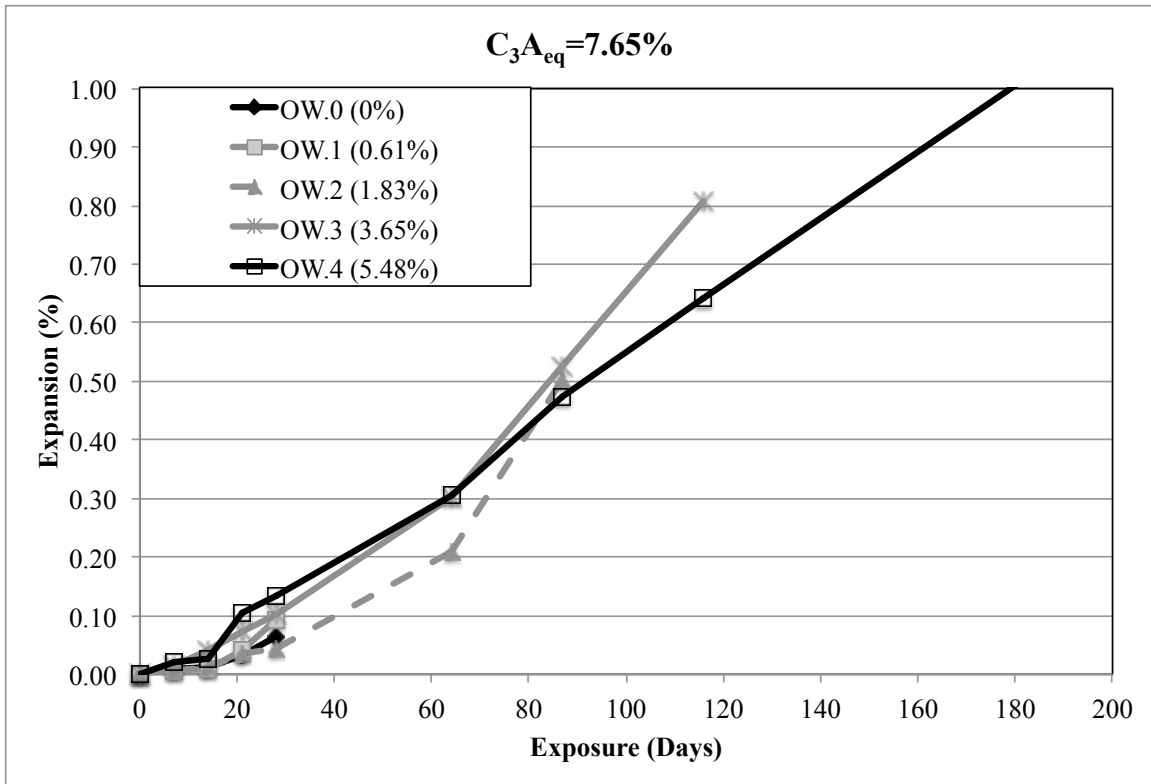


Figure 8-7: Length change for blended OW/HC with varying gypsum dosages in 5% Na_2SO_4 solution (% gypsum addition)

8.5 MICROSTRUCTURAL EVALUATION

8.5.1 XRD Rietveld analysis

X-ray diffraction analyses were performed for all blended mixtures prior to sulfate exposure. Quantitative Rietveld analysis was conducted on all diffraction patterns. Table 8-5 shows the amount of ettringite, monosulfate, gypsum and portlandite present in the system by mass percent prior to sulfate exposure (i.e., “zero” measurement). The equivalent tricalcium aluminate (C_3A_{eq}) content for each fly ash cement blend is also provided.

The formation of ettringite was evident with increasing gypsum mineral addition for all mixtures. For example, mixture C1.4 containing the highest gypsum addition

(9.04%), showed the most ettringite present of all mixtures with approximately 12.69% in the system. The results demonstrate that the formation and stabilization of ettringite at early ages did result in improved sulfate resistance based on the observed physical measurements and visual appearance of the mortar bars exhibiting moderate expansion values with minor deterioration at the corners (see Figure 8-3 and 8-4). Interestingly, the ettringite contents were roughly the same for mixtures having no gypsum addition showing only minor differences with decreasing equivalent tricalcium content. Similarly, the monosulfate and calcium hydroxide contents showed a minor decrease in amount with increasing gypsum content.

It is worth reemphasizing the gypsum additions were selected based on the calculated C_3A_{eq} content for each fly ash cement blend and divided in equal increments to investigate the varying combinations. It was assumed that the aluminate available to react from external sulfate attack was a result of the tricalcium aluminate (C_3A) content in the cement and one-third of the bulk chemical alumina content of the HC fly ash (Freeman, 1992; Freeman & Carrasquillo, 1995; Dhole, 2008). These values are converted to a total equivalent tricalcium aluminate (C_3A_{eq}) content for the cement-fly ash combination. Thus, enough gypsum was added initially to promote the conversion of C_3A_{eq} to ettringite during the fresh state and reduce the potential of ettringite formation during the hardened state. The Rietveld analysis revealed significantly less ettringite formation with decreasing C_3A_{eq} content. Intuitively, this would assume to be the case for lower C_3A_{eq} contents and thus, reducing the need for ettringite formation to improve the sulfate performance. However, the expansion results reveal differently showing severe expansion and deterioration, particularly in the OW cements having the lowest C_3A content.

Table 8-5: Quantitative Rietveld analysis of fly ash/cement blends with varying gypsum replacements prior to sulfate exposure

Cement/Fly Ash Blend	Gypsum (% Addition)	Ettringite (Wt. %)	Monosulfate (Wt. %)	Gypsum (Wt. %)	Portlandite (Wt. %)
C1/HC ($C_3A_{eq}=11.41\%$)	0%	2.16	2.37	0.82	3.54
	1.01%	1.96	2.13	3.69	3.53
	3.01%	3.33	1.31	1.65	2.30
	6.03%	8.52	1.65	2.68	2.58
	9.04%	12.69	1.52	0.86	2.40
C2/HC ($C_3A_{eq}=9.51\%$)	0%	1.97	1.72	1.07	4.62
	0.85%	1.72	1.66	0.96	4.18
	2.56%	3.34	1.63	0.07	3.09
	5.13%	6.77	1.46	1.07	3.32
	7.69%	10.78	1.30	0.83	2.59
C5/HC ($C_3A_{eq}=8.58\%$)	0%	1.55	1.86	0.67	5.12
	0.70%	1.39	1.23	0.73	4.89
	2.10%	2.79	1.44	0.44	4.12
	4.21%	4.56	1.55	0.88	4.34
	6.31%	7.89	1.69	0.59	3.76
OW/HC ($C_3A_{eq}=8.03\%$)	0%	1.79	1.13	0.47	4.16
	0.61%	2.46	1.46	0.30	4.89
	1.83%	2.14	1.63	0.61	4.22
	3.65%	4.02	1.38	0.32	3.84
	5.48%	5.26	1.58	0.54	3.67

Figure 8-8 and 8-9 present the phase contents formed pre- and post- exposure to 5% sodium sulfate. Ettringite clearly indicated a linear trend with increasing amount of

sulfates in the ternary system. A small reduction in the calcium hydroxide was noticeable. However, the formation of ettringite related to the SO_3 content was not clear after 6 months of exposure to sodium sulfate as shown in Figure 8-9.

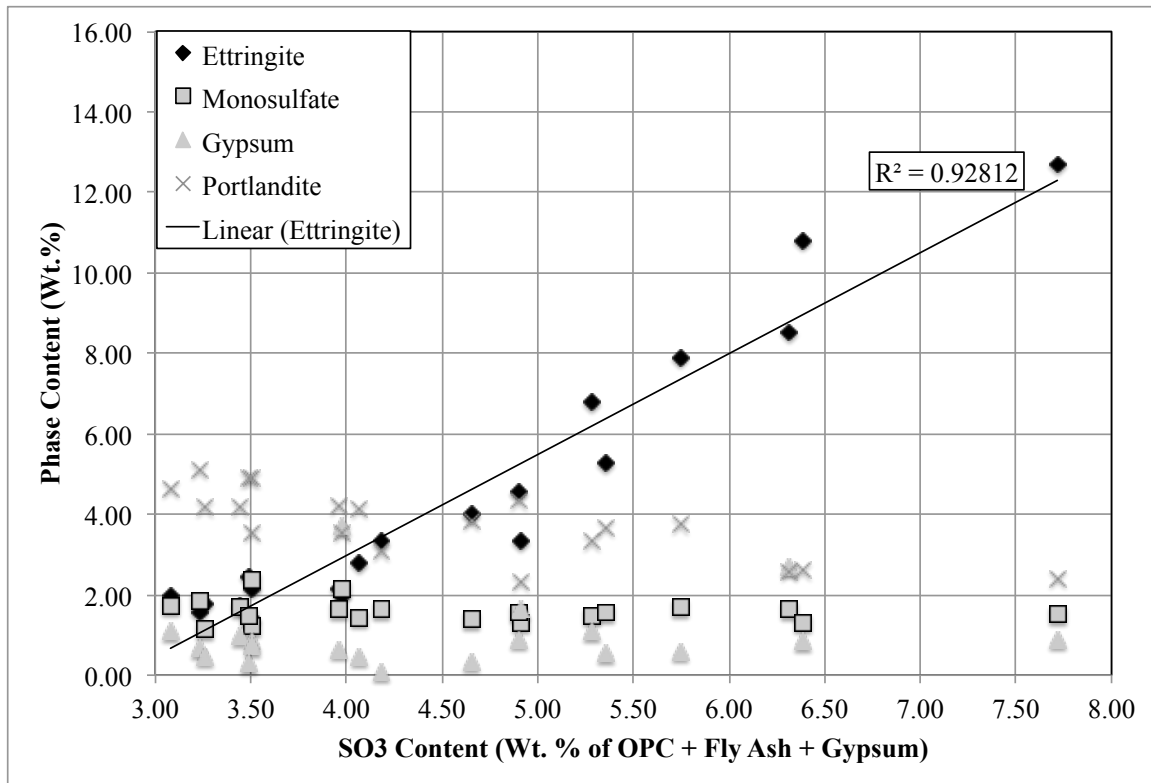


Figure 8-8: Phase content of reaction products prior to sulfate exposure and different levels of SO_3

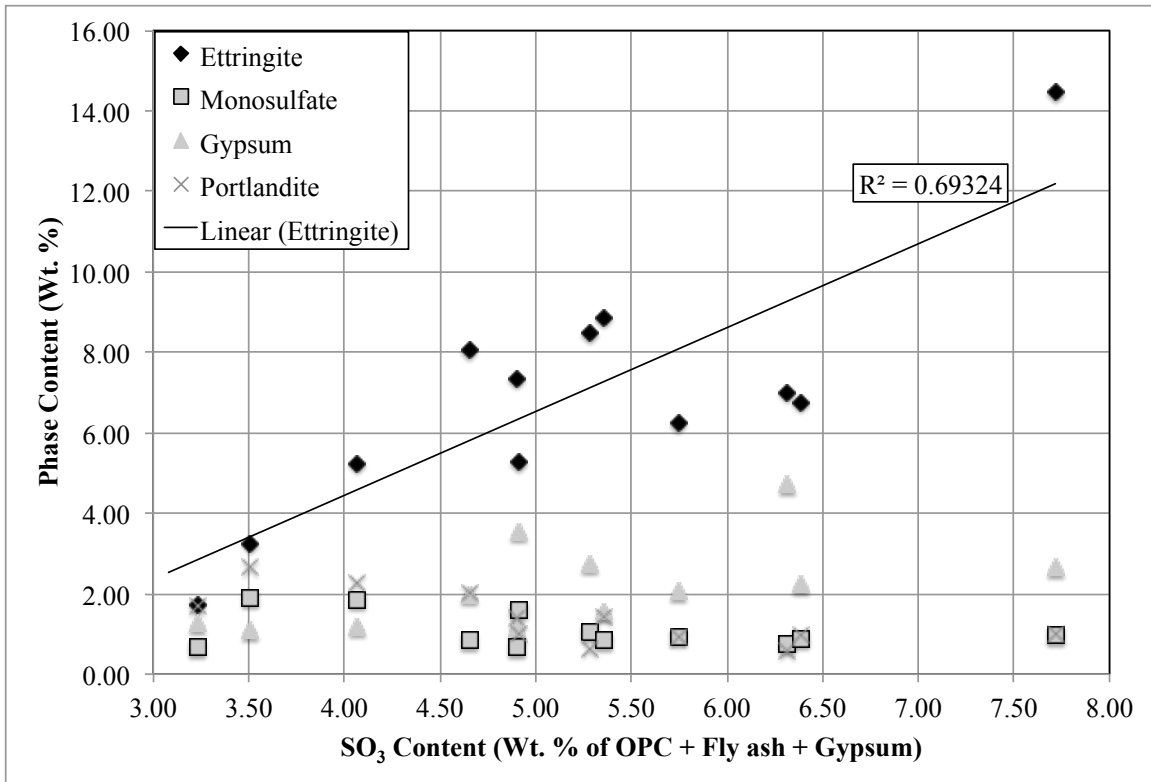


Figure 8-9: Phase content of reaction products after six months exposure to 5% Na₂SO₄ and different levels of SO₃

Figure 8-10 present the weight percent of ettringite in mixtures C1.0-1.4 as a function of time. The figure shows the amount of ettringite formed after 0, 2, 4, and 26 weeks exposure to 5% Na₂SO₄ solution; mixtures C1.0 and C1.1 were no longer measurable after 8 weeks and thus no results are presented at 26 weeks. The figure clearly illustrates the significant ettringite formed early on with increasing gypsum addition. Interestingly, a reduction in the amount of ettringite present was observed up to 4 weeks exposure. Thereafter, an increase was observed and likely attributed to the observed expansion in the mortar bars.

The reduction in the amount of ettringite is likely associated with an imbalance of sulfate ions to aluminate ions (SO₄²⁻/Al) in the system. The rapid formation of ettringite

early on is primarily a result of the conversion of tricalcium aluminate (C_3A) from the cement reacting with the gypsum whereas, the high-calcium fly ash is likely not participating in the early stages of the reaction due to its lower pozzolanic reactivity dormant period during the initial stages of hydration. From further hydration and reactivity, the availability of alumina in the fly ash reduces the ratio of sulfate ions to aluminate ions and favors the formation of monosulfate instead of ettringite during the early stages of hydration (Tishmack et al., 1999). Consequently, the ingress of external sulfates leads to additional ettringite formation during the hardened state.

Figure 8-11 shows the ettringite formation as a function of time for plain and blended mixtures using OW cement. The reduction of ettringite at 4 weeks is not as prevalent as blended C1 mixtures; however, there is a significant increase in ettringite after 6 months in sodium sulfate solution.

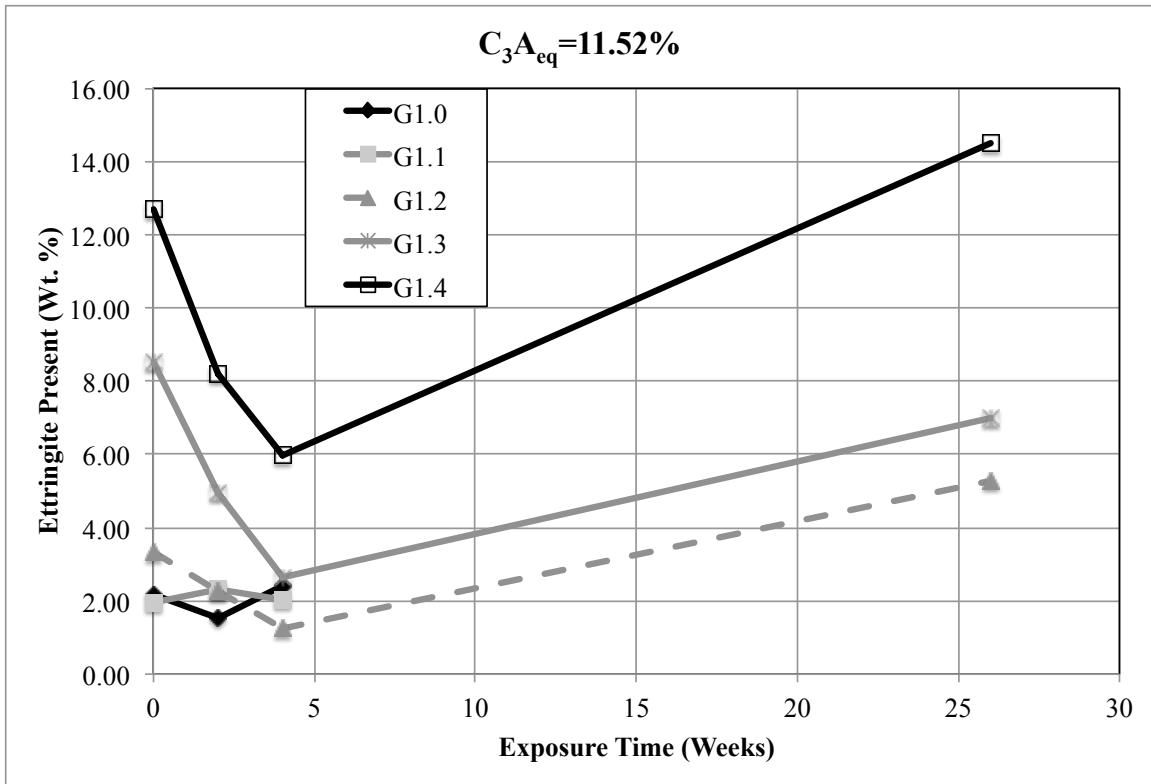


Figure 8-10: Ettringite formation as a function of time in 5% Na_2SO_4 in blended C1/HC mixture with varying gypsum dosages

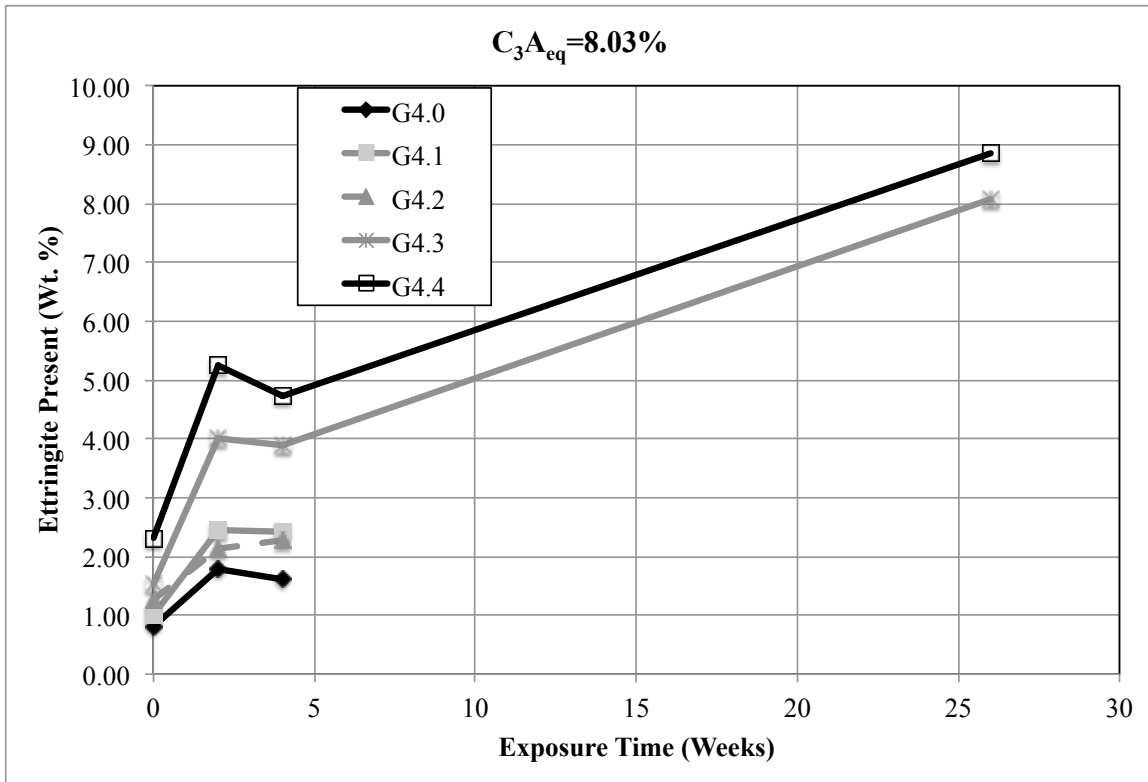


Figure 8-11: Ettringite formation as a function of time in 5% Na_2SO_4 in blended OW/HC mixture with varying gypsum dosages

8.5.2 SEM/EDS

The XRD results confirmed the presence of ettringite in significant quantities; however, it was unclear how well dispersed ettringite was in the system. Therefore, SEM analysis was used to study the effect of gypsum addition and ettringite disbursement in within the bulk portion of the mortar bar samples. Mixtures C1.0 and C1.4 were selected due to the significant differences in ettringite formation and length change results shown in the previous sections.

In order to determine the presence of ettringite at various locations in the sample, EDS point analysis was performed in two areas:

- Within the bulk paste matrix of the sample; and

- Near and around the outer edge of the sample

For each area, approximately 50 points in the paste selected at two different locations were analyzed and used to provide an indication the main phase present in the system. Figure 8-11 presents the EDS point analysis results for the two samples. The results for the edge of the sample clearly display the presence of ettringite as the main phase present for mixture C1.4; however, minor traces of monosulfate is still present. Mixture C1.0 revealed scattered results showing a mix of CSH, monosulfate, and ettringite present at the edge of the sample (see Figure 8-12). Interestingly, the EDS point analysis showed a significant shift in the phases present in the bulk area of the mortar samples, particularly for mixture C1.4. The bulk area showed a higher presence of monosulfate in both mixes. Consequently, this may result in formation of ettringite from the ingress of external sources of sulfate provided enough time and cracking is observed at the surface to encourage penetration. Furthermore, the latter method may be attributing to the observed expansion previously shown.

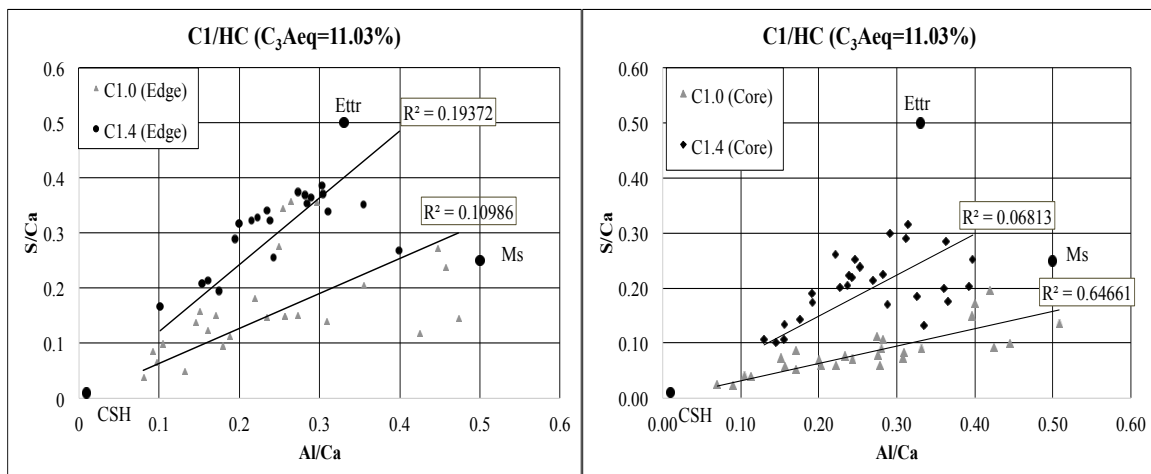


Figure 8-12: EDS point analysis of left) outer edge portion of sample; and right) bulk paste matrix

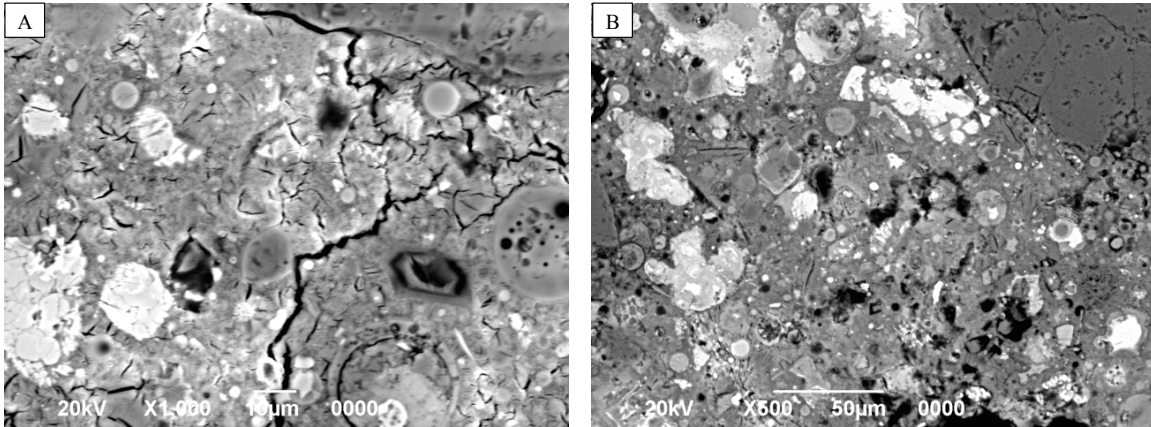


Figure 8-13: BSE images of samples prior to exposure of A) C1.4 showing large deposits of ettringite near the edge; and B) C1.0 with abundant monosulfate

8.7 HEAT OF HYDRATION

Paste samples prepared using a combination of C1, HC and gypsum were analyzed using isothermal calorimetry and qualitative XRD to study the effects of pre-blending the gypsum and fly ash for improving their reactivity. Isothermal calorimetry can be a useful screening tool for evaluating cement hydration and identifying mixture incompatibilities in a reasonable time, as shown in Figure 7-13. The results presented are an average of four samples. As expected, the addition of HC fly ash showed a longer deceleration phase as compared to the control. Furthermore, significant differences were noted for blended mixtures comprising 1.01% and 9.04% gypsum. For the mixtures comprising of 1.01% gypsum, a slight retardation as well as a larger second peak was observed, which is attributed to the hydration of the aluminate phase; however, the use of a finer particles size for the HC fly ash resulted in slight acceleration of the heat flow curve and most likely attributed to an effect of enhanced nucleation and growth of hydration products. A similar trend was observed in the mixtures comprising 9.04% gypsum showing a slight acceleration in the second peak; however, the second peak was not observed until after 24 hours. Unfortunately, the calorimetry curve for the mixture

comprising 9.04% gypsum and “unsieved” HC fly ash was not obtained due to the initial agreement to only run the sample for 24 hours. Furthermore, due to time constraints, the mixture was not re-evaluated in the isothermal calorimetry.

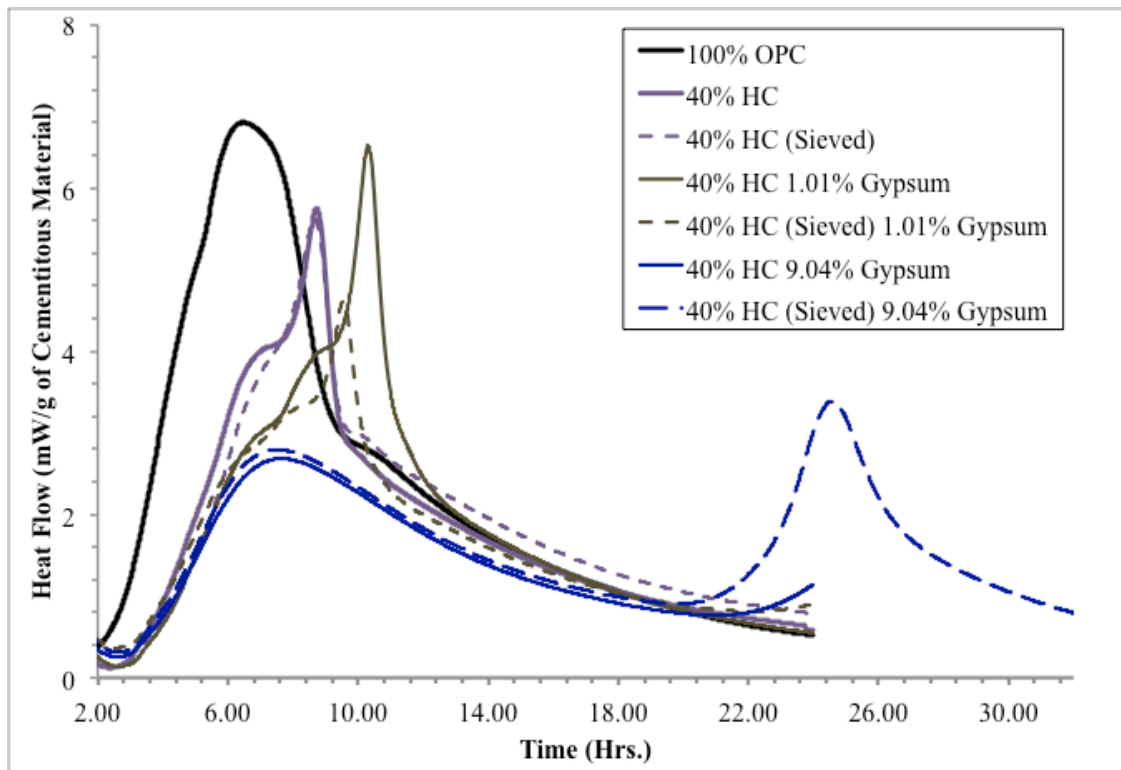


Figure 8-14: Heat flow curve for paste samples maintained at an isothermal temperature of 35 °C (95 °F)

The diffraction patterns for the eight paste mixtures pre- and post- exposure to 5% sodium sulfate solution is presented in Figure 8-13. The main objective here was to qualitatively investigate the changes in the hydration products resulting from sulfate exposure in mixtures containing C1, HC, and gypsum. Additionally, the impact of pre-blending finer fly ash particles prior to mixing was evaluated.

Ettringite is shown to be relatively stable as gypsum dosages increase in blended fly ash cement mixtures. The absence of monosulfate in most of these mixtures is most likely attributed to the aluminate phases being consumed to form ettringite during hydration. This was not the case however, for the mixture comprising 9.04% gypsum and sieved fly ash where the ettringite peak was not as strong pre-exposure. As a result, it is difficult to generate any conclusive explanations of the performance of the mixtures on the basis of the qualitative XRD. Nevertheless, it is evident from the XRD patterns that the addition of gypsum favored the formation of more ettringite at the expense of monosulfate.

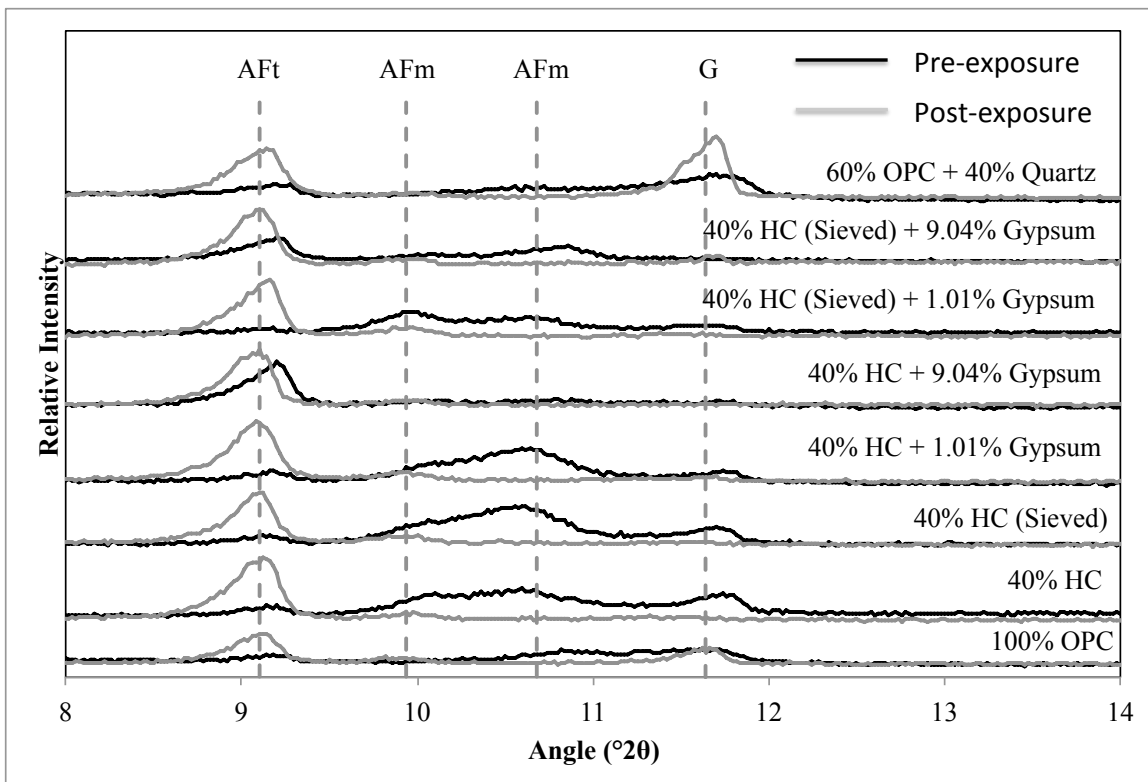


Figure 8-14: XRD patterns of paste samples pre- and post-exposure to 5.0% Na₂SO₄

8.8 CONCLUSION

- In comparison to plain high-calcium fly ash cement blended mixtures, the addition of gypsum showed improved sulfate performance. However, the performance was only slightly improved with most mixtures still exhibiting significant expansion and immeasurable after only 9 months of exposure to 5% Na₂SO₄
- In this study, the results clearly indicated that the tricalcium aluminate (C₃A) content has a substantial effect on the sulfate performance from the addition of gypsum at varying levels. Highest C₃A content combined with the highest gypsum addition greatly outperformed the other blended mixtures.
- The formation of ettringite during the early stages of hydration was clearly evident in the microstructural investigation in this study. However, SEM analysis revealed ettringite was found to mainly form near the surface edge of the mortar bar. Monosulfate was the dominant phase present at the center and likely contributed to the observed expansion in the mortar bars.
- Proper selection of the amount of gypsum to add to a given cement/Class C fly ash system to reduce the severity of sulfate attack deserves more attention, especially given that more and more Class C fly ash is likely to be available in the coming years.

Chapter 9: Conclusions and Recommendations

This chapter summarizes the main findings from this research and describes areas for future research.

9.1 CONCLUSIONS

9.1.1 Accelerated Performance Testing

Two methods of accelerating sulfate-induced expansion were evaluated. From the results presented, the following conclusions can be made:

- The proposed accelerated method involving the acceleration of sulfate ions by intentionally inducing microcracking in the cement matrix accelerated expansion, when compared to the conventional ASTM C 1012. Plain and blended mixtures using Type I cement showed accelerated results and exhibited a shorter time to failure (i.e., $\geq 0.10\%$ expansion); however, mixtures using Type I/II and Type V cement did not observe similar results. It was suggested that the modified heating regime the mortar bars were subjected to might have influenced the maturity of these mixtures.
- The use of vacuum impregnation was found to effectively increase the rate of sulfate ingress, resulting in significantly faster rates of expansion.
- Accelerated testing of mortar proved to be significantly shorter than companion mixtures using concrete specimens. This is mainly attributed to the specimen size as well permeability of the specimens. However,

concrete specimens cast using a relatively high w/cm showed significant improvements in terms of obtaining results in a shorter period

- Concrete prisms that were cast and sliced along each face exposing the bulk paste matrix accelerated the rate of expansion more than any method investigated; however, the results were inconsistent between mixtures. Nonetheless, the findings suggest that the permeability and exposure conditions have a significant impact on sulfate resistance.
- From accelerated performance testing, the rate of expansion was not significantly influenced when calcium and magnesium sulfate were used as the testing solution. The rate of expansion from highest to lowest for each sulfate type tested was: sodium > magnesium > calcium sulfate.
- Although calcium sulfate is typically regarded as the least aggressive of the commonly known sulfate types in the field, deterioration was observed in the Type I mixture after only one year of exposure.

9.1.2 Field Performance

- The use of high-calcium fly ash exhibited poor sulfate resistance when tested at the outdoor sulfate exposure site in Austin, TX. The performance was exasperated with increasing replacements of fly ash. However, for the companion prisms placed in 0.89%, only minor deterioration evident, particularly for those mixtures having a $w/cm=0.40$.
- The influence of w/cm was clearly evident in concrete made with a $w/cm=0.55$ exhibiting higher expansion rates and severe deterioration.

- Ternary blends of high-calcium fly ash, silica fume and portland cement proved to provide superior durability in sulfate environments.
- Field specimens correlated fairly well with companion concrete samples placed in controlled laboratory condition, showing similar distress and modes of failure.
- The influence of temperature fluctuations, environmental conditions, and fluctuating sulfate concentration on sulfate performance was evident. Sulfate deterioration was typically accelerated for field specimens.

9.1.3 Mechanisms of Sulfate Attack

- Mixtures immersed in 5% sodium sulfate typically exhibited a faster onset of expansion and deterioration compared to 0.89%.
- Although the formation of ettringite and gypsum was evident in samples placed in both 5% and 0.89% sodium sulfate, ettringite was found to be the dominant phase present at 5% and the primary source of expansion.
- Ettringite was the primary phase observed in samples placed in calcium and sodium sulfate, whereas the formation of ettringite, gypsum, and magnesium silicate hydrate (MSH) was observed in mixtures placed magnesium sulfate.
- Expansion, cracking and in some cases warping of the bars was associated for prisms placed in sodium sulfate solution; only minor expansion was observed in mortar bars placed in calcium sulfate whereas the main mode of deterioration as primarily cracking and softening of the mortar bars; lastly, cracking of bars at the edges and corners was the main deterioration

observed in bars placed in magnesium sulfate solution with minor to moderate expansion.

- The addition of gypsum in blended high-calcium fly ash mixtures resulted in the formation of ettringite early on and thus improving the sulfate resistance; however, the decrease in tricalcium aluminate (C_3A) resulted in worse performance.
- Unlike the Type I cement, where the sulfate performance was significantly improved with increasing gypsum addition, Class H oil well cement was essentially unaffected by the addition of gypsum in the system.

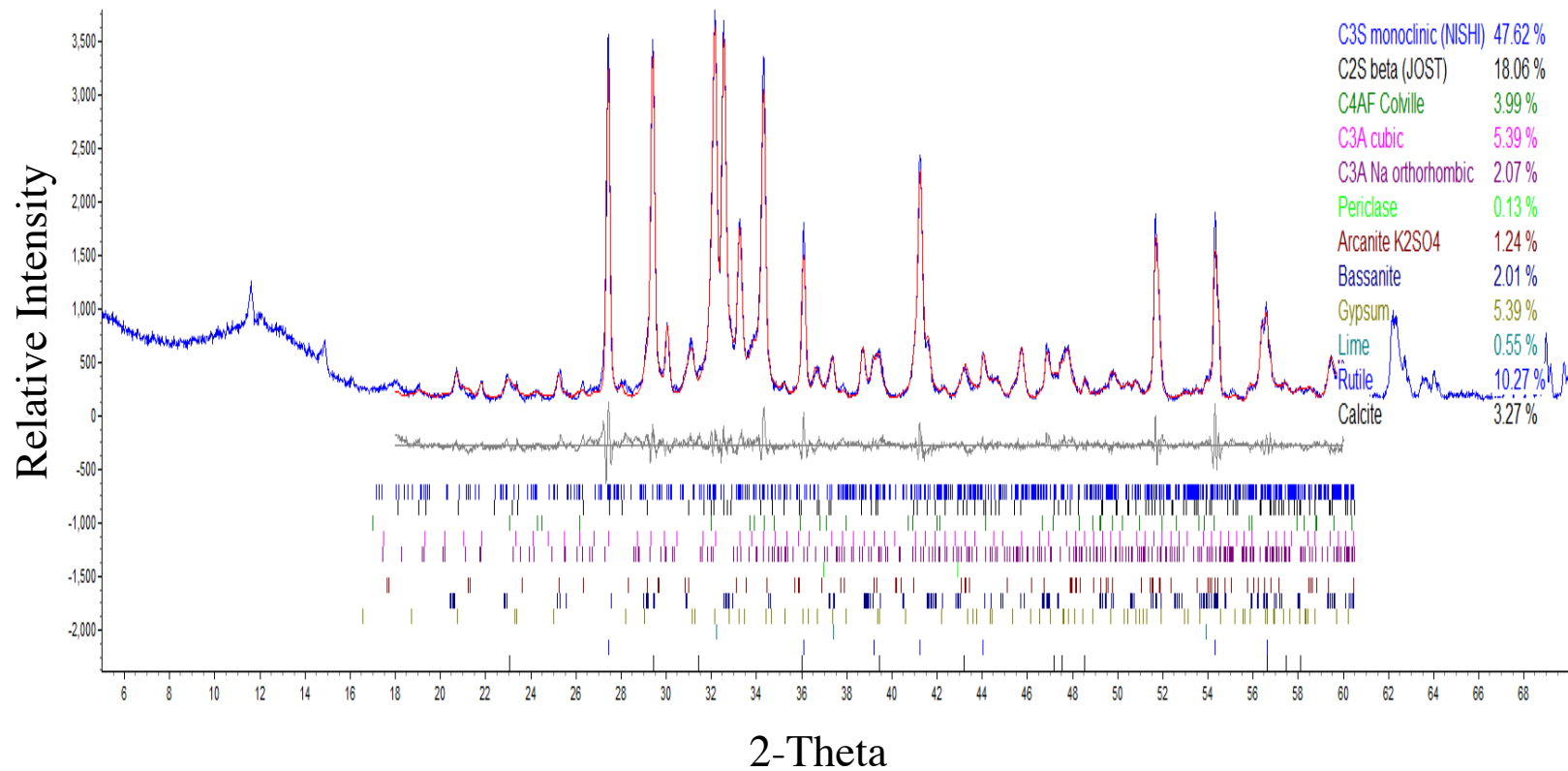
9.2 FUTURE WORK

This dissertation focused on the performance cementitious systems in various sulfate environments including field and laboratory investigations. Furthermore, this study presents an innovative accelerated test method to evaluate the sulfate performance using concrete specimens. Although the accelerated method demonstrate superior results, future research is needed that focuses on:

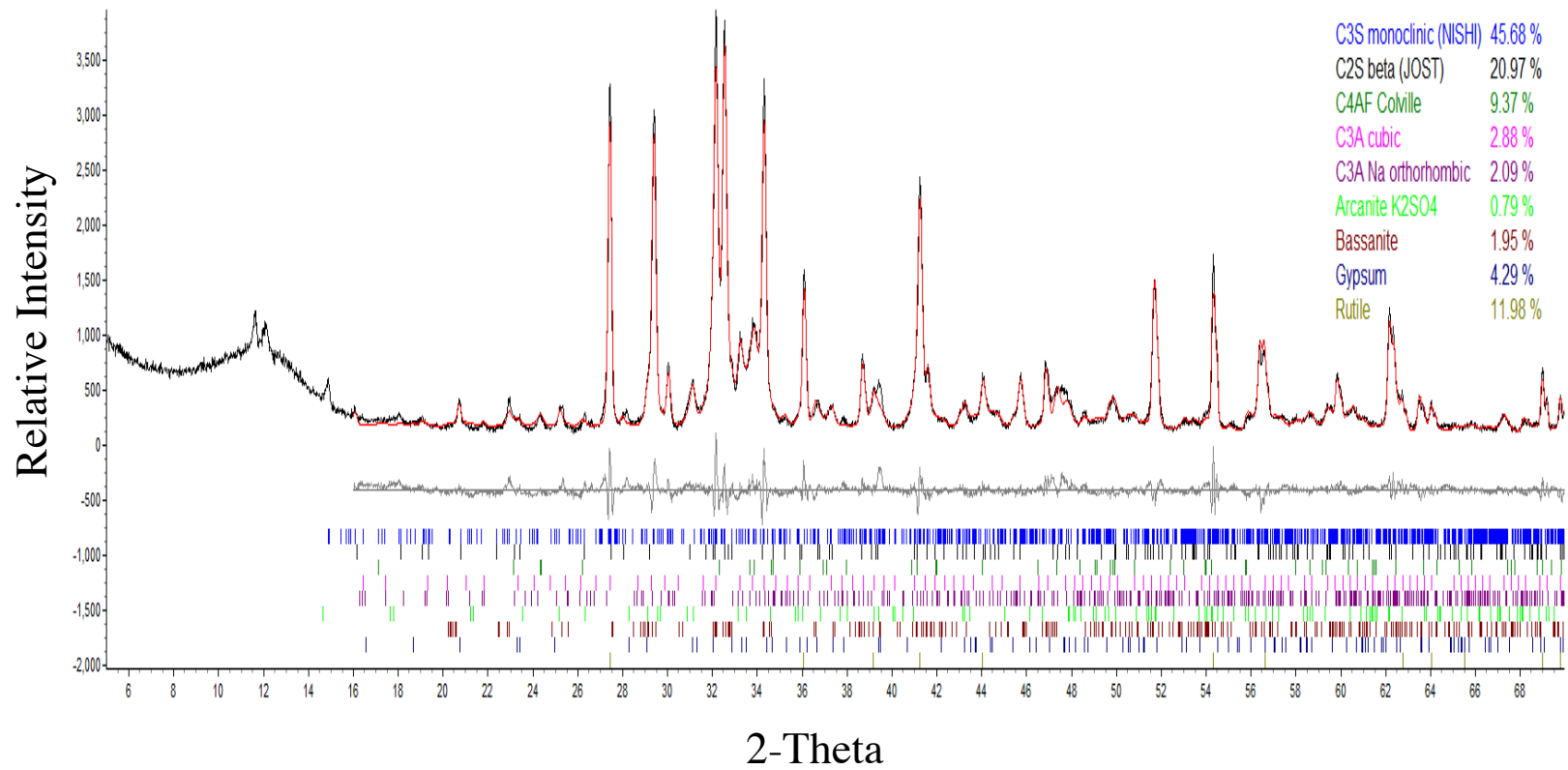
- Studying the repeatability of the accelerated performance test within a laboratory as well as between laboratories.
- Improving the accuracy and further reducing the duration of the test by studying the effects of constant pH, temperature, sulfate concentration, sulfate type, specimen sizes and w/cm ratio.
- Investigating the performance of the accelerated method on number of other cementitious materials such rapid repair, alkali-activated, and performance cements.

Lastly, it is recommended that additional concrete samples be evaluated under field conditions or using outdoor exposure sites, with the ultimate goal of benchmarking accelerated laboratory tests.

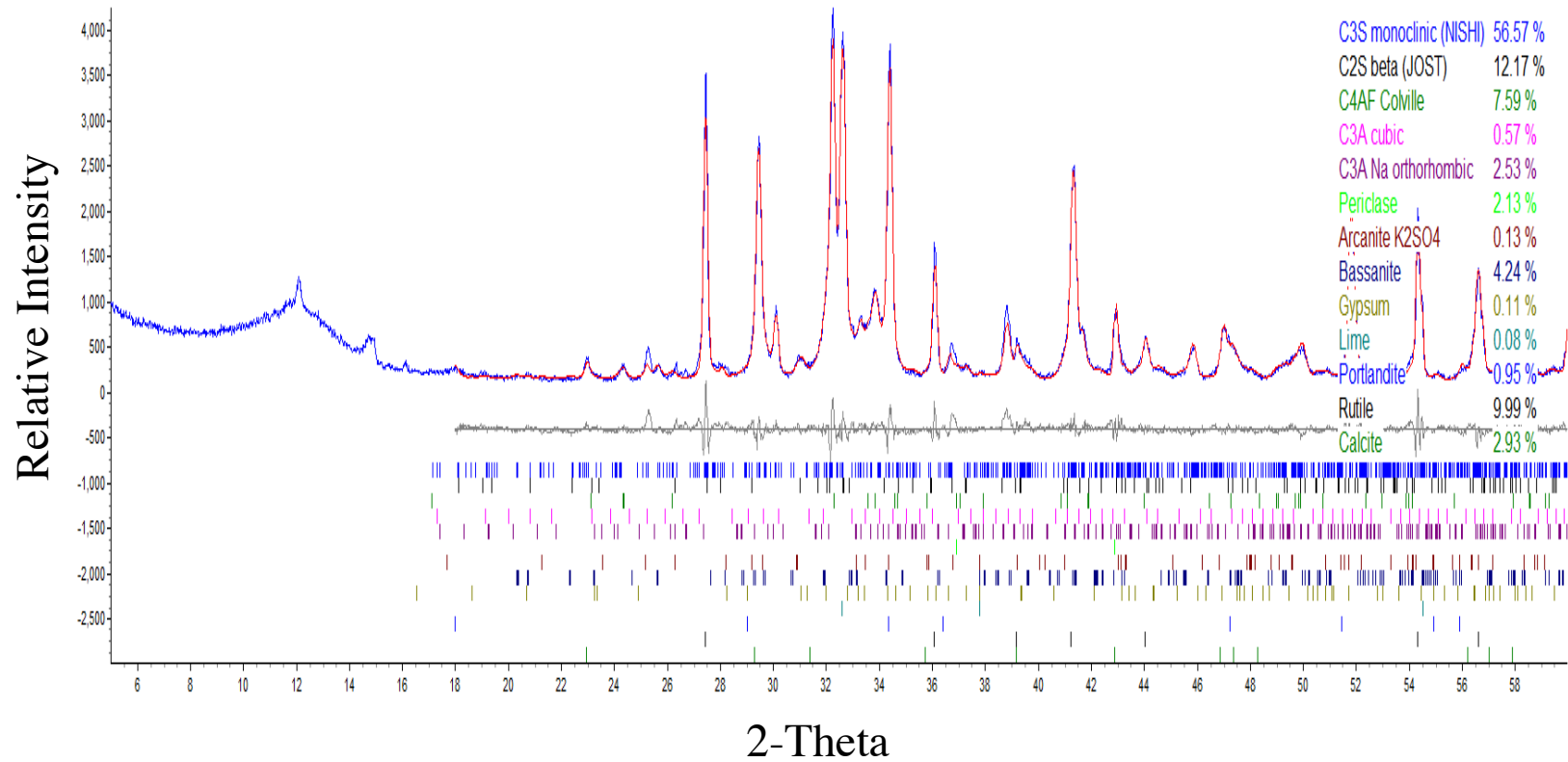
Appendix A – Rietveld Analysis for Cementitious Materials



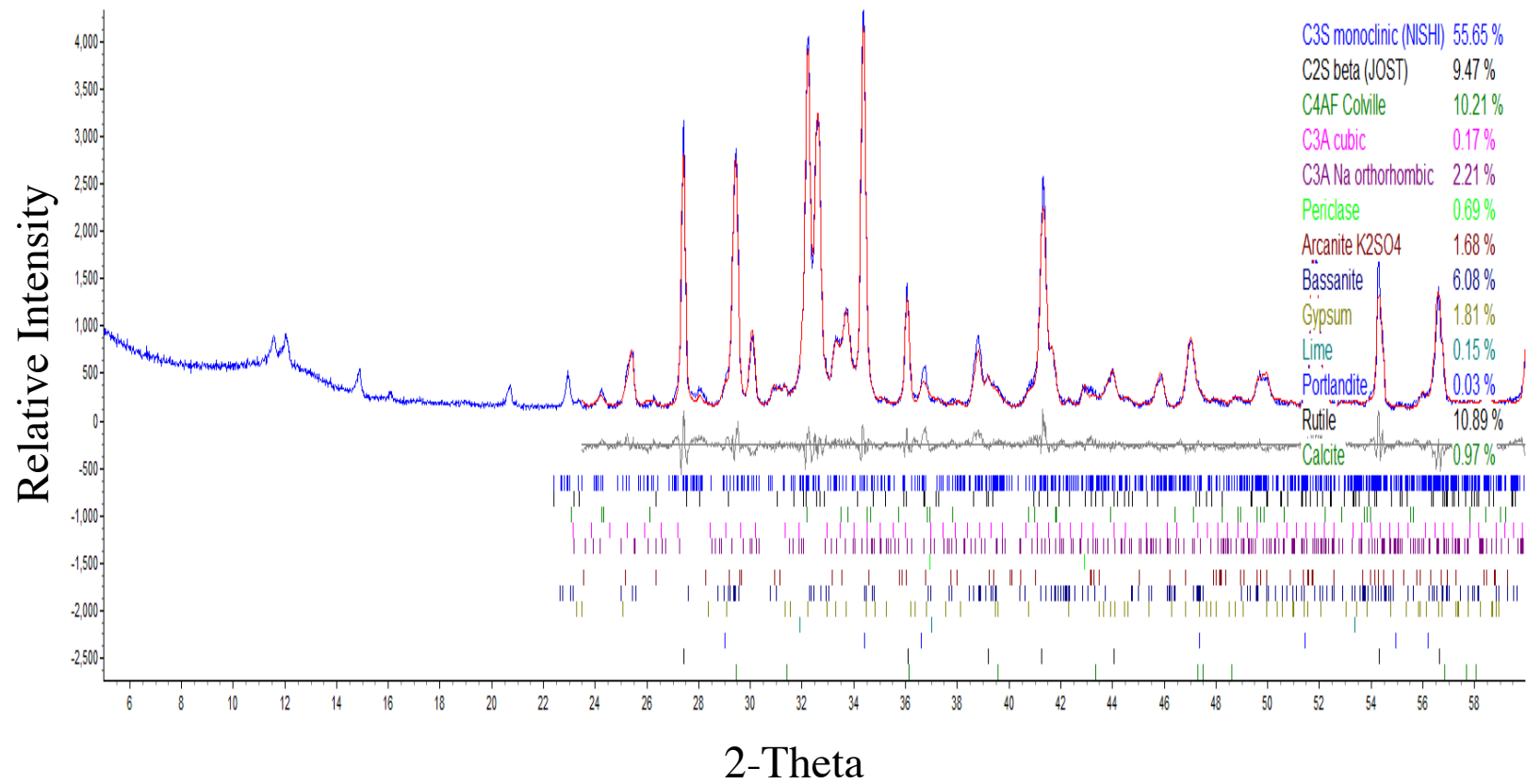
A.1: X-Ray Diffraction Pattern and Rietveld Analysis for Type I Cement



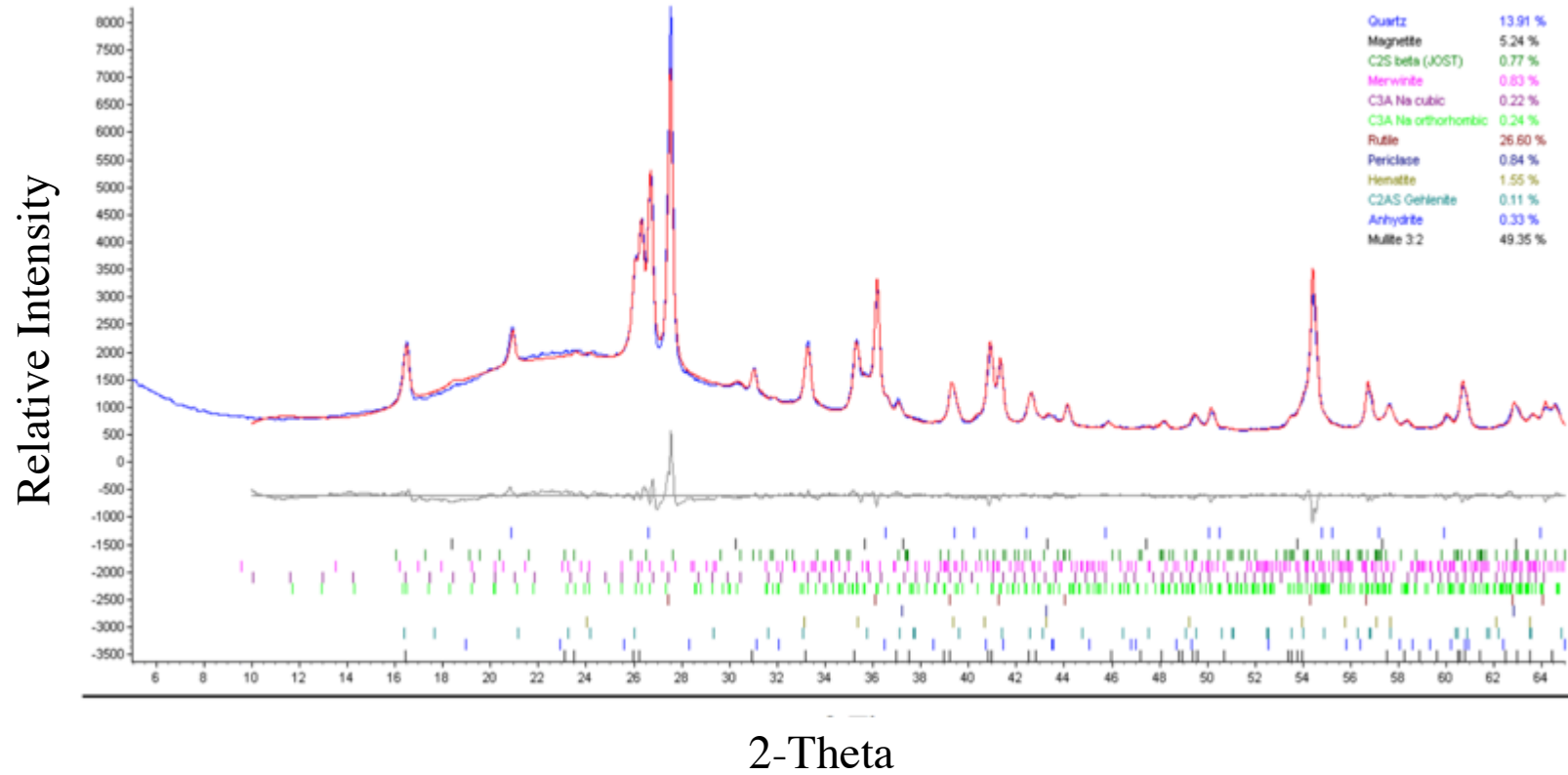
A.2: X-Ray Diffraction Pattern and Rietveld Analysis for Type I/II Cement



A.3: X-Ray Diffraction Pattern and Rietveld Analysis for Type V Cement



A.4: X-Ray Diffraction Pattern and Rietveld Analysis for Class H Oil Well Cement



A.5: X-Ray Diffraction Pattern and Rietveld Analysis for High-Calcium Class C Fly Ash

Appendix B –Procedure for Performing the Accelerated Vacuum Impregnation Technique

Vacuum impregnation of 25 x 25 x 285 mm (1 x 1 x 11.25 in) mortar bars immersed in Na₂SO₄

- A sufficient number of 25 x 25 x 285 mm (1 x 1 x 11.25 in) mortar bars and 50 mm (2 in) cubes are cast and cured at 35 °C ± 3 °C (73°F ± 5°F) for 23.5 hr ± 0.5 hr
- After demolding, mortar cubes are evaluated for their strength. Each mixture must obtain a strength of 20 MPa (2,850 psi) prior to beginning of the test
- Once strength is achieved, mortar bars are placed at 38°C for drying for a minimum of 14 days (or constant mass is achieved). At the end of the drying period, bars are weighed and measured for their length;
- Following the drying period, bars are then placed in a large pressure tank and subjected to a high-vacuum for 4 hours;
- Still under vacuum, the tank containing the mortar bars is introduced with sulfate solution (at the same concentration that is being considered for testing, in this case 5.00% Na₂SO₄) to entirely cover the specimens. Vacuum is adjusted if needed;
- After 20 hours of immersion (24 hour cycle), vacuum is released and bars are weighed and measured for their initial length (“zero-measurement”)
- The bars are stored at 23 °C ± 2°C (73 °C ± 4 °F) in solution at the same concentration as that used in the vacuum impregnation technique;
- Expansion and mass change is monitored periodically and visual degradation noted for at least 12 months